

MECHANICAL BEHAVIOR OF ASPHALT-MINERAL
POWDER COMPOSITES AND ASPHALT-MINERAL
INTERACTION

FEBRUARY 1971— NUMBER 5



BY

DAVID A. ANDERSON

JHRP

JOINT HIGHWAY RESEARCH PROJECT
PURDUE UNIVERSITY AND
INDIANA STATE HIGHWAY COMMISSION

Progress Report

MECHANICAL BEHAVIOR OF ASPHALT-MINERAL
POWDER COMPOSITES AND ASPHALT-MINERAL INTERACTION

TO: J. F. McLaughlin, Director
Joint Highway Research Project

February 2, 1971

FROM: H. L. Michael, Associate Director
Joint Highway Research Project

Project: C-36-6Y

File: 2-4-25

The attached is a Progress Report on the HPR-1 (8) Part II research project "Cracking in Bituminous Mixtures". The report is titled "Mechanical Behavior of Asphalt-Mineral Powder Composites and Asphalt-Mineral Interaction". It has been authored by the principal investigator Mr. David A. Anderson, Graduate Instructor in Research on our staff, under the direction of Professor W. H. Goetz. The report is presented as the final report on Phase I of this research project.

This phase of the research has taken much longer to complete than originally anticipated due to difficult technical problems which had to be solved in order to achieve results. The perseverance and ability of the investigator resulted in solutions to these problems and the attainment of the objectives of the study.

The findings have been utilized in developing a Plan of Study for Phase II of this project. That Plan of Study will be submitted shortly for review, comment and approval.

This Progress Report is presented to the Board for information and for acceptance as fulfilling the objectives of the Phase I Plan of Study approved by the Board on March 14, 1967. The Report will also be submitted to the ISHC and the FHWA for similar review, comment and acceptance.

Respectfully submitted,

Harold L. Michael

Harold L. Michael
Associate Director

HLM:ms

cc: F. L. Ashbaucher
W. L. Dolch
W. H. Goetz
W. L. Grecco
M. J. Gutzwiller
G. K. Hallock

M. E. Harr
R. H. Harrell
M. L. Hayes
E. M. Mikhail
R. D. Miles
J. W. Miller

C. F. Scholer
M. B. Scott
W. T. Spencer
N. W. Steinkamp
H. R. J. Walsh
K. B. Woods
E. J. Yoder

Progress Report

MECHANICAL BEHAVIOR OF ASPHALT-MINERAL
POWDER COMPOSITES AND ASPHALT-MINERAL INTERACTION

by

David A. Anderson
Graduate Instructor in Research

Joint Highway Research Project

Project No: C-36-6Y

File No: 2-4-25

Prepared as Part of an Investigation

Conducted by

Joint Highway Research Project
Engineering Experiment Station
Purdue University

in cooperation with the

Indiana State Highway Commission

and the

U. S. Department of Transportation
Federal Highway Administration

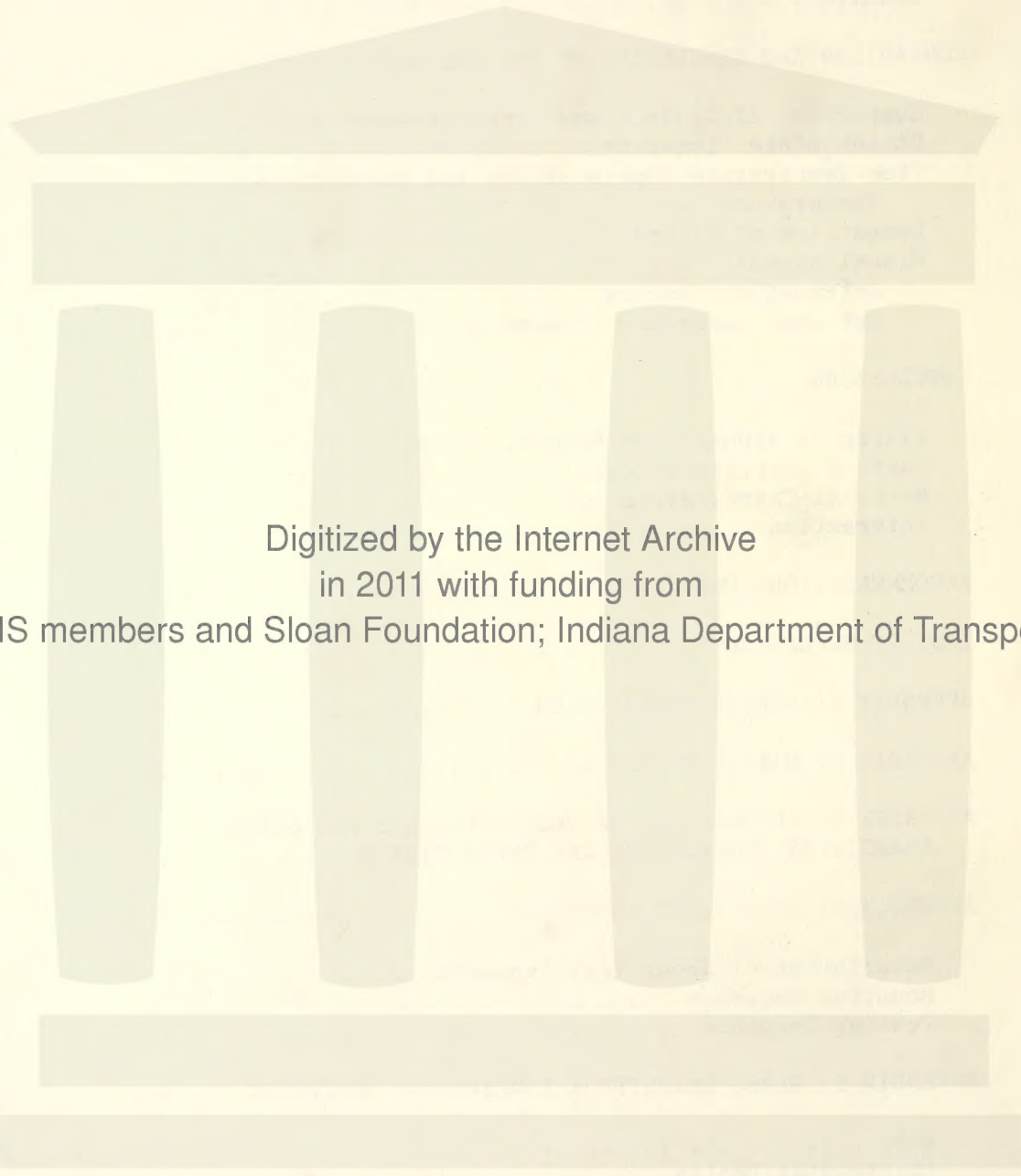
The opinions, findings and conclusions expressed in this
publication are those of the authors and not necessarily
those of the Federal Highway Administration.

Purdue University
Lafayette, Indiana
February 2, 1971

TABLE OF CONTENTS

	Page
LIST OF TABLES	vi
LIST OF FIGURES	viii
NOMENCLATURE	xiv
ABSTRACT	xvii
INTRODUCTION	1
Scope	1
Background	2
Review of Literature	3
Statement of Problem	8
MATERIALS AND SAMPLE PREPARATION	11
Mineral Powders - Selection and Preparation	11
Mineral Powders - Characterization	13
Air Permeability and Nitrogen Adsorption Measurements	15
Scanning Electron Microscope	20
Physico-Chemical Surface Properties	24
Summary	26
Description of Asphalts	29
Preparation and Description of Powder-Asphalt Mixtures	30
CHARACTERIZATION OF MECHANICAL BEHAVIOR	33
General	33
Test Procedures	37
Dynamic Measurements	39
Time-Temperature Superposition	48
Dynamic Testing - Results	57
Retardation Spectra	78
Creep Measurements	81
Creep Testing - Presentation and Discussion of Results	85
Summary	105

	Page
GLASS TRANSITION TEMPERATURE MEASUREMENTS	108
Background	108
Experimental	109
Results	113
COMPARISON AND DISCUSSION OF THE VARIOUS RESULTS	119
Comparison of Dynamic and Creep Measurements	119
Steady State Viscosity	123
Time-Temperature Superposition and Glass Transition Temperature	129
Comparison of Effect of Fillers on Compliance	136
Miscellaneous	155
Retardation Spectra	155
Specimen Aging and Treatment	159
CONCLUSIONS	166
Mixing of Asphalt and Mineral Powder	166
Surface Characterization	166
Material Characterization	167
Interaction	168
RECOMMENDATIONS FOR FURTHER RESEARCH	170
LIST OF REFERENCES	173
APPENDIX A: POWDER PREPARATION	179
APPENDIX B: MIXING PROCEDURE	187
APPENDIX C: PREPARATION OF TEST SPECIMENS FOR GLASS TRANSITION TEMPERATURE AND SHEAR TESTING	192
APPENDIX D: SHEAR TEST PROCEDURE	196
Description of Shear Test Apparatus	196
Mounting Sequence	202
Testing Sequence	203
APPENDIX E: GLASS TRANSITION TEMPERATURE EQUIPMENT	205
Bath	205
Dilatometer Design	207



Digitized by the Internet Archive
in 2011 with funding from
LYRASIS members and Sloan Foundation; Indiana Department of Transportation

	Page
APPENDIX F: REDUCTION OF DYNAMIC TEST DATA	213
APPENDIX G: REDUCED DYNAMIC DATA	223
Program	224
Sample Data	226
Reduced Data	227
APPENDIX H: REDUCTION OF CREEP DATA	252
APPENDIX I: REDUCED CREEP DATA	259
Program	260
Reduced Data	262
Sample Data	263

LIST OF TABLES

Table	Page
1. Description of Minerals	12
2. Properties of Specially Prepared Finely Divided Mineral Powders	14
3. Results of Surface Acidity Measurements	27
4. Asphalt Properties	29
5. Identification of Asphalt-Mineral Powder Composites	32
6. Values of $\log a_T$ and T_s for B3056 Mixtures	50
7. Values of $\log a_T$ and T_s for B3603 Mixtures	51
8. Values of $\log a_T$ and T_s for Aged Mixtures	52
9. Calculated Coefficients, WLF Equation	56
10. Calculated Retardation Spectra, Sample 108	79
11. Average Differences Between Rise and Fall T_g Values for Various B3056 Mixtures	114
12. Average Values of T_g for B3056 Mixtures	116
13. Average Values of T_g for B3603 Mixtures	117
14. Comparison of Glass Transition Temperatures	117
15. Calculated Values of J_e and η	127
16. Relative Values of J_e and η : B3056 Mixtures	128
17. Summary of Experimental Values of a_T	130
18. Comparison of Mechanically and Dilatometrically Determined Values of T_g for CaCO_3 and SiO_2 Mixtures	134
19. Comparison of Mechanically and Dilatometrically Determined Values of T_g for B3056 Asphalt with $< 2.5\mu\text{m}$ Powders	134

LIST OF TABLES, cont.

Table	Page
A1. Specific Gravity and Time of Fall for Powders	181, 182
D1. Filter Attenuation Factors	201

LIST OF FIGURES

Figure	Page
1. Schematic of Air Permeability Manometer	17
2. Sample Cup	18
3. Drop Weight Compacting Device	18
4. Scanning Electron Photomicrograph, 10-20 μm Quartz, 300x	21
5. Scanning Electron Photomicrograph, 10-20 μm Calcite, 300x	21
6. Scanning Electron Photomicrograph, 10-20 μm Quartz, 3000x	21
7. Scanning Electron Photomicrograph, 10-20 μm Calcite, 3000x	21
8. Scanning Electron Photomicrograph, 2.5-5.0 μm Quartz, 1500x	22
9. Scanning Electron Photomicrograph, 2.5-5.0 μm Calcite, 1300x	22
10. Scanning Electron Photomicrograph, 0.63-1.25 μm Quartz, 1000x	22
11. Scanning Electron Photomicrograph, 0.63-1.25 μm Calcite, 1000x	22
12. Scanning Electron Photomicrograph, < 2.5 μm Apatite, 3000x	23
13. Scanning Electron Photomicrograph, < 2.5 μm Bytownite, 3000x	23
14. Scanning Electron Photomicrograph, < 2.5 μm Magnesite, 3000x	23
15. Scanning Electron Photomicrograph, < 2.5 μm Microcline, 3000x	23

Figure	Page
16. Typical Plot of $\text{Log } J^* $ Versus $\text{Log } 1/\omega$	42
17. Typical Plot of $\text{Log } J'$ Versus $\text{Log } 1/\omega$	43
18. Typical Plot of $\text{Log } J''$ Versus $\text{Log } 1/\omega$	44
19. Typical Plot of $\text{Log Tan } \delta$ Versus $\text{Log } 1/\omega$	45
20. Peak to Peak Stress Versus Peak to Peak Strain	47
21. Experimentally Determined a_T	54
22. Determination of T_g	55
23. Dynamic Compliance Components, Sample No. 105: B3056 Asphalt, 10.-20. μm Calcite	58
24. Dynamic Compliance Components, Sample No. 106: B3056 Asphalt, 2.5-5.0 μm Quartz	59
25. Dynamic Compliance Components, Sample No. 107: B3056 Asphalt, 10.-20. μm Quartz	60
26. Dynamic Compliance Components, Sample No. 108: B3056 Asphalt, 2.5-5.0 μm Calcite	61
27. Dynamic Compliance Components, Sample No. 109: B3056 Asphalt, Graded Calcite	62
28. Dynamic Compliance Components, Sample No. 118: Unfilled B3056 Asphalt	63
29. Dynamic Compliance Components, Sample No. 119: B3056 Asphalt, Graded Quartz	64
30. Dynamic Compliance Components, Sample No. 120: B3056 Asphalt, 2.5-5.0 μm Quartz	65
31. Dynamic Compliance Components, Sample No. 121: B3056 Asphalt, 2.5-5.0 μm Calcite	66
32. Dynamic Compliance Components, Sample No. 123: Unfilled B3603 Asphalt	67
33. Dynamic Compliance Components, Sample No. 124: B3603 Asphalt, 10.-20. μm Calcite	68

Figure	Page
34. Dynamic Compliance Components, Sample No. 125: B3603 Asphalt, 10.-20. μm Quartz	69
35. Dynamic Compliance Components, Sample No. 126: B3056 Asphalt, < 2.5 μm Magnesite	70
36. Dynamic Compliance Components, Sample No. 127: B3056 Asphalt, < 2.5 μm Bytownite	71
37. Dynamic Compliance Components, Sample No. 128: B3056 Asphalt, < 2.5 μm Microcline	72
38. Dynamic Compliance Components, Sample No. 129: B3056 Asphalt, < 2.5 μm Apatite	73
39. Dynamic Compliance Components, Sample No. 130: B3603 Asphalt, 2.5-5.0 μm Calcite	74
40. Dynamic Compliance Components, Sample No. 131: B3603 Asphalt, 2.5-5.0 μm Quartz	75
41. Dynamic Compliance Components, Sample No. 132: B3056 Asphalt, 0.63-1.25 μm Calcite	76
42. Dynamic Compliance Components, Sample No. 133: B3056 Asphalt, 0.63-1.25 μm Quartz	77
43. Retardation Spectra, Sample No. 108	80
44. Typical Unshifted Creep Data, Sample No. 108	82
45. Construction of Superposed Creep Curve	84
46. Extension of Creep Data by Superposition	86
47. Creep Compliance, Sample No. 105: B3056 Asphalt, 10.-20. μm Calcite	88
48. Creep Compliance, Sample No. 106: B3056 Asphalt, 2.5-5.0 μm Quartz	89
49. Creep Compliance, Sample No. 107: B3056 Asphalt, 10.-20. μm Quartz	90
50. Creep Compliance, Sample No. 108: B3056 Asphalt, 2.5-5.0 μm Calcite	91

Figure	Page
51. Creep Compliance, Sample No. 109: B3056 Asphalt, Graded Calcite	92
52. Creep Compliance, Sample No. 118: Unfilled B3056 Asphalt	93
53. Creep Compliance, Sample No. 119: B3056 Asphalt, Graded Quartz	94
54. Creep Compliance, Sample No. 120: B3056 Asphalt, 2.5-5.0 μm Quartz	95
55. Creep Compliance, Sample No. 121: B3056 Asphalt, 2.5-5.0 μm Calcite	96
56. Creep Compliance, Sample No. 123: Unfilled B3603 Asphalt	97
57. Creep Compliance, Sample No. 124: B3056 Asphalt, 10.-20. μm Calcite	98
58. Creep Compliance, Sample No. 125: B3603 Asphalt, 10.-20. μm Quartz	99
59. Creep Compliance, Sample No. 130: B3603 Asphalt, 2.5-5.0 μm Calcite	100
60. Creep Compliance, Sample No. 131: B3603 Asphalt, 2.5-5.0 μm Quartz	101
61. Creep Compliance, Sample No. 132: B3056 Asphalt, 0.63-1.25 μm Calcite	102
62. Creep Compliance, Sample No. 133: B3056 Asphalt, 0.63-1.25 μm Quartz	103
63. Idealized Volume - Temperature Relationship	110
64. Typical Data for Determination of the Glass Transition Temperature	112
65. Comparison of $ \bar{J}^* $ and $J(t)$ at $\omega = 1/t$, B3056 Asphalt . .	121
66. Comparison of $ \bar{J}^* $ and $J(t)$ at $\omega = 1/t$, B3603 Asphalt . .	122
67. Estimation of Steady State Viscosity and Equilibrium Compliance	126

Figure	Page
68. $ \bar{J}^* $, B3056 - SiO_2 Mixtures	139
69. Comparison of Storage Compliance for B3056, CaCO_3 Mixtures	140
70. Comparison of Storage Compliance for B3056, SiO_2 Mixtures	141
71. Effect of Filler Type on Storage Compliance, B3056 Mixtures	142
72. Storage and Loss Compliance for B3603 Mixtures	143
73. Creep Compliance for CaCO_3 Mixtures, B3056 Asphalt	145
74. Creep Compliance for SiO_2 Mixtures, B3056 Asphalt	146
75. Creep Compliance, SiO_2 and CaCO_3 Mixtures Compared	148
76. Creep Compliance for B3603 Mixtures, B3603 Asphalt	149
77. $ \bar{J}^* $, $< 2.5 \mu\text{m}$ B3056 Mixtures	150
78. Ratio, $J^0(t)/J(t)$ for Selected B3056 and B3603 Mixtures	152
79. Comparison of the Results of the Unfilled Asphalts With Those of Other Authors	153
80. Retardation Spectra, SiO_2 - B3056 Mixtures	156
81. Retardation Spectra, CaCO_3 - B3056 Mixtures	157
82. Retardation Spectra, B3603 Mixtures	158
83. J' , J'' for Unaged and Aged B3603, 2.5-5.0 μm Calcite	161
84. J' , J'' for Unaged and Aged B3603, 2.5-5.0 μm Quartz	162
85. J' , J'' for Unaged and Aged B3056, 0.63-1.25 μm Calcite	163
86. J' , J'' for Unaged and Aged B3056, 0.63-1.25 μm Quartz	164

Appendix Figures

A1. Schematic of Gravity Sedimentation Equipment	183
A2. Freeze Dry Apparatus	186

Figure	Page
B1. Photograph of Mixing Equipment	188
B2. Schematic of Mixing Equipment	189
C1. Test Specimen Preparation Sequence	193
D1. Overall Picture of Test Set Up	197
D2. Details of Plate Assembly being Mounted in Water Bath . .	197
D3. Assembled Sample Plates	198
D4. LVDT Assembly	200
D5. Flow Chart for Test Sequence	204
E1. Controlled Temperature Bath	206
E2. Typical Time-Temperature Plot from T_g Bath	208
E3. First Design T_g Dilatometer	209
E4. Second Design T_g Dilatometer	211
F1. Sample Lissajous Patterns, x-y Recorder	214
F2. Sample Lissajous Patterns, Oscilloscope	215
F3. Schematic Lissajous Pattern	216
F4. Sample Data Sheet, Dynamic	222
H1. Sample Creep Curve	253
H2. Sample Data Sheet, Creep	254

NOMENCLATURE

A	Cross-section area, cm sq
a	Scale divisions in Y direction at center of Lissajous Pattern
a_T	Shift function
Δa_T	Change in a_T between two adjacent test temperatures
c_v	Volume concentration of solids
c_v^{\max}	Volume concentration of solids at densest packing
c_1^0, c_2^0	Constants in one form of WLF equation
d	Particle diameter, cm
e	Base of natural logarithm
e_{ij}	Deviatoric strain tensor, cm/cm
F	Correction factor to correct for filter attenuation
\bar{G}^*	Complex modulus, dynes/cm sq
$G(t)$	Creep modulus, dynes/cm sq
H_o	Hammett and Deyrup acidity function
h	Height of fall, cm
J_e	Equilibrium compliance, cm sq/dyne
J_e^0	Equilibrium compliance of unfilled asphalt, cm sq/dyne
J_g	Glassy compliance, cm sq/dyne
J_i	Compliance of i^{th} spring, cm sq/dyne
$J(p)$	Transformed compliance
$J(t)$	Creep compliance, cm sq/dyne

$J^o(t)$	Creep compliance of unfilled bitumen, cm sq/dyne
\bar{J}^*	Complex compliance, cm sq/dyne
J'	Storage compliance, cm sq/dyne
J'_o	Storage compliance of unfilled bitumen, cm sq/dyne
J''	Loss compliance, cm sq/dyne
L	Length, cm
$L(\tau)$	Retardation function, cm sq/dyne
MC	Recorder sensitivity millivolts/division
m	Slope of $\log J(t)$ versus \log time plot
p	LaPlace transform parameter
R	Sensitivity of MTS output signal grams or inch/division
\bar{r}	Hydraulic radius of voids in dry packed powder, cm
s_{ij}	Deviatoric stress tensor, dynes/cm sq
T	Test temperature, degrees Kelvin or Centigrade
T_g	Glass transition temperature, degrees Centigrade
T_h	Thickness of sample (2 sides), inch
T_o	Reference temperature, 298 degrees Kelvin
T_s	Standard temperature as used in WLF equation
t	Time, seconds
t_u	Time of removal of step load, seconds
w	Mass, grams
X_o	Scale divisions, peak to peak X direction, Lissajous Pattern
x	Scale divisions in X direction at any time t
x_k	Scalar, distance in k direction
Y_o	Scale divisions, peak to peak, in Y direction, Lissajous Pattern

y	Scale divisions in Y direction at any time t
γ	Strain, cm/cm
γ_o	Peak to peak strain, cm/cm
$\dot{\gamma}$	Shear strain rate, cm/cm-sec
δ	Phase angle as strain lags stress, radians
ϵ	Porosity, volume of voids divided by total volume
η	Coefficient of steady state (newtonian) viscosity, dyne-sec/cm sq
η_o	Steady state viscosity of unfilled asphalt, dyne-sec/cm sq
η_{rel}	Ratio of mixture viscosity to bitumen viscosity
θ	Variable of integration representing time, seconds
ν	Poisson's ratio
ρ	Density of bitumen at any temperature, T , grams/cm ³
ρ_o	Density of bitumen at reference temperature, T_o , grams/cm ³
ρ_p	Density of powder, grams/cm ³
σ	Stress, dyne/cm sq
σ_o	Step stress, or peak to peak sinusoidal stress, dynes/cm sq
τ	Retardation time, seconds
τ_i	Retardation time of i^{th} element, seconds
ω	Frequency, radians/second

ABSTRACT

Anderson, David Albert. Ph.D., Purdue University, January 1971. Mechanical Behavior of Asphalt-Mineral Powder Composites and Asphalt-Mineral Interaction. Major Professor: William H. Goetz.

This study was initiated in order to study the extent and nature of the interfacial interaction between mineral aggregate and bitumen. Ideally, such a study should include a direct observation of the mineral-bitumen interface. From a technical standpoint, however, such an observation is very difficult. Instead, an indirect approach was taken by choosing a system wherein a varying amount of surface (interfacial) area could be generated. Several well defined mineral powders of differing size (surface area) were added to two different bitumens. The stress-strain behavior of these composites was then determined and compared for evidence of interfacial interaction.

Six different minerals (calcite, quartz, apatite, bytownite, magnesite and microcline) were dry ground to a fine powder and then separated into varying size fractions in different aqueous solutions according to Stokes' law.

Size measurements were determined from air permeability data and from adsorption (N_2 , BET) and the scanning electron microscope. The measured "size" from the different methods was found in good agreement. The scanning electron microscope showed the fractions to be well separated and of similar physical appearance.

The powders were mixed with two different asphalt cements (AC-20 grade) using a specially designed vacuum mixing apparatus. The vacuum mixing was necessary in order to achieve a homogeneous, air free mixture.

In order to determine the stress-strain relation for the various composites and unfilled asphalts, the sample to be tested was mounted as a pair of thin discs sandwiched between three steel plates. A dynamic or static shear stress was then imparted to the sample by shearing the center plate with respect to the two outer plates. Tests were performed at 5, 15 and 25 C and at frequencies from 0.053 to 50.3 Hertz and up to 120 seconds in creep. The testing was limited to linear behavior (strains of a few per cent or less).

Linear viscoelastic behavior was verified in the dynamic measurements by the independence of compliance on stress level and by the sinusoidal response to a sinusoidal input. No thixotropic effect was noticed: steady state response (dynamic) was attained after only a few cycles. Linear viscoelastic behavior in creep was verified by the independence of compliance on stress level and by the additivity of stress history (Boltzmann superposition principle).

Dilatometric glass transition temperature measurements were obtained on the filled and unfilled asphalts.

With verification of linear viscoelastic behavior, the creep and dynamic compliances were found interconvertible and thermorheologically simple. The same shift function characterized both the loss and storage compliance and the creep compliance. The form of the shift function was compatible with the WLF equation but $T_s - T_g$ was found

dependent on asphalt type and independent of the presence of filler.

In contrast to values estimated from the WLF equation, dilatometrically determined values of T_g were dependent on filler properties.

Using the established linear viscoelastic characterization as a medium of comparison, the minerals were found to interact with the asphalt but to a varying degree depending on powder size and type and the asphalt type. Whereas the classical equations adequately predict the stiffening effect of the filler over the entire range of measured compliance from the mixtures for the one asphalt (B3603), they are valid only for the short-term compliances for the second asphalt (B3056). At longer times and higher temperatures where the flow term, t/η , predominates the interaction of the filler becomes apparent, resulting in a "stiffening" of the response that increases with increasing surface area.

INTRODUCTION

This study was initiated in order to examine the extent and nature of the interfacial interaction between mineral aggregate and bitumen. The common practice with bituminous paving mixtures is to design on the basis of properties measured on bulk bitumen. This implies that the bulk properties are valid indicators of the properties of the bitumen as it exists in the mixture and that there is a lack of bitumen-mineral interaction. It is possible that the presence of an interfacial interaction may have an important effect on the various mechanical properties such as the viscoelastic moduli, failure (fracture) parameters, etc.

Scope

Ideally, a study of interfacial interaction should include a direct observation of the interface. Technically this is a difficult task. Instead, for this study, an indirect observation was made by choosing a system wherein a large amount of specific surface (interfacial area) could be generated. Several well defined mineral powders of differing size (and specific surface) were added to two different bitumens to give various mineral powder-bitumen composites. The stress-strain behavior of these composites was then determined and compared for evidence of bitumen-mineral interaction.

The composites were, in essence, well-defined mixtures of bitumen and mineral filler where mineral filler is loosely defined as any mineral matter a certain percentage of which will pass a 200 mesh sieve.⁽¹⁾ In bituminous paving mixtures, this is the material that forms the binder for the coarser aggregate framework. Therefore, in the process of evaluating the extent and nature of the interaction between mineral and bitumen a comprehensive evaluation of the stress-strain behavior of the mineral filler-bitumen system was obtained.

Background

Bituminous concretes are mixtures of three components: mineral aggregate, bitumen, and air. The proportion of each component and the gradation of the aggregate is generally determined by one of several mixture design methods.⁽¹⁾ Additional constraints are generally placed on the individual components in terms of bitumen consistency and aggregate characteristics.

In the usual dense-graded bituminous concrete the aggregate portion is well graded from the coarsest size down to the 200 mesh size (74 μ m). The intent of the close gradation is to build an aggregate framework with maximum particle contact wherein each subsequent size just fills the voids of the larger size.⁽²⁾

Typically, the minus 200 material may be 5 per cent of the total mixture volume and the bitumen 13 per cent. Allowing some of the bitumen to be adsorbed or otherwise trapped in the plus 200 fraction, a minus 200-bitumen ratio as high as 40-60, by volume, is very realistic. At a 40-60 ratio the mineral is floating in the bitumen and particle-

particle contact between the aggregate particles no longer predominates. The 40 value represents a solids concentration less than that at densest packing. (3,4)

Under these conditions, the mixture consistency is controlled by the volume filling and physico-chemical reinforcing of the filler rather than by the nature of the Mineral to mineral contact. This is in contrast to the behavior of the overall mixture where a significant contribution to the load-deformation behavior is made by the nature of the binder as well as by the nature of the particle-particle contact. (5,6)

It is customary to specify a range of consistency for the bitumen used in bituminous concrete. To assume that this in turn specifies a similar range of consistency in the filler-bitumen matrix of the bituminous concrete implies that the consistency of the bitumen in the matrix is uninfluenced by the nature of the filler. In other words, the tacit assumption in customary usage is that the bulk bitumen consistency is a valid predictor of the bitumen when incorporated into the matrix, regardless of the filler properties, and that there is an absence of interaction between the bitumen and the filler.

Review of Literature

Different filler-bitumen systems have been reported on in the literature, both as separate systems and as incorporated into bituminous concrete. Perhaps one of the earliest references is to the work of Clifford Richardson. (7) He postulated that the function of the filler was more than mere void filling, implying that some sort of physical-chemical phenomenon was operative. Richardson reported that silica,

limestone, and portland cement made successively better fillers as they adsorbed a correspondingly thicker film of bitumen. When supplied as commercial fillers, silica, limestone, and portland cement is a very likely order of increasing fineness.

By the late 1930's many studies on the bitumen-mineral filler system had been completed in an attempt to characterize fillers with respect to their potential for stiffening the system. Traxler ⁽⁸⁾ reported on a series of extensive investigations in which the findings were, essentially, (a) that the relative viscosity (η_{rel} , defined as mixture viscosity divided by viscosity of the bitumen at zero solids concentration) for varying filler concentrations, C_v , was independent of the nature and consistency of the suspending medium, (b) that the stiffening effect of the filler could not always be adequately predicted by the per cent voids in the dry compacted filler, and (c) that only by mixing the filler and bitumen and testing it could a reliable prediction of the ensuing stiffening be made. Traxler considered size and size distribution as the fundamental filler parameters in that they affect the void content and average void diameter of packed powders. More recent articles by Traxler are in essential agreement with the earlier findings. ⁽⁹⁾

Mitchell and Lee ⁽¹⁰⁾ also conducted research in an attempt to find a parameter that would adequately predict the ability of a mineral filler to reinforce the bitumen to which it is added. Their data were taken for relatively small solid concentrations and indicated that the bulk settled volume of filler in benzene is a good predictor of the

reinforcement to be expected. The actual experiment consisted of allowing different fillers to settle in benzene and adding equal bulk settled volumes of different fillers to a constant volume of asphalt: it was found that for small filler-bitumen ratios equal settled volumes gave equivalent reinforcement (η_{rel}). It has been demonstrated by others that the settled volume in benzene is directly related to fineness.

A very extensive series of experiments on mineral fillers and mineral filler-bitumen composites has been reported by Rigden.⁽¹¹⁾ His viscosity data were collected from experiments using both a Couette viscosimeter and a uniaxial tension test (on the more viscous material). Surface area, settled volume in benzene, and permeability measurements (of dry packed powder) were made.

At the higher volume concentrations no valid correlation between any of the primary physical properties of the powders and η_{rel} was found, nor did the settled bulk volume in benzene provide a valid correlation. By measuring the average hydraulic radius of the voids in the dry packed powder, \bar{r} , an improved correlation was possible by plotting $\log \eta_{rel}$ vs $c_v \sqrt{\frac{1}{\bar{r}}}$. However, there were still deviations of over an order of magnitude in η_{rel} in this correlation. Rigden calculated η_{rel} for the different systems at the arbitrary shear stress of 6×10^4 dynes/cm sq. One of his figures suggests strains of 30 per cent in the testing, hardly a small strain.

According to the data presented by Rigden, at the higher filler concentrations, both the temperature susceptibility and the degree of complex flow are functions of the volume concentration.

More recently Winniford ⁽¹²⁾ has used the sliding plate micro-viscosimeter to study filler-bitumen systems. Several different viscosity increasing mechanisms were postulated by Winniford: in addition to the mechanism provided by volume filling, they were, (a) gelation of the asphalt by the surface with attendant non-newtonian flow and lowered temperature susceptibility, (b) formation of thick viscous coatings which increased the effective solids concentration and (c) surface shielding by adsorbed asphaltenes.

Steady state viscosity values were obtained on fillers of differing size but of the same mineral type. Roughly it was shown that reinforcement was more pronounced with the smaller sized material: two 10 μm and 25 μm CaCO_3 fillers gave essentially the same η_{rel} but this was not true of the more finely divided fillers.

Winniford also compared a surface-treated filler to an untreated filler. By treating the silica surfaces with dichlorodimethylsilane the relative viscosity of the systems was increased. The surface treatment was interpreted as disallowing an adsorbed layer of "asphaltic material" which, when present, shields the particles, lowering the interparticle van der Waals forces. Calcium carbonate was considered to strongly adsorb asphaltenes and in the process significantly increase its effective volume concentration.

Warden, et al. ⁽¹³⁾ presented data on filler-bitumen systems in conjunction with field observations. These authors, motivated by field failures which they attributed to filler type, sought an easily measurable parameter that would predict the performance of the filler in the pavement. The tests performed on the fillers were empirical tests

currently in vogue in asphalt technology. A re-examination of the early work by Traxler proved once again inconclusive in that no one single parameter was capable of predicting the reinforcement to be expected from a given mineral filler. The softening point of the filler systems was found to be quite critical to filler type.

Recently Tunnicliff has written a review paper on the subject of mineral fillers.⁽¹⁴⁾ A substantial portion of his paper is devoted to a definition of mineral filler; it is his desire to define the filler as that part of the fine aggregate that acts as though it is a "part of the binder." It is suggested that the influence of the surface may be extended into the bitumen through a surface energy gradient. A later paper by Tunnicliff⁽¹⁵⁾ contains another review and again concludes that the filler should be defined as that material suspended in the asphalt. These two papers by Tunnicliff contain a comprehensive listing of references on mineral fillers.

Much of the work reported in the literature for filler-bitumen systems has been done by comparing steady state viscosity measurements of the filled system to those of the original unfilled bitumen (η_{rel}). This steady state viscosity is usually determined by applying a load to the sample in question and waiting for the resulting displacement versus time plot to become linear. The stress divided by the slope of this plot is then given as the coefficient of viscosity.⁽¹⁶⁾ Because most bitumens at their service temperatures exhibit elastic effects that retard the viscous flow mechanism, it is necessary to pursue large strains before viscous flow is approached. In addition,

because the approach to linearity is exponential, it is very difficult to be certain exactly when the steady state situation has been obtained.

Even if it were possible to easily define a steady state condition, the η_{rel} approach cannot account for elastic effects: additional parameters are needed to characterize short term behavior. Except for perhaps long-term creep, the elastic effects are important in determining the response of the material in time and temperature regions often encountered in the pavement system. The use of η_{rel} by itself appears to be of useful but limited value and a more comprehensive characterization of the mineral filler-bitumen system is needed.

Statement of Problem

In light of the foregoing remarks, it was decided that, for two different reasons, additional research on the nature of the composite produced by the addition of finely divided mineral powder to asphalt was justified. These two different reasons are:

1. Adequate characterization of mechanical behavior.

Previous characterization of mineral powder-asphalt composites have been based on η_{rel} determinations at necessarily large strains. This is inadequate to characterize the composites over the time, temperature, and strain ranges encountered in the pavement.

For the present study, it was decided to test the validity of a linear viscoelastic (LVE) characterization. Different mineral powder-asphalt composites were prepared and tested in dynamic and creep shear and the

various criteria for a LVE material were then applied.

2. Interaction between mineral surface and asphalt. Having established a means for adequately characterizing the mineral powder-asphalt composite over a wide range of the time-temperature spectrum, it was felt that the different composites should provide a good expedient for establishing the presence and or extent of any interfacial interaction between the mineral and asphalt. To the extent that the interactions were surface phenomena the effect of their presence, for a given mineralogical composition, should be a function of the surface area (size) of the powder comprising the composite. Therefore, it was decided to prepare different powders of different size fractions and different mineralogical compositions. Two different asphalts were used to give a range in asphalt composition.

In summary, the purpose of this work was to first establish a method of characterizing the mechanical behavior of a mineral powder-asphalt composite and then to use that characterization to establish the presence and or nature and extent of the interaction between the mineral surface and bitumen.

In the sections that follow, the preparation of the various powders and their characterization are described in detail. The asphalt and the means of mixing it with the mineral is described next, followed by a description of the various tests used to characterize the mechanical behavior of the composites.

MATERIALS AND SAMPLE PREPARATION

Previous work on filled bituminous systems has, for the most part been done with commercially used fillers. Such materials have included crusher dust, silt, flyash and so forth. These materials are by nature ill defined, both in terms of mineralogical composition and particle size distribution. The series of mineral powders used in this study were carefully prepared and specifically sized. They are described in detail below.

Two different asphalts as supplied by the Bureau of Public Roads were mixed with the powders using a specially developed mixing procedure.

Mineral Powders - Selection and Preparation

In the present work six different minerals were selected for use and prepared to give a well-defined size character. Quartz and calcite were used in the bulk of the work because they were readily available in pure form and are generally considered to represent the range of materials between acidic and basic used as fillers in bituminous mixtures. The other materials used were microcline, bytownite, magnesite, and apatite. A summary of the source of each mineral is given in Table 1.

An x-ray diffraction pattern was determined for each of the finely divided mineral powders. Each powder produced a pattern in keeping

Table 1
Description of Minerals

Mineral	Density*	Supplier, Source and Form
Quartz	2.65	Sil-co-sil. Finely divided Ottawa Sand, Ottawa, Ill.
Calcite	2.72	Naturally occurring crystals, collected at France Stone Co., Logansport, Ind.
Apatite	3.18	Ward's Natural Science Estab. Inc. Ontario, Canada Translucent green single crystals
Bytownite	2.74	Ward's Natural Science Estab. Inc. Crystal Bay, Minnesota Massive translucent grayish green crystals
Magnesite	3.04	Ward's Natural Science Estab. Inc. Chewaleh, Washington White mass of fine crystals
Microcline	2.55	Ward's Natural Science Estab. Inc. Parry Sound Ontario Massive pink crystals

*From reference (17).

with its description and no unexplained peaks were found.

All the mineral powders, except the quartz, were prepared by first crushing the original crystal fragments to a fine sand size. This material was then ground in a ball mill until the majority of it passed the 400 mesh sieve. The quartz was obtained as a powder but required considerable grinding before the majority of it would pass the 400 mesh sieve. The crushing and grinding process is described in Appendix A.

After grinding, each powder was fractionated into several different fractions by allowing very dilute suspensions of the powders to sediment for various periods of time. A detailed description of this procedure is also given in Appendix A. The different sized powders that were prepared and used are listed in Table 2. The size given is a nominal value according to time of sedimentation.

Mineral Powders - Characterization

The nominal size determined from a sedimentation process must be used with caution because of the many assumptions made for the process. (18) This is particularly true with the smaller sized particles. With this in mind alternative methods for characterizing particle size were used.

It should be noted that an accurate determination of particle shape and size is a complete study in itself and that much research has been done on this topic. (19,20) In such a study the first problem is an exact definition of size. This may be the extreme length of a particle, the diameter of the smallest enclosing circle, the smallest square the particle will pass through (sieve), and a whole host of others.

Table 2. Properties of Specially Prepared Finely Divided Mineral Powders

Material	Sedimentation Size, μm	Porosity		From Air Permeability		N_2 Sorption Surface Area, sq m/gram
		10 blows at 100 grams	20 blows at 100 grams	Size, μm	Surface area, sq m/gram	
Quartz	10-20	0.53	0.51	7.3	0.31	
	2.5-5.0	0.53	0.51	2.1	1.1	1.5
	0.63-1.25	0.55	0.54	.59	3.8	4.4
	XFDG*	0.43	0.41	1.8	1.2	
Calcite	10-20	0.52	0.51	6.9	0.32	
	2.5-5.0	0.51	0.51	2.1	1.1	
	0.63-1.25	0.48	0.47	1.4	1.6	2.4
	XFDG*	0.35	0.34	3.0	0.74	
Apatite	< 2.5	0.52	0.51	0.53	3.6	
Eytownite	< 2.5	0.54	0.53	0.60	3.6	
Magnesite	< 2.5	0.55	0.54	0.61	3.2	
Microcline	< 2.5	0.53	0.51	0.60	3.9	

*XFDG was a graded material, ground to size, no sedimentation used.

Secondly there is the matter of defining shape and again there are a multitude of definitions. Finally, in order that the measurements be truly representative, statistical methods must be applied. This elaborate procedure was considered unnecessary in the present work.

Air Permeability and Nitrogen Adsorption Measurements

As an alternative size measurement, air permeability measurements were made on packed beds of each of the powders. This technique for determining surface area and particle size is well documented and accepted.⁽²⁰⁻²⁴⁾ Particle sizes determined by this technique generally agree quite well with determinations from other methods.

The air permeability method is based on a relationship between particle size and the rate of flow of a fluid (gas or liquid) through a packed bed of the powder. The equations used are derived from Poiseulles' Law, assuming that the packed bed consists of a large number of parallel flow paths. The particle size is then related to the hydraulic radius of the flow path.

Unfortunately, the actual flow mechanism is more complicated than assumed by Poiseulles' Law. As the particle diameter gets less than about 5 micrometers, the mean free path of the gas molecules becomes large compared to the pore radius and the flow is not purely viscous. Instead the gas is considered, to a degree, to "slip" through the pores, hence the terminology "slip flow". The complete consideration of this phenomenon is long and cumbersome and is reviewed in the literature.^(21, 22, 23)

The experimental procedure used was that of Kamak.⁽²⁴⁾ A schematic of the equipment used is shown in Figures 1 through 3. The measurement procedure is to first displace (suck) the fluid up one side of the manometer U tube to just beyond the timing marks, Figure 1. The sample cup, Figure 2, with its precompacted sample is then put in place and the fluid released. The head of pressure drives the entrapped air through the sample and the time required for the fluid to fall a given height is recorded. With several apparatus constants, the rate of flow, hydraulic radius, particle size, and, in turn, surface area can be calculated.

In order to accomodate the range in power sizes, four different combinations of manometer fluid and monometer U tube diameter were used:

1. dibutylphthlate, 0.500 inch I D,
2. dibutylphthlate, 0.250 inch I D,
3. mercury, 0.250 inch I D,
4. mercury, 0.125 inch I D.

The procedure for compacting the powders in the sample cup was as follows: the cup was first placed on a large block of steel and a single layer of wiping tissue (Kimberly-Clark, "Kimwipe") was placed in the cup bottom. Sufficient powder to give a compacted bed about 0.5 cm thick was then placed in the cup, followed by another tissue and a snug fitting perforated teflon disc. The entire assembly was then compacted using a drop weight compaction hammer. The hammer weight and fall height were kept constant at 100 grams and 3 centimeters.

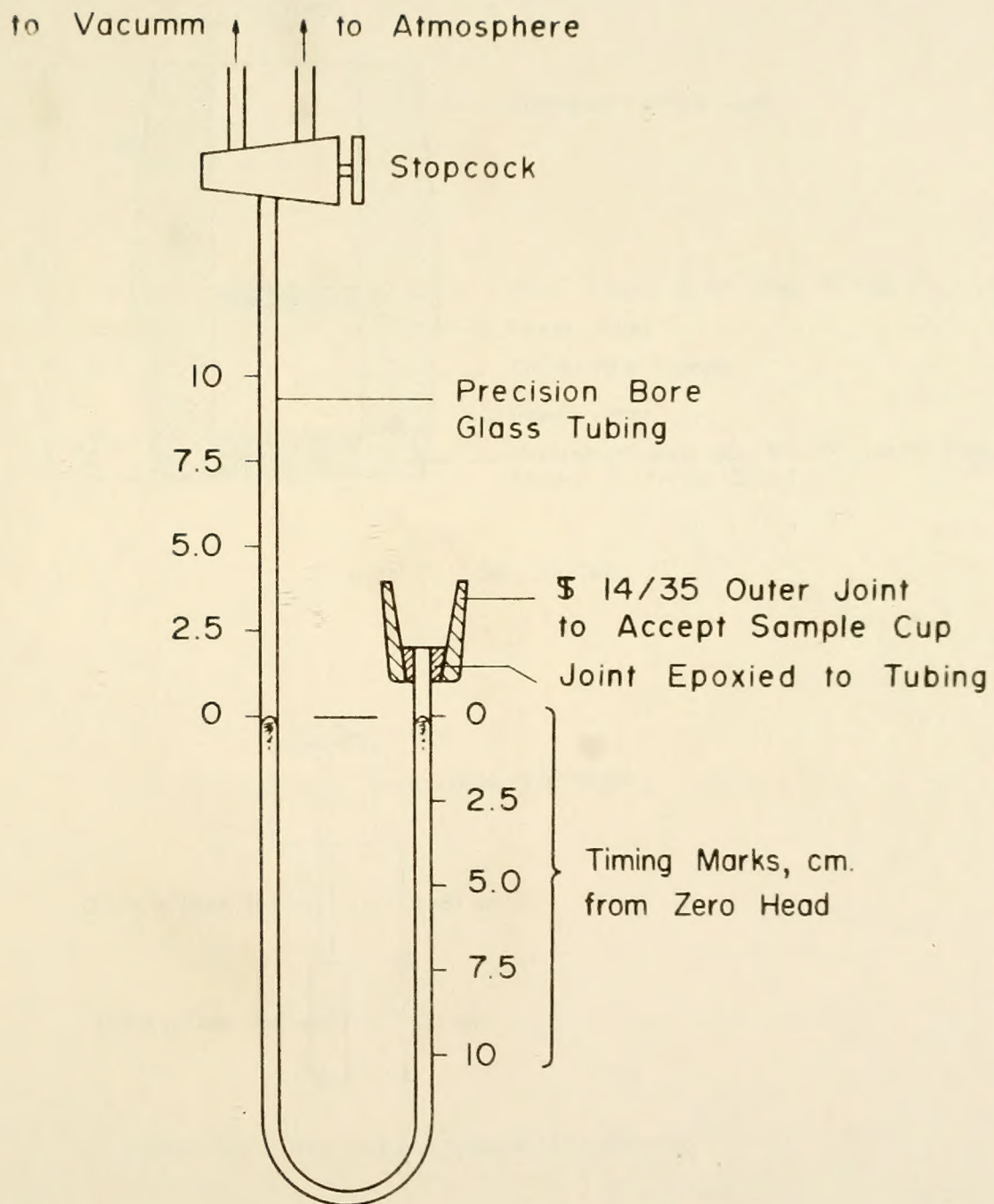


Figure 1. Schematic of Air Permeability Manometer

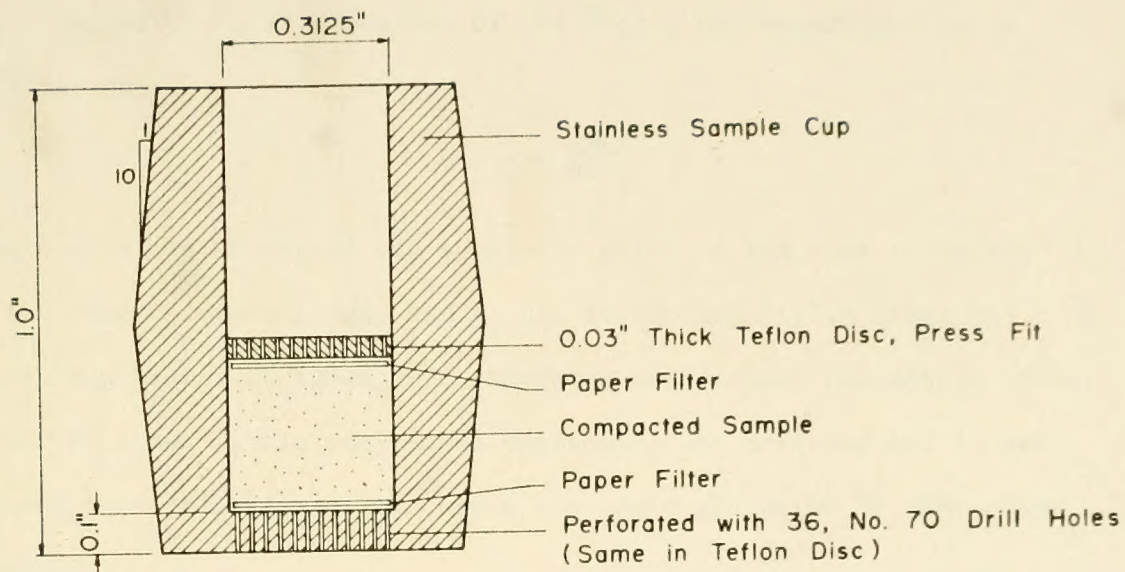


Figure 2. Sample Cup

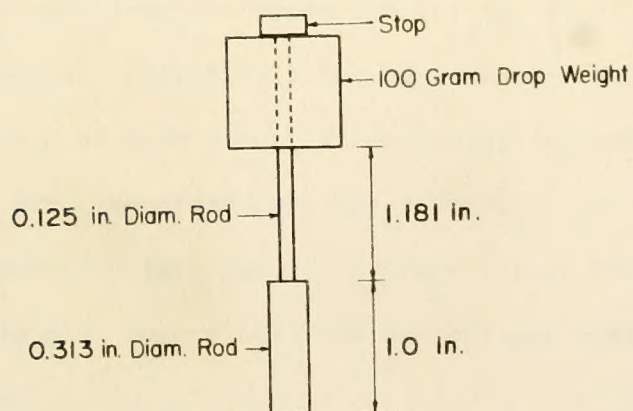


Figure 3. Drop Weight Compacting Device

Varying degrees of compaction were produced by varying the number of hammer blows. In this way, beds of differing porosity were prepared.

Porosity, ϵ , is a measure of the degree of compaction and is defined as:

$$\epsilon = 1 - \frac{m}{AL\rho_p}$$

where m is the weight of the sample in grams, A the area in cm sq, L the sample length in cm, and ρ_p the powder density in grams/cm³. By trial and error, 20 blows were chosen as the maximum compactive effort. After 20 blows little additional compaction was achieved and it was feared that additional blows would produce degradation of the powder particles.

Values of surface area and particle size were calculated according to the equations derived by Kamak.⁽²⁴⁾ The calculated values were found to be independent of the head of fluid in the manometer (i.e., the pressure gradient producing the gas flow) over the range 5 to 20 centimeters. Essentially the same surface area and particle size were calculated at each porosity (degree of compaction). The reported values are, therefore, average values for several different porosities and monometer fluid heads. Average values for surface area and particle size determined from the air permeability data are given in Table 2.

As a check on the surface area values calculated from the air permeability measurements, several surface area values were determined from nitrogen adsorption. A commercial instrument made by the American Instrument Company was used for this purpose. The treatment of data from this equipment is in accordance with the usual BET theory.⁽²⁵⁾

The values calculated from measurements taken with this instrument are given in Table 2. In each case the values are greater than those measured by the air permeability method. This is as expected due to the nature of the measurement. The permeability measurement considers the streamlined flow path around the particle while the gas adsorption measurement is based on the gas adsorbed on the entire surface and in particle interstices. The agreement between the air permeability and nitrogen measurements is considered good.

Scanning Electron Microscope

In order to compare the physical appearance of the individual powder particles a scanning electron photomicrograph was obtained from a sample of each of the powders. The photomicrograph samples were prepared by dusting the powder onto a wet plastic film and gently blowing the excess powder off after the plastic had dried. A typical photomicrograph for each of the powders is given in Figures 4 through 15.

Particle sizes scaled from the photomicrographs agree quite well with the air permeability data of Table 2 and are quite consistent with the relative fineness of the different powders. Looking at Figures 4, 5, and 8 through 11, the one-sized nature of the various size fractions is quite apparent. The 0.63-1.25 μm calcite is definitely larger in size than the 0.63-1.25 μm quartz. This is consistent with the air permeability data. (Recall that the 0.63-1.25 is a nominal designation according to time of sedimentation.) In addition, Figure 11 shows some contamination from larger particles while the quartz is quite clean.

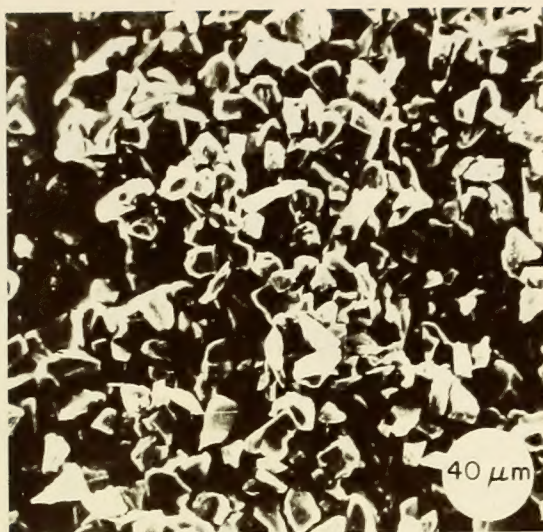


Figure 4. Scanning Electron
Photomicrograph, 10-20 μm
Quartz, 300x.



Figure 5. Scanning Electron
Photomicrograph, 10-20 μm
Calcite, 300x.



Figure 6. Scanning Electron
Photomicrograph, 10-20 μm
Quartz, 3000x.

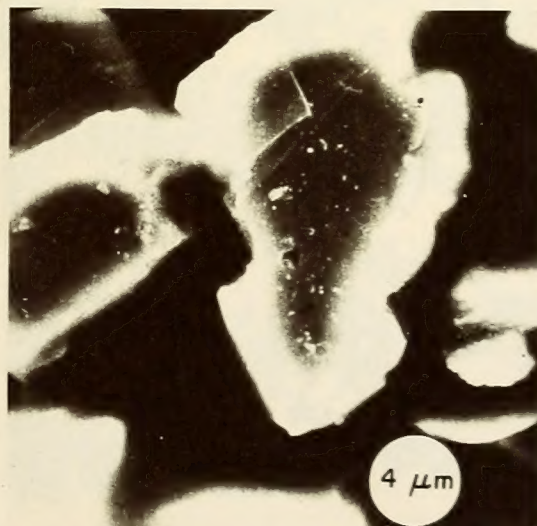


Figure 7. Scanning Electron
Photomicrograph, 10-20 μm
Calcite, 3000x.

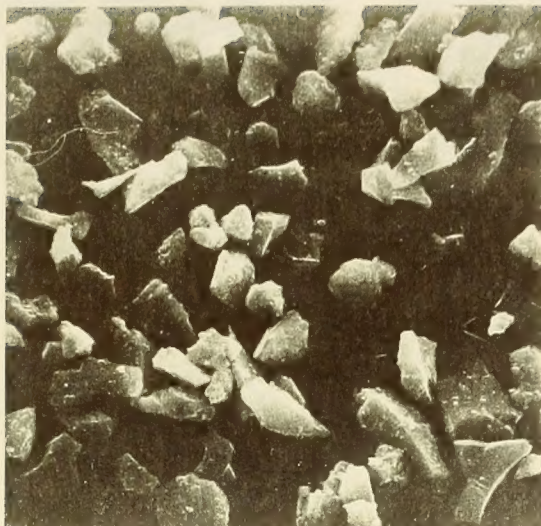


Figure 8. Scanning Electron
Photomicrograph, 2.5-5.0 μm
Quartz, 1500x.

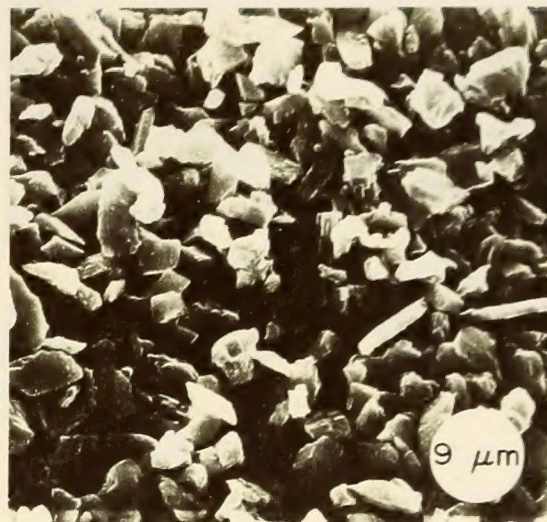


Figure 9. Scanning Electron
Photomicrograph, 2.5-5.0 μm
Calcite, 1300x.



Figure 10. Scanning Electron
Photomicrograph, 0.63-1.25 μm
Quartz, 1000x.

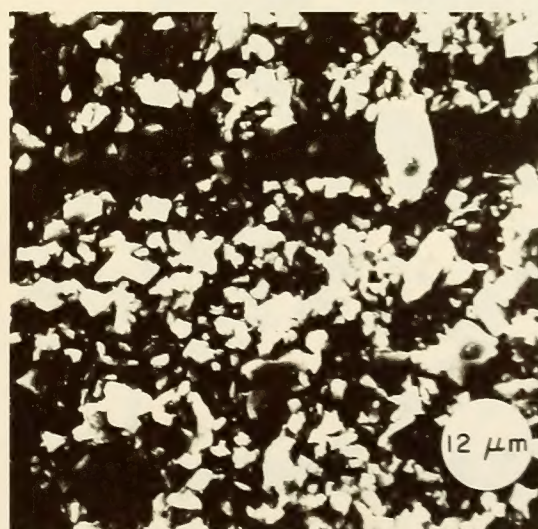


Figure 11. Scanning Electron
Photomicrograph, 0.63-1.25 μm
Calcite, 1000x.

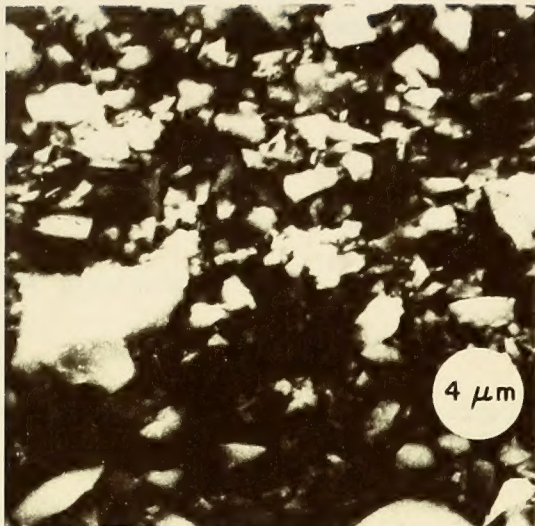


Figure 12. Scanning Electron Photomicrograph, < 2.5 μm Apatite, 3000x.

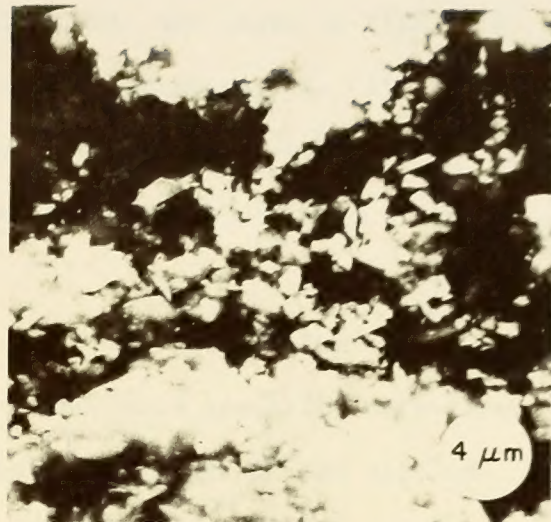


Figure 13. Scanning Electron Photomicrograph, < 2.5 μm Bytownite, 3000x.

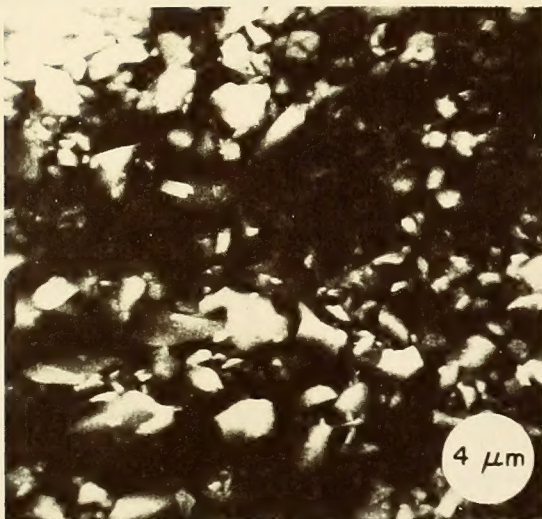


Figure 14. Scanning Electron Photomicrograph, < 2.5 μm Magnesite, 3000x.

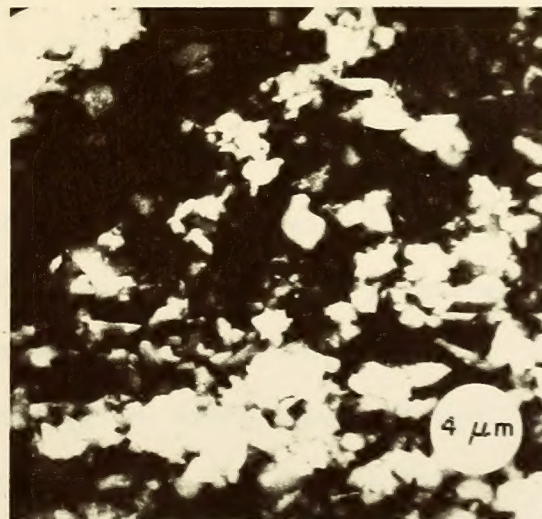


Figure 15. Scanning Electron Photomicrograph, < 2.5 μm Microcline, 3000x.

Enlarged particles of quartz and calcite are shown in Figures 6 and 7. Each has a small degree of surface contamination. It is uncertain what this material is or how strongly it is bound to the surface. It is assumed that it is parent material, abraded during the grinding process.

All the materials are certainly angular. The calcite tends toward a blocky character with a rectangular appearance appearing more often than the anticipated rhombohedral shape. The edges on the calcite appear a bit more dulled than on the other materials although this may be an artifact produced in the process of generating the picture. In general the individual particles are angular and show their length on one axis to be slightly longer than on the other, but this is a mild effect and certainly the particles cannot be classified as strongly elongated.

Physico-Chemical Surface Properties

A literature search was made for techniques applicable to this study that would adequately characterize physico-chemical surface properties of the various powders. Unfortunately this is a relatively little studied area and the literature search was unproductive. The problem is additionally complicated because the exact nature of the components in the bitumen is uncertain and little insight can be gained into exactly what surface properties should be measured.

Consideration was given to measuring the preferential adsorption from the bitumen onto the mineral surface. Because of the high viscosity of the bitumen, the bitumen must be dissolved in a solvent

in order to recover the mineral powder. The effect of the solvent on the bitumen is uncertain and makes the results very questionable as they relate to adsorption in the absence of the solvent.⁽²⁶⁾

Additionally, most of the work done in this area has been done with aqueous solutions and the principles, theories, and techniques are not generally valid for the adsorption from non-electrolytes.⁽²⁷⁾

One rather straightforward technique for characterizing the surface acidity of powders was suggested. In this technique, a series of indicators, called Hammett indicators,⁽²⁸⁾ are dissolved in a suitable solvent (benzene) and allowed to come in contact with the powder. To the extent that there are acid sites on the surface, the adsorbed indicator is converted from the neutral base to its conjugate acid with a resulting color change. The surface acid strength of a powder measured by this technique is defined as the proton donating ability of the surface (Bronsted acid). The various indicators have been chosen by the previous investigators so that their acid forms will not be masked by the basic form. In this way, only a small fraction of the surface need contribute to the classification.

The usual series of indicators were purchased from the Aldrich Chemical Company and additional indicators prepared as described by Benesi.⁽²⁹⁾ A list of the results for the powders used is given in Table 3 where H_0 is the Hammett and Deyrup acidity function.

As a check the indicators were referenced to one of the clays (clay Spur, Wyoming bentonite) described in the paper by Benesi. The color changes found in the laboratory were identical to those reported in his paper. Benesi cited a range of + 4.0 to + 6.8 for silica gel,

attributing this to silicic acid groups on the surface. This is the range reported for the quartz in Table 3. No adsorption was found for the calcite powders.

Summary

One of the necessary steps in this study was the preparation of a series of closely sized powders with similar physical properties but of dissimilar mineralogical composition. A close look at the SEM photomicrographs and the data of Table 2 shows that this has been accomplished for the quartz and the calcite material, and for the apatite, bytownite, magnesite, and microcline. The sized fractions are exceptionally clean in terms of contamination from fine, adhered particles, and the "cuts" are very sharp.

As was expected, the nominal sedimentation size did not agree exactly with the other size determinations. The air permeability data and the nitrogen sorption data show good agreement. The nitrogen surface area values are larger than those from permeability but to a degree that is not unexpected. Although there are an insufficient number of particles to do a statistical size and shape analysis in the SEM photomicrographs, the range of sizes that can be scaled from the photomicrographs agree quite well with those given in Table 2.

The porosity values given in Table 2 show a remarkable consistency. The sized materials all show porosities in the range 0.51 to 0.54 except for the calcite which has a value of 0.47. These data reflect the cleanliness of the cuts (lack of gradation) and a similarity in shape and texture. The 0.63 μm - 1.25 μm calcite shows some contamination

Table 3. Results of Surface Acidity Measurements

Material	H_o
Quartz	+ 4.0 to + 6.8
Calcite	no adsorption
Apatite	+ 4.0 to + 6.8
Eysowrite	+ 4.0 to + 6.8
Magnesite	+ 4.0 to + 6.8
Microcline	+ 4.0 to + 6.8

from coarse material (more graded), and this is reflected in the slightly lowered (0.47 from 0.51 to 0.54) porosity value. The two XFDG materials show a definitely lower porosity and this is attributed to the fact that they are graded materials.

A method of determining surface acidity is presented. A more comprehensive treatment of physico-chemical surface properties was desired but was found to be outside the resources of the researcher.

In summary it can be stated that:

1. The powder preparation has yielded a series of well-defined powders of similar shape and texture.
2. Porosity produced in the sized materials are uniform from 0.51 to 0.54. The effect of gradation is to decrease the voids.
3. Four different methods of determining size (sedimentation, air permeability, nitrogen adsorption and SEM photomicroscopy) all gave comparable results; any discrepancies are readily explainable.
4. A method of rating of surface acidity is given. All the materials were rated between + 4.0 and + 6.8 except the calcite for which there was no apparent adsorption. Most likely it lies outside the range of the indicators used.
5. A comprehensive description of the surface of mineral powders will require a close collaboration between the surface chemist and the asphalt

chemist. New techniques and measurements in both fields will probably be needed.

Description of Asphalts

The two different asphalts used in this study were AC-20 grade material furnished by Mr. James M. Rice of the Bureau of Public Roads, U. S. Department of Transportation. The two materials, designated B-3603 and B-3056, were from a group of study asphalts reported on at length in the literature.⁽³⁰⁻³²⁾

Viscosity data were obtained on the supplied material at 77 F and 275 F. These values are reported in Table 4 and agree quite well with values reported by other investigators.⁽³⁰⁾ At 77 F the B-3603 asphalt behaves as a newtonian fluid in the sliding plate microviscosimeter while the B-3056 asphalt is non-newtonian.

Table 4. Asphalt Properties

<u>Sample</u>	<u>B 3056</u>	<u>B 3603</u>
Viscosity, centistokes, 275 F	431	309
Viscosity, megapoises, 77 F, 0.05 sec ⁻¹	10.5	3.9
Penetration, 77 F, 100g, 5 sec	34	45
Ductility, 77 F, 5 cm/min	250 +	250 +

Preparation and Description of Powder-Asphalt Mixtures

A special technique was developed for mixing the asphalt and mineral powder. Initially, the materials were mixed by hand in a beaker immersed in a heated oil bath. The resulting mixes were not homogeneous. When the material was examined, after it had cooled, small pockets of uncoated powder were invariably found. This problem was solved by combining and mixing the two components in a closed system under vacuum. The equipment and mixing procedure is detailed in Appendix B. In this equipment, provision was made for preheating both powder and asphalt prior to combination and for the slow addition of the powder to the asphalt. Slow addition was necessary because the asphalt foamed excessively when the powder was dumped rapidly, in mass, into the asphalt.

After mixing, small discs of sample material were cast for later testing according to the procedure outlined in Appendix C. A visual observation of the interior of some of these sample discs showed them to be uniform. No signs that the powder had settled in the asphalt were observed; the appearance of the material at the top and bottom of the disc was similar.

It was anticipated that the vacuum process would have a measurable effect on the viscosity of the asphalt, especially in view of the fact that it was exposed not only to the heat and vacuum but to the stirring action as well. Viscosity data were obtained on asphalt sampled after ten and forty minutes in the mixing chamber. Within experimental error, no change in the 0.05 sec^{-1} viscosity value for

Table 5. Identification of Asphalt-Mineral Powder Composites

Sample Number	Asphalt Type	Powder Type	Powder Size, μm	Treatment
105	B3056	Calcite	10. - 20.	Mixed in vacuum
106	B3056	Quartz	2.5- 5.0	Mixed in vacuum
107	B3056	Quartz	10. - 20.	Mixed in vacuum
108	B3056	Calcite	2.5- 5.0	Mixed in vacuum
109	B3056	Calcite	XFDG*	Mixed in vacuum
116	B3056	None	---	None, as supplied
117	B3056	None	---	None, as supplied
118	B3056	None	---	Mixed in vacuum
119	B3056	Quartz	XFDG*	Mixed in vacuum
120	B3056	Quartz	2.5- 5.0	Mixed in air
121	B3056	Calcite	2.5- 5.0	Mixed in air
122	B3603	None	---	None, as supplied
123	B3603	None	---	Mixed in vacuum
124	B3603	Calcite	10. - 20.	Mixed in vacuum
125	B3603	Quartz	10. - 20.	Mixed in vacuum
126	B3056	Magnesite	< 2.5	Mixed in vacuum
127	B3056	Bytownite	< 2.5	Mixed in vacuum
128	B3056	Microcline	< 2.5	Mixed in vacuum
129	B3056	Apatite	< 2.5	Mixed in vacuum
130	B3603	Calcite	2.5- 5.0	Mixed in vacuum
131	B3603	Quartz	2.5- 5.0	Mixed in vacuum
132	B3056	Calcite	0.63- 1.25	Mixed in vacuum
133	B3056	Quartz	0.63- 1.25	Mixed in vacuum

*XFDG was a graded material, ground to size, no sedimentation used.

the B-3603 asphalt was observed. The coefficient of viscosity for B-3056 asphalt increased to 10.7 and 12.5 megapoises (from the original 10.5) after ten and forty minutes. The lack of a viscosity increase during the vacuum treatment was rather surprising but was later substantiated by a similar trend in the compliance data (compare samples 117 and 118, and 122 and 123, Appendices G and I). Perhaps this attests to the reported importance of the atmosphere in the aging process of bitumens. (33)

A list of the different samples that were prepared are given in Table 5. All the mixtures containing mineral powder were in the proportion 40 powder to 60 bitumen, by volume.

Each mixture received a sample number as described in Table 5. Note that samples 120 and 121 were not mixed under vacuum but were mixed in air. Five asphalt samples were tested without the addition of any mineral powder: samples 116, 117 and 122 were tested as supplied, without any vacuum treatment while samples 118 and 123 were placed under vacuum and mixed as though powder was being added.

CHARACTERIZATION OF MECHANICAL BEHAVIOR

The primary objective of material characterization is to establish the relationship between stress and strain. Two different groups of problems are recognized;⁽³⁴⁾ the prediction of strain from stress and, its inverse, the prediction of stress from strain. In this study a selected stress (both sinusoidal and quasi-static) was applied to the specimen and the resulting strain level observed. The functions relating strain to stress have units of cm^2/dyne and are commonly called compliances.

General

A number of different mathematical techniques are available for characterizing the stress-strain relation. The classical approach is to consider the material as composed of a number of linear springs and newtonian dashpots. When a single spring and dashpot are paired in parallel they are known as a Voigt model. The strain, $\gamma(t)$ resulting from a step stress, σ_0 , is given by:⁽³⁵⁾

$$\gamma(t) = \sigma_0 [J(1 - e^{-t/\tau})] \quad 1$$

where J is the compliance of the spring, t is time, and τ , the retardation time, is defined as equal to ηJ where η is the coefficient of viscosity of the dashpot. A single Voigt element is inadequate

THE HISTORY OF THE UNITED STATES

The history of the United States is a story of growth and development. It begins with the first settlers who came to the continent in search of a new life. They found a land of vast resources and a people who were determined to build a new nation. The story of the United States is a story of the struggle for freedom and the pursuit of the American dream. It is a story of the triumph of the human spirit over adversity and the power of unity in the face of challenge. The history of the United States is a story that continues to inspire and guide us today.

CHAPTER I

The first chapter of the history of the United States is the story of the early settlers. These brave men and women came to the continent in search of a new life. They found a land of vast resources and a people who were determined to build a new nation. The story of the United States is a story of the struggle for freedom and the pursuit of the American dream. It is a story of the triumph of the human spirit over adversity and the power of unity in the face of challenge. The history of the United States is a story that continues to inspire and guide us today.

CHAPTER II

The second chapter of the history of the United States is the story of the early years of the nation. This period was marked by the struggle for independence and the establishment of the new government. The story of the United States is a story of the struggle for freedom and the pursuit of the American dream. It is a story of the triumph of the human spirit over adversity and the power of unity in the face of challenge. The history of the United States is a story that continues to inspire and guide us today.

to describe real materials and is therefore expanded to an infinite number of elements arranged in series,

$$\gamma(t) = \sigma_0 \sum_{i=1}^{\infty} J_i (1 - e^{-t/\tau_i}) \quad 2$$

The application of a step load to a real material can produce an instantaneous strain and a steady state flow. To account for this, Equation 2 is modified to include J_g and t/η ,

$$\gamma(t) = \sigma_0 [J_g + \sum_{i=1}^{\infty} J_i (1 - e^{-t/\tau_i}) + t/\eta] \quad 3$$

where J_g represents the instantaneous or glassy response and η is the steady state coefficient of viscosity. The summation term represents the contribution to the strain by a discrete spectrum of retardation times τ_i . This can be replaced by a continuous spectra where

$$\gamma(t) = \sigma_0 [J_g + \int_{-\infty}^{+\infty} L(\tau) (1 - e^{-t/\tau}) d \ln \tau + t/\eta] \quad 4$$

The function $L(\tau)$ has the nature of a distribution function such that $L(\tau) d \ln \tau$ represents the contribution to compliance between $\ln \tau$ and $\ln \tau + d \ln \tau$. The retardation spectrum, $L(\tau)$, can be inferred from a phenomenological consideration of material behavior without recourse to models.⁽³⁵⁾ Although $L(\tau)$ is not commonly used in direct calculations, it is useful in phenomenological considerations and for interrelating the different forms of the viscoelastic function.

A detailed mathematical consideration of the various viscoelastic functions, their interconvertibility and application, is beyond the scope of this paper. The mathematical theory of viscoelasticity is considered at length by such authors as Ferry, Gross, Bland, Lee and Schapery.⁽³⁵⁻³⁹⁾

Other representations than those developed from the traditional spring-dashpot analogy of viscoelastic behavior are also possible. For example, by observing that over a part of its range the retardation spectrum may be represented by a power law, a considerable simplification of the viscoelastic functions is possible. Alternatively a series of exponentials may be used to describe the experimental data,^(39, 40) or the data may be described in linear differential operator form in which the various constants are obtained from curve fitting techniques.

Taking LaPlace transforms of the operator form,⁽⁴¹⁾ expressions such as

$$2\bar{e}_{ij}(X_{K,p}) = J(p) \bar{s}_{ij}(X_{K,p}) \quad 5$$

may be developed. Equation 5 reveals the analogy between elastic behavior and viscoelastic behavior in the transform plane where \bar{e}_{ij} and \bar{s}_{ij} are the p transformed deviatoric strain and stress respectively and $J(p)$ is the transformed compliance. $J(p)$ is defined by the ratio of the transformed strain and stress when the stress is a unit step function. With $J(p)$ defined, the strain response to any arbitrary load may be calculated by inverting Equation 5.

A continuum mechanics representation of the relation between stress and strain may be given as⁽⁴²⁾

$$\gamma_{ij}(x,t) = \int_{-\infty}^t J_{ijkl}(x,t-\theta) \frac{\partial \sigma_{k,l}(x,\theta)}{\partial \theta} d\theta \quad 6$$

where $\gamma_{ij}(x,t)$ is the strain as a function of position, x , and time, t , and θ is a time variable.

In the work to follow, the materials are assumed homogeneous and isotropic. This reduces the characterization functions of Equation 6 to two variables that can be written as $J(t)$ and $\nu(t)$ when ν is Poisson's ratio. It is further assumed that the bulk modulus is large relative to the shear modulus which is equivalent to assuming $\nu(t) = 0.5$.⁽¹¹⁾

Several considerations make the use of the LVE representation desirable. If a satisfactory form can be found for the various visco-elastic moduli they can be used to solve boundary value problems using the methods of solid mechanics. A good deal of work is reported in the literature on both the manipulation and interconvertability of the moduli and their use in boundary value problems. The LVE characterization has been applied to many other time dependent materials as well as asphalt. In addition, trends in the moduli can often be explained phenomenologically.

In the pages to follow a brief description of the test procedures used is first given, followed by a description of the dynamic measurements. This is followed by a consideration of temperature dependency

and a retardation spectra representation of the data. Finally the creep measurements are presented and a summary of the mechanical measurements is given.

Test Procedures

Each of the mixtures (Table 5) were tested in dynamic and creep shear. The sample to be tested was mounted as a pair of thin discs between three steel plates (stacked face to face). The shearing displacement was recorded as the displacement of the center plate relative to the outside plates as they were sheared with respect to each other. A detailed description of the mounting procedure and test equipment is given in Appendix D.

Each sample prepared was observed under a sinusoidally varying load (dynamic) and a step load (creep). From these data, the complex compliance, $|\bar{J}^*|$ and the creep function, $J(t)$, were determined. Each is discussed in subsequent sections under the appropriate heading.

From the nature of the test, the sinusoidal data are considered to be more reliable than the creep data. This is due to the fact that, during testing, any drift from zero by the loading function of the testing machine was reflected as a drift in the displacement of the sample which was often difficult to observe. As a given creep test proceeded and the rate of displacement became small, a small error in zero significantly influenced the shape of the creep curve (see Figure H1, Appendix H).

The sinusoidal data, on the other hand, were much less influenced by a zero drift for several reasons. First, the time of measurement

was much shorter and the loads for a given displacement much larger, thus reducing the relative effect of a zero drift. Secondly, the presence of a zero drift was more easily recognized as a drifting of the repeating trace of the Lissajous pattern (x-y recorder and oscilloscope). Lastly, each set of dynamic compliance data represents a series of tests on five or more frequencies whereas the creep compliance is really only one test carried out over a longer period of time.

The range of the testing variables was limited by the test equipment. Loads below a few hundred grams were difficult to control, limiting the testing at high temperatures and low loading rates where the materials are easily deformed. At low temperatures ("stiffer" material response) the loads became excessive for the sample mounts and at high frequencies the hydraulic capacity of the machine was taxed.

An effort was made to perform all the testing at sufficiently low strains such that linear behavior was preserved. No attempt was made to ascertain the onset of non-linear behavior because after each test point the samples were subsequently used for another data point. It was feared that exposure to the non-linear region might irreversibly affect subsequent behavior.

Occasionally, during the dynamic testing, a load sufficiently large to cause distortion in the Lissajous figure was applied. Although this did not occur with sufficient frequency to establish a definite pattern, most likely the onset of nonlinearity is a function

of both time and temperature. Linearity was observed over a wider range of strains and/or stresses at longer times and higher temperatures.

A sample plate after being deformed to several hundred per cent strain was disassembled and the shape of the deformed material examined. The leading and trailing edges of the sheared sample were seen to be linear, as opposed to say an "S" shape that would have implied a non-uniform strain across the sample.

Dynamic Measurements

The dynamic data were obtained by applying a sinusoidally varying stress,

$$\sigma(\omega) = \sigma_0 \sin \omega t \quad 7$$

to the test samples. $\sigma(\omega)$ is the stress in dynes per square centimeter, σ_0 the peak to peak stress, ω the angular frequency and, t , the time in seconds. If a material is linear viscoelastic, the response must also be sinusoidal but lagging the input by a phase angle, δ .⁽³⁵⁾

The response can then be written as

$$\gamma(\omega) = \gamma_0 \sin (\omega t - \delta) \quad 8$$

where $\gamma(\omega)$ is strain in cm per cm, γ_0 the peak to peak strain, and δ the phase angle in radians.

It is convenient to write the dynamic property that relates stress to strain as a complex variable, \bar{J}^* , where,⁽³⁶⁾

$$\bar{J}^*(\omega) = \frac{\gamma_0 e^{i(\omega t - \delta)}}{\sigma_0 e^{i\omega t}} \quad 9$$

and

$$\bar{J}^* = \frac{\gamma_0}{\sigma_0} \cos \delta - \frac{\gamma_0}{\sigma_0} i \sin \delta \quad 10$$

Equation 10 separates the complex compliance into two parts, an in-phase component, J' and an out-of-phase component, J'' , defined as

$$J' = \frac{\gamma_0}{\sigma_0} \cos \delta \quad 11$$

$$J'' = \frac{\gamma_0}{\sigma_0} \sin \delta \quad 12$$

where, from the usual vector diagram⁽⁴³⁾

$$|\bar{J}^*| = \frac{\gamma_0}{\sigma_0} \quad 13$$

The real part, J' , is commonly called the storage compliance because it represents stored or recoverable energy. The imaginary part, J'' , represents lost, nonrecoverable energy and is commonly called the loss compliance.

Equations 11, 12, and 13 were used to calculate the three components of compliance. A description of these calculations and a set of sample calculations is presented in Appendix F. A tabulation of the logarithm of the reduced data is given in Appendix G. Because the numerical values of compliance and time vary so widely, it is customary to consider the logarithm of the values. The time value is given as $1/\omega$; dimensionally $1/\omega$ is equivalent to time, and, as discussed later, is roughly equal to time, t , in the creep experiment.

Note that the data have been reduced to a reference temperature, T_0 by multiplying each of the compliance components by the ratio:

$$\frac{T}{T_0}$$

where T is the test temperature in degrees Kelvin and T_0 is arbitrarily taken as 298 K.

Theoretically,⁽³⁵⁾ the reduction should be

$$\frac{T \rho}{T_0 \rho_0}$$

14

where ρ and ρ_0 are the densities of the test material at T and T_0 respectively. The contribution from ρ is very small as the volume coefficient of expansion of asphalt is of the order of $10^{-3} \text{ cm}^3/\text{cm}^3/\text{C}$,⁽³⁰⁾ and, over the range of temperatures used, ρ/ρ_0 is very close to 1. Actually, the same is true of T/T_0 ; at 5 C, the logarithm of T/T_0 is only -0.03. The effect of the T/T_0 correction is a change in the 5 C data by -0.03 units.

A typical plot for each of the various compliance components and the phase angle versus the reciprocal of the angular frequency is given in Figures 16 through 19.

As cited above, a necessary condition for a linear viscoelastic material is that a sinusoidal input (load) give a sinusoidal output (deformation). This condition was verified by examining the shape of the Lissajous patterns produced while recording the data. Two sine waves combine to produce an ellipse and deviations from the ellipsoidal shape are very sensitive to distortions in the component signals.⁽⁴⁴⁾

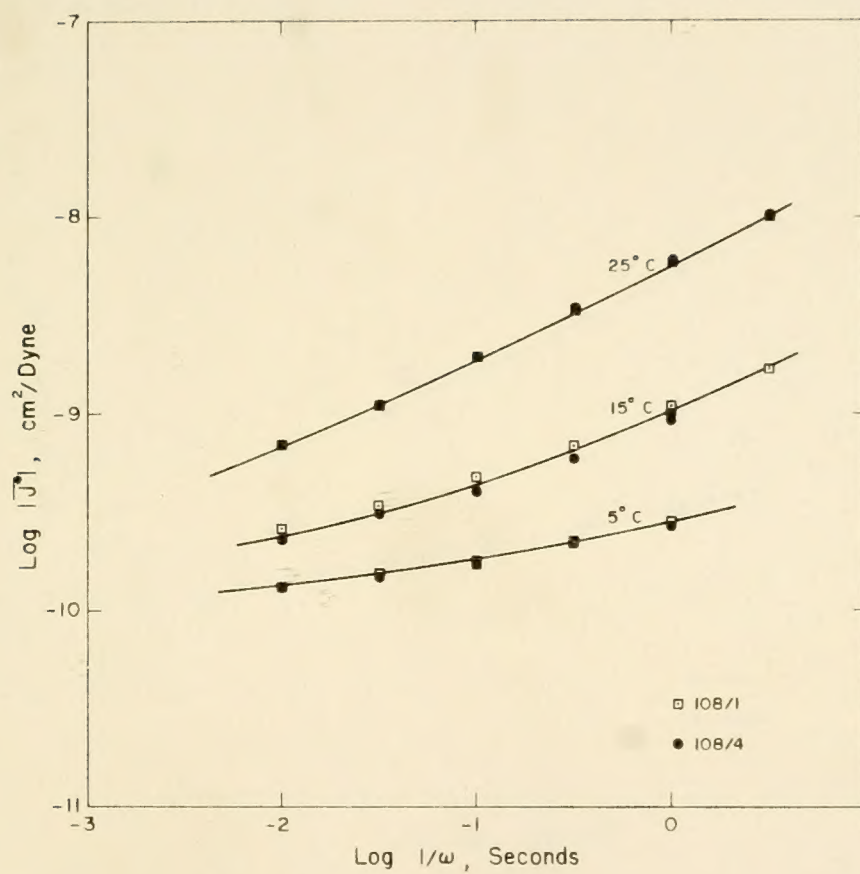


Figure 16. Typical Plot of $\text{Log } |\bar{J}^*|$ Versus $\text{Log } 1/\omega$.

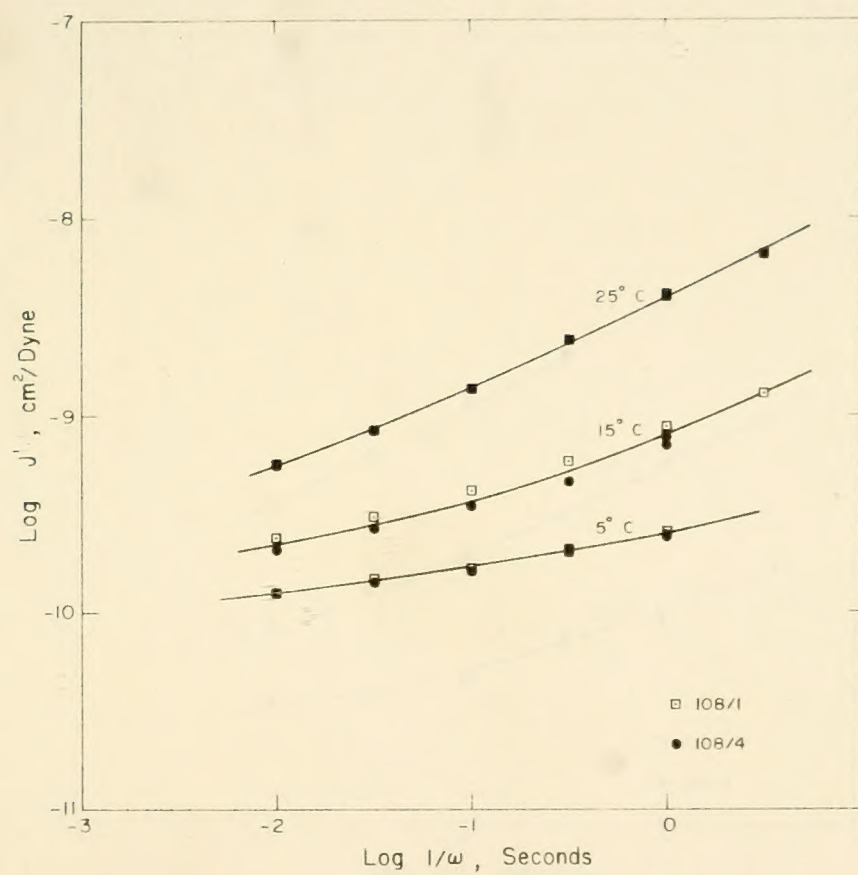


Figure 17. Typical Plot of $\text{Log } J'$ Versus $\text{Log } 1/\omega$.

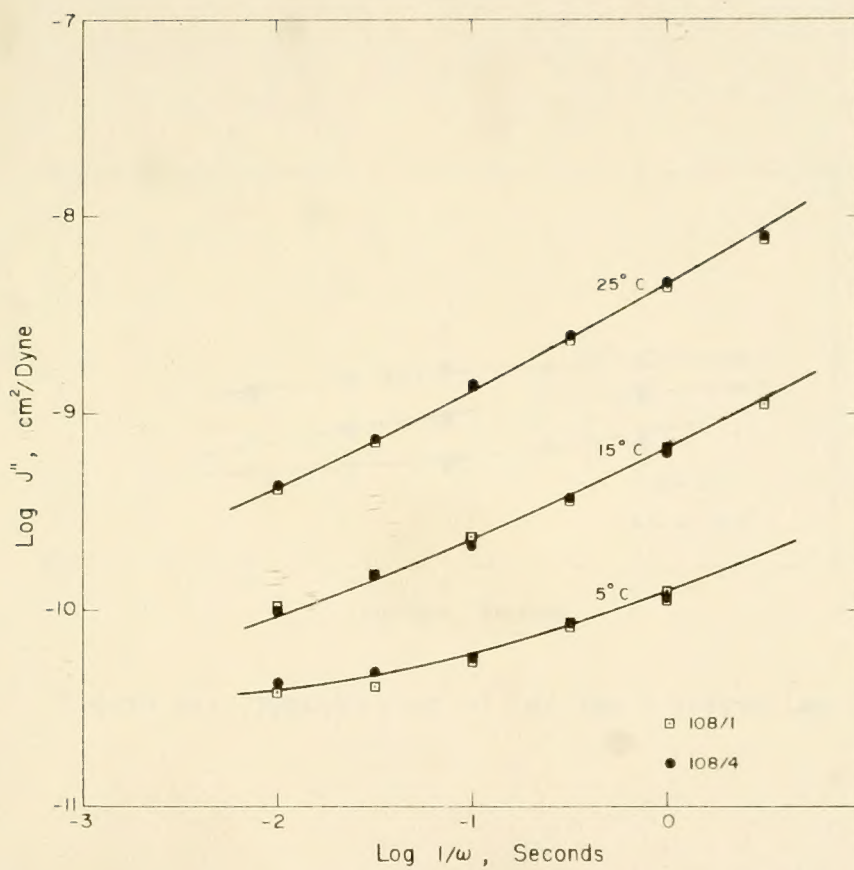


Figure 18. Typical Plot of $\text{Log } J''$ Versus $\text{Log } 1/\omega$.

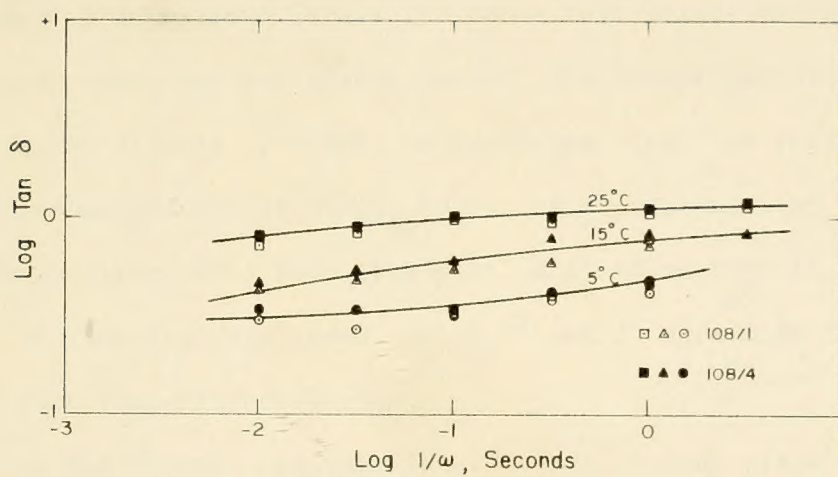


Figure 19. Typical Plot of $\text{Log Tan } \delta$ Versus $\text{Log } 1/\omega$.

Typical Lissajous patterns are shown in Figures F1 and F2, Appendix F. Their smooth ellipsoidal shape shows that the sine in - sine out criterion was satisfied.

A second condition necessary for linearity is the independence of $|\bar{J}^*|$ on the load level at any given frequency and temperature.⁽⁴⁵⁾ This condition was shown to be valid by preparing plots of maximum stress versus maximum strain for those test points where data were taken at more than one stress level. The reciprocal of the slope of this curve defines $|\bar{J}^*|$ and, to the degree that the curve is linear, $|\bar{J}^*|$ is independent of stress level. A typical plot of this type is shown in Figure 20. From this plot, and others like it, a good indication of linearity was shown. Both J' and J'' were also found to satisfy this same linearity criterion.

In the dynamic testing, in all cases, steady state displacement was obtained after only a few cycles at the predetermined load, and repeated cycling did not change the level of the displacement. In a few instances prior levels of stress and frequency were reapplied after testing at other stress and frequency levels. In each case the original output was obtained within experimental error. This implies the absence of any thixotropy or structural breakdown in the material and, concomitantly, any artifacts in the data due to test history.

Sample No. 116 deserves special comment. Referring to the dynamic data, Appendix G, (no creep data were taken), sample plates spaced at 0.005 inches gave essentially the same moduli as those spaced at 0.04 inches. This is a near eightfold difference in thickness. If

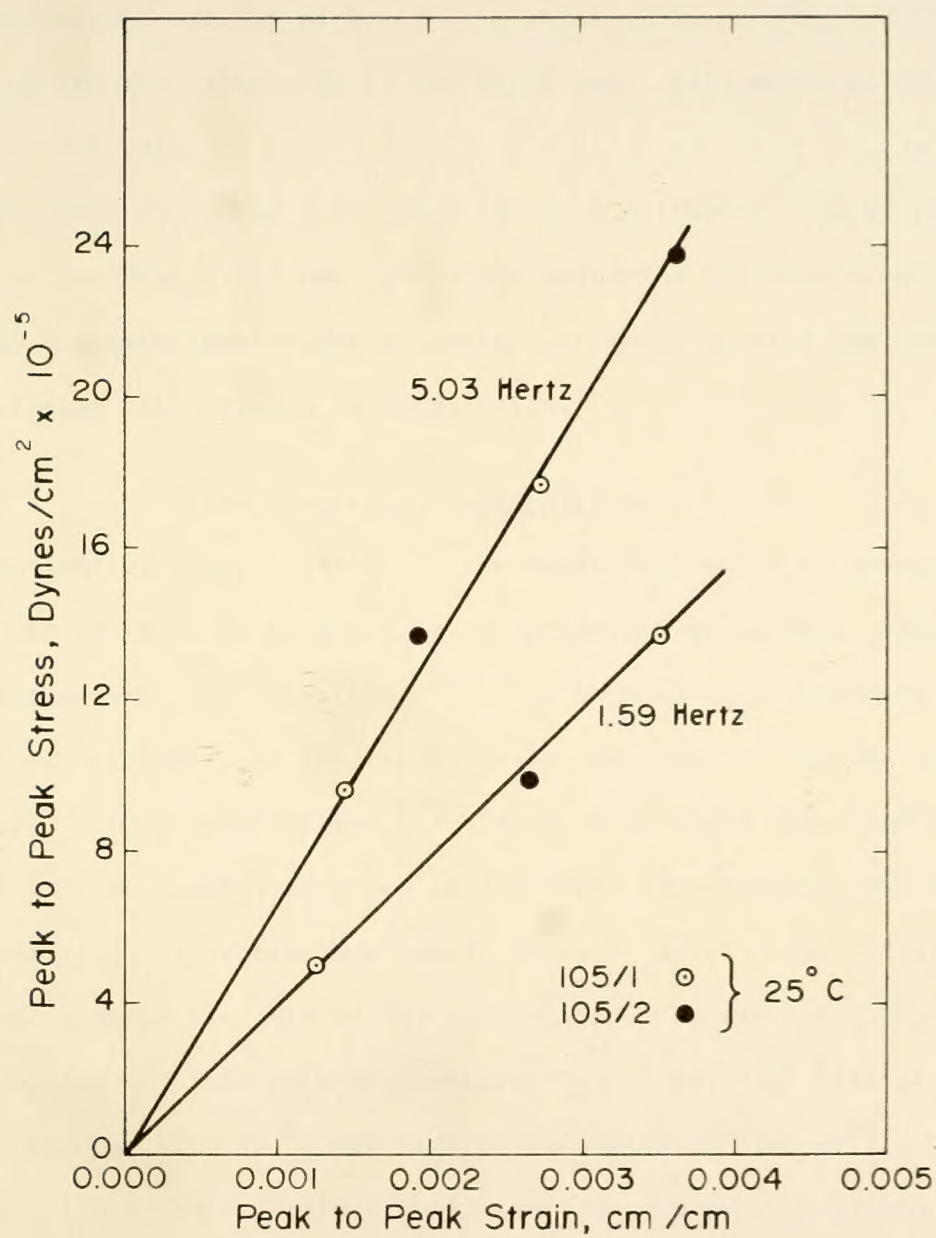


Figure 20. Peak to Peak Stress Versus Peak to Peak Strain.

there was any considerable error from a slippage or deformation effect in the test setup, the net effect of the error would have been 8 times as great in the thin sample as in the thick one. This error is not revealed in the data.

Sample Nos. 119/1 and 119/2 were run at a different area to thickness ratio than Nos. 119/3 and 119/4. By comparing the tabulated data, the moduli are seen independent of plate thickness, showing the data to be invariant with respect to sample size.

Time-Temperature Superposition

A substantial simplification in the characterization of mechanical behavior may be obtained by applying the principle of reduced variables or time-temperature superposition.⁽⁴⁶⁾ The technique is suggested by the shape of the curves of the viscoelastic functions in Figures 16 through 19. With an appropriate shifting of the curves along the time axis, the various curves, obtained at different temperatures, can be made to coincide, generating one smooth "master curve". The shifting is done relative to the data at one arbitrarily selected temperature which is called the reference temperature; T_0 . A material that is shiftable as described is termed thermorheologically simple.⁽⁴⁷⁾ The series of shift factors, defined as the various distances shifted, yield a smooth continuous "shift function", $a_T(T-T_0)$, which is a function of temperature only.

Having generated the master curve and a_T function, it is then possible to generate the viscoelastic function in question for any intermediate values of time (or frequency) and temperature.

Experimentally, the test to determine if a material is thermorheologically simple is to first plot the data, reduced by $T_0/T_0 \rho_0$, on transparent paper versus the logarithm of time. The curves are then adjusted along the time axis, without any vertical shift, so that the curves at the different temperatures comprise one single smooth curve.

In this work, the technique was applied to the values of $|\bar{J}^*|$ and smooth curves were generated without any vertical shift. Values obtained for the $\log a_T$ are tabulated in Tables 6 through 8. Note that 298 K was used as the reference temperature, T_0 .

While the matching of the curves of plotted data is a necessary criterion for the applicability of time-temperature superposition, two other criteria should be tested when possible: ⁽³⁵⁾ (a) the one a_T function should be unique to all the viscoelastic functions and, (b) the a_T function for the material in question must be consistent with experience.

The uniqueness criterion was tested by applying the a_T values generated from the $|\bar{J}^*|$ data to J' , J'' , and the creep function, $J(t)$. A discussion of these tests is presented in those sections where the appropriate reduced data are presented.

A widely accepted functional form of a_T is given by the WLF equation as ⁽⁴⁶⁾

$$\log a_T = \frac{-8.86 (T - T_s)}{101.6 + T - T_s}$$

Table 6. Values of $\log a_T$ and T_s for B3056 Mixtures.

Sample No.	Mineral	$\log a_T$		$T_s, ^\circ\text{C}$
		15 C	5 C	
105	10-20 CaCO_3	1.56	3.36	43
108	2.5-5 CaCO_3	1.57	3.22	41
132	0.63-1.25 CaCO_3	1.50	3.21	41
109	XFDG CaCO_3	1.53	3.45	43
107	10-20 SiO_2	1.53	3.22	41
106	2.5-5 SiO_2	1.64	3.37	43
133	0.63-1.25 SiO_2	1.47	3.15	41
119	XFDG SiO_2	1.58	3.34	43
126	Magnesite	1.53	-	44
127	Bytownite	1.25	-	37
128	Microcline	1.51	-	44
129	Apatite	1.52	-	44
117	None**	1.55	3.30	43
118	None***	1.43	3.23	42
120	2.5-5 SiO_2 *	1.44	3.34	42
121	2.5-5 CaCO_3 *	1.54	3.48	43
-	Average	1.53	3.31	

* Mixed in air

** As supplied, no vacuum treatment

*** Mixed in vacuum

Table 7. Values of $\log a_T$ and T_s for B3603 Mixtures

Sample No.	Mineral	$\log a_T$		$T_s, ^\circ\text{C}$
		15 C	5 C	
124	10-20 CaCO_3	1.38	2.87	37
125	10-20 SiO_2	1.41	2.86	37
130	2.5-5 CaCO_3	1.21	-	35
131	2.5-5 SiO_2	1.21	2.73	34
122	None*	1.42	2.83	37
123	None**	1.35	2.84	37
-	Average	1.33	2.85	-

* As supplied, no vacuum treatment

** Mixed in vacuum

Table 8. Values of $\log a_T$ and T_s for Aged Mixtures*

Sample No.	Mineral	$\log a_T$		$T_s, ^\circ\text{C}$
		15 C	5 C	
130	2.5-5 CaCO_3	1.21	-	35
230	2.5-5 CaCO_3	1.29	2.73	35
330	2.5-5 CaCO_3	1.47	2.75	35
131	2.5-5 CaCO_3	1.21	2.73	34
231	2.5-5 SiO_2	1.21	2.68	34
331	2.5-5 SiO_2	1.19	2.68	34
132	0.63-1.25 CaCO_3	1.50	3.21	41
232	0.63-1.25 CaCO_3	1.28	2.95	38
332	0.63-1.25 CaCO_3	1.54	3.26	41
133	0.63-1.25 SiO_2	1.47	3.15	41
233	0.63-1.25 SiO_2	1.26	2.75	35
333	0.63-1.25 SiO_2	1.50	3.18	41

* 100 series samples were tested when prepared, 200 series were tested 2 months later, 300 series were tested just after reheating at 2 months. Thus, those samples with the same last two digits are the same samples except for the time of test.

where the reference temperature, T_s , is an adjustable parameter, generally about 50 C above the glass transition temperature, T_g . The empirical constants 8.86 and 101.6 represent data from many different polymer systems. Equation 15 implies a unique a_T function for all materials, provided they are referenced to the appropriate reference temperature, T_s .

A plot of experimentally determined values of $\log a_T$ versus T for the two different asphalts used in this study is given in Figure 21. The values plotted are the averages for all the mixtures made with the two different asphaltic materials.

Figure 22 shows the results of shifting (horizontally and vertically without rotation) the values from Figure 21 so that they best fit on the empirical equation for a_T as predicted by Equation 15. The value of T_s was read from Figure 22 at the point corresponding to $T = 0$ (using the scale of Figure 21). A complete set of T_s values for each mixture, obtained by this procedure, is given in Tables 6, 7 and 8.

Experimentally, for many different materials, including asphalts, it has been found that T_s is approximately 50 C above the experimentally measured glass transition temperature, T_g . (35, 46, 48-50) Values of T_s in Tables 6, 7, and 8 range between 35 C and 44 C for the two different asphalts and the mixtures made with them. If the 50 C value is valid, it would imply T_g values of -15 C to -6 C.

A more satisfactory approach to define the functional form of a_T is to compute the constants in the equation:

$$\log a_T = \frac{-c_1^0 (T - T_0)}{c_2^0 + T - T_0} \quad 16$$

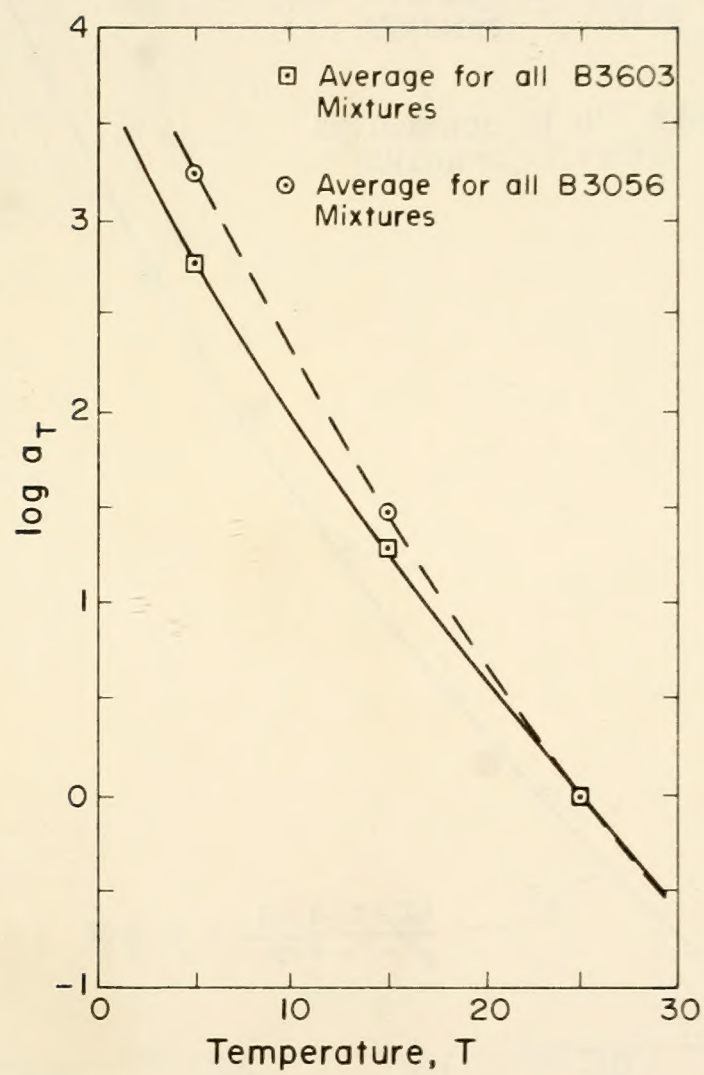


Figure 21. Experimentally Determined a_T .

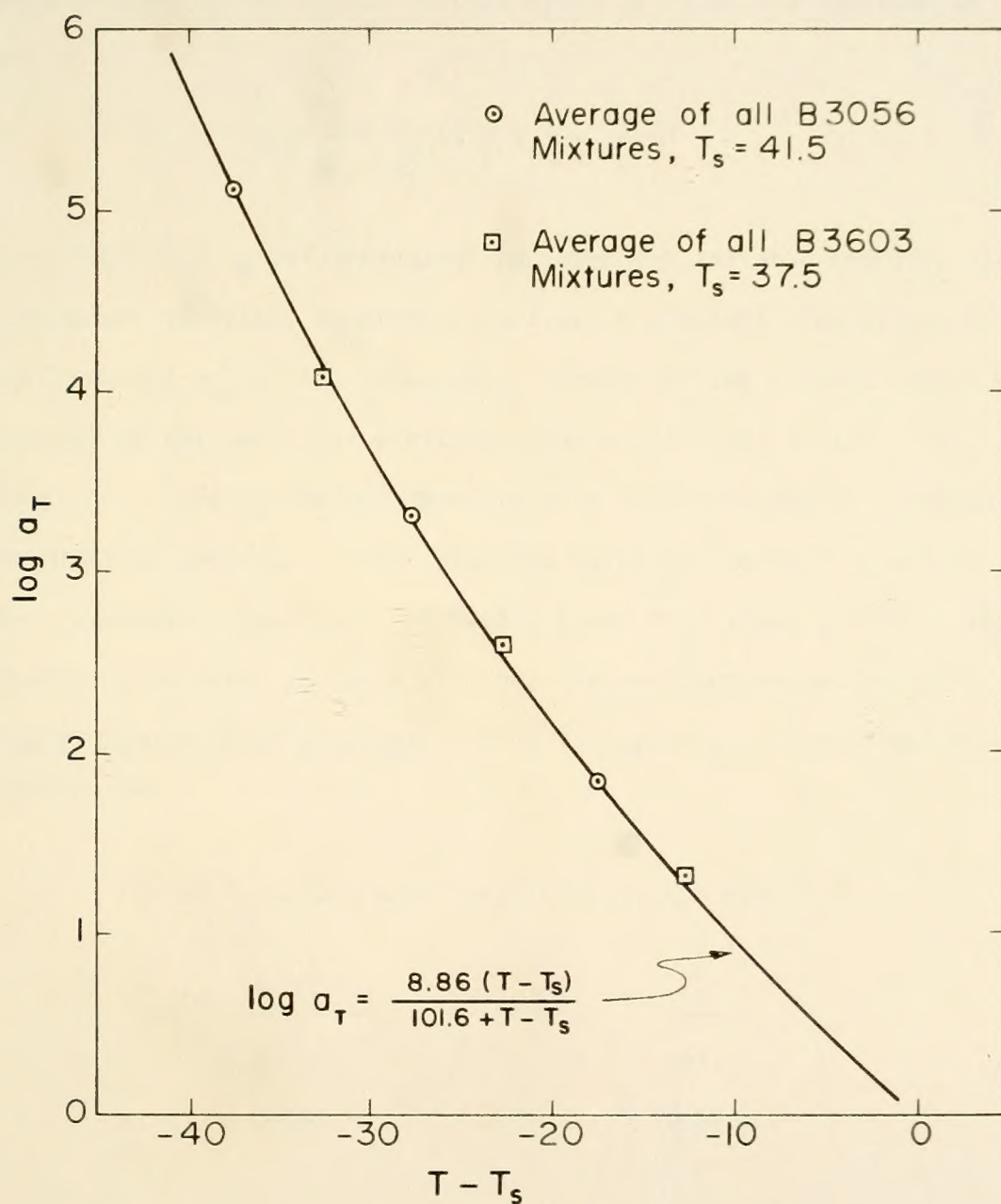


Figure 22. Determination of T_s .

where c_1^0 and c_2^0 are constants referred to the temperature T_0 .⁽³⁵⁾

The constants c_1^0 and c_2^0 can be calculated by rewriting Equation 16 as

$$\frac{T - T_0}{\log a_T} = \frac{1}{c_1^0} (T - T_0) + \left(\frac{-c_2^0}{c_1^0} \right) \quad 17$$

When $(T-T_0)/\log a_T$ is considered the dependent variable and $T-T_0$ the independent variable, Equation 17 defines a straight line with $-1/c_1^0$ the slope and $-c_2^0/c_1^0$ the intercept. Because of the limited number of data points available for plotting Equation 17 ($T-T_0 = -10^\circ, -20^\circ$) values of c_1^0 and c_2^0 for each mixture were rather sporadic. Instead, two plots of Equation 17 were prepared using the average values for the two asphalt types given in Tables 6 and 7. Values c_1^0 and c_2^0 were determined as shown in Table 9. These values, referenced to 298 K, compare favorably to published values for asphalt and other materials. (35, 51, 52).

Table 9. Calculated Coefficients, WLF Equation.

Asphalt	c_1^0	c_2^0
B3056	19	133
B3603	21	169

The ability of the form of the WLF equation as given by Equation 15 to fit the plotted data of Figure 22 and the magnitude of the calculated values of c_1^0 and c_2^0 reinforce the applicability of the time-temperature superposition principle for both the filled and unfilled systems. Previous authors have shown the principle valid for unfilled asphalts. (48, 50, 51, 53)

Dynamic Testing - Results

The results of the dynamic testing are presented in Figures 23 through 42. The data for $|\bar{J}^*|$, J' and J'' have been shifted according to the procedure outlined in the previous section by matching the curves of $|\bar{J}^*|$ at 25, 15, and 5 C. In the interest of clarity, the individual data points for $|\bar{J}^*|$ are not shown. For reference, the curve representing $|\bar{J}^*|$ for the corresponding unfilled asphalt is shown on each graph as a dashed line.

One of the checks on the validity of the time-temperature superposition is the ability of the a_T function to shift the various viscoelastic functions (page 49). In the shifting in Figures 23 through 42 the same a_T value has been applied to both J' and J'' (Tables 6 and 7) and a single curve drawn through each set of data points. A close examination of the shifted data points shows that they fit a single curve quite nicely, validating the use of the same a_T function for $|\bar{J}^*|$, J' and J'' .

Although Figures 23 through 42 represent data for several different systems, the trends are quite similar. At the higher frequencies (more negative values of $\log (1/\omega a_T)$) the samples show a "stiffer"

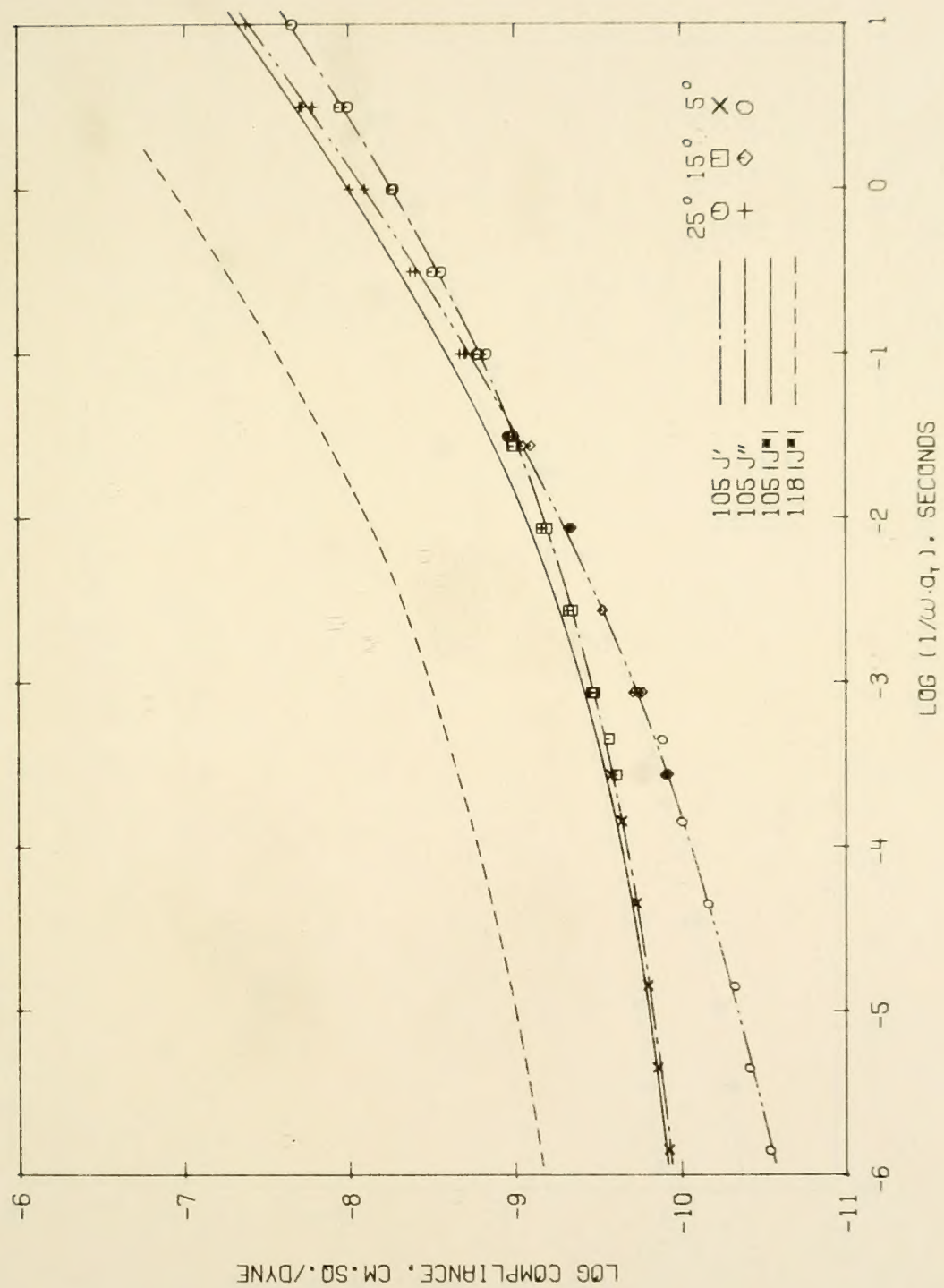


Figure 23. Dynamic Compliance Components, Sample No. 105: B3056 Asphalt, 10.-20. μm Calcite.

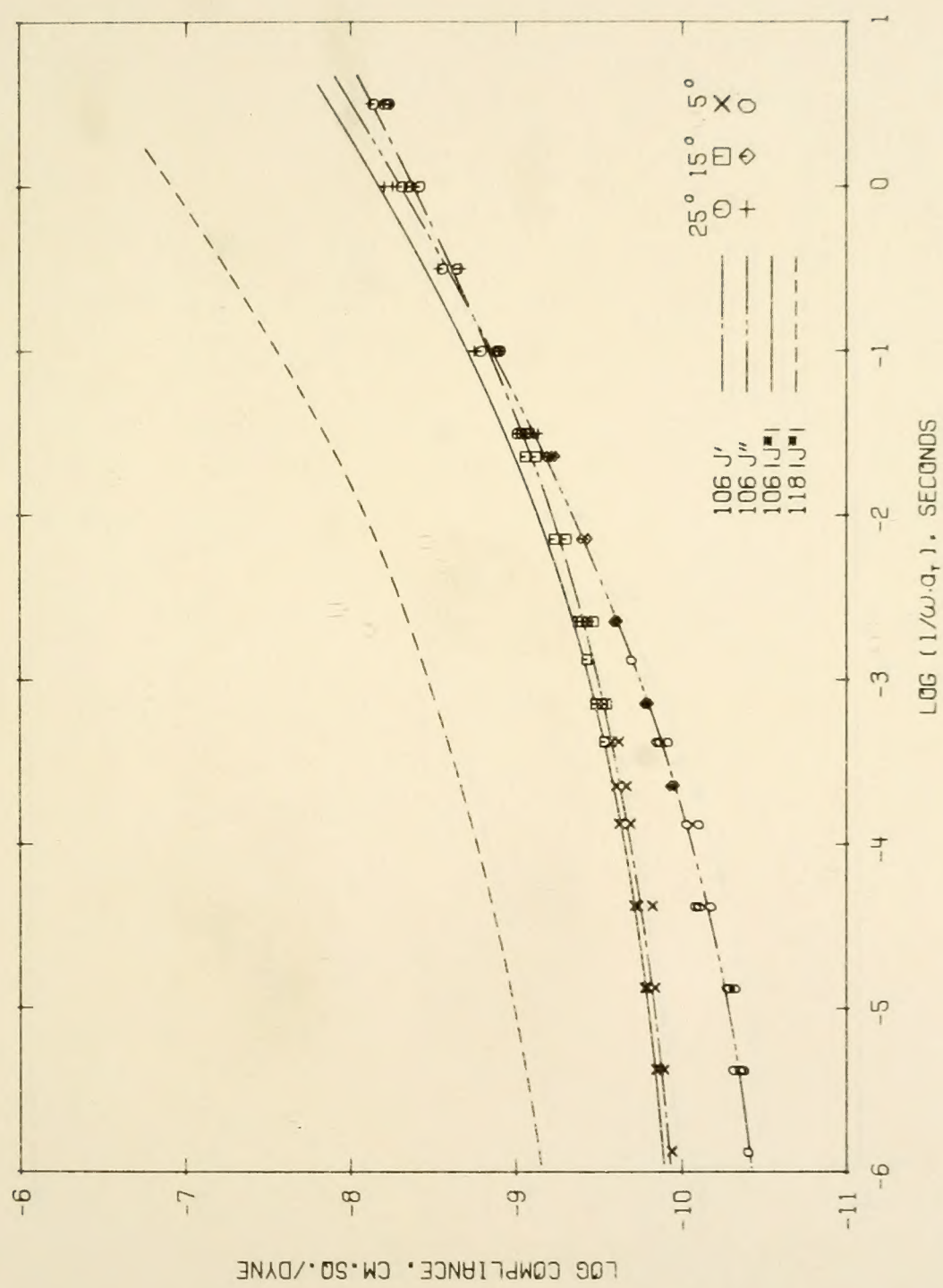


Figure 24. Dynamic Compliance Components, Sample No. 106: B3056 Asphalt
2.5-5.0 μm Quartz.

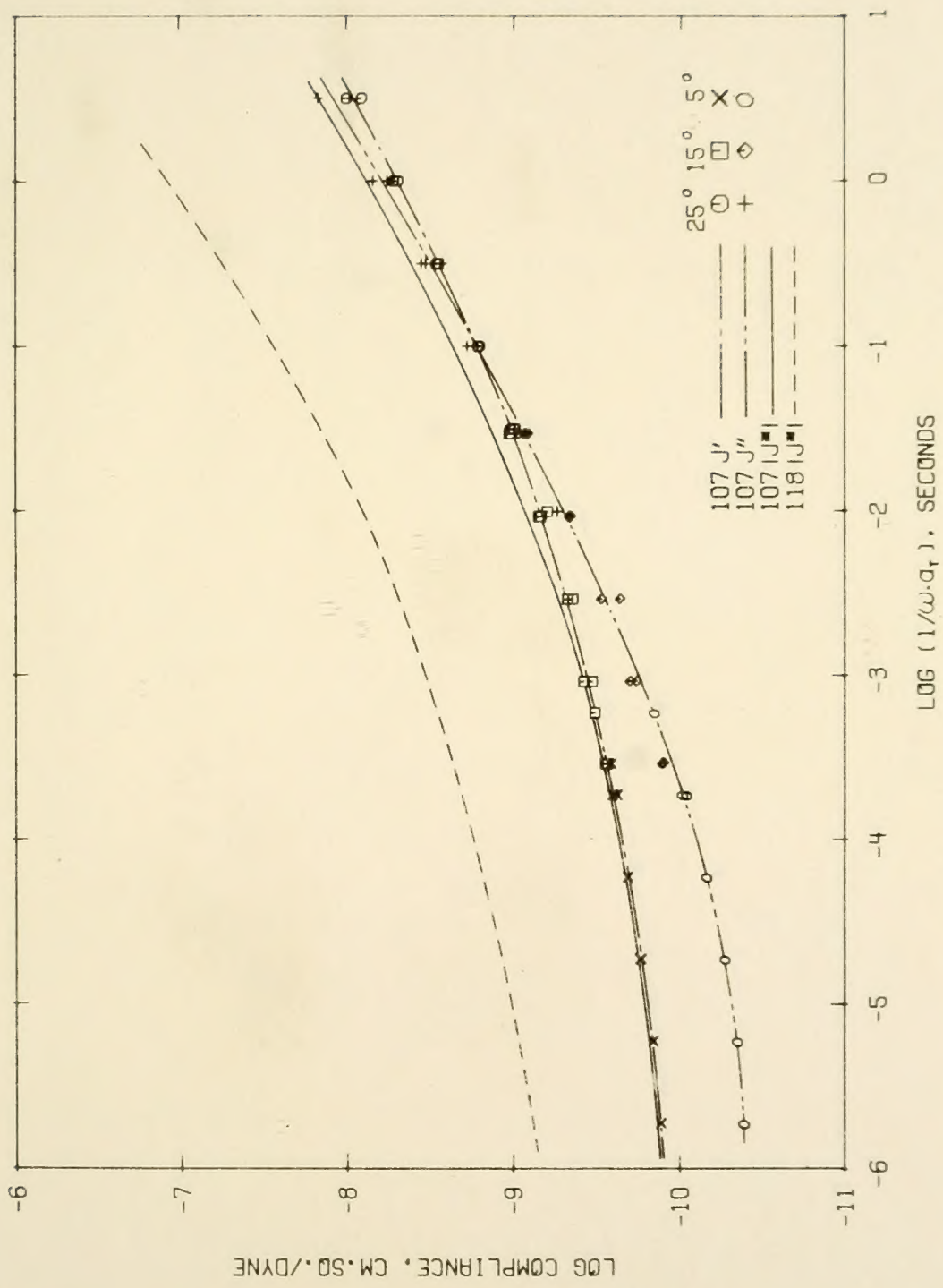


Figure 25. Dynamic Compliance Components, Sample No. 107: B3056 Asphalt, 10.-20. μm Quartz

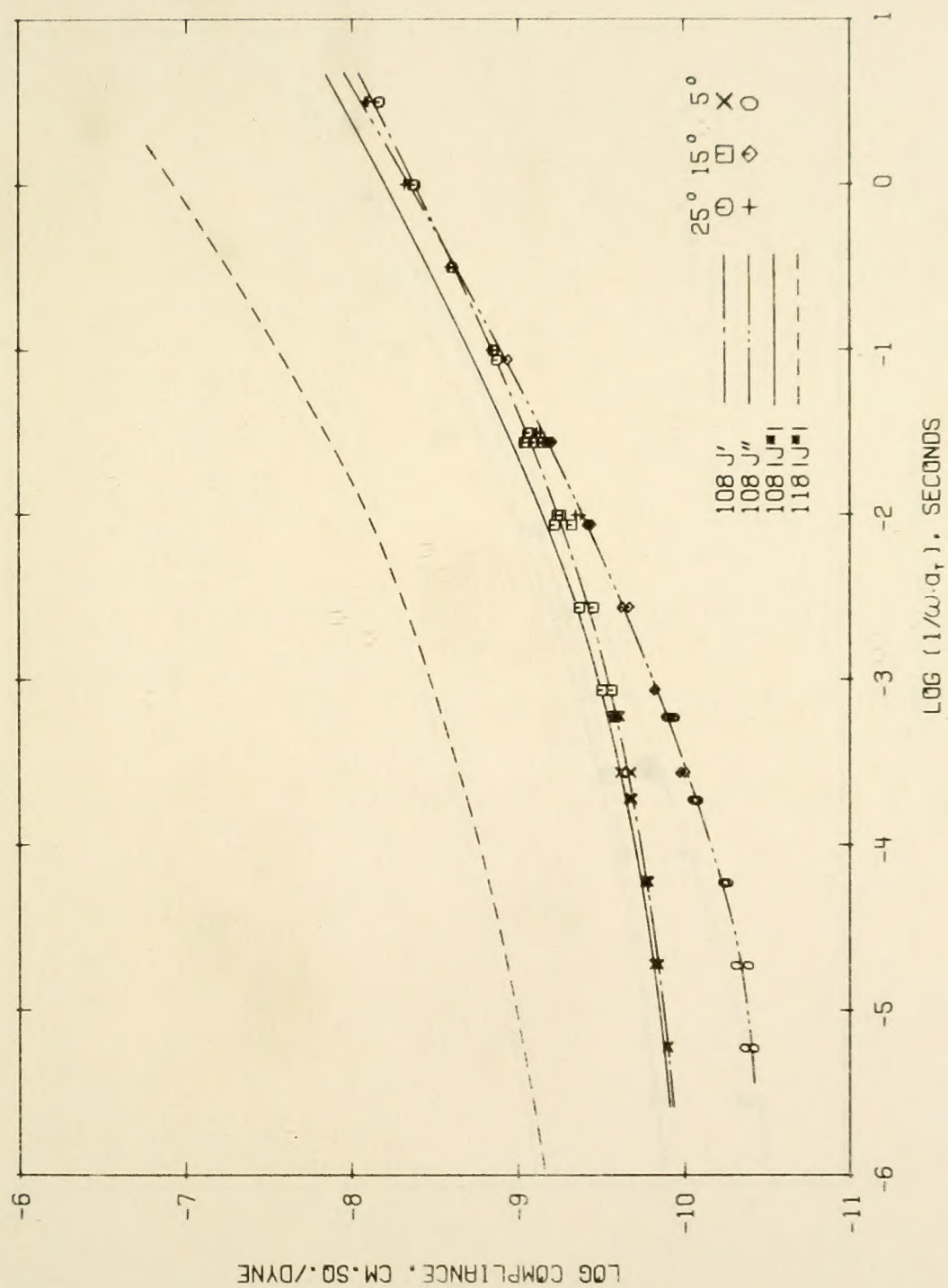


Figure 26. Dynamic Compliance Components, Sample No. 108: B3056 Asphalt,
2.5-5.0 μm Calcite.

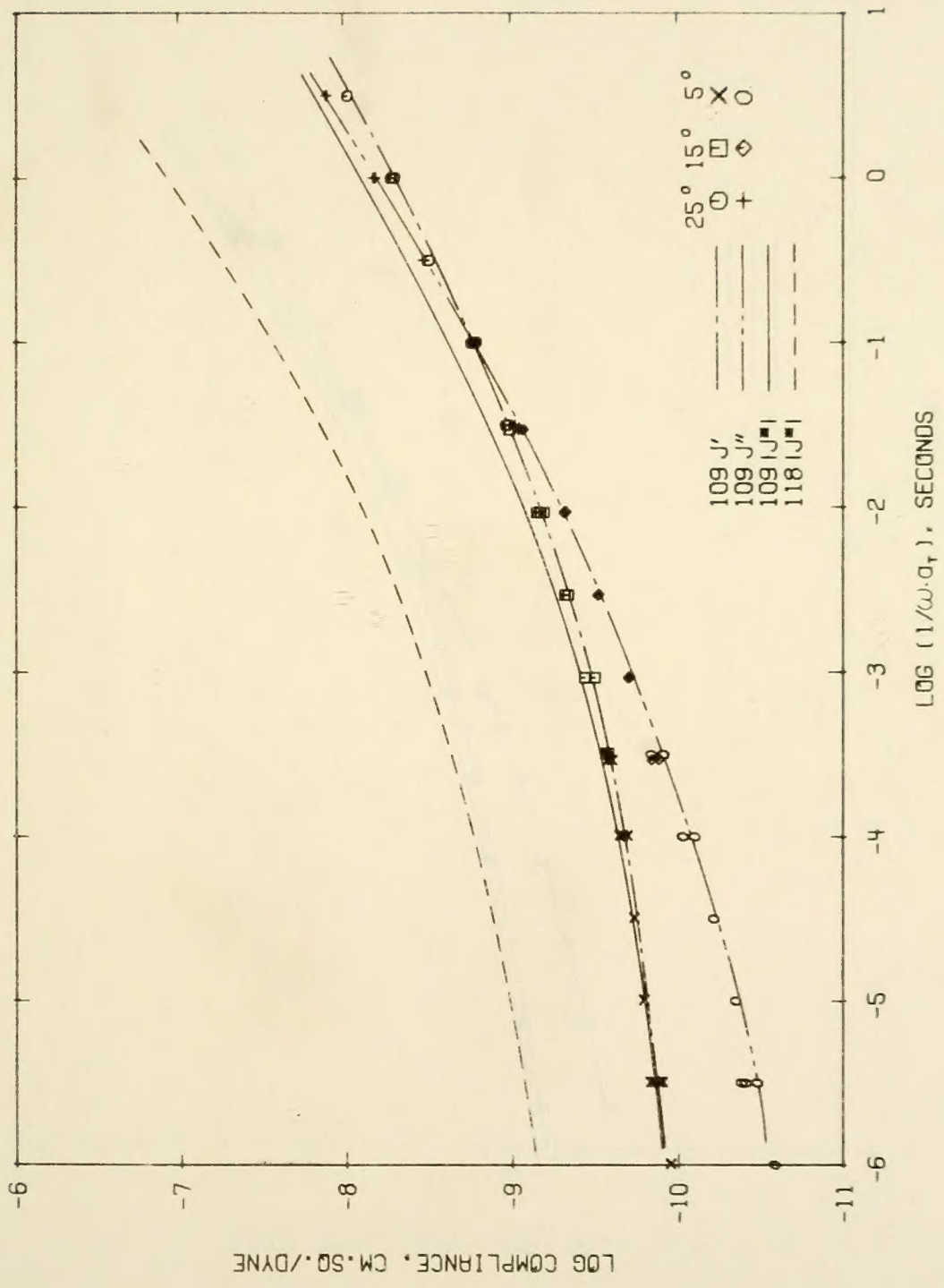


Figure 27. Dynamic Compliance Components, Sample No. 109: H3056 Asphalt, Graded Calcite.

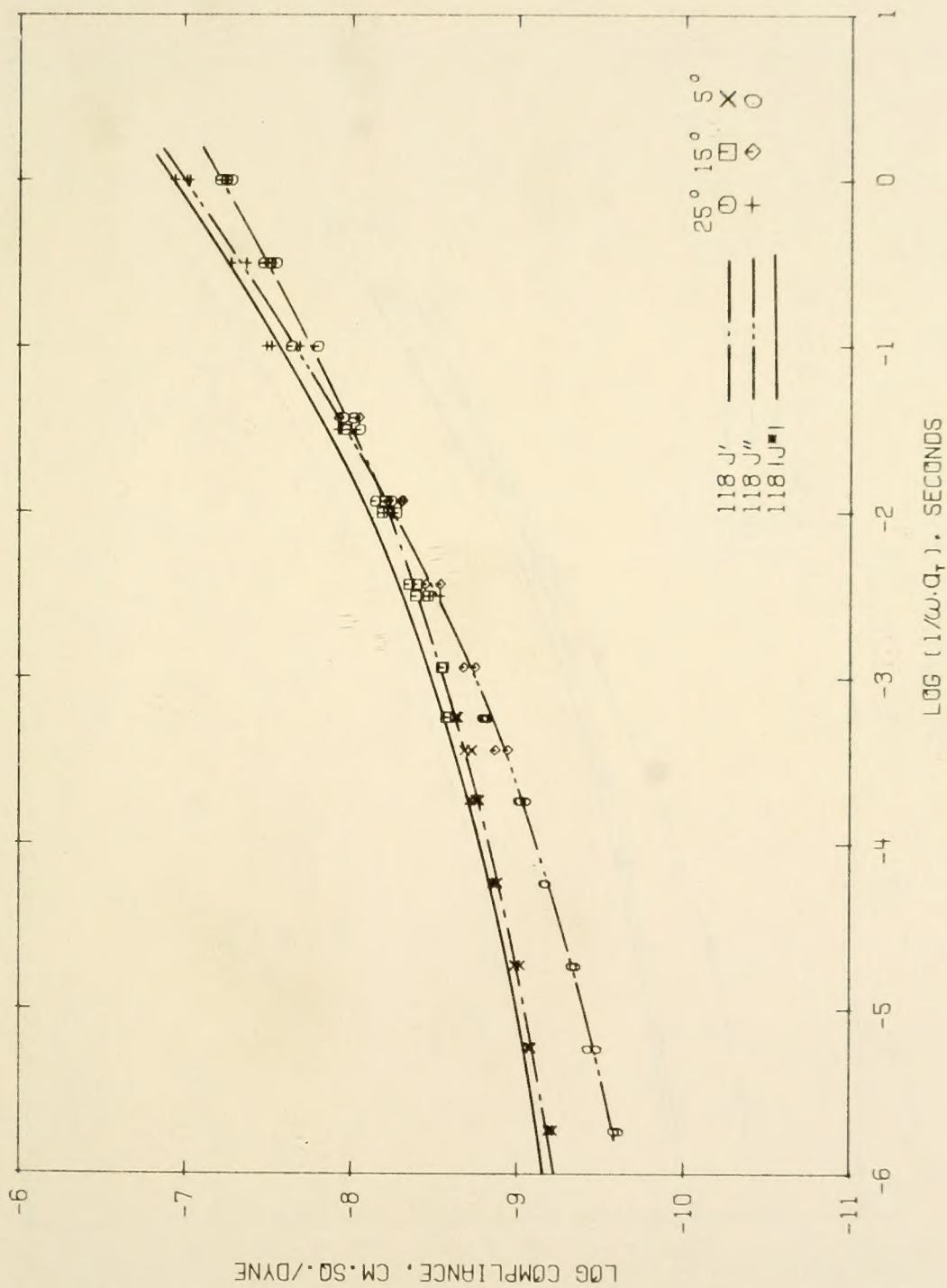


Figure 28. Dynamic Compliance Components, Sample No. 118: Unfilled B3056 Asphalt.

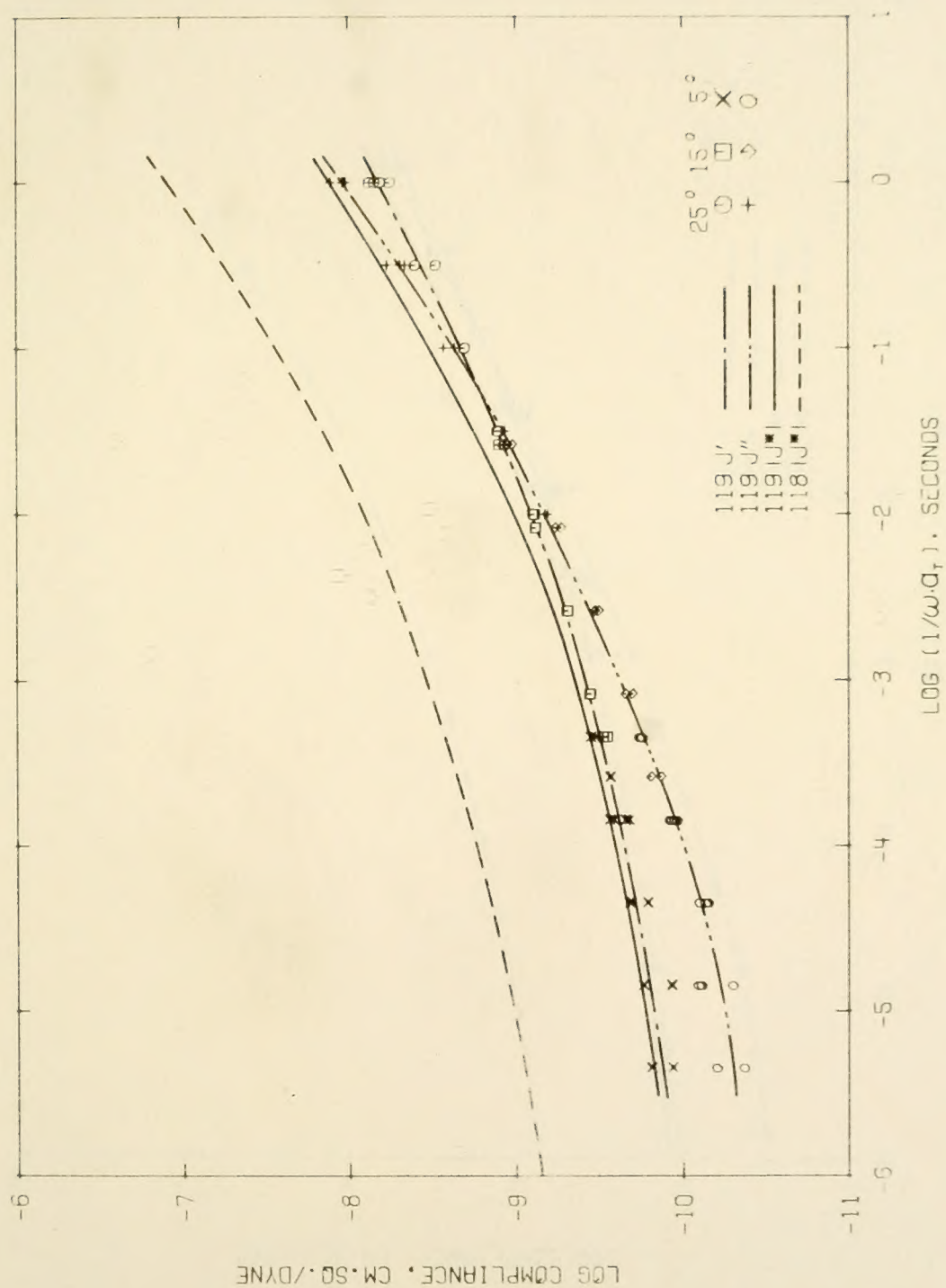


Figure 29. Dynamic Compliance Components, Sample No. 119: B3056 Asphalt, Graded Quartz.

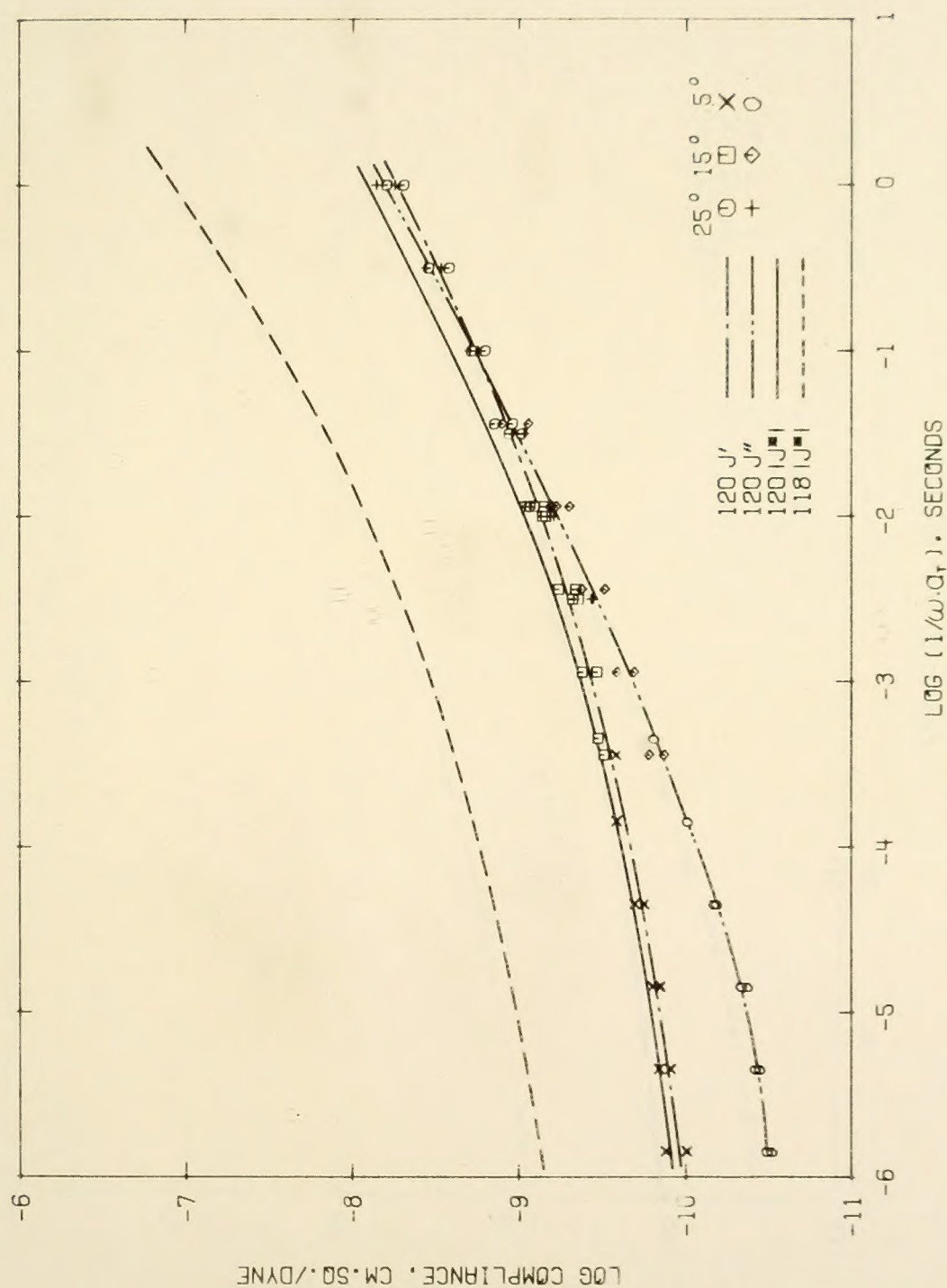


Figure 30. Dynamic Compliance Components, Sample No. 120: B3056 Asphalt, 2.5-5.0 μ m Quartz.

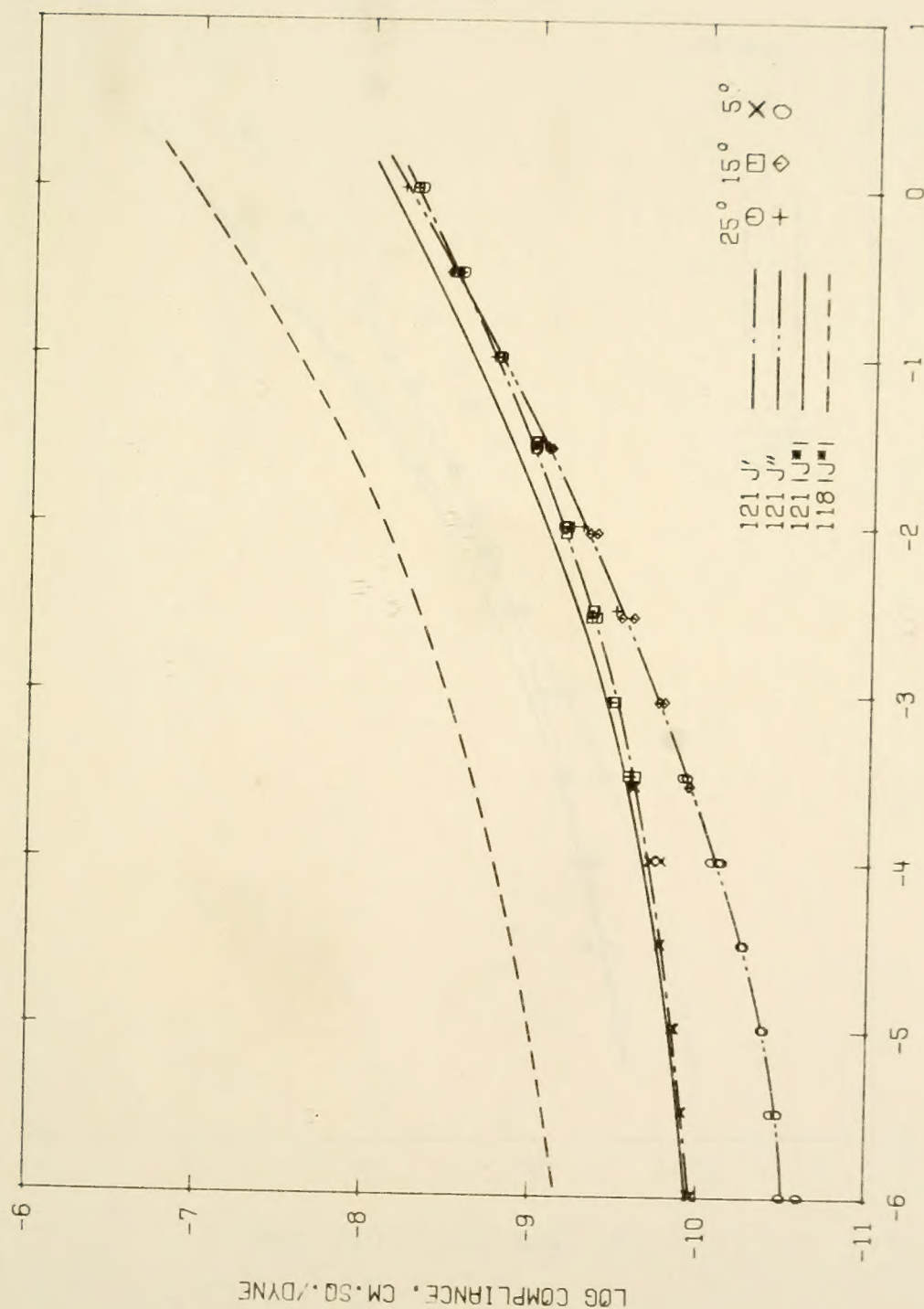


Figure 31. Dynamic Compliance Components, Sample No. 121: B3056 Asphalt, 2.5-5.0 μm Calcite.

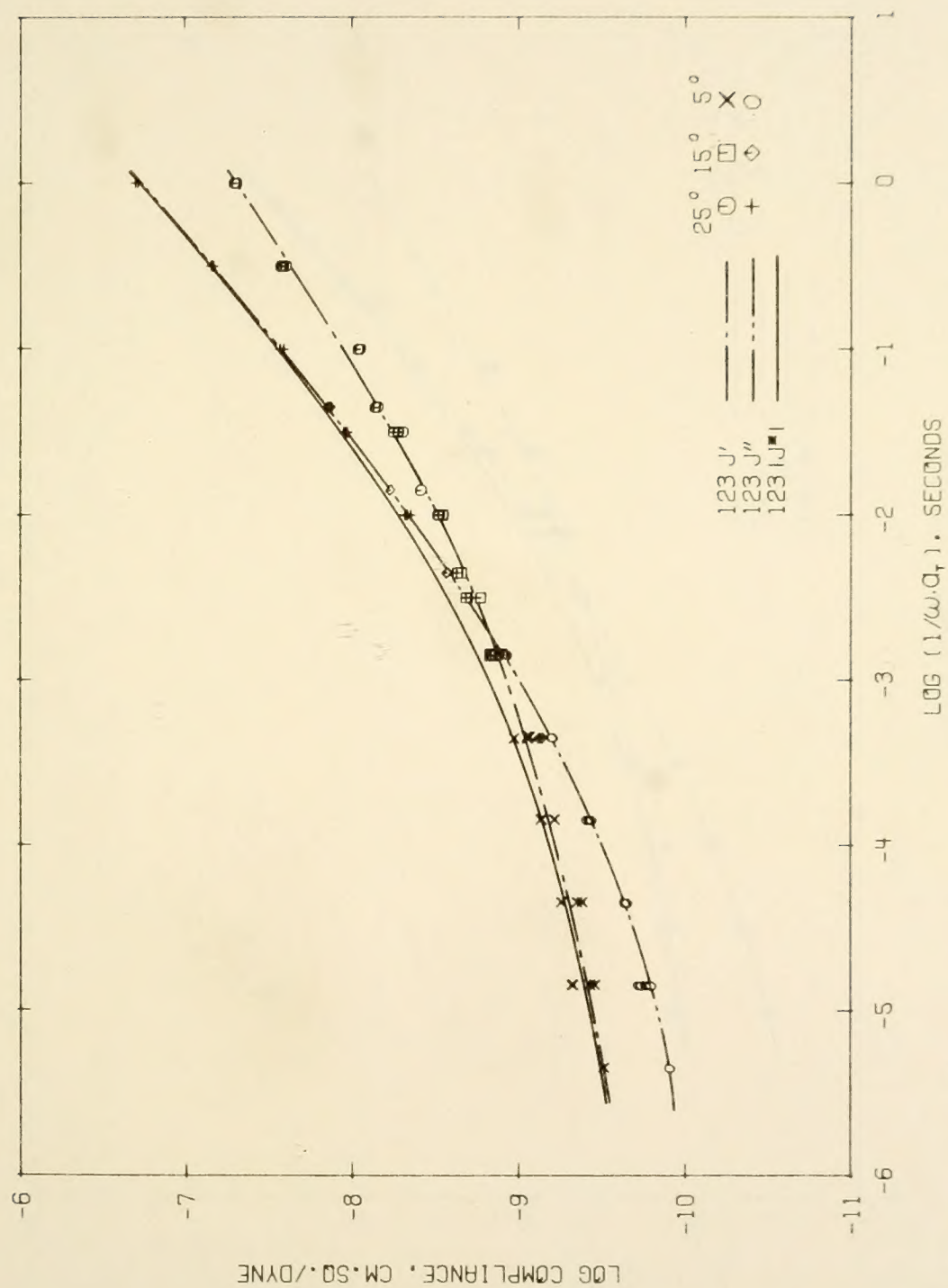


Figure 32. Dynamic Compliance Components, Sample No. 123: Unfilled B3603 Asphalt.

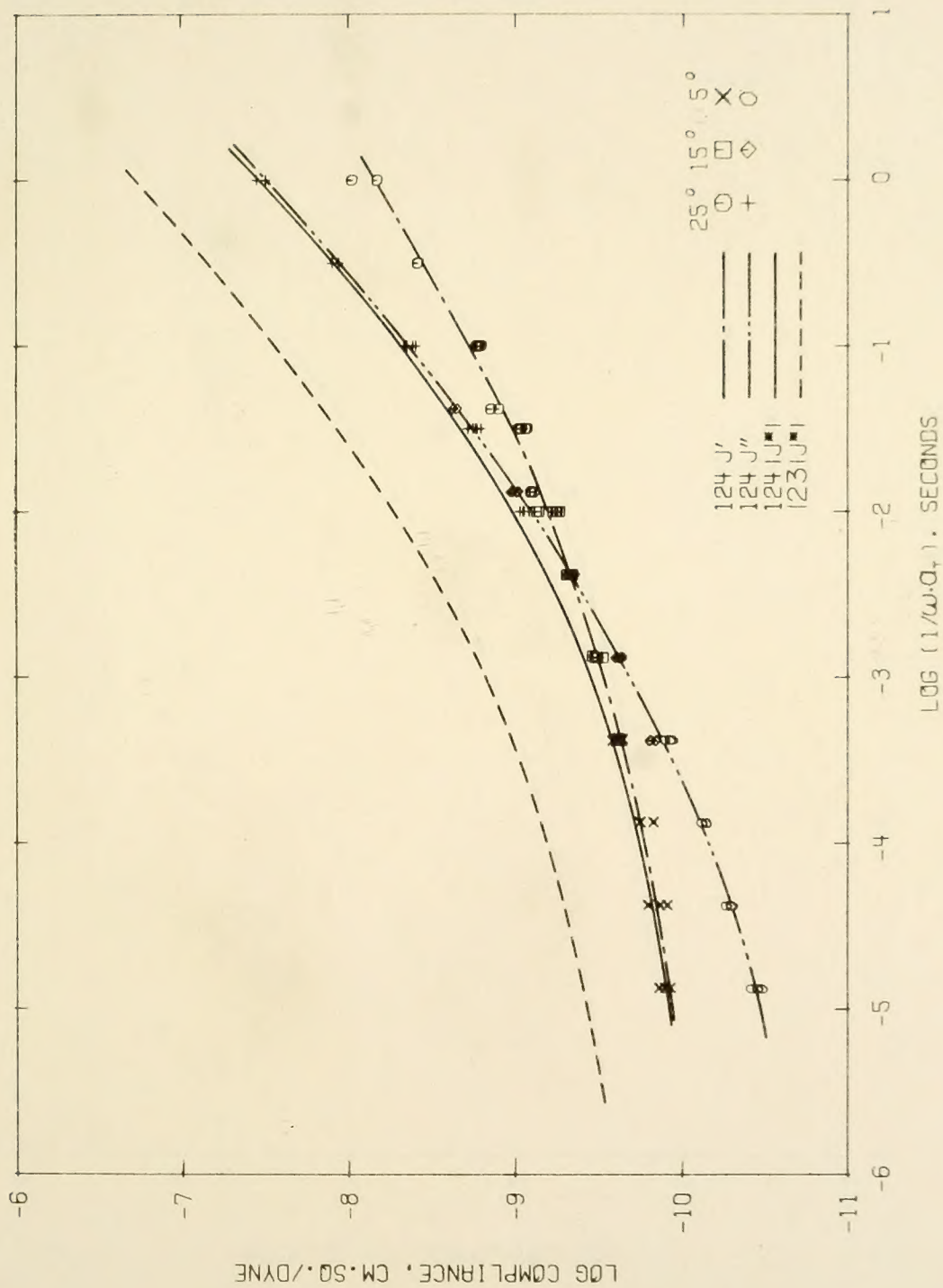


Figure 33. Dynamic Compliance Components, Sample No. 124: B3603 Asphalt, 10.-20. μm Calcite.

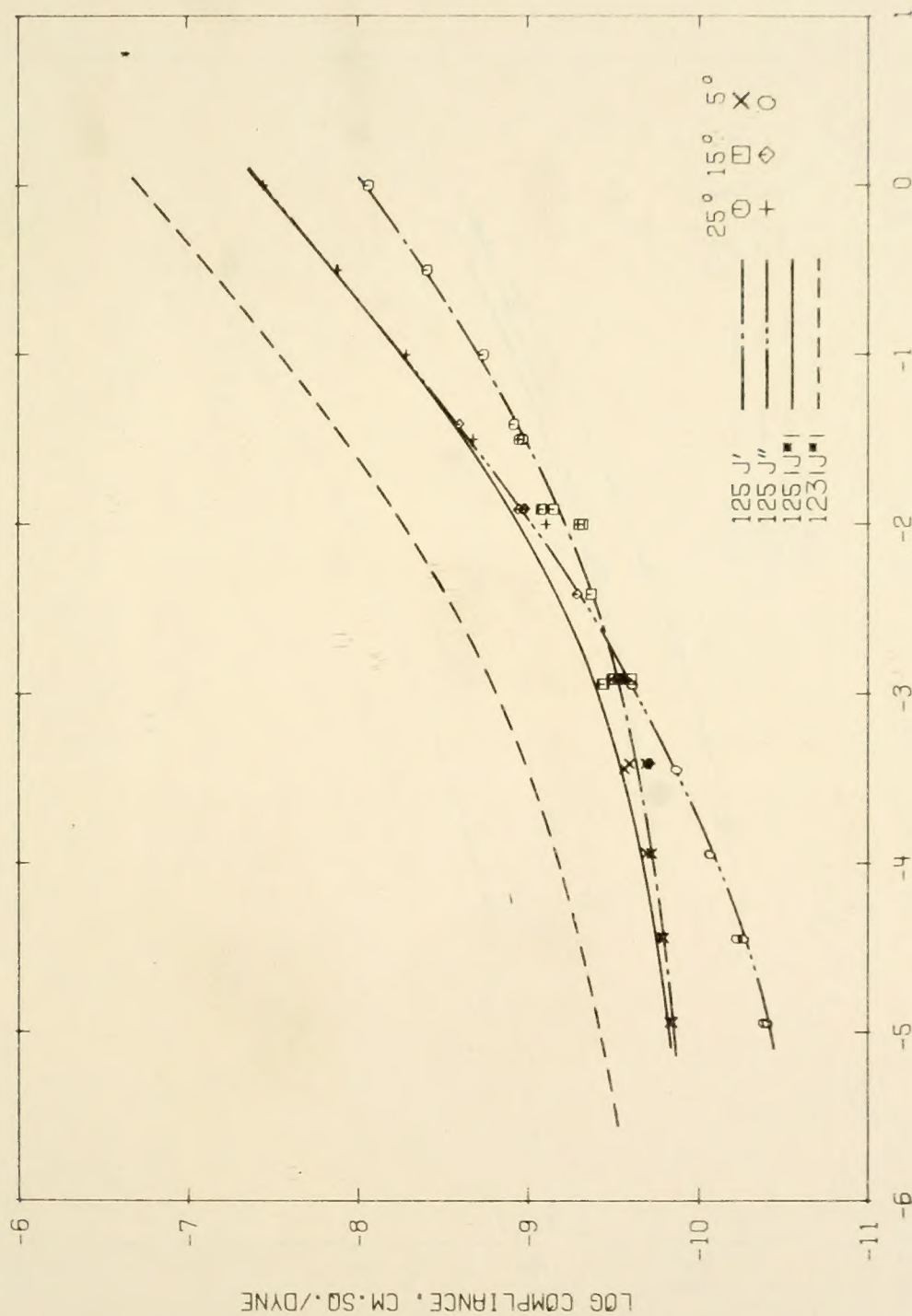


Figure 34. Dynamic Compliance Components, Sample No. 125: B3603 Asphalt, 10.-20. μ m Quartz.

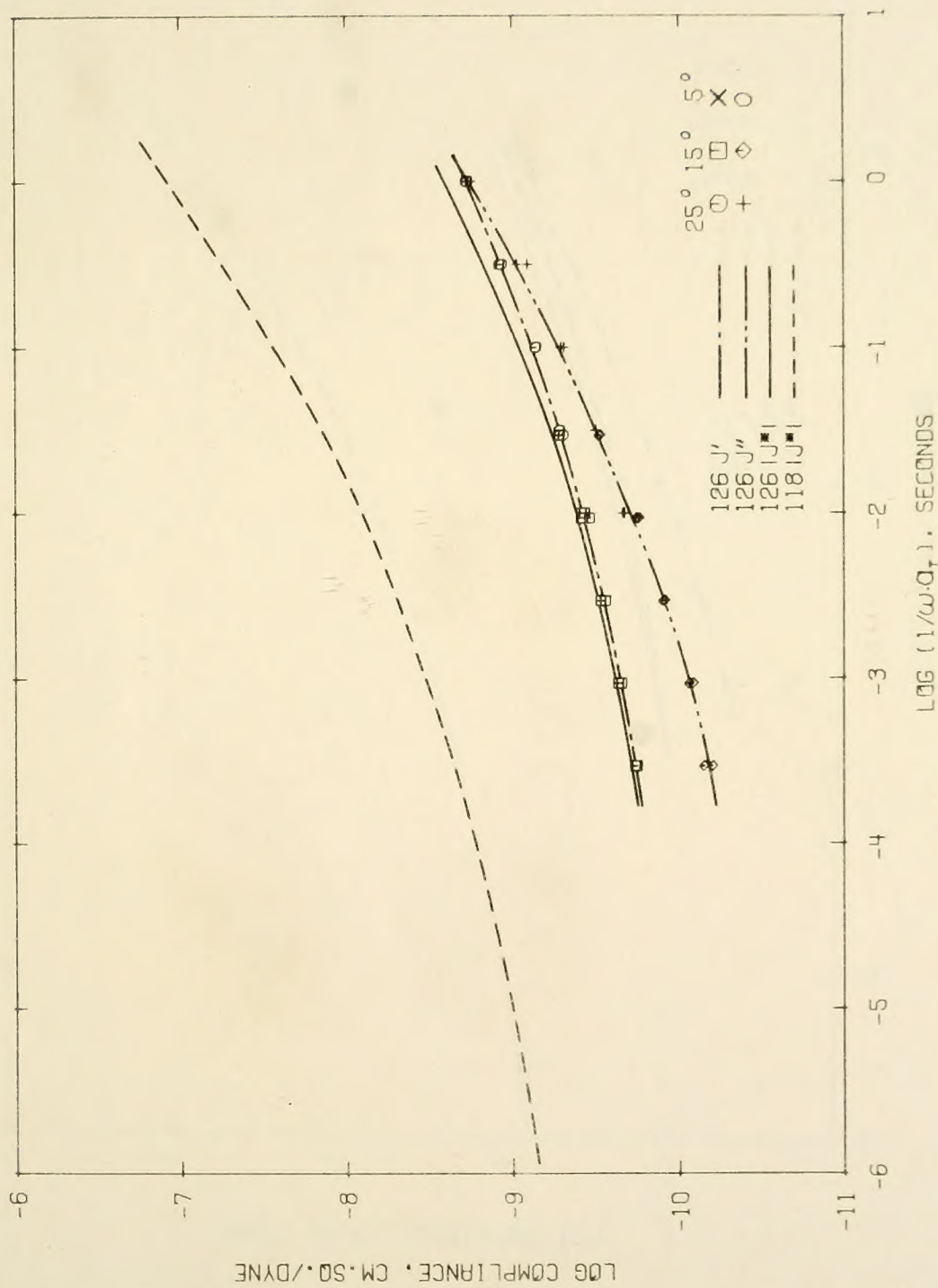


Figure 35. Dynamic Compliance Components, Sample No. 126: B3056 Asphalt, < 2.5 μm Magnesite.

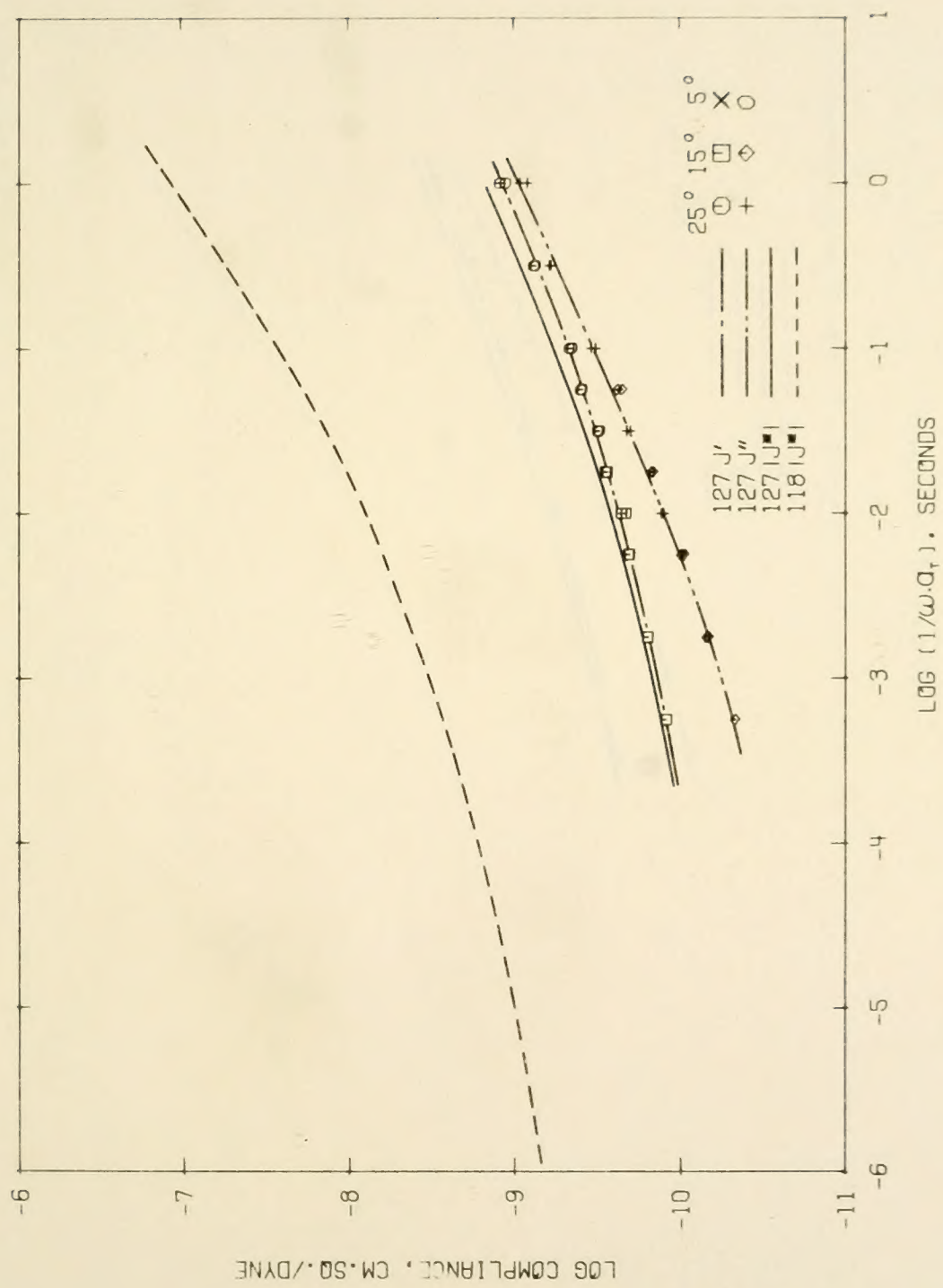


Figure 36. Dynamic Compliance Components, Sample No. 127: B3056 Asphalt, < 2.5 μm Bytownite.

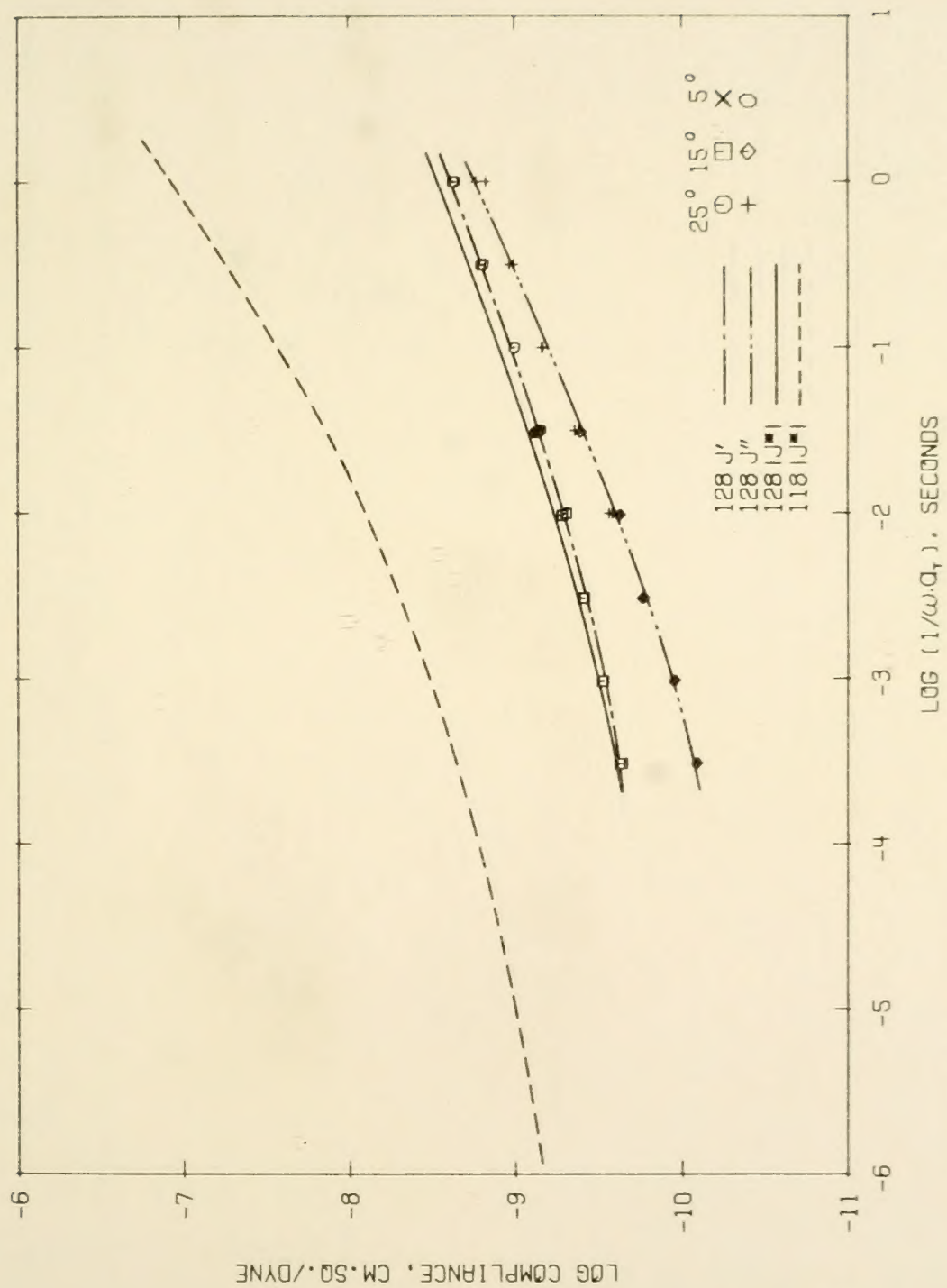


Figure 37. Dynamic Compliance Components, Sample No. 128: B3056 Asphalt, < 2.5 μm Microcline.

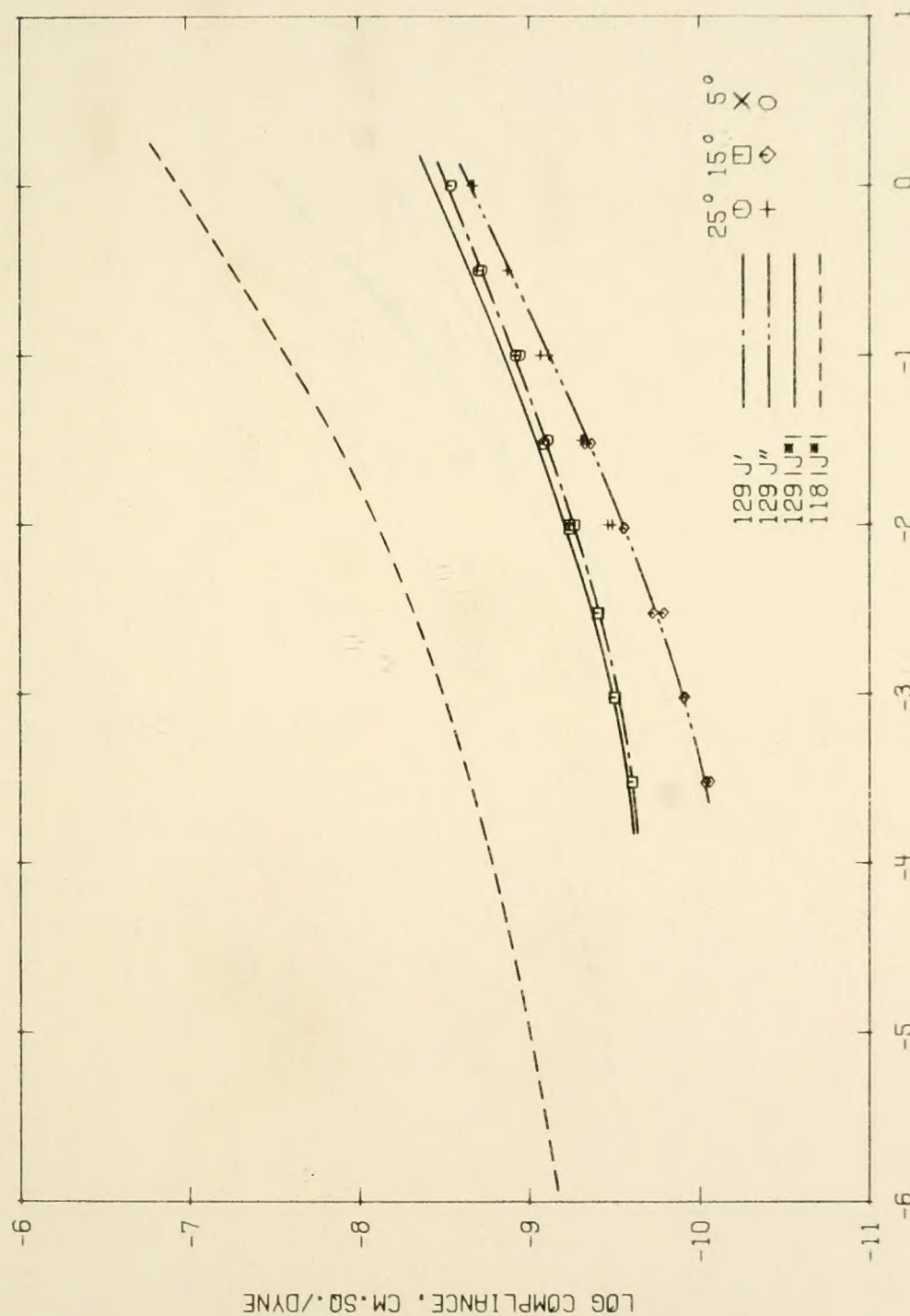


Figure 38. Dynamic Compliance Components, Sample No. 129: B3056 Asphalt, < 2.5 μm Apatite.

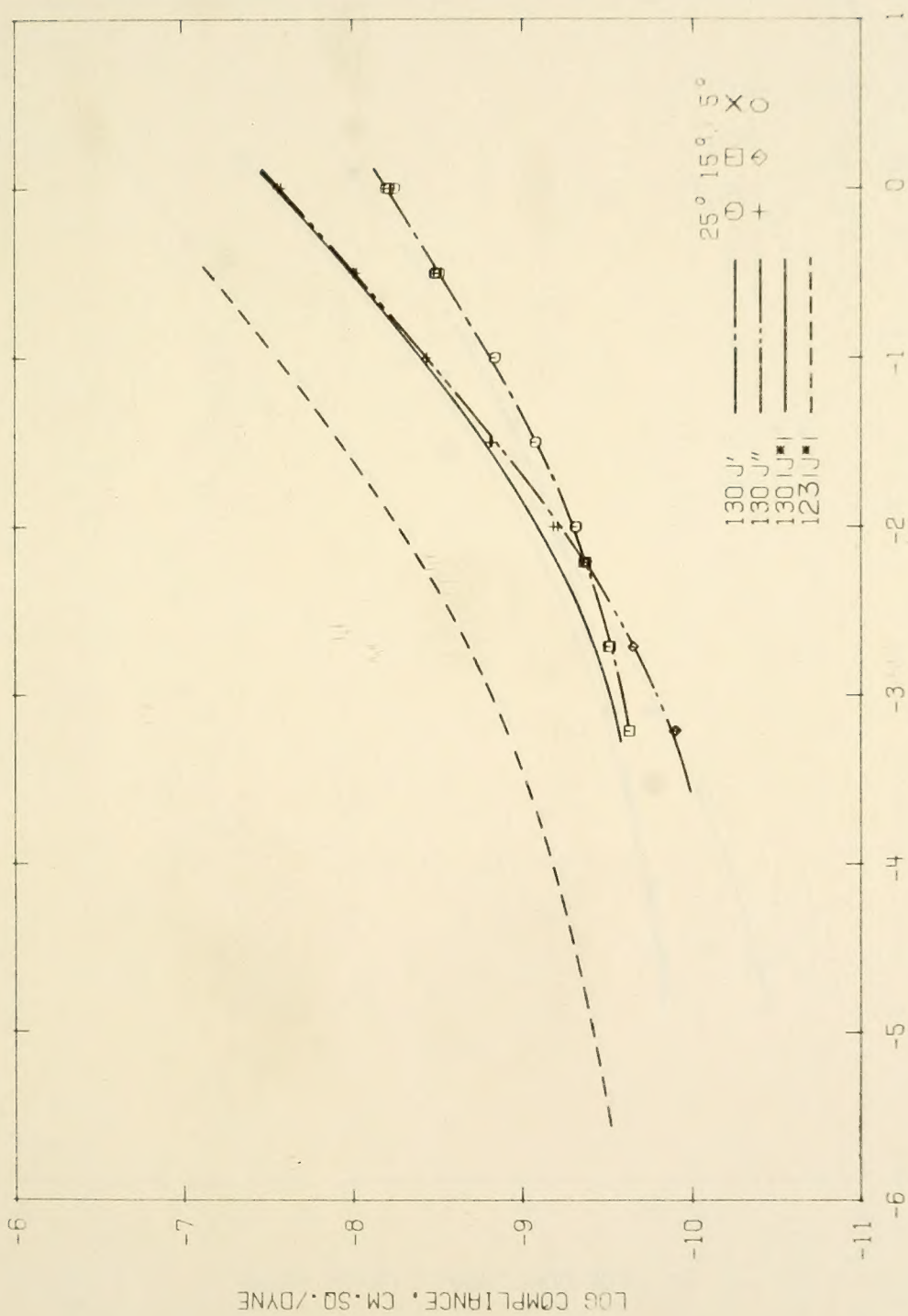


Figure 39. Dynamic Compliance Components, Sample No. 130: B3603 Asphalt, 2.5-5.0 μm Calcite.

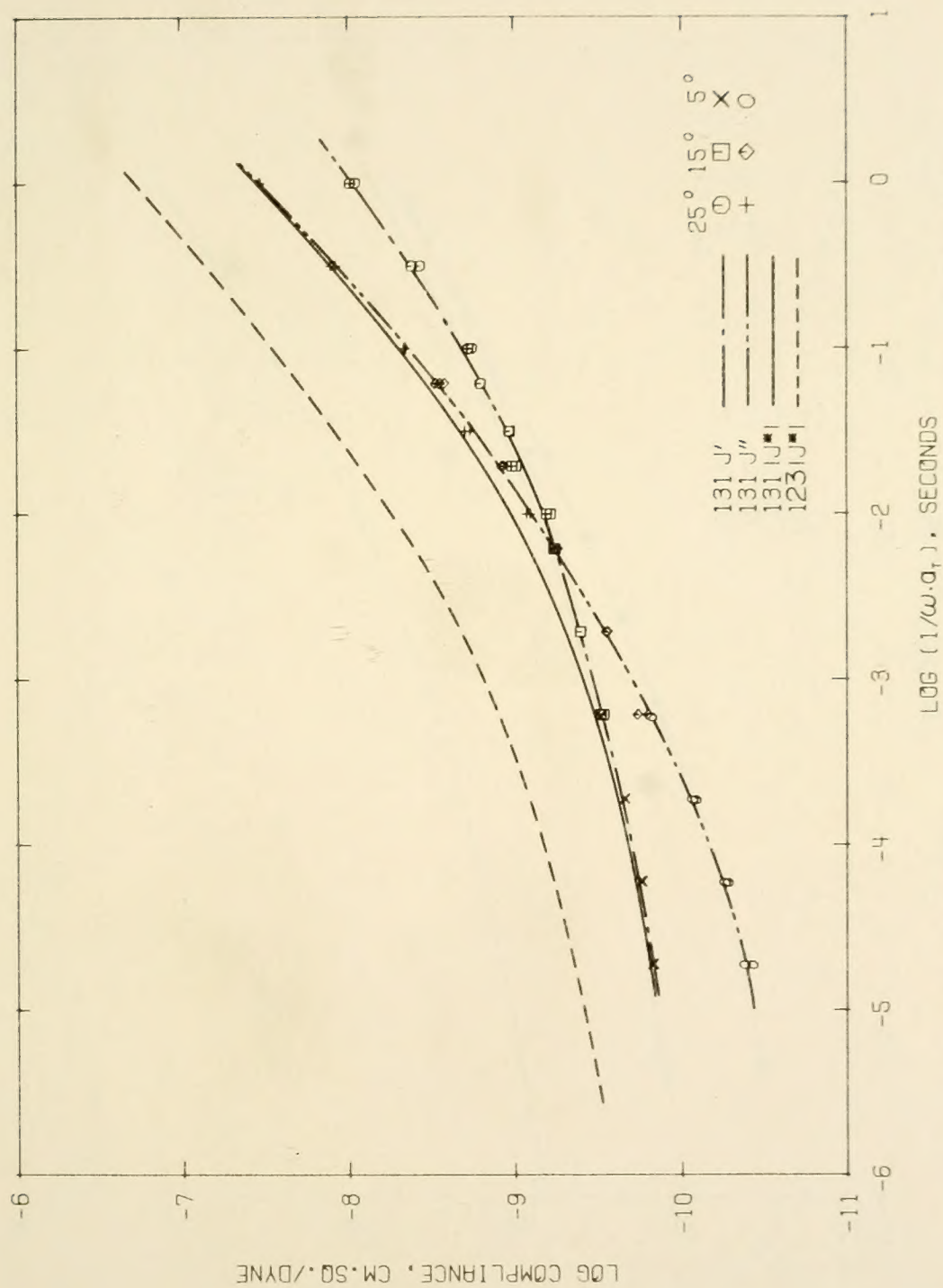


Figure 40. Dynamic Compliance Components, Sample No. 131: B3603 Asphalt, 2.5-5.0 μ m Quartz.

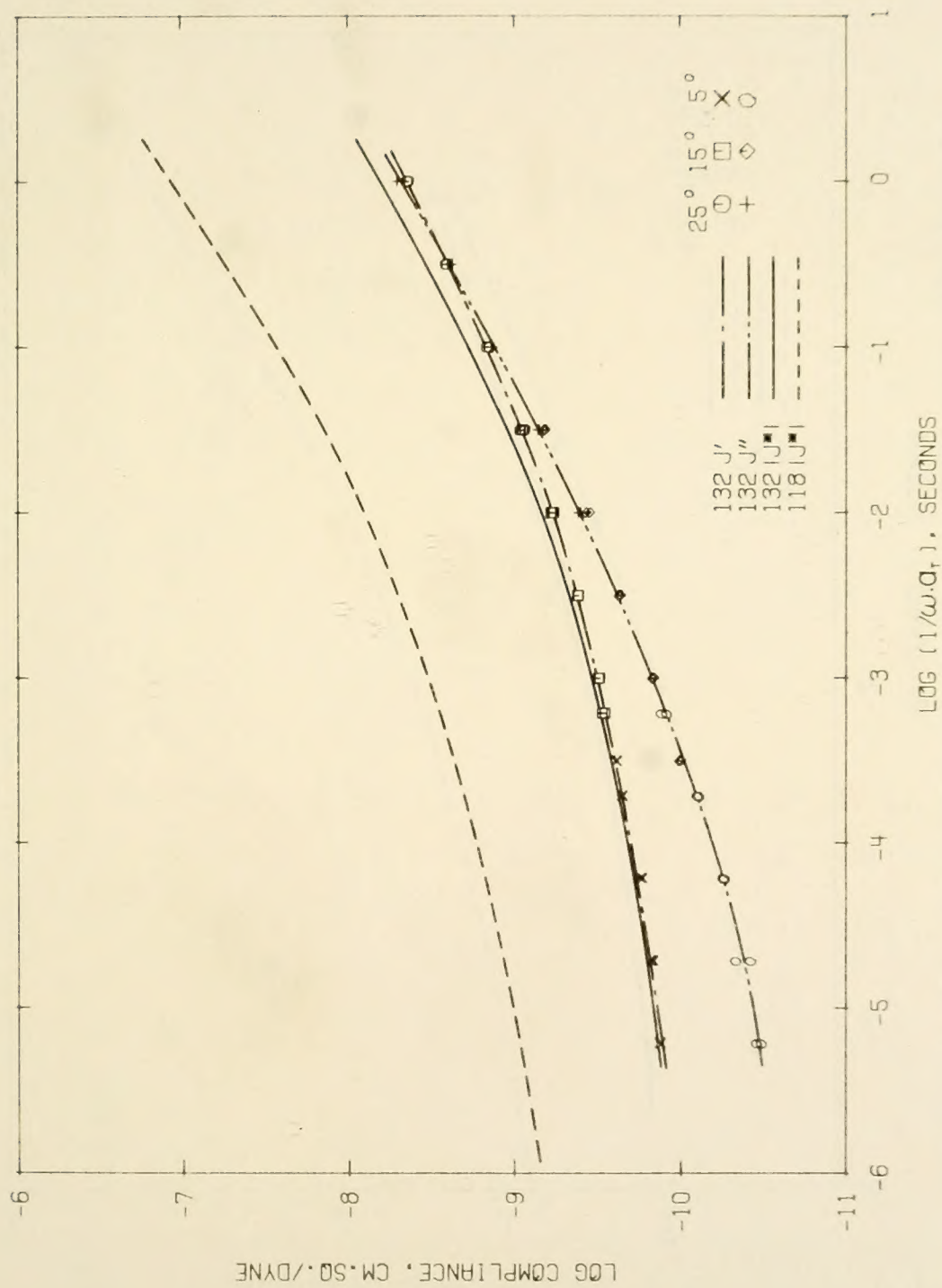


Figure 41. Dynamic Compliance Components, Sample No. 132: B3056 Asphalt, 0.63-1.25 μm Calcite.

behavior as evidenced by a reduction in the compliance components. The more elastic behavior at higher frequencies is reflected by the convergence of $|\bar{J}^*|$ and J' .

The "softer" behavior and the dominance of viscous flow at the lower frequencies (right hand side of the Figures) is reflected by the increase in the compliance components and the convergence of J'' and $|\bar{J}^*|$.

Retardation Spectra

The two dynamic compliance components, J' and J'' were used to calculate retardation spectra. While the retardation function, $L(\tau)$, is not usually of direct value in engineering calculations, it is often used by the chemist to characterize molecular processes in time-dependent materials.

Two different approximate methods, after Ninomiya and Ferry⁽⁵⁴⁾ and Williams and Ferry⁽⁵⁵⁾ were used to calculate $L(\tau)$. The average of the values determined by the two methods, calculated for both J' and J'' from sample 108, is given in Table 10. The data in this table have been plotted in Figure 43. While some local variances are noted, these are considered errors in the reduction scheme, and in general the two data points for any given τ lie quite close together.

Both J' and J'' should yield the same $L(\tau)$ function and agreement of the $L(\tau)$ values calculated from the two components is a good measure of the authenticity of the two components.⁽⁵⁶⁾ Figure 43 is typical of the data. Although some spread is occasionally noted at the high or low end of the time scale, the spread shown is considered minimal, supporting the validity of the individual J' and J'' curves.

Table 10. Calculated Retardation Spectra, Sample 108.

<u>τ</u>	<u>$\text{Log } L(\tau), J'$</u>	<u>$\text{Log } L(\tau), J''$</u>
0.00	- 8.74	- 8.72
-0.25	- 8.87	- 8.84
-0.50	- 8.96	- 8.95
-0.75	- 9.09	- 9.13
-1.00	- 9.21	- 9.29
-1.25	- 9.35	- 9.36
-1.50	- 9.47	- 9.46
-1.75	- 9.59	- 9.59
-2.00	- 9.69	- 9.70
-2.25	- 9.79	- 9.80
-2.50	- 9.93	- 9.90
-2.75	-10.06	-10.00
-3.00	-10.17	-10.07
-3.25	-10.27	-10.16
-3.50	-10.36	-10.29
-3.75	-10.44	-10.35
-4.00	-10.50	-10.41
-4.25	-10.58	-10.48
-4.50	-10.66	-10.54
-4.75	-10.76	-10.58

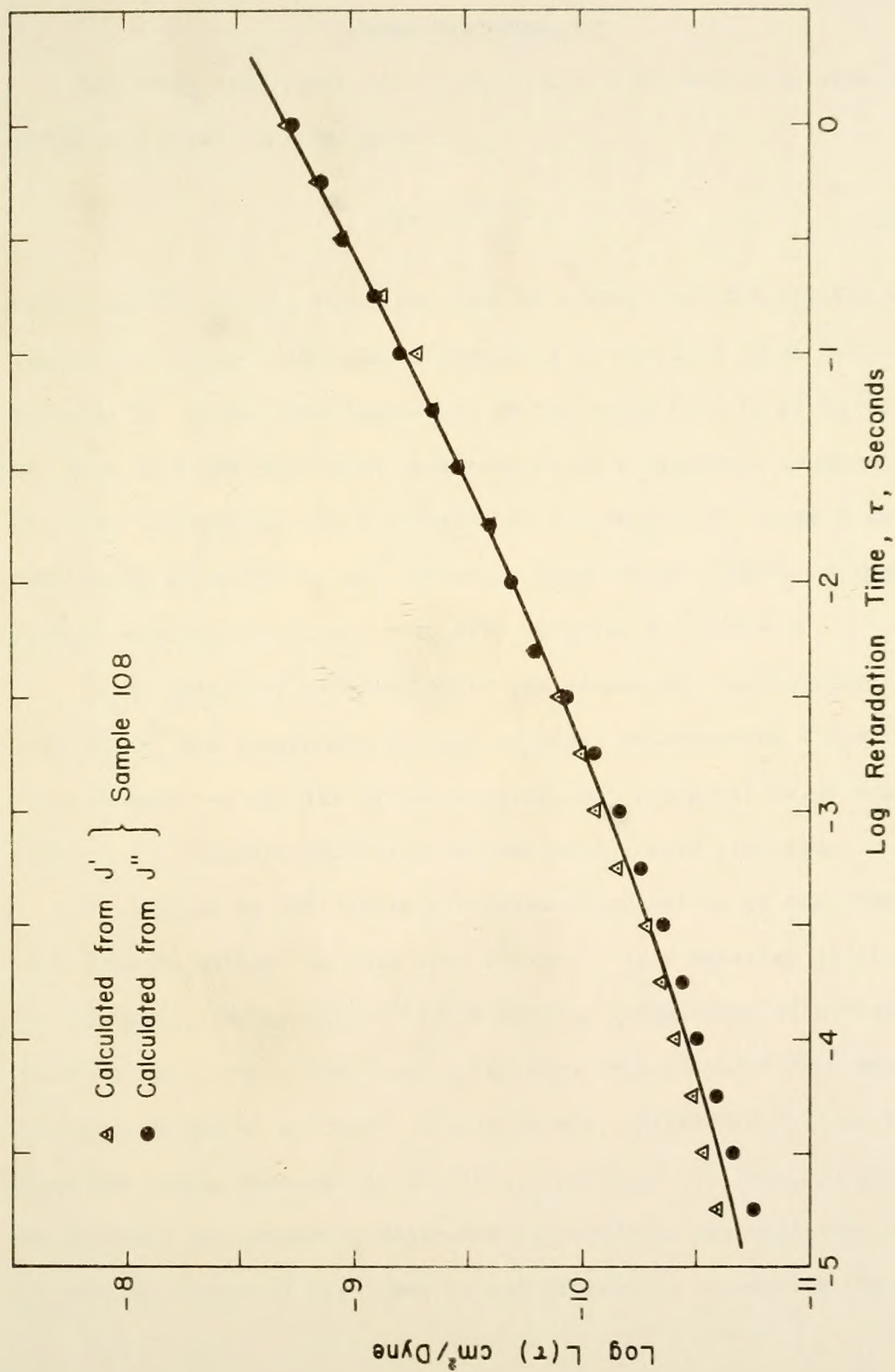


Figure 43. Retardation Spectra, Sample No. 108.

Creep Measurements

The creep compliance, $J(t)$, gives the relationship between shear strain and stress according to

$$J(t) = \frac{\gamma(t)}{\sigma_0} \quad 18$$

where the stress, σ_0 , takes the form of a step function applied at $t = 0$. Values of $J(t)$ were calculated according to Equation 18 as described in Appendix H. A complete tabulation of the creep data is given in Appendix I. Note that the data have been reduced to a reference temperature of 298 K by multiplying the $J(t)$ value by the ratio T/T_0 where T is the test temperature and T_0 the reference temperature, 298 K. A typical plot of reduced unshifted creep data is given in Figure 44.

Creep data were recorded after one second of loading time. A rise time for σ_0 was programmed at 0.06 seconds, representing a good compromise between the ability of the machine, the minimization of transient effects and the desirability of a reasonably rapid rise time.

Two checks on the linear viscoelastic character of the creep data were imposed before the data were shifted. If a material is linear viscoelastic, the creep compliance must be independent of stress.⁽⁴⁷⁾ This was found valid for creep compliance data computed from replicate tests performed at different stress levels. Reference is made to the data for sample numbers: 117/2, 25 C; 123/3, 25 C; 124/1, 25 C; etc., in Appendix H. Comparing values of $\log J(t)$ for the replicate tests at similar values of \log time, little difference is seen in the $\log J(t)$

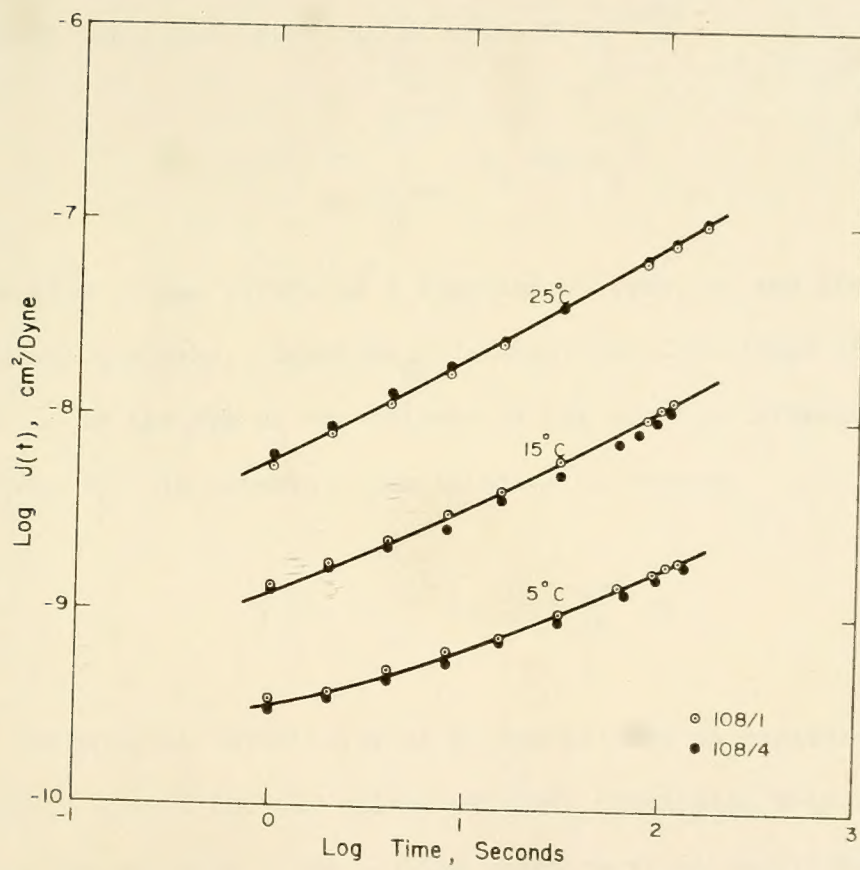


Figure 44. Typical Unshifted Creep Data, Sample No. 108.

values. (Note: stress levels are not given in the Appendix but differences are readily visualized by noting that stress is proportional to strain.)

A second check involves an application of the Boltzmann superposition principle which can be written as: ⁽⁴⁷⁾

$$\gamma(t) = \sum_{t_i=0}^{t_i=t} \sigma_i J(t-t_i) \quad 19$$

where $\gamma(t)$ is the strain as a function of time, t , and $J(t - t_i)$ is the creep function. Equation 19 states that the strain at any given time, t , is the sum of the effects of the previous stresses, σ_i , applied at times t_i . In integral form Equation 19 becomes

$$\gamma(t) = \int_0^t J(t-\theta) \frac{d\sigma}{d\theta} d\theta \quad 20$$

Assuming the additivity of stress history as expressed by Equations 19 and 20, the values of creep compliance were extended by adding the recovery curve and the creep curve at equivalent times. A schematic of the construction is given in Figure 45.

The recovery curve may be considered as the sum of σ_0 applied at t_0 and $-\sigma_0$ applied at t_u ;

$$\gamma(t) \Big|_{t > t_u} = \sigma_0 J(t) + (-\sigma_0) J(t-t_u) \Big|_{\text{recovery}}$$

The superposed curve, Figure 45, may be considered as the sum of three loads; σ_0 applied at $t = 0$ and $(+\sigma_0)$ and $(-\sigma_0)$ applied at $t - t_u$.

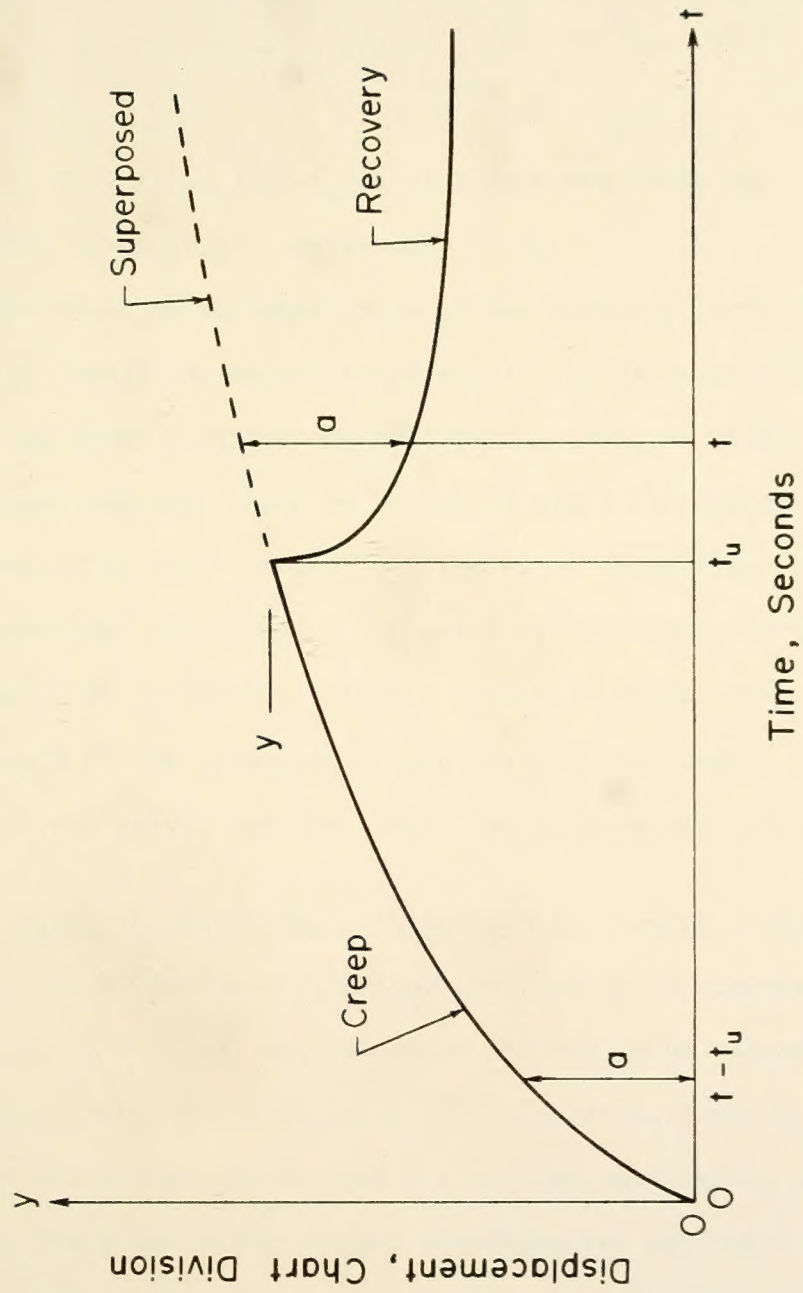


Figure 45. Construction of Superposed Creep Curve.

$$\begin{aligned}
 \gamma(t) \Big|_{t > t_u} &= \sigma_o J(t) + (-\sigma_o)J(t-t_u) + \sigma_o J(t-t_u) \Big|_{\text{superposed}} \\
 &= \sigma_o J(t) \Big|_{\text{creep}}
 \end{aligned}
 \tag{21}$$

where $\sigma_o J(t) + (-\sigma_o)J(t-t_u)$ is the recovery curve and $\sigma_o J(t-t_u)$ is the creep curve with t_o referenced to t_u .

The check on the additivity of the recovery portion and the validity of the Boltzmann superposition principle is the equality of the superposed and creep portions of Equation 21. Typical plots of creep and superposed data are shown in Figure 46 where the superposed data are represented by open circles. To the extent that they form smooth curves, the superposed data predict the shape of the creep curve with good accuracy. No attempt to extend a replicate creep curve to the extended time scale of the superposed curve was made because of the smoothness of the creep curves and the later time-temperature shifting of the data.

Creep Testing - Presentation and Discussion of Results

The creep data are presented graphically in Figures 47 through 62. Before being plotted, the data were shifted using values of a_T determined from the shifting of $|\bar{J}^*|$, Tables 6, 7 and 8. An examination of the figures shows that the shifted data define a single, smooth curve. There are a few obvious discrepancies but these are attributable to experimental errors. (See "Test Procedures" section) From the appearance of the plotted data a single a_T function is seen to shift both $|\bar{J}^*|$, J' , J'' and $J(t)$.

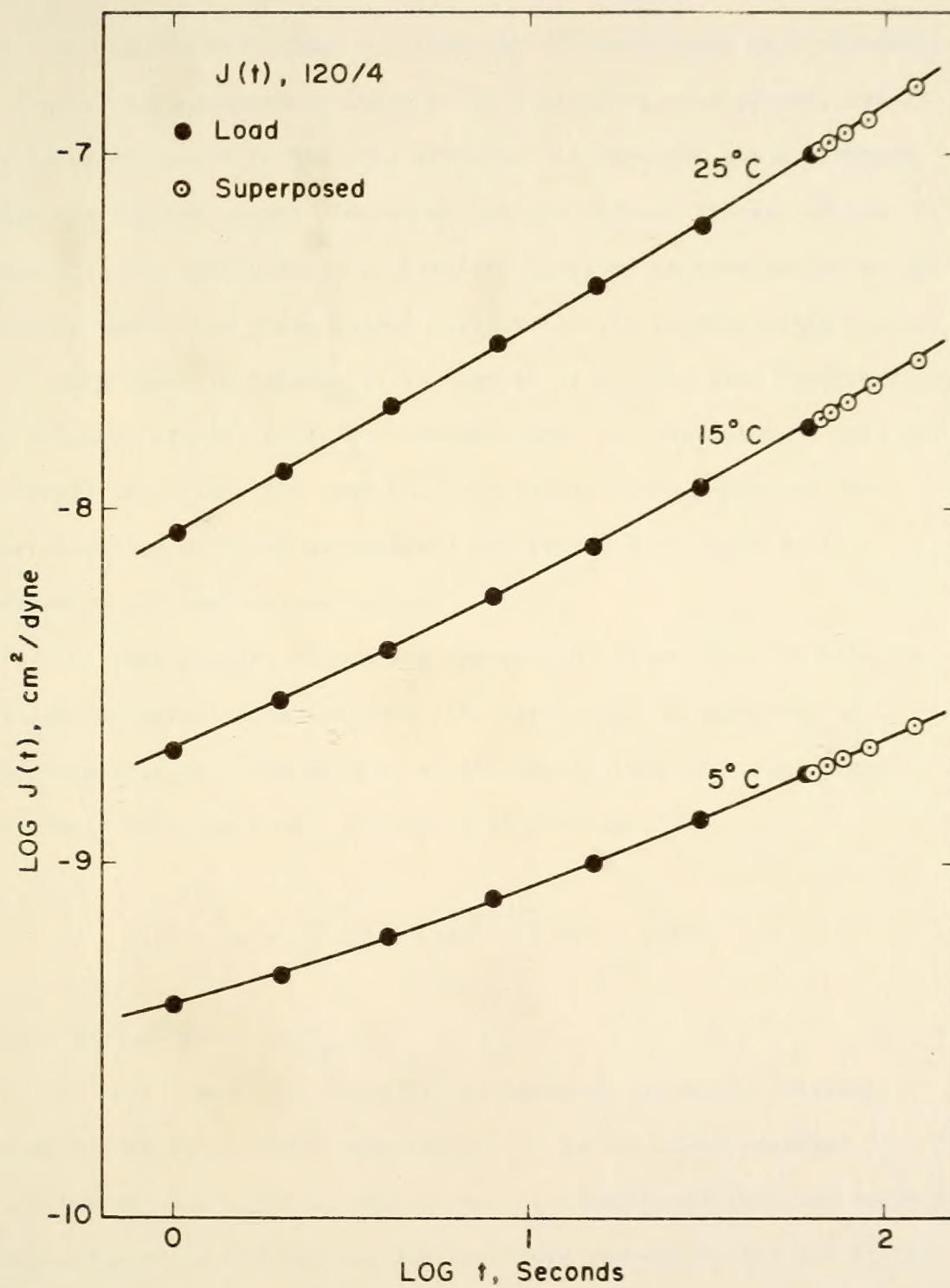


Figure 46. Extension of Creep Data by Superposition.

In Figures 47 through 62, each set of data points that represent a single creep experiment include two superposed data points, calculated as discussed in the last section. In each set the superposed data are the two points plotted at the two largest times. As was the case with the unshifted data (previous section) an examination of the Figures shows that these points blend well with adjacent data points.

Also shown in Figures 47 through 62 is a solid line, representing an estimate of $J(t)$ using the dynamic data. A discussion of this is deferred until the next section. The dashed lines represent the corresponding unfilled asphalt and are intended to serve as a reference for the various curves.

The same general trends are observable in the data for both the filled and unfilled materials. $J(t)$ approaches an asymptote of approximately 10^{-10} cm sq/dyne at the short times and rises monotonically with log time. According to Equation 4:

$$J(t) = J_g + \int_{-\infty}^{+\infty} L(\tau) (1 - e^{-t/\tau}) d \ln \tau + t/\eta \quad 22$$

where the asymptote is J_g .

At long times, the value of the integral becomes a constant, equal to the equilibrium compliance J_e . In the model analogy, J_e is obtained only after all the stress is transferred from the dashpots (excepting η) to the springs and therefore represents the sum of the compliances of all the springs. J_e represents energy stored and recoverable only after the occurrence of flow in the dashpots and therefore is termed delayed elasticity.

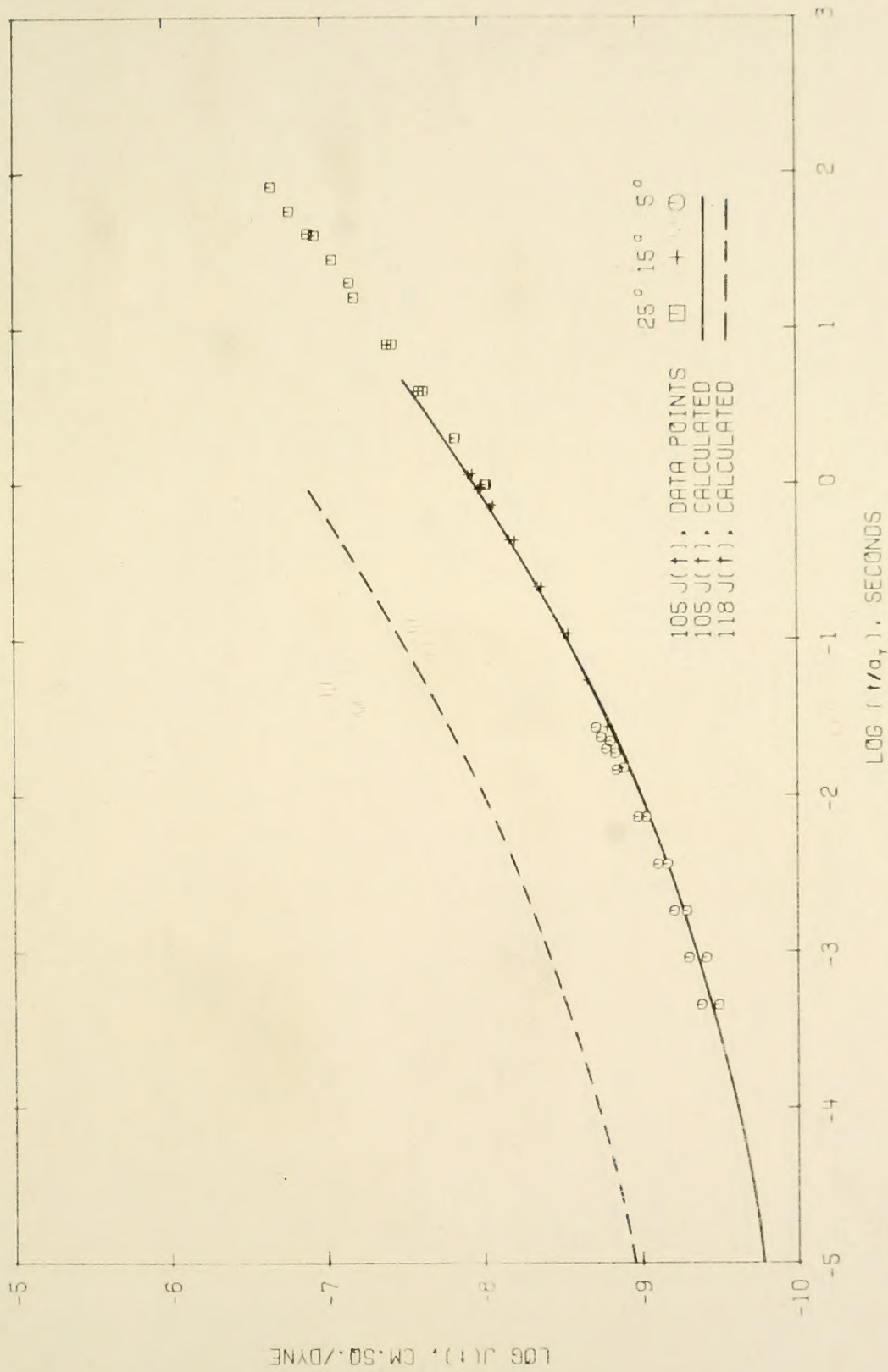


Figure 47. Creep Compliance, Sample No. 105: B3056 Asphalt, 10.-20. um Calcite.

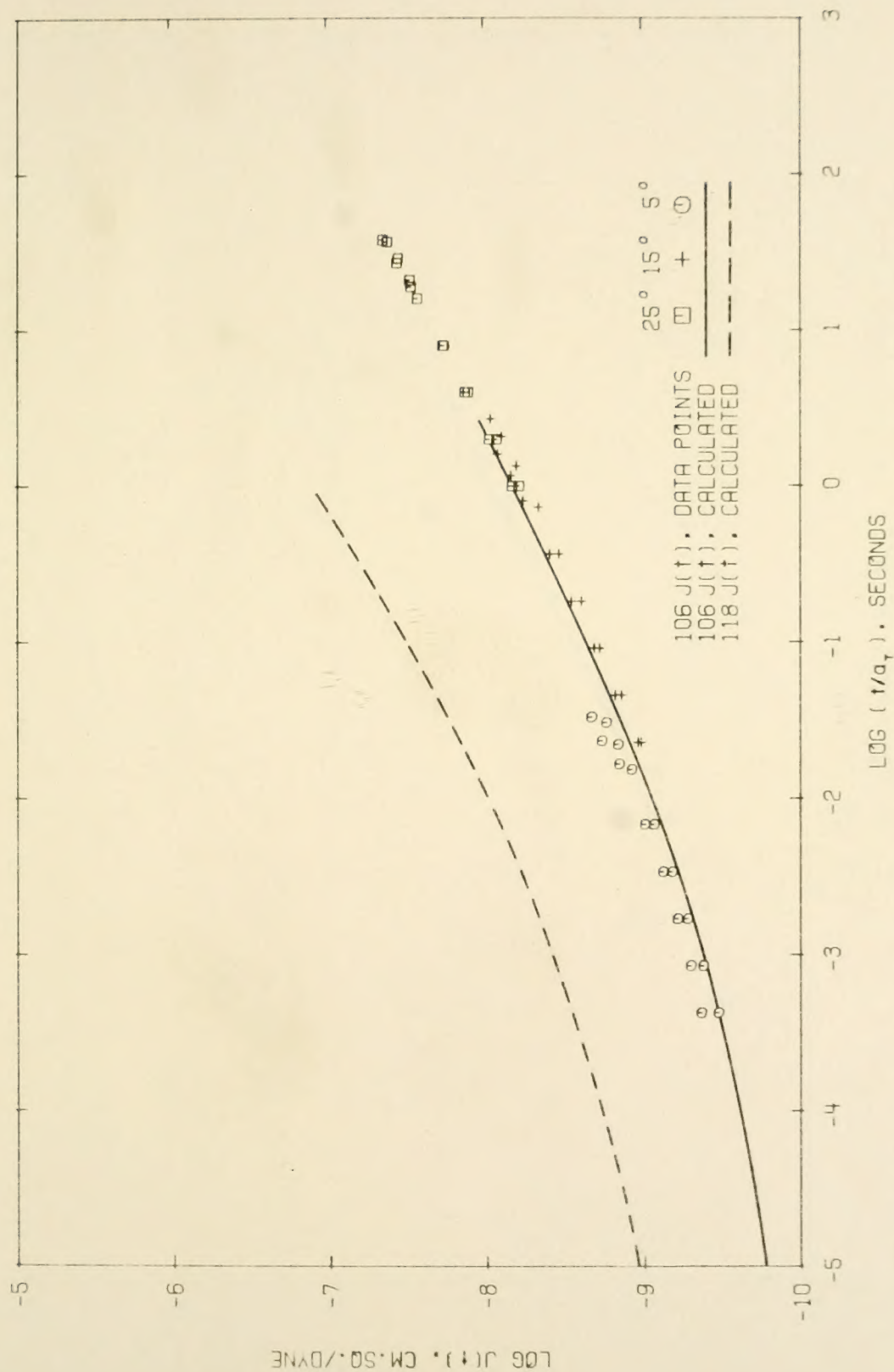


Figure 48. Creep Compliance, Sample No. 106: B3056 Asphalt, 2.5-5.0 μm Quartz.

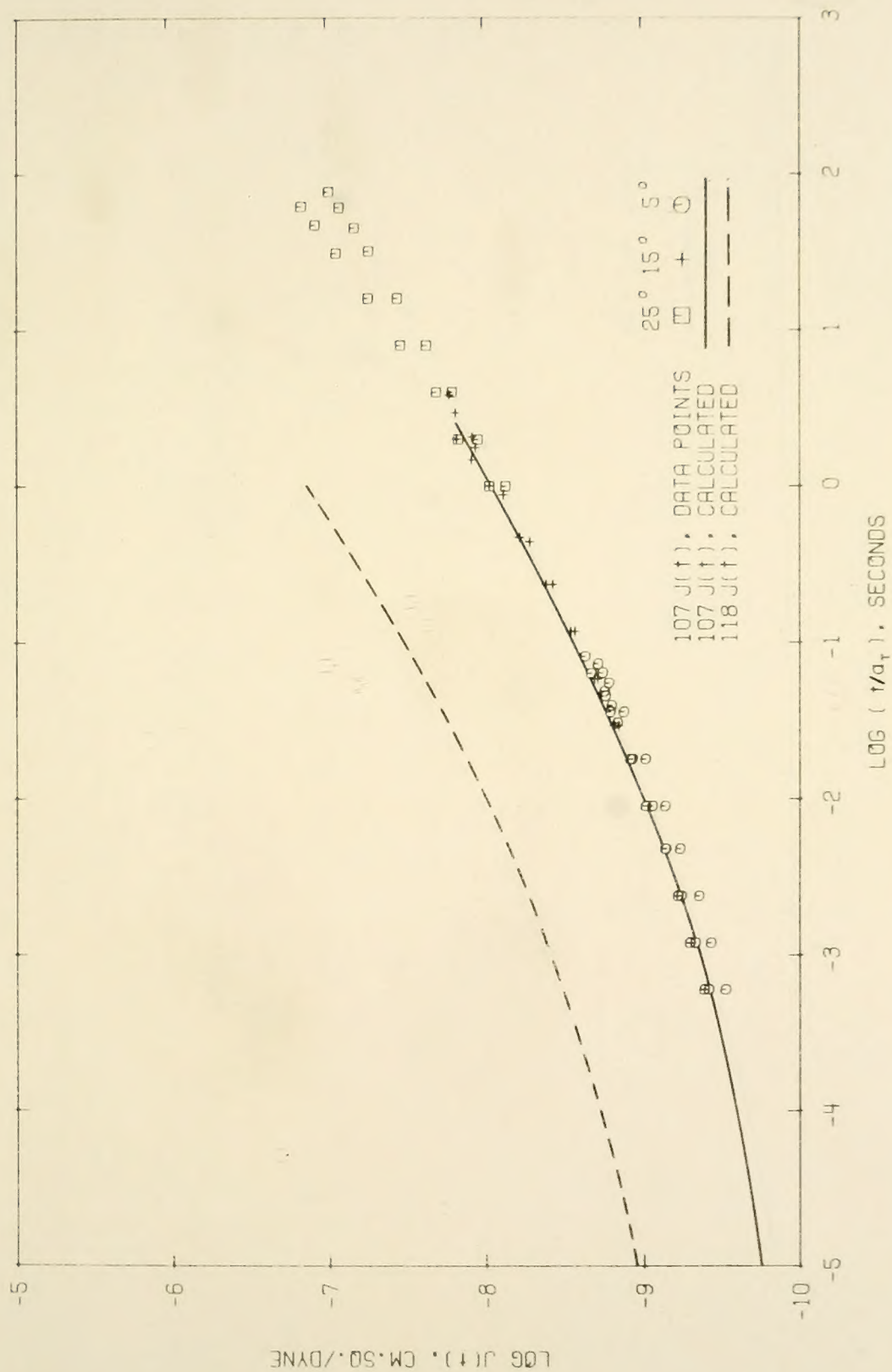


Figure 49. Creep Compliance, Sample No. 107: B3056 Asphalt, 10.-20. μm Quartz.

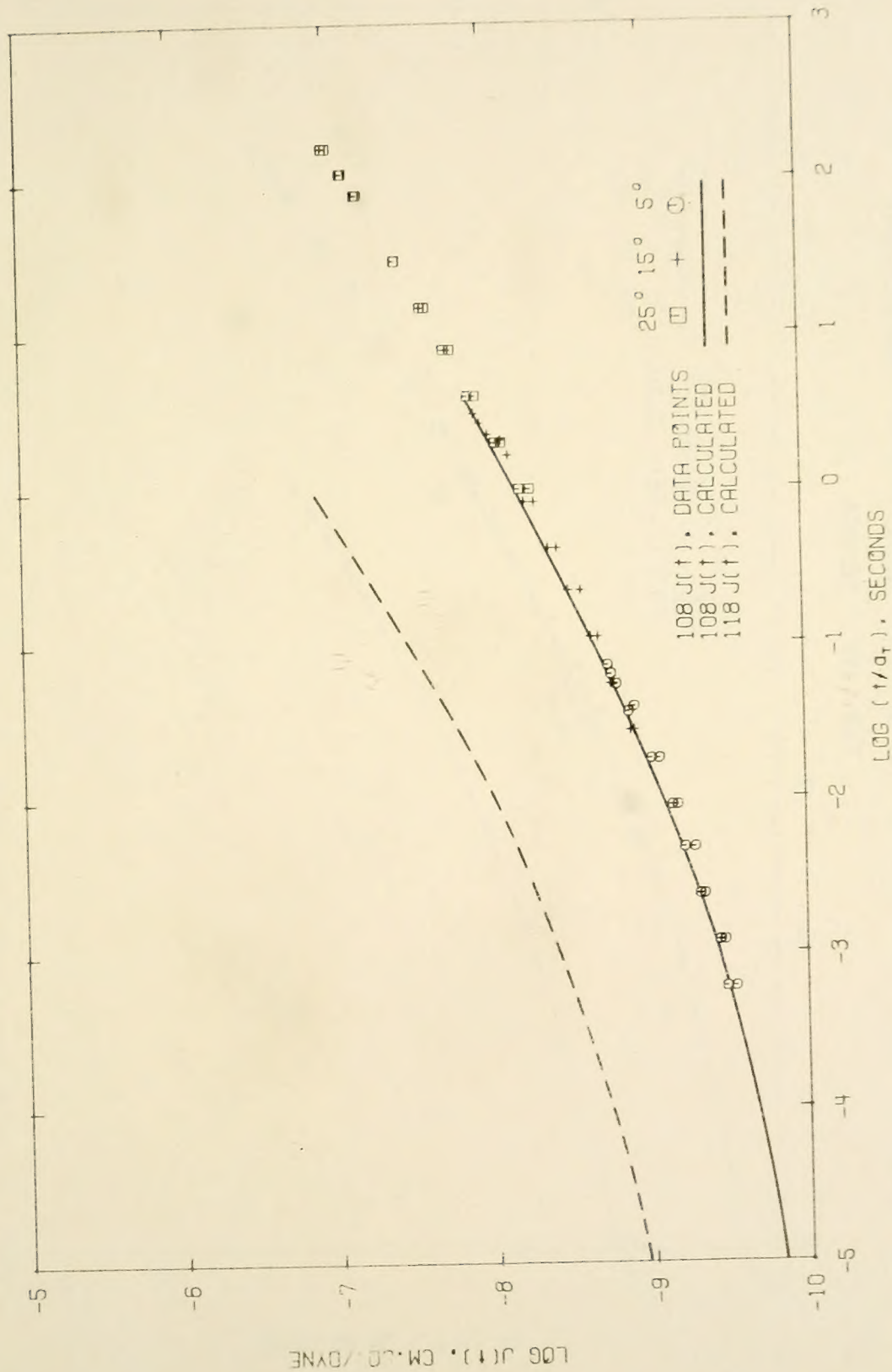


Figure 50. Creep Compliance, Sample No. 108: B3056 Asphalt, 2.5-5.0 μ m Calcite.

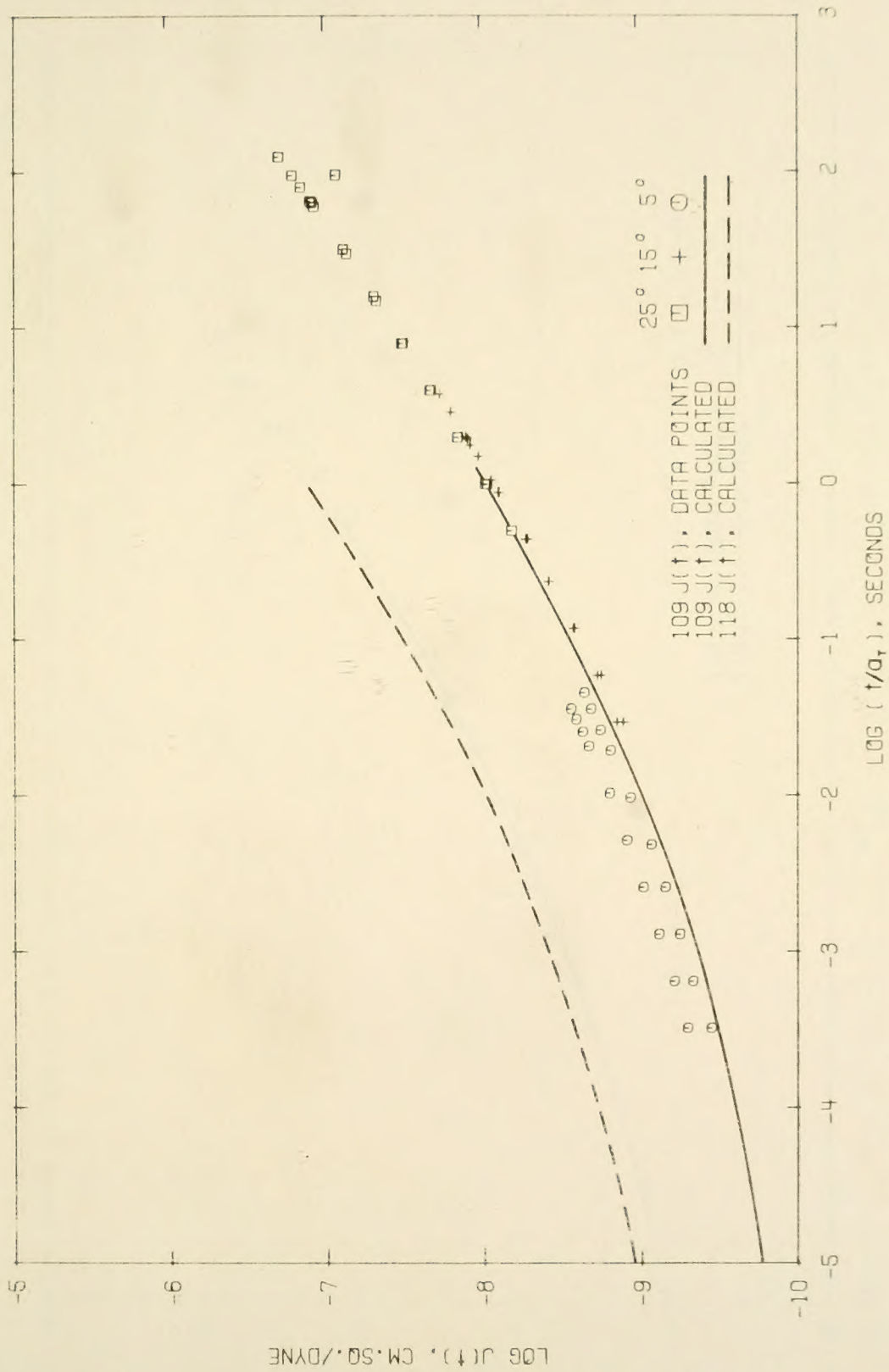


Figure 51. Creep Compliance, Sample No. 109: B3056 Asphalt, Graded Calcite.

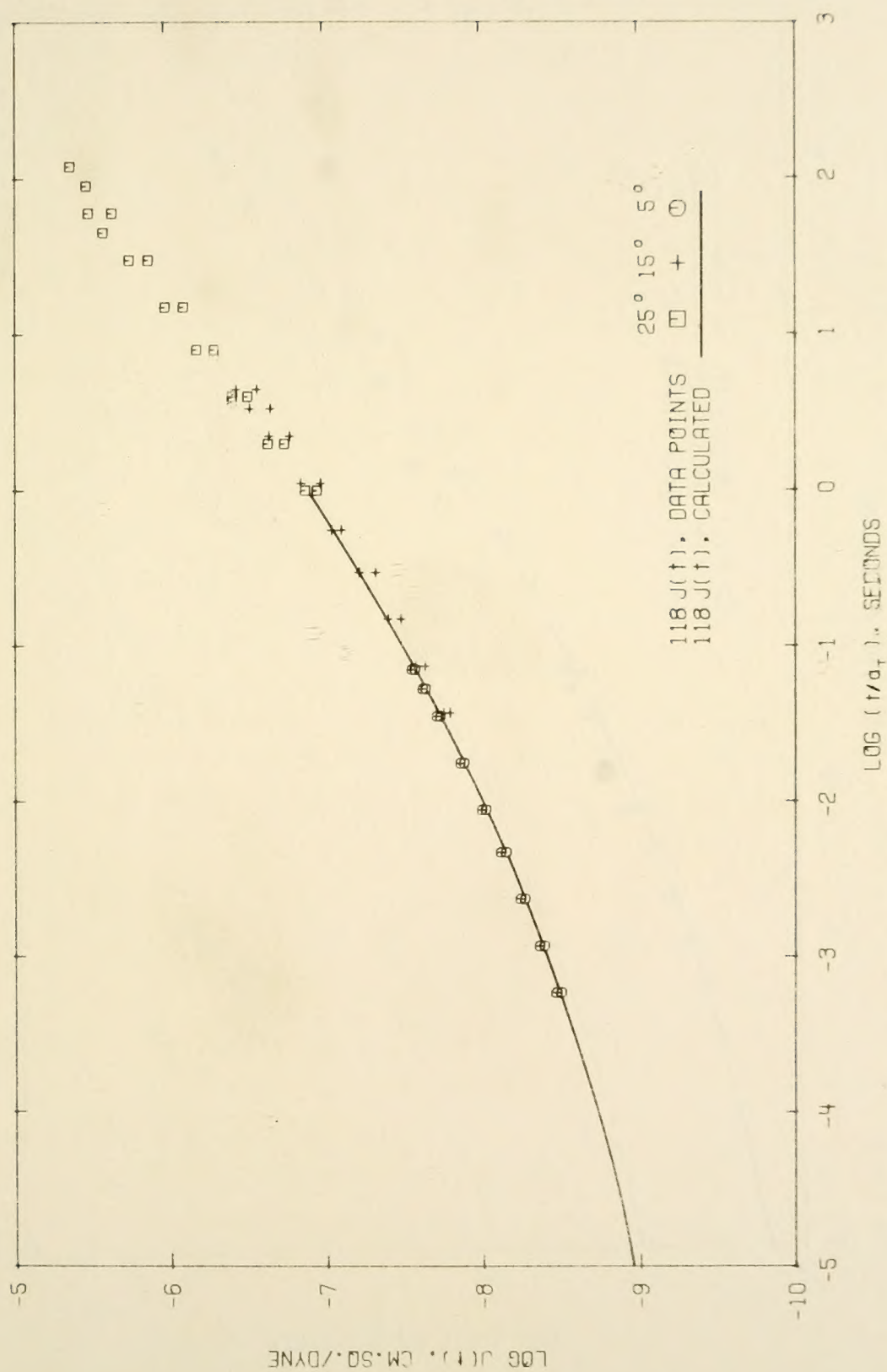


Figure 52. Creep Compliance, Sample No. 118: Unfilled B3056 Asphalt.

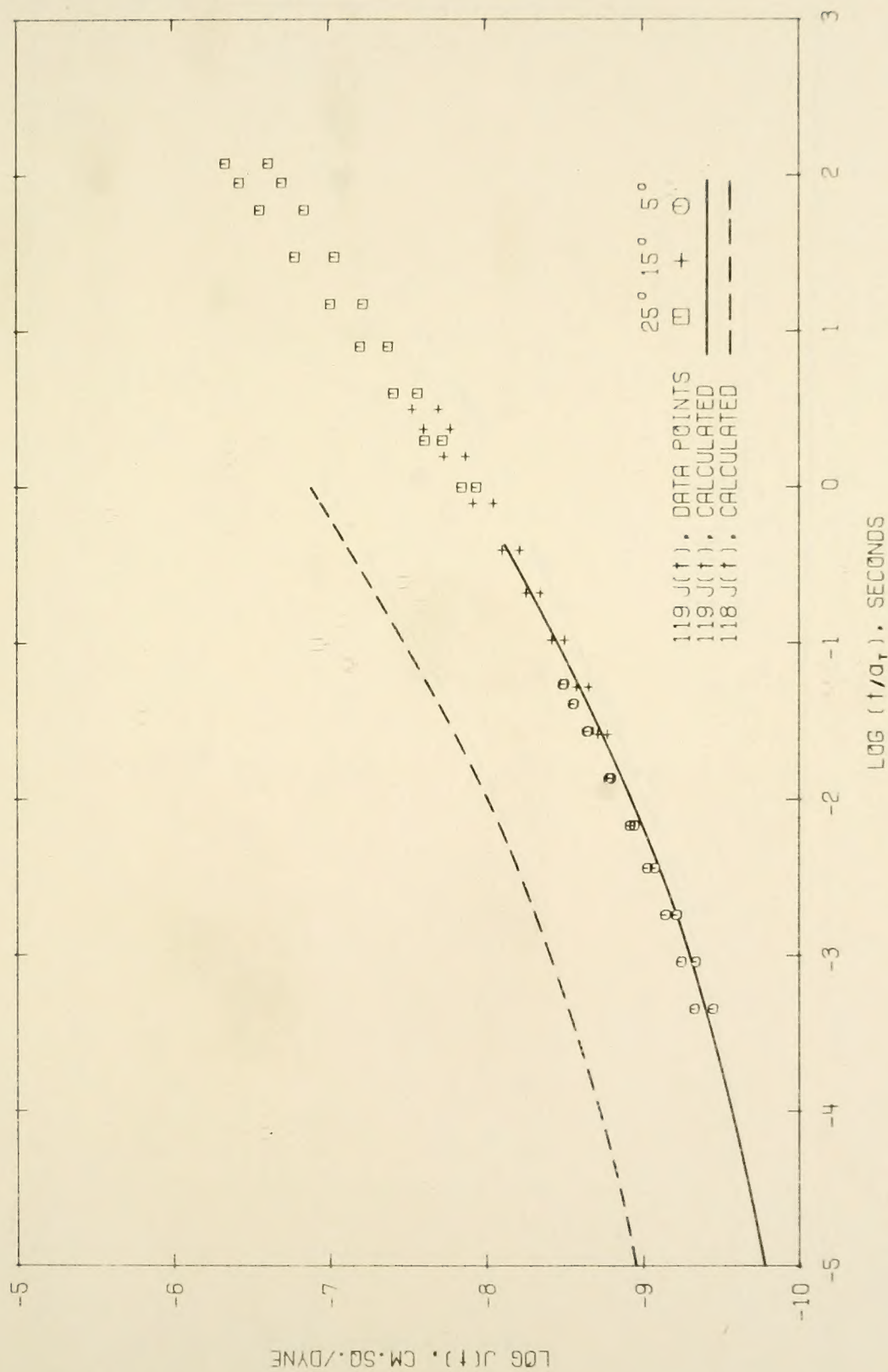


Figure 53. Creep Compliance, Sample No. 118: B3056 Asphalt, Graded Quartz.

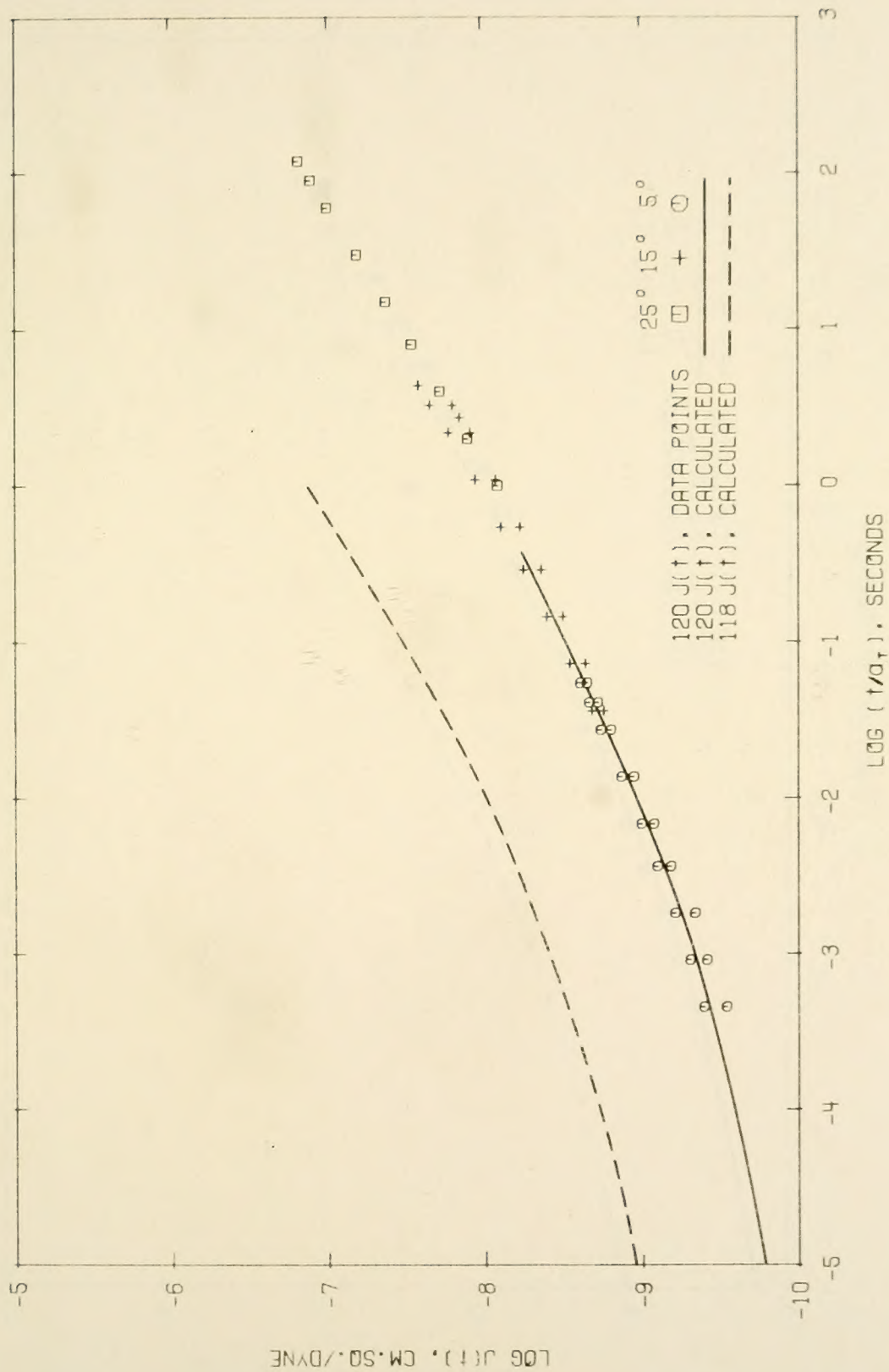


Figure 54. Creep Compliance, Sample No. 120: B3056 Asphalt, 2.5-5.0 μm Quartz.

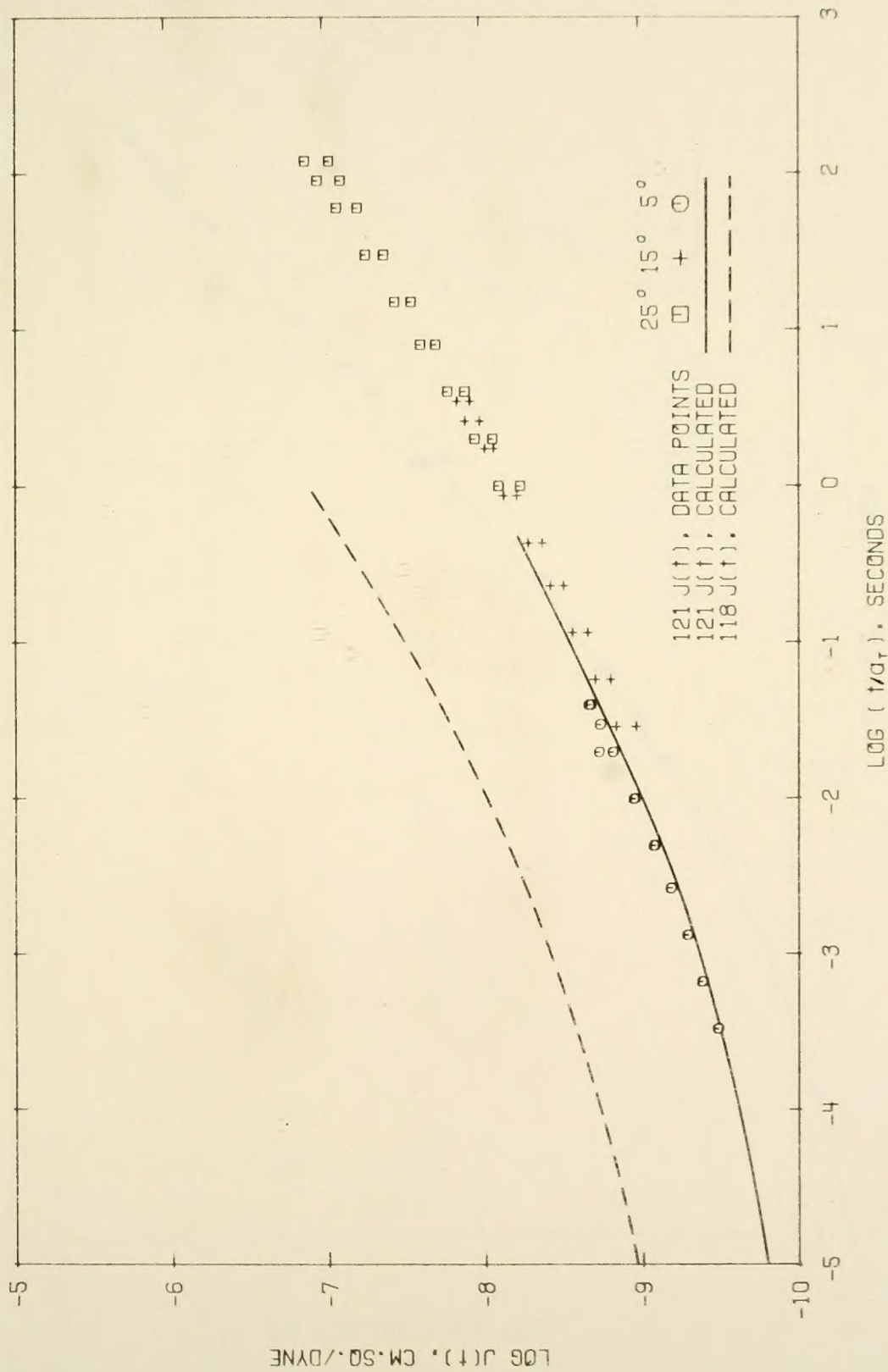


Figure 55. Creep Compliance, Sample No. 121: B3056 Asphalt, 2.5-5.0 μm Calcite.

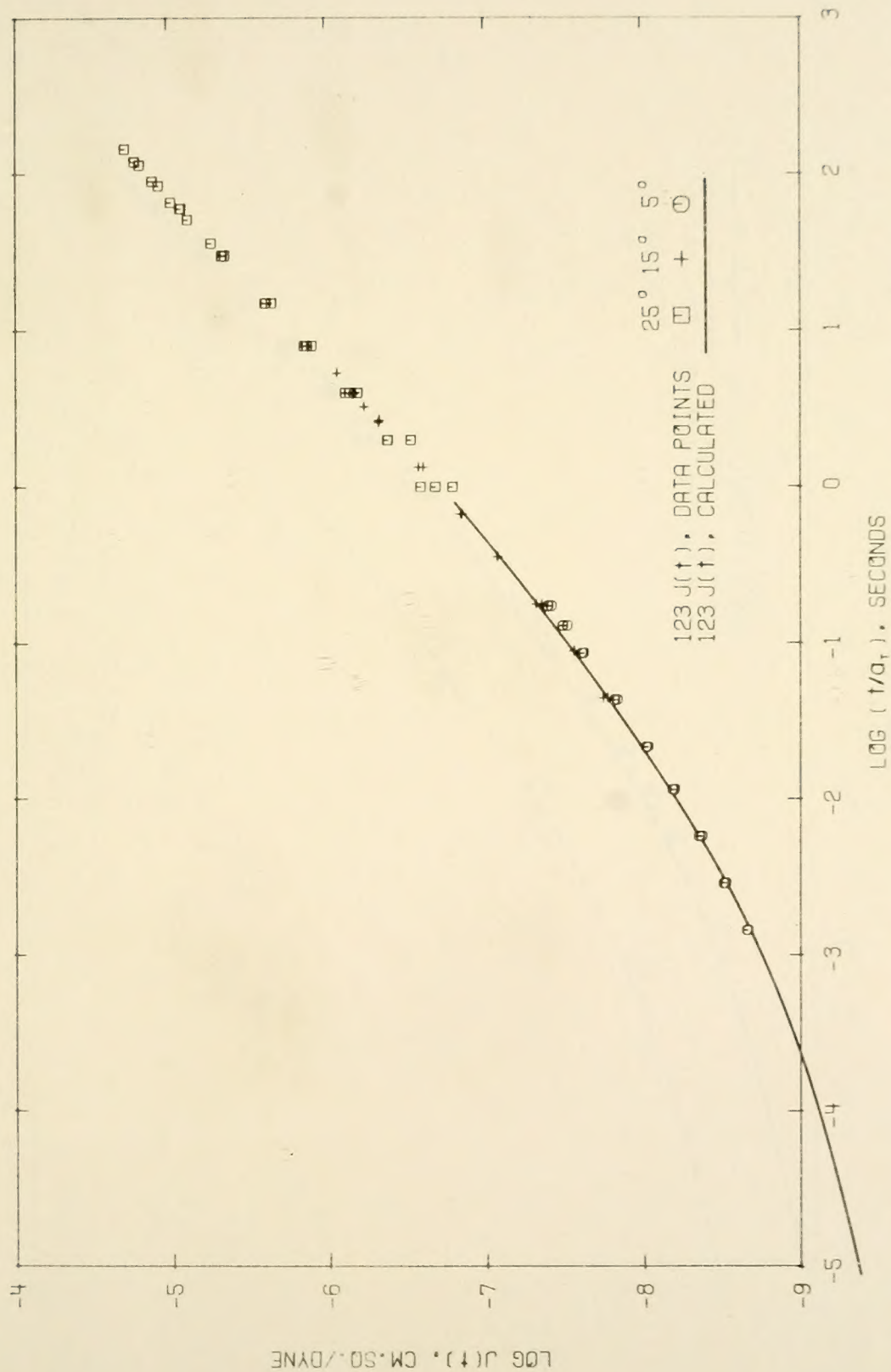


Figure 56. Creep Compliance, Sample No. 123: Unfilled B3603 Asphalt.

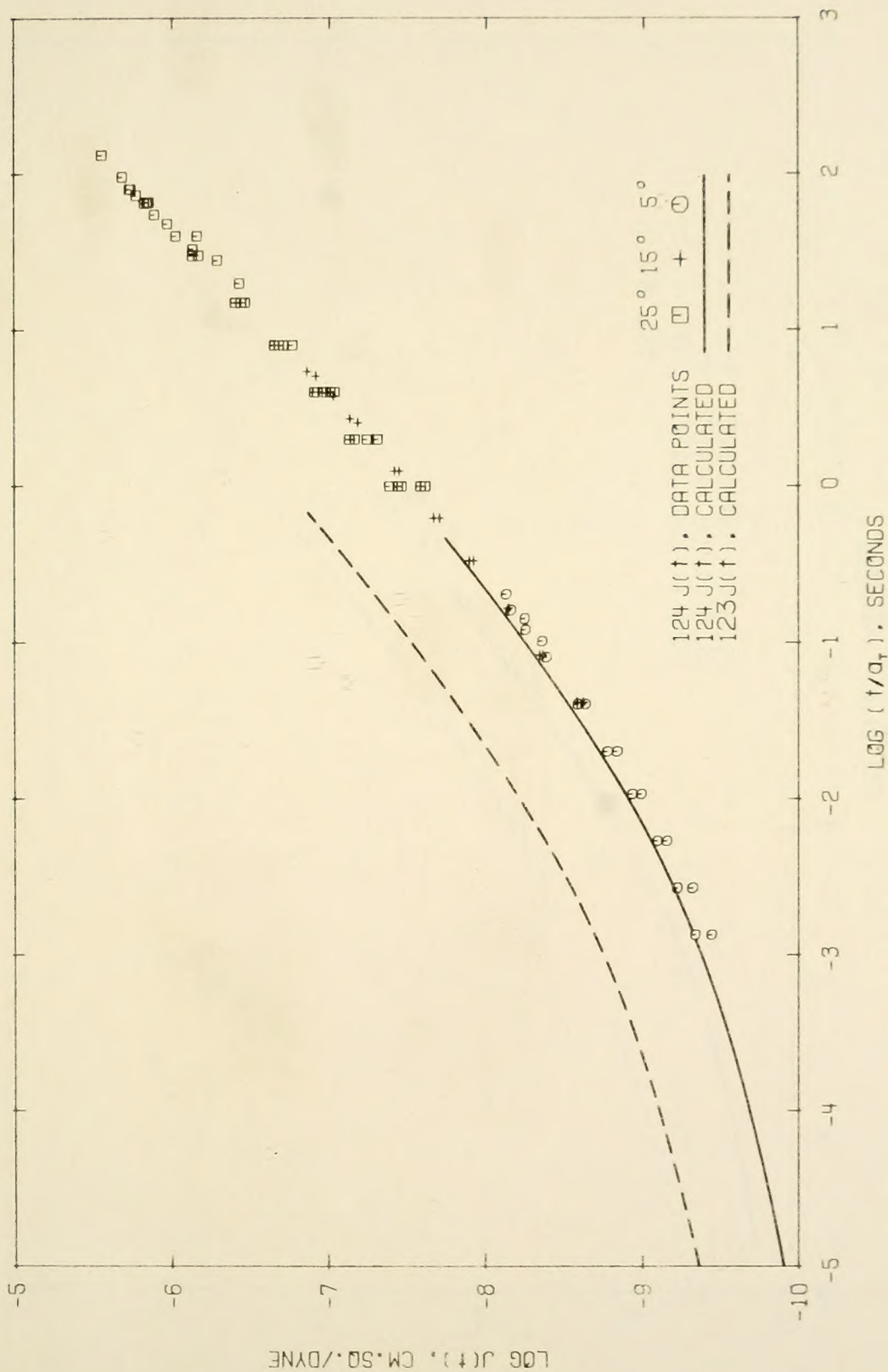


Figure 57. Creep Compliance, Sample No. 124: B3603 Asphalt, 10.-20.µm Calcite.

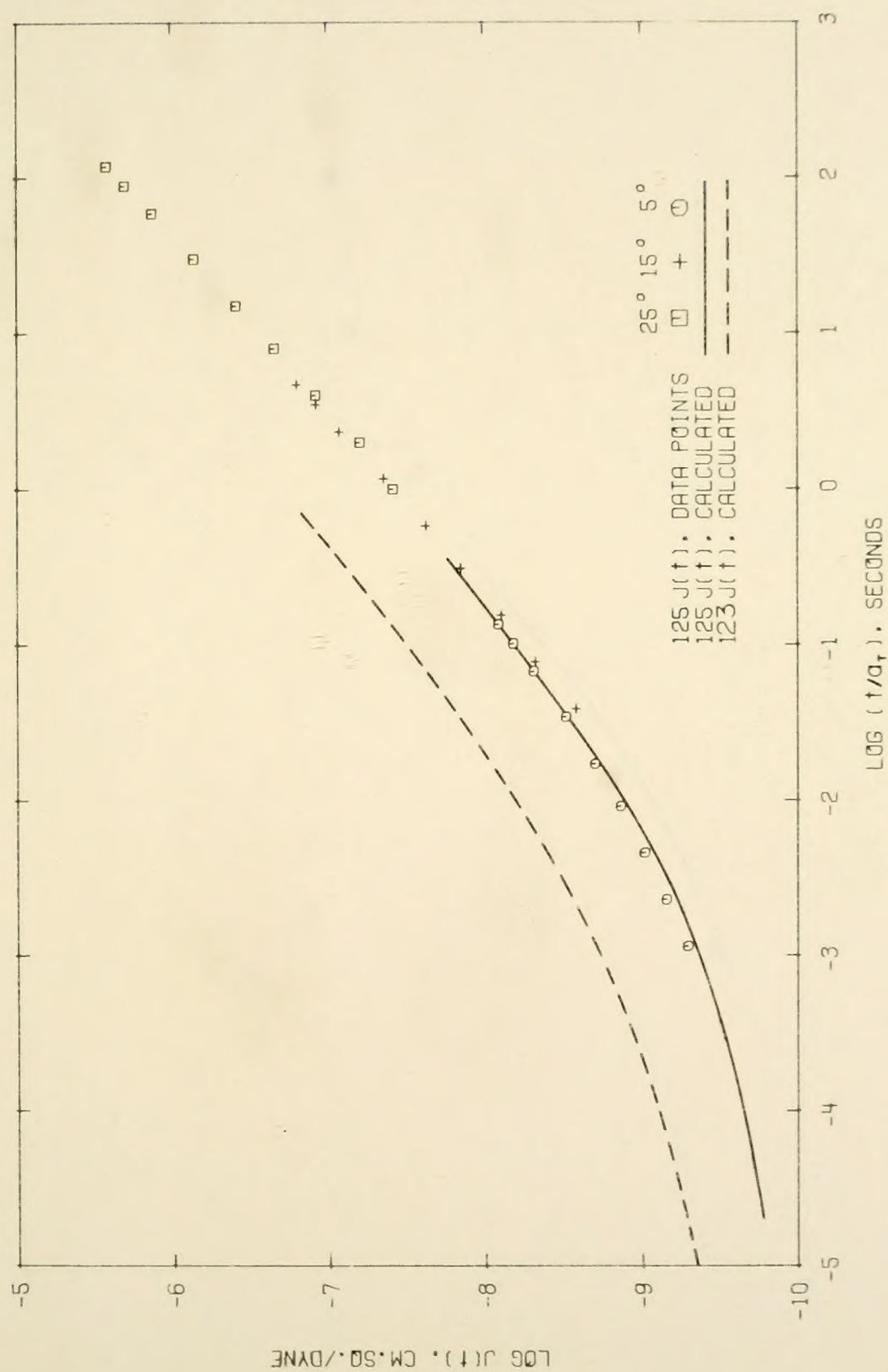


Figure 58. Creep Compliance, Sample No. 125: B3603 Asphalt, 10.-20. μm Quartz.

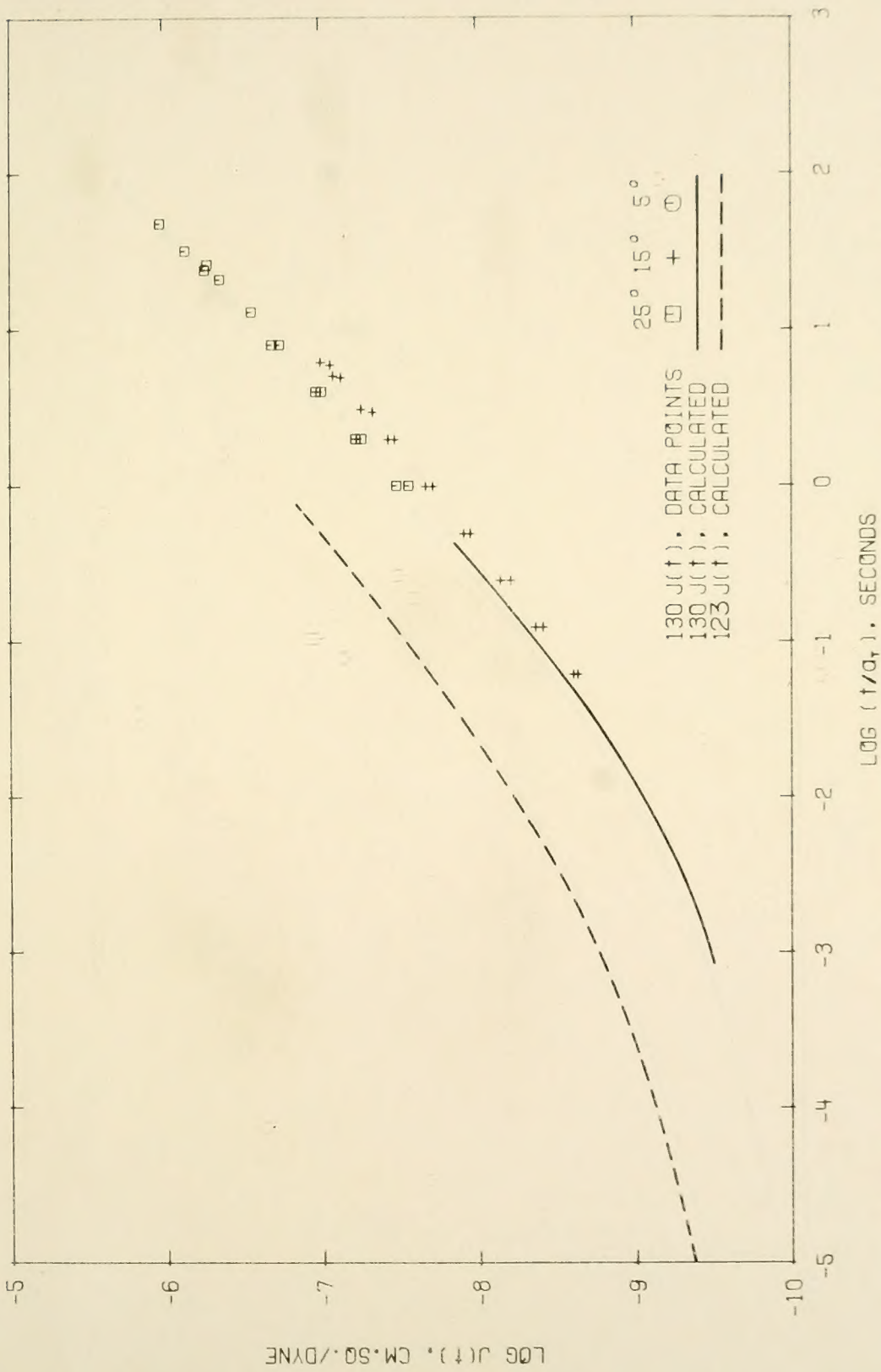


Figure 59. Creep Compliance, Sample No. 130: H3603 Asphalt, 2.5-5.0 μm Calcite.

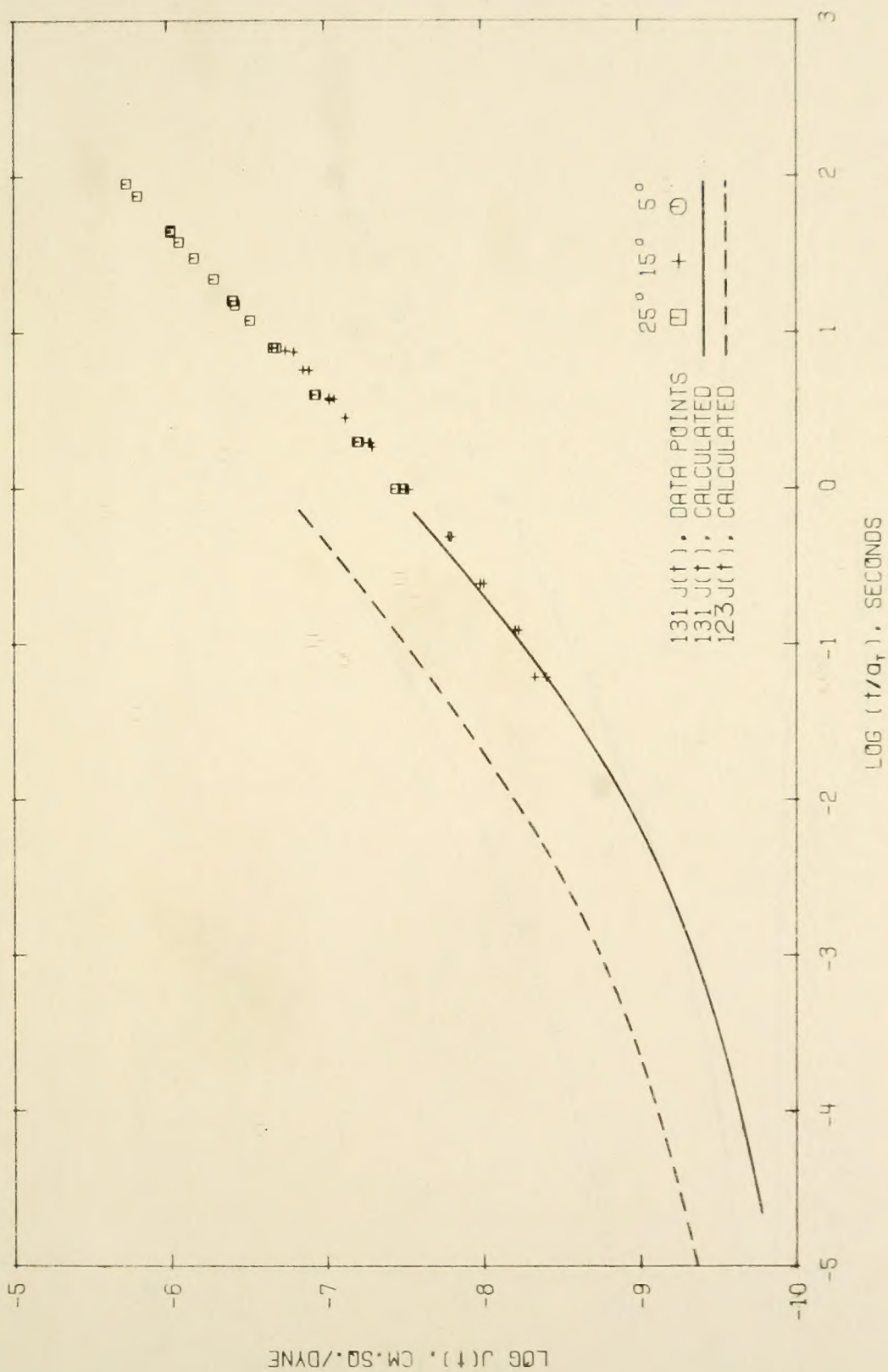


Figure 60. Creep Compliance, Sample No. 131: B3603 Asphalt, 2.5-5.0 μm Quartz.

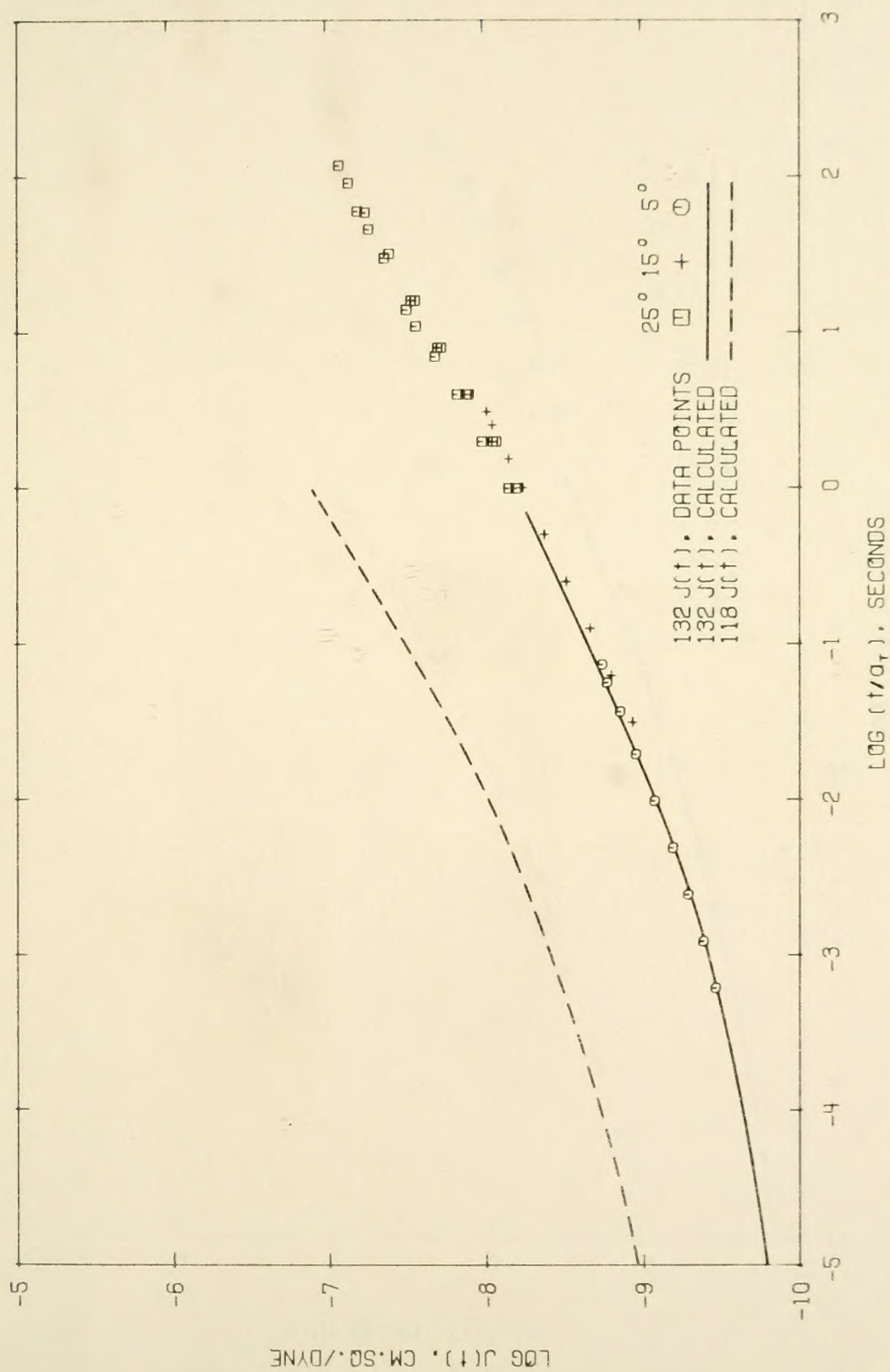


Figure 61. Creep Compliance, Sample No. 132: B3056 Asphalt, 0.63-1.25 μm Calcite.

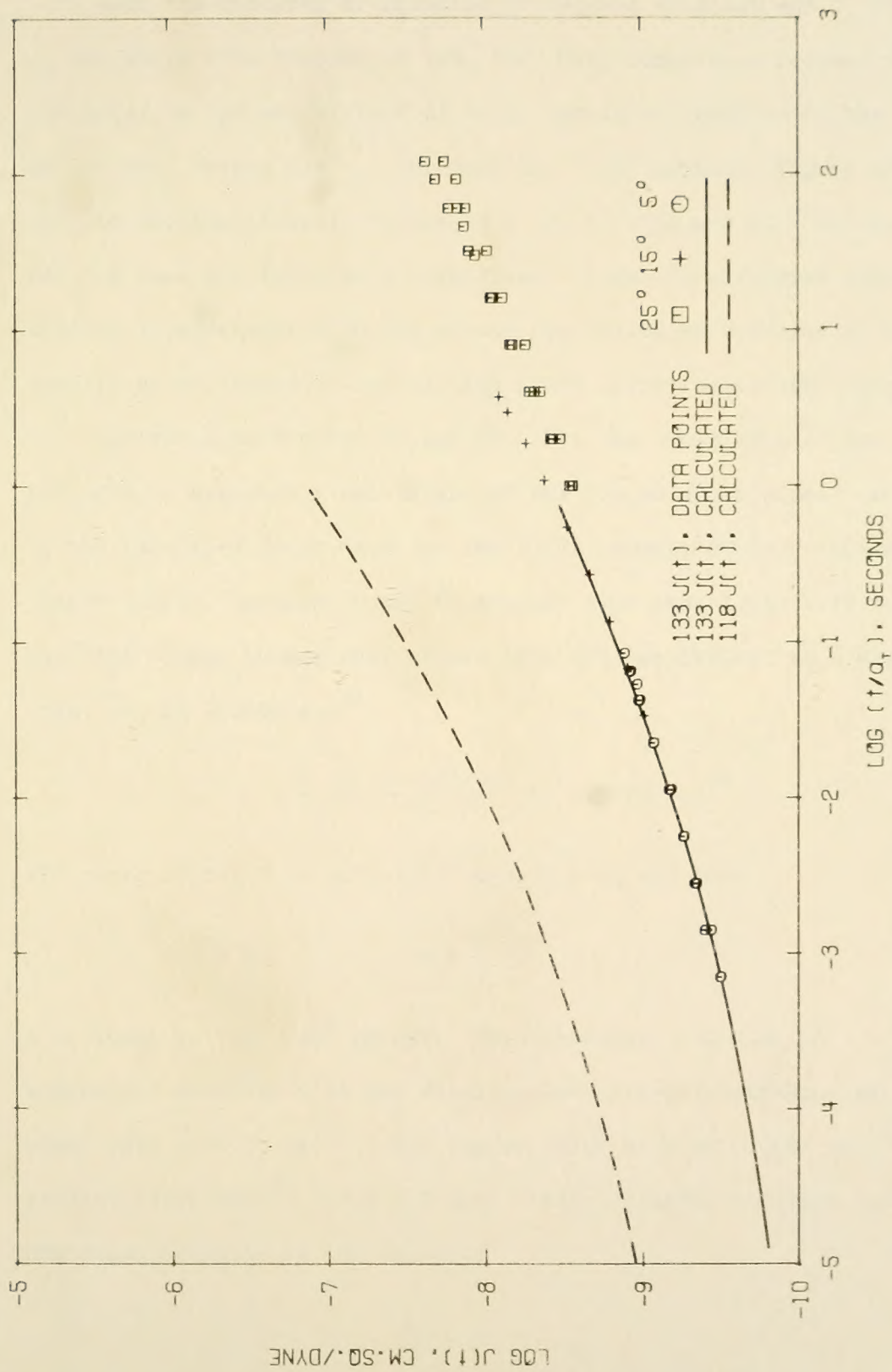


Figure 62. Creep Compliance, Sample No. 133: B3056 Asphalt, 0.63-1.25 μ m Quartz.

When the integral of Equation 22 becomes constant and J_e and J_e are small with respect to t/η , the creep compliance becomes proportional to t/η and a slope of unity should be obtained in the plot of $\log J(t)$ versus $\log t$. For both the B3056 asphalt, Figure 52, and the B3056 mixtures, Figures 47 - 51, 53 - 55 and 61 - 62, this is not the case and there is a significant effect from delayed elasticity. This is in agreement with the stated non-newtonian behavior of B3056 asphalt as evidenced in the sliding plate microviscosimeter (page 29).

Referring to Figures 56 and 57 - 60, the B3603 asphalt and B3603 mixtures do approach a unit slope at the longer creep times. Referring to the tabulated creep data for the B3603 asphalt at 25 C (Appendix I, Sample 123/3), between 30 and 60 seconds (log time 1.48, 1.78 respectively) the change in per cent strain is 1.202, equivalent to a shear rate, $\dot{\gamma}$, of 0.0004 sec^{-1} .

$$\dot{\gamma} = \frac{1.202/100}{30 \text{ sec}} = 0.0004 \text{ sec}^{-1}$$

The shear stress σ is 3.04×10^3 dynes/cm sq and from

$$\eta = \frac{\sigma}{\dot{\gamma}}$$

η is equal to 7.5×10^6 poises. This compares with the 3.9 megapoises measured with the sliding plate microviscosimeter at a shear rate of 0.05 sec^{-1} . The larger value of η at 0.0004 sec^{-1} may reflect experimental error but more likely reflects a slight non-newtonian behavior in the asphalt.

Summary

A number of important results have been obtained relative to the mechanical characterization of both the filled and unfilled asphaltic materials. Each of these results demonstrates that these materials may be characterized as linear viscoelastic according to a number of different definitions, any one of which may be considered a necessary condition for linearity. Listed by definition the various results are:

A. Invariance of compliance on stress or strain level.

Stress-strain plots, for both dynamic and creep data, give a linear relationship indicating that the compliance (reciprocal of slope) is independent of stress and strain.

Load levels were kept sufficiently low so that the per cent strain was below a few per cent in creep and well below a per cent in the dynamic tests.

B. Sine in - Sine out criterion.

A sinusoidal input (load) produced a sinusoidal output (strain) as required of a linear material.

C. Time-temperature superposition.

The following comments apply to both the filled and unfilled asphalts.

1. Smooth curves were generated when both the dynamic and creep data were shifted.
2. For each material one unique a_T function was found valid for $|\bar{J}^*|$, J' , J'' and $J(t)$.
3. Numerical values calculated for the WLF equation were consistent with values reported in the literature and the experimental data were in close agreement with a commonly accepted form of the WLF equation (Equation 15).

D. Retardation spectra.

Retardation spectra calculated independently from J' and J'' were in close agreement.

E. Additivity of creep and recovery curves.

As a test of the Boltzmann Superposition principle, the creep and recovery curves were added to effect an extension of the creep curve. This superposed data faithfully predicted the creep curve validating the superposition principle.

During the dynamic testing a sinusoidal load was instantaneously applied to the specimens and the steady state response was obtained almost immediately without any discernable delay in the response. This indicates a lack of thixotropy and/or structural breakdown in the materials under the conditions imposed by the test.

The compliances were invariant with respect to sample thickness and size (from sample 116) and minimal error was present from any "softness" in the sample plates and fixtures.

CLASS TRANSITION TEMPERATURE MEASUREMENTS

As seen in the previous section, the glass transition temperature can be estimated from the WLF relationship using mechanical data. A more direct measurement was obtained from dilatometric measurements on both the filled and unfilled asphalt.

Background

The temperature at which an amorphous material undergoes the transition from a rubberlike or flexible behavior to a glasslike or brittle behavior is called the glass transition temperature, T_g .⁽⁵⁷⁾ The transition is dramatically illustrated by bending a sheet of the material in question. Above the transition temperature, T_g , it will repeatedly flex with no sign of damage whereas below T_g it will readily shatter. Unfortunately, a bending test is too subjective to qualify as an accurate measure of T_g . The onset of brittle behavior is influenced by the rate of loading, thickness of sample and so forth. In addition, the approach to brittleness is gradual, blurring the actual T_g point.

A more satisfactory evaluation of T_g is obtained from volume-temperature data. Two different coefficients of thermal expansion are observed, one above T_g and one below, giving two linear portions on a volume-temperature plot. The intersection of the two portions is termed T_g .⁽⁵⁷⁾

An explanation of the existence of the two different coefficients includes the concept of a free volume in the material. (57, 58) The free volume consists of "holes" between the molecules, created by their thermal rotation. As the material is cooled to the T_g temperature, this rotation ("writhing action") ceases, and the free volume becomes collapsed. Below T_g volume change is due only to van der Waals' bonding whereas above T_g volume change is due to both van der Waals' bonding and the free volume expansion. The presence of these two phenomena is shown graphically in Figure 63.

As a material passes through its T_g temperature the usual abrupt changes in material properties that characterize a first order transition are missing. There is no abrupt change in volume, latent heat of fusion, etc. Instead, the T_g point is a second order transition, marking a change in the temperature derivative of the material properties. Although a host of material properties exhibit this change, (57, 59, 60) the criterion used to define T_g for this study was the volume change as measured in a dilatometer.

Experimental

Glass transition temperatures were determined for both the filled and unfilled asphalts from volume-temperature data obtained with methanol-filled dilatometers. The design of the dilatometers and the controlled temperature bath is explained in detail in Appendix E. The samples were round discs, 1/8-inch thick by 3/4-inch in diameter, prepared as described in Appendix C.

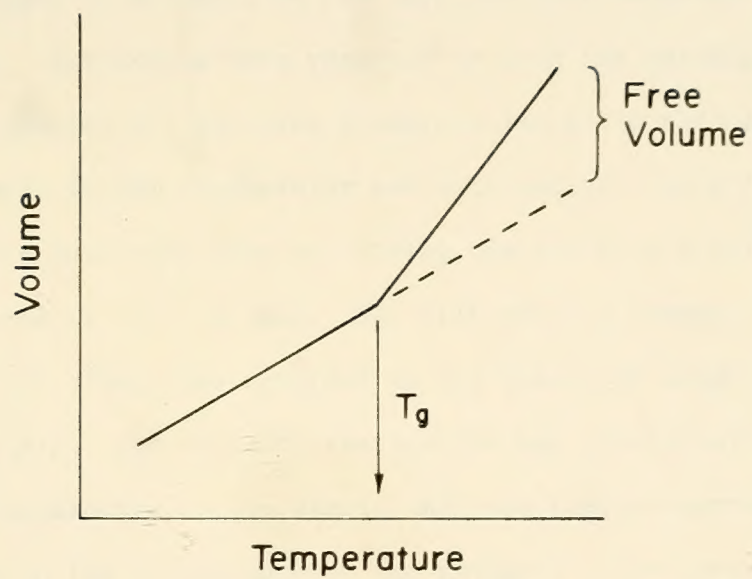


Figure 63. Idealized Volume - Temperature Relationship.

Briefly, the dilatometers consisted of a sample chamber connected to a precision bore capillary tube which was open to the atmosphere at its top end. The sample was placed in the chamber and the chamber and tube were filled with methanol. As the chamber was cooled in a bath, the height of methanol in the capillary was recorded at intervals of about 5 C. The levels were recorded in both the heating and cooling mode to the nearest 0.1 mm using a scale attached to the capillary tube.

A methanol-filled thermometer was constructed from a 1.4 mm precision bore capillary tube by fitting one end with a bulb roughly 0.7 cm in diameter by 6 cm long. The bulb end was immersed in the bath and temperature change was recorded as the change in height of methanol in the capillary. The methanol thermometer was calibrated by placing an ASTM 6C thermometer in the sample bath and taking several simultaneous readings on the 6C thermometer and methanol. The precision of the methanol thermometer was needed more for the plotting of the volume-temperature curve than precision in determining actual T_g temperature.

In the process of establishing the T_g values, direct measurements of volume were not used but instead plots were made of fluid level in the dilatometers versus fluid level in the methanol thermometer. The intersection of the upper and lower straight line portion of this plot then defined the T_g temperature, in cm, referred to the methanol thermometer. Conversion was made to degrees Centigrade by projecting the methanol thermometer value to the plot generated with the ASTM 6C thermometer. A typical data plot and the procedure for determining T_g are given in Figure 64.

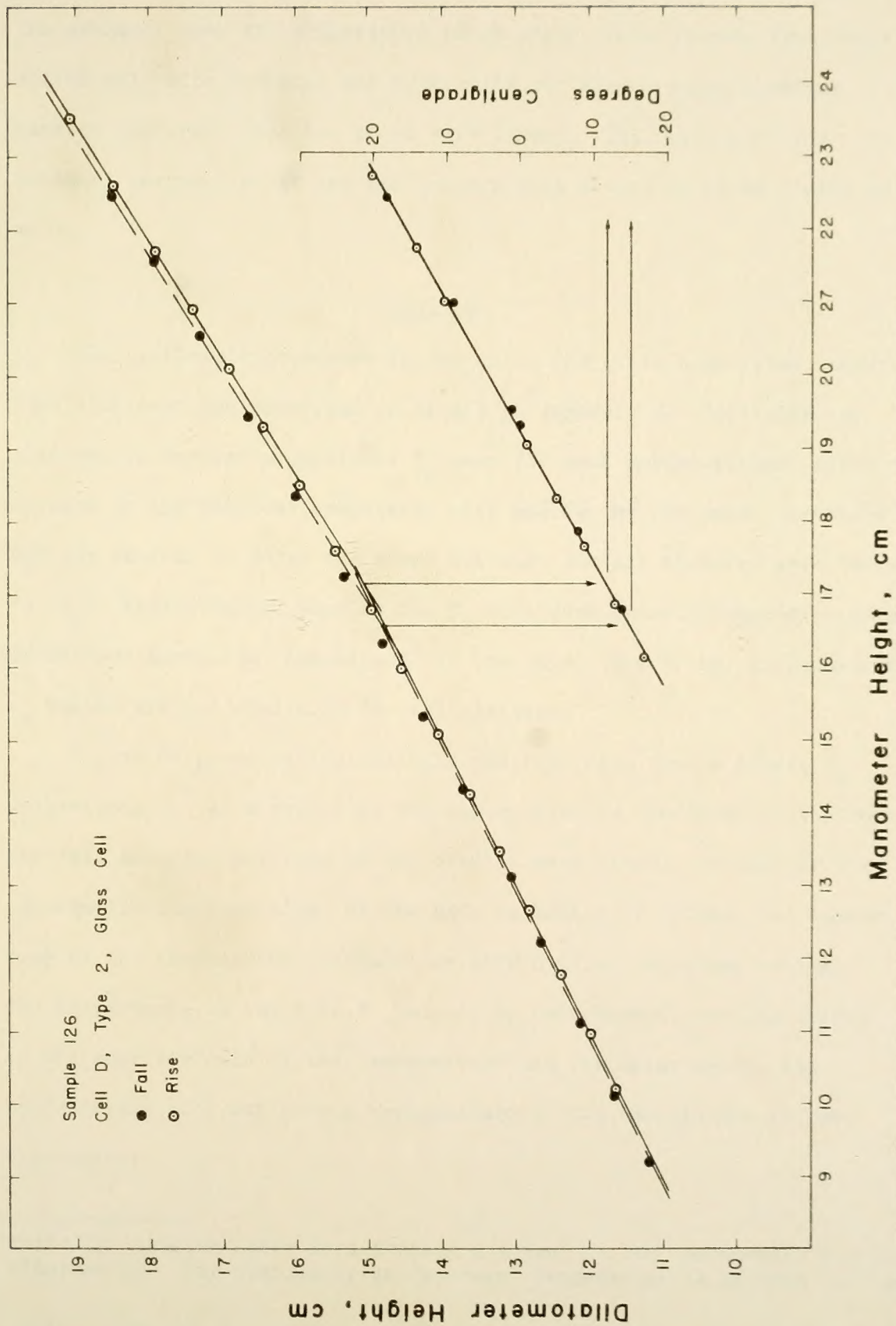


Figure 64. Typical Data for Determination of the Glass Transition Temperature.

The above technique is predicated on a linear volume change in the methanol over the temperature range used. Data plotted from cells filled only with methanol and from cells containing dummy aluminum samples confirmed that the plots were linear. Calibration of the methanol thermometer at several temperatures showed it to be linear as well.

Results

The problems encountered in designing the glass-transition temperature equipment are described in detail in Appendix E. Initially the plan was to perform a duplicate T_g test for each powder-bitumen mixture. Because of the problems associated with making the equipment operative and not wanting to delay the shear testing, not all mixtures were tested for T_g . Additionally, some of the T_g data were later discarded because of obvious anomalies (Appendix E) in the data. Therefore, dilatometric T_g values are not available for all mixtures.

Figure 64 presents typical fall and rise data from a single T_g determination. As a result of the nonequilibrium condition of the test, the fall and rise portions do not overlap each other. Because of the non-equilibrium condition, as the bath is heated or cooled, the temperature of the thermometer (methanol or ASTM 6 C) and dilatometer lags the temperature in the bath.* Unless, by coincidence, the lag effect is the same for each of the thermometers and the dilatometer, the thermometers will not give a true measure of the temperature in the dilatometer.

*Strictly speaking there is a thermal gradient in the thermometer and the dilatometer. For simplicity an "average" temperature is assumed for each.

The net result of the thermal lag effect is a horizontal displacement of the rise and fall curve when plotted as in Figure 64; i.e., for a given dilatometer height a different apparent temperature is recorded in rise and fall. From data taken with an aluminum sample, the thermal lag between the thermometers and dilatometer was evaluated as being approximately 1 C.

A second consideration that might be expected to show the effects of thermal lag between the different components results from the differences in construction of the two dilatometer cells. The first cell was constructed of aluminum as opposed to the use of less conductive glass in the second design. From the data of Table 11, there is no decided difference between the lag measured for the two designs as might be expected from the differing conductivities of glass and aluminum.

Table 11. Average Differences Between Rise and Fall T Values for Various B3056 Mixtures

	Unfilled	Filled
Aluminum Cell	5.2 C (11)*	5.3 C (5)
Glass Cell	4.0 C (4)	5.0 C (10)

*Number in brackets indicates number of tests included in this average.

Since the thermal conductivity for minerals is several times greater than for asphalt⁽⁶¹⁾, if a major source of the rise and fall differential were due to a lack of temperature response in the sample,

then a narrower spread between rise and fall T_g might be expected for the filled material than for asphalt alone. From Table 11 this is seen not to be the case as there is little difference between the average rise and fall data for filled and unfilled systems.

Another factor that contributes to the difference in the fall and rise data is the viscoelastic nature of the material itself. Any response to an applied stress, in this case thermally induced, requires a finite time for all the strain to relax. This point is discussed by Buche in conjunction with relaxation spectra.⁽⁵⁷⁾ For this reason the observed T_g is dependent on the rate of heating or cooling and the "true" T_g value should lie somewhere between those obtained in the cooling and heating modes.

A complete tabulation of T_g values is given in Tables 12 and 13. Each of these values represents at least two data points; the rise and fall points were first averaged to give an average for the single test and then the duplicate test values were averaged. The two B3603 mixtures show T_g values quite close to the unfilled B3603. Most of the values for the B3056 mixtures are also quite close to that for the unfilled B3056 asphalt. There are several notable exceptions, however; the two 0.63-1.25 μm materials show a definite increase in T_g as do the bytownite and magnesite mixtures.

Except for the four mixtures showing definitely higher values for T_g , the range between the filled and unfilled T_g values is 3.0 C or less. The high values may represent experimental error (perhaps caused by entrapped air) and, even though all the values (except 2.5-5.0 μm SiO_2 with B3603 asphalt) are on the high side of the unfilled

Table 12. Average Values of T_g for B3056 Mixtures.

B3056	-21.0 C
10-20 μm SiO_2	-18.8
10-20 μm CaCO_3	-20.8
2.5-5.0 μm SiO_2	-18.0
0.63-1.25 μm SiO_2	- 8.8
0.63-1.25 μm CaCO_3	-10.0
< 2.5 μm Apatite	-18.6
< 2.5 μm Bytownite	-13.5
< 2.5 μm Magnesite	-13.2
< 2.5 μm Microcline	-20.3

Table 13. Average Values of T_g for B3603 Mixtures.

B3603	-19.2 C
2.5-5.0 μm SiO_2	-19.7
2.5-5.0 μm CaCO_3	-18.8

Table 14. Comparison of Glass Transition Temperatures.

	B3056	B3603
Schmidt and Santucci	-18.8 C	-21.1 C
This study	-20.9 C	-19.2 C

asphalt, the incorporation of mineral matter does not appear to cause a marked rise in T_g value.

A comparison of the values obtained by Schmidt and Santucci⁽³⁰⁾ with those of this study is given in Table 14. Considering the nature of the test, this is considered good reproducibility.

COMPARISON AND DISCUSSION OF THE VARIOUS RESULTS

The results of the mechanical characterization (viscoelastic moduli) of both the filled and unfilled asphalts have been presented in graphical form. The data were found thermorheologically simple and from the shift function, an estimate of the glass transition temperature, T_g , was presented. This was augmented by a dilatometric measure of T_g .

In this section, the various results from the sections on powder characterization, creep and dynamic viscoelastic moduli, and glass transition temperature measurements are compared. The comparisons are made with the intent of evaluating the extent and nature of the reinforcement contributed by the mineral powder to the various mineral powder-bitumen composites.

Comparison of Dynamic and Creep Measurements

Early in the study it was decided to obtain both quasi static and dynamic shear data in order to effectively extend the time span of the measurements within the available test equipment (MTS machine). Dynamic measurements are convenient for short-time characterization, while the creep measurements are convenient for long times. These measurements can be interrelated.

A number of different methods are available for relating creep and dynamic data. Most simply, van der Poel^(62,63) has shown that good equivalence is obtained by setting

$$|\bar{J}^*|_{t=1/\omega} = J(t) \quad 23$$

According to van der Poel, the error is, at most, 40 per cent, occurring in the transition region. The results of applying Equation 23 to the filled and unfilled B3056 and B3603 asphalt are shown in Figures 65 and 66, respectively. In each case the mineral powder is 10.0-20.0 μm calcite. Good agreement is shown over the range of times in common with both curves and the shapes of both show good alignment.

By the mathematical manipulation of the different viscoelastic variables, exact relations that relate the creep and dynamic compliance components can be written, either in terms of each other or in terms of the retardation function. In the latter case⁽³⁵⁾

$$J' = J_g + \int_{-\infty}^{\infty} \frac{L(\tau)}{1+\omega^2\tau^2} d\ln \tau \quad 24$$

$$J'' = \int_{-\infty}^{\infty} \frac{L(\tau)\omega\tau}{1+\omega^2\tau^2} d\ln \tau + \frac{1}{\omega\eta} \quad 24a$$

Equations 24 and 24a pose several problems: $L(\tau)$ must be defined and integrated over its entire range and values must be available for both J_g and η .

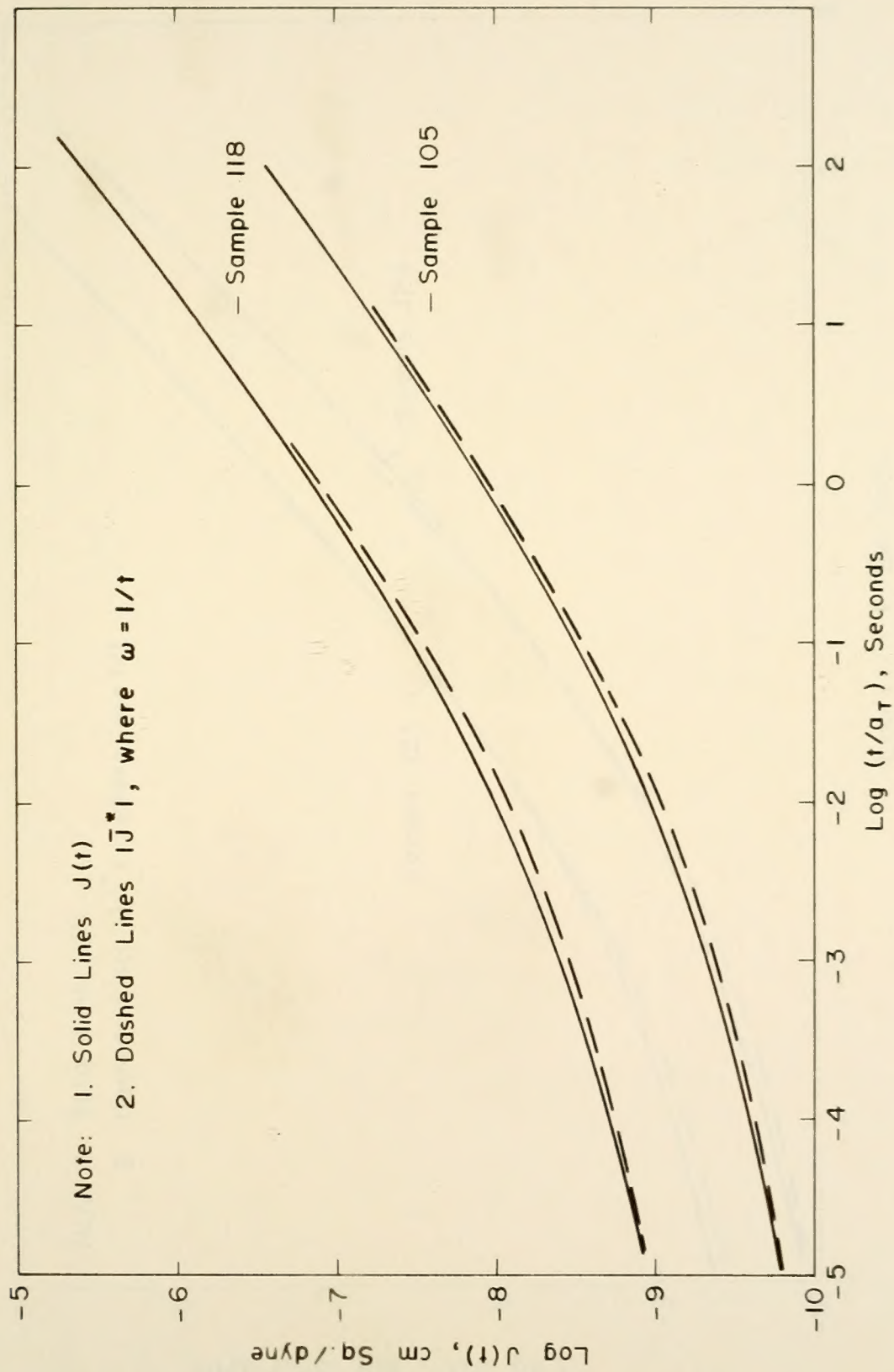


Figure 65. Comparison of $|\bar{J}^*|$ and $J(t)$ at $\omega = 1/t$, B3056 Asphalt

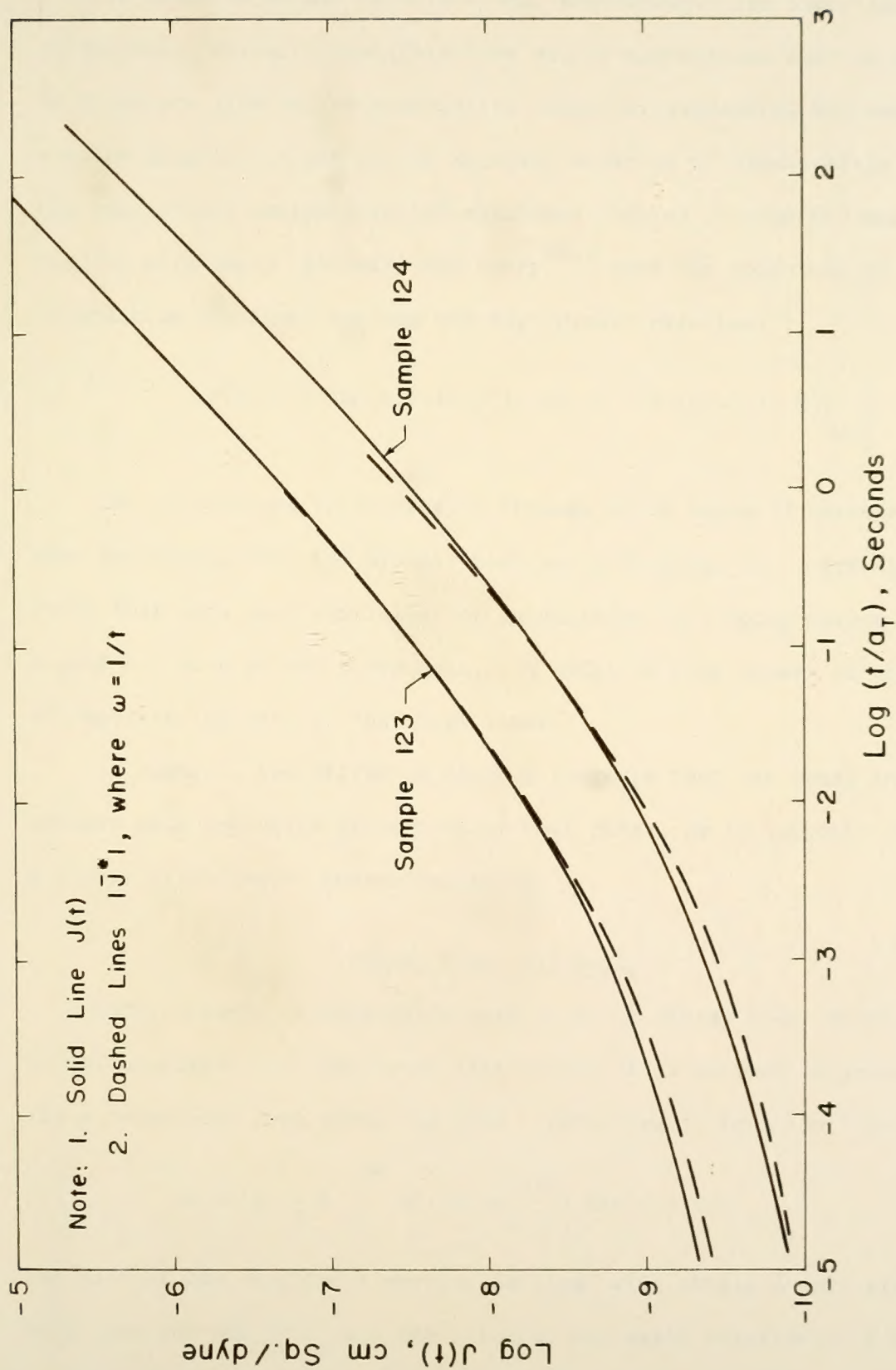


Figure 66. Comparison of $|\bar{J}^*|$ and $J(t)$ at $\omega = 1/t$, B3603 Asphalt

In order to obtain relations that are suitable for numerical calculation, certain simplifications and/or assumptions must be made in equations like 24, or alternative means for expressing the moduli must be sought. In the latter approach a series of exponentials or the appropriate manipulation of equations such as 5 (page 35) may be used to advantage. Ninomiya and Ferry⁽⁵⁴⁾ have, by operating on the retardation function, derived the approximate relation:

$$J(t) = J'(\omega) + 0.40 J''(0.40 \omega) - 0.14 J''(10 \omega) \Big|_{\omega = \frac{1}{t}} \quad 25$$

The solid lines in Figures 47 through 62 on pages 88 through 103 were calculated from the dynamic data using Equation 25. Over the range that data were available for calculation, the solid curves give a good estimate of the creep data. In addition they appear to properly extrapolate the data at the short times.

In summary, two different methods indicate that the creep and dynamic data are valid predictors of each other, as is expected from a linear viscoelastic characterization.

Steady State Viscosity

Unfortunately, a straightforward value of steady state viscosity is not available from the creep test unless it is allowed to proceed for a relatively long period of time. Referring to Equation 4 and 18:

$$J(t) = J_g + \int_{-\infty}^{\infty} L(\tau)(1 - e^{-t/\tau}) \, d\ln \tau + t/\eta$$

the plot of log compliance versus log time will attain a unit slope only when the sum of J_g and the integral are small relative to t/η

(i.e. $J(t) \propto t/\eta$). It will be recalled that in the plots of creep compliance (Figures 47 through 62), linearity (slope of unity on log-log plot) was approached at the longer times for the B3603 materials but not for the B3056 materials. As a consequence some other estimate of η was required of the B3056 data.

From a theoretical standpoint all that is necessary to attain linearity is to extend the creep curve to long times. However this was impractical for two reasons: first the drift in the machine at the low loads required was troublesome beyond a few minutes. Secondly, even if this were not the case, the long times imply large strains and the onset of nonlinearity.

In principle the recovery curve should provide a good estimate of η . The non-recoverable strain remaining after complete recovery represents viscous flow that occurs during the duration of the step load. Using this value, η may be calculated by dividing σ_0 by the displacement, divided by the time of duration of the step load. Experimentally, very long periods of time were required for complete recovery and this technique was also considered impractical.

Ninomiya⁽⁶⁴⁾ has suggested a convenient method for approximating both the steady state viscosity, η , and the steady state compliance, J_e . Plots of $J(t)/t$ and $mJ(t)/t$ versus $1/t$ are prepared and curves drawn through the data with m equal to $d \log J(t)/d \log t$. The intercept is the same for both curves and defines $1/\eta$ while the initial tangent of the $J(t)/t$ curve is an estimate of J_e . The purpose of the factor m is to reduce the curvature in the plot giving a more accurate

estimate of the intercept. A sample construction for the data of Sample No. 108 is shown in Figure 67. Calculated values for J_e and η are given in Table 15. The estimated value of η for the unfilled B3603 asphalt is listed as 6 megapoises, compared to 3.9 for the sliding plate microviscosimeter and 7.5 from a direct calculation using the creep data (see Table 4 and the section titled "Creep Measurements"). The estimated value for the plain B3056 asphalt is 32 megapoises as compared to 10.5 measured in the microviscosimeter (Table 4). To the extent that these values are valid they reflect the severe degree of non-newtonian flow evident in the B3056 asphalt and the inability of the routine microviscosimeter test to measure steady state viscosity.

The data for the B3056 mixtures made with SiO_2 show a greater decrease in compliance and increase in viscosity than those made with the CaCO_3 . (Recall that a decrease in J implies a "stiffening".) No values of J_e are given for the plain B3603 asphalt and for the B3603 - CaCO_3 mixtures, indicating that the t/η effect (flow) was large in comparison to the effect of J_e : plots as given in Figure 67 were parallel to the $1/t$ axis.

The viscosity for the B3056 mixtures is apparently particle size dependent, increasing with decreasing size. The ratio η/η_0 ranges to, and above, 100 for the B3056 mixtures (see Table 16) but is only about 7, and independent of size, for the B3603 mixtures.

As will be discussed later, at a volume concentration of 0.40 solids, a value of η/η_0 of approximately 4 would be expected. This

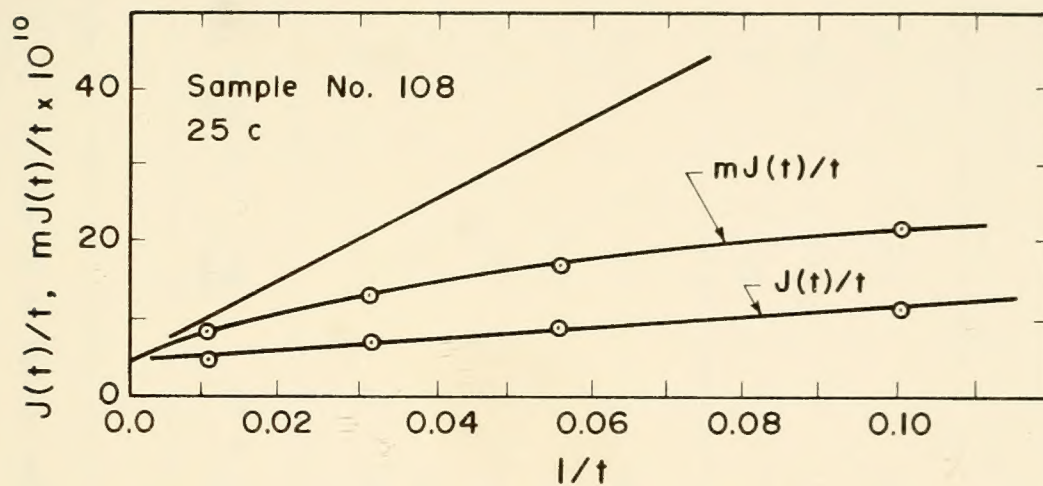


Figure 67. Estimation of Steady State Viscosity and Equilibrium Compliance

Table 15. Calculated Values of J_e and η .

Description	CaCO ₃				SiO ₂			
	Sample No.	$J_e \frac{\text{cm}^2}{\text{dyne}} \times 10^{-8}$	$\eta \frac{\text{dyne sec}}{\text{cm}^2} \times 10^6$	Sample No.	$J_e \frac{\text{cm}^2}{\text{dyne}} \times 10^{-8}$	$\eta \frac{\text{dyne sec}}{\text{cm}^2} \times 10^6$	Sample No.	$J_e \frac{\text{cm}^2}{\text{dyne}} \times 10^{-8}$
Plain B3056	118	80	32	118	80	32		
10-20 μm	105	8	530	107	8	1300		
2.5-5 μm	108	6	2000	106	3	3300		
.63-1.25 μm	132	3	2500	133	3	6700		
XFDG	109	6	2000	119	8	500		
Plain B3603	123	-	6	123	-	6		
10-20 μm	124	-	44	131	16	42		
2.5-5 μm	130	-	42	123	9	47		

would indicate that the asphalt in the B3603 mixtures is only slightly reinforced* (4 compared to 7) but that the asphalt in the B3056 mixtures is strongly reinforced (4 compared to 100).

Summarizing, it can be stated that, according to the approximate method of estimating η and J_e :

1. There is a very significant difference in the behavior of the two asphalts: the B3056 asphalt is strongly reinforced by the presence of the mineral ($\eta/\eta_o \rightarrow 100$) while the B3603 asphalt is only very slightly reinforced.
2. The effect of reinforcement is more pronounced in η than in J_e . Both J_e and η change with particle size, but the change is more pronounced with the SiO_2 than with the CaCO_3 mixtures. This is summarized in Table 16.

Table 16. Relative Values of J_e and η : B3056 Mixtures

Size	CaCO_3		SiO_2	
	J_e^o/J_e	η/η_o	J_e^o/J_e	η/η_o
10-20 μm	10	17	10	41
2.5-5.0 μm	13	62	26	103
0.63-1.25 μm	26	78	26	210

NOTE: Superscripts and subscripts "o" refer to unfilled material.

*Borrowing terminology from work with filled elastomers, (65) a filler is said to be reinforcing if the polymer composite formed with the filler has some enhanced physical property greater than that due to only the volume filling effect of the filler.

Time-Temperature Superposition and Glass Transition Temperature

The principle of time-temperature superposition has been shown experimentally valid for both the filled and unfilled asphalts. The plotted a_T data were seen to fit a generally accepted form of the WLF equation and were used to successfully generate the constants in a second, more specific form of the equation. In addition, graphically determined values of T_g generated reasonable values of the glass transition temperature, T_g .

The function a_T may be considered a measure of temperature susceptibility. When comparing data of similar slope on the log-log plot of compliance versus time, the more widely spaced (vertically) the individual curves (i.e. more temperature dependent) the larger the value of a_T required to obtain coincidence. Therefore, for curves of similar shape, the larger value of a_T indicates a more temperature susceptible material.

Unfortunately, it was not convenient to test at the half dozen and more temperatures needed to accurately define a_T and, at most, only two values of a_T were determined for each mixture. Values of $\log \Delta a_T$ from the CaCO_3 and SiO_2 composites are shown in Table 17. The values given are the number of logarithmic cycles needed to get coincidence between the 15-25 C and 5-15 C data. Although perhaps a bit unorthodox, in an attempt to compare better the limited data, the averages of the two values are also given.

From the data shown no trends attributable to either particle size or mineral type are apparent. The values for the B3603 material,

Table 17. Summary of Experimental Values of a_T .

Sample Description	$\log a_T, \text{CaCO}_3$			$\log a_T, \text{SiO}_2$		
	15-25 C	5-15 C	Avg.	15-25 C	5-15 C	Avg.
B3056 Asphalt	1.43	1.80	1.62	1.43	1.80	1.62
10-20 μm	1.56	1.80	1.73	1.53	1.69	1.61
2.5-5.0 μm	1.57	1.65	1.61	1.64	1.73	1.69
0.63-1.25 μm	1.50	1.71	1.61	1.47	1.68	1.58
B3603 Asphalt	1.35	1.49	1.42	1.35	1.49	1.42
10-20 μm	1.38	1.49	1.44	1.41	1.45	1.43
2.5-5.0 μm	1.21	--	--	1.21	1.53	1.37

its flow resistance from the mechanical particle-particle contact between the aggregate particles.⁽⁶⁾ This contact would not be expected to be noticeably temperature-dependent, with the net effect being a lowering of the temperature susceptibility of the composite. To the extent that any particular test mobilizes particle-particle contact, a differing influence on the a_T function might be expected.

For the mixes tested in this study, the space between the mineral grains was sufficient such that it is difficult to imagine any noticeable effect on mechanical behavior from intergranular contact. Referring to Table 2, the majority of the materials had a dry packed porosity of about 0.51. In all the mixtures the percentage volume of asphalt was 60 per cent which would correspond to a porosity of 0.60, considering the asphalt volume as interparticle voids. This is, then, about 9 percentage points above that required to just fill the voids between the mineral grains at densest packing and is in contrast to ordinary bituminous concrete where the asphalt and air occupy only about 13 per cent of the total volume.

A number of studies have been carried out on filled polymeric systems in the range of filler concentration used in this study, principally by investigators interested in solid rocket propellants.^(56, 70-73) At volume concentrations, c_v , in the range of 0.40, it is reported that the form of the temperature dependence does not change.⁽⁷³⁾ As described earlier (page 53) by comparing the standard curve (Equation 15) to the experimental curves, it is possible to graphically determine T_g for both the filled and unfilled polymer.

however, were decidedly lower than those for the B3056 material. The two values for the B3603 asphalt mixed with the two 2.5-5.0 μm minerals are admittedly low when compared with the other B3603 values but with the scatter in the data this may well represent experimental error rather than any trend in the data. Therefore, there is no apparent effect on a_T from mineral size or type: the effect of asphalt type outweighs that of the mineral powder.

Varying results are reported in the literature on the effect of fillers on the shift factor, a_T . When compared to the binder alone, while the individual values of a_T may change, the form of the a_T versus temperature curve is generally retained, as given by Equation 15.

The data available on filled bituminous materials are from tests performed on bituminous concrete. Some authors report little change in the a_T values^(66,67) while data presented by others^(68,69) suggest a considerable lowering of the values of Δa_T due to the effect of the aggregate. In the latter case, for a 20 C temperature change values of Δa_T of one logarithmic decade or less are reported while values of Δa_T for the unfilled asphalts are on the order of 2.5 to 3.5 logarithmic decades.

It is also reported that the effect on a_T is a function of the type of test⁽⁶⁹⁾, the best agreement with the unfilled bitumen coming from a stress relaxation test, the poorest from extrapolated steady state viscosity data. In all instances the effect is a reduction in the value of a_T . To the extent that the lower values of a_T can be considered a reduction in temperature susceptibility this is not surprising as the highly filled bituminous concrete develops much of

T_g may then be determined by taking $T_s - T_g$ equal to an appropriate value, either assumed or measured experimentally, for the pure polymer.

Using the above procedure, Landel⁽⁵⁶⁾ reports an increase in T_g of 2, 5, and 7 C for a non-crosslinked polyisobutylene-glass bead composite. The increase was in the order of increase in the filler concentration of 9, 20, and 37 per cent and was attributed to cross-linking in regions of polymer adsorption.

For each of the mixtures in this study the above procedure was followed and the resulting values of T_g are reported in Tables 6-8. For pure asphalt, $T_s - T_g$ is reported on the order of 50 C with one author reporting 56 C. Estimates of T_g using the latter value are given in Tables 18 and 19 along with values of T_g determined dilatometrically.

The data in Table 18 for the B3603 materials agree quite well. A slight decrease in T_g for the 2.5-5.0 μm material is noted but this is within experimental error.

The data for the B3056 materials are more variable. Looking first at the CaCO_3 and SiO_2 mixtures, little variation is seen in the mechanically determined T_g values, reflecting the uniformity of the a_T values given in Table 17. The dilatometrically determined values are also relatively uniform except for the two 0.63-1.25 μm materials which show a definite increase in the T_g temperature in contrast to the mechanically determined values.

A slight increase is noted for the SiO_2 dilatometric data, proceeding from the unfilled to the 2.5-5.0 μm material. Although systematic and corresponding to the increased interaction of the SiO_2 over the

Table 18. Comparison of Mechanically and Dilatometrically Determined Values of T_g for CaCO_3 and SiO_2 Mixtures.

Description	CaCO_3		SiO_2	
	Mechanical	Dilatometric	Mechanical	Dilatometric
B3056 Asphalt	-14	-21	-14	-21
10-20 μm	-13	-21	-15	-19
2.5-5.0 μm	-15	-	-13	-18
0.63-1.25 μm	-15	-14	-15	- 9
XFDG	-13	-	-13	-
B3603 Asphalt	-19	-19	-19	-19
10-20 μm	-19	-	-19	-
2.5-5.0 μm	-21	-19	-22	-20

Table 19. Comparison of Mechanically and Dilatometrically Determined Values of T_g for B3056 Asphalt with < 2.5 μm Powders

Description	Mechanical	Dilatometric
B3056 Asphalt	-14	-21
< 2.5 μm Apatite	-12	-19
< 2.5 μm Bytownite	-19	-14
< 2.5 μm Magnesite	-12	-13
< 2.5 μm Microcline	-12	-20

CaCO_3 , (see e.g. Table 16 or next section) no assurance can be made that the small 3 C change is not attributable to experimental error.

In contrast to the B3603 material the $T_g = T_s - 56$ assumption does not bring the B3056 dilatometric and mechanical data into agreement. For this case $T_s - T_g$ is closer to 63 C, indicating that the technique of using T_s to estimate T_g must be used with discretion. The constants in the WLF equation are then functions of asphalt type as shown in Table 9, in agreement with the conclusions of Jongepier and Kuilman.⁽⁷⁴⁾

No good explanation is offered for the larger dilatometrically determined values of T_g , as compared to the mechanical ones for the 0.63-1.25 μm B3056 mixtures. If the data are indeed valid, a different controlling mechanism is perhaps indicated in the thermal volume expansion than in the shear behavior. For example, Wada and Hirose suggest that the asphaltene concentration controls T_g ; perhaps the finer powders can accommodate an increased asphaltene adsorption which is reflected more in the dilatometric result than in the stress-strain result.

The T_g data in Table 19 for the four graded materials, apatite, bytownite, magnesite and microcline are somewhat conflicting. The mechanical T_g value for bytownite (-19 C) would appear questionable as it represents a decrease in T_g against the established trend which indicates an increase in T_g on the addition of filler. Because only one value of a_T is available for the $< 2.5 \mu\text{m}$ materials (two points on $\log a_T$ vs. T), the mechanical T_g values may be of limited reliability.

The two increases in the dilatometric T_g for bytownite and magnesite are in keeping with the trends in the dynamic compliance as shown in the next section.

In summary it can be said that:

1. Except for the 0.63-1.25 μm SiO_2 and CaCO_3 mixes made with the B3056 asphalt, values of a_T are relatively unchanged by the type or size of filler; the effect of the type of asphalt outweighs the effect of the type of filler.
2. Values of $T_s - T_g$ for the unfilled asphalts vary with the asphalt type and for the two asphalts reported were 56 and 63 C. The data also suggest that the constants in the WLF equation vary with asphalt type.
3. Dilatometric values of T_g are sensitive to particle size whereas those determined from $T_s - T_g$ are not.

Comparison of Effect of Fillers on Compliance

At this point the various viscoelastic moduli, both dynamic and quasi-static have been shown thermorheologically simple and interconvertible. A comparison of the shifted and interconverted data for the different mixtures follows in an attempt to evaluate the nature and extent of the interaction between mineral and bitumen.

One of the earliest and perhaps most famous evaluations of the effect of the concentration dependence of a filled viscous system was that of Einstein.⁽⁷⁵⁾ His work was done for dilute suspensions where it can be assumed there is no overlapping of the perturbations caused

by the individual particles. Einstein's relationship is given as

$$\eta = \eta_0 (1 + 2.5 c_v) \quad 26$$

and is valid only for very dilute suspensions.

In the intervening years a good deal of attention has been given to the problem of accounting for more concentrated suspensions, but little has been forthcoming in terms of theoretical treatments. Instead, a host of empirical equations have been developed, some tempered by theoretical considerations. A logical extension of Equation 26 is given by

$$\eta = \eta_0 (1 + 2.5 c_v + 14.1 c_v^2)$$

after Guth⁽⁷⁶⁾ and Smallwood.⁽⁷⁷⁾ Eilers and Van Dijk⁽⁷⁸⁾ have developed an empirical relation which can be written as

$$\frac{J_e^0}{J_e} = \left[\left(1 + \frac{1.25 c_v}{1 - 1.28 c_v} \right)^2 \right]$$

Here J_e^0 is the glossy compliance of the unfilled polymer and c_v is the volume fraction at closest packing. Additional relationships have been developed by others which when used for regularly shaped particles that do not interact with the binder, closely predict the effect of the filler. In addition, it can be shown that the ratio of stiffening offered by the steady state viscosity is also realized in the moduli,^(35, 79) therefore,

$$\frac{\eta}{\eta_0} = \frac{1/J'}{1/J_0'}$$

At a volume concentration of 0.40 the stiffening effect predicted by the above equations is equivalent to an increase in moduli or viscosity of about four times, and, from experiment appears independent of particle size.

Guided by the above relationships, the first attempt was to compare $|\bar{J}^*|$ from the filled and unfilled asphalts by making a vertical shift on the unfilled asphalt equal to the logarithm of 4.0. A typical result is shown in Figure 68 where it is quite obvious that a single vertical shift is not sufficient to match the curves. The data are convergent at the short times and tend to diverge at longer times. This is true of both the unfilled curve as compared to the filled and, within the filled curves. Extrapolated to the small end of the time scale, as J' approaches J_g , the factor 4.0 gives a good account of the effect of the filler. This behavior is typical of all the mixtures.

Figures 69 through 72 offer a comparison of the relative effect of different filler types on the storage compliance. It is striking that, although there is a definite difference among the curves at the large end of the time spectrum, at the small end all the filled curves tend to converge at the same value of $|\bar{J}^*|$, about 10^{-10} cm sq/dyne. At the lower temperatures and shorter times the behavior among all the systems is similar, independent of particle size and type, and asphalt type.

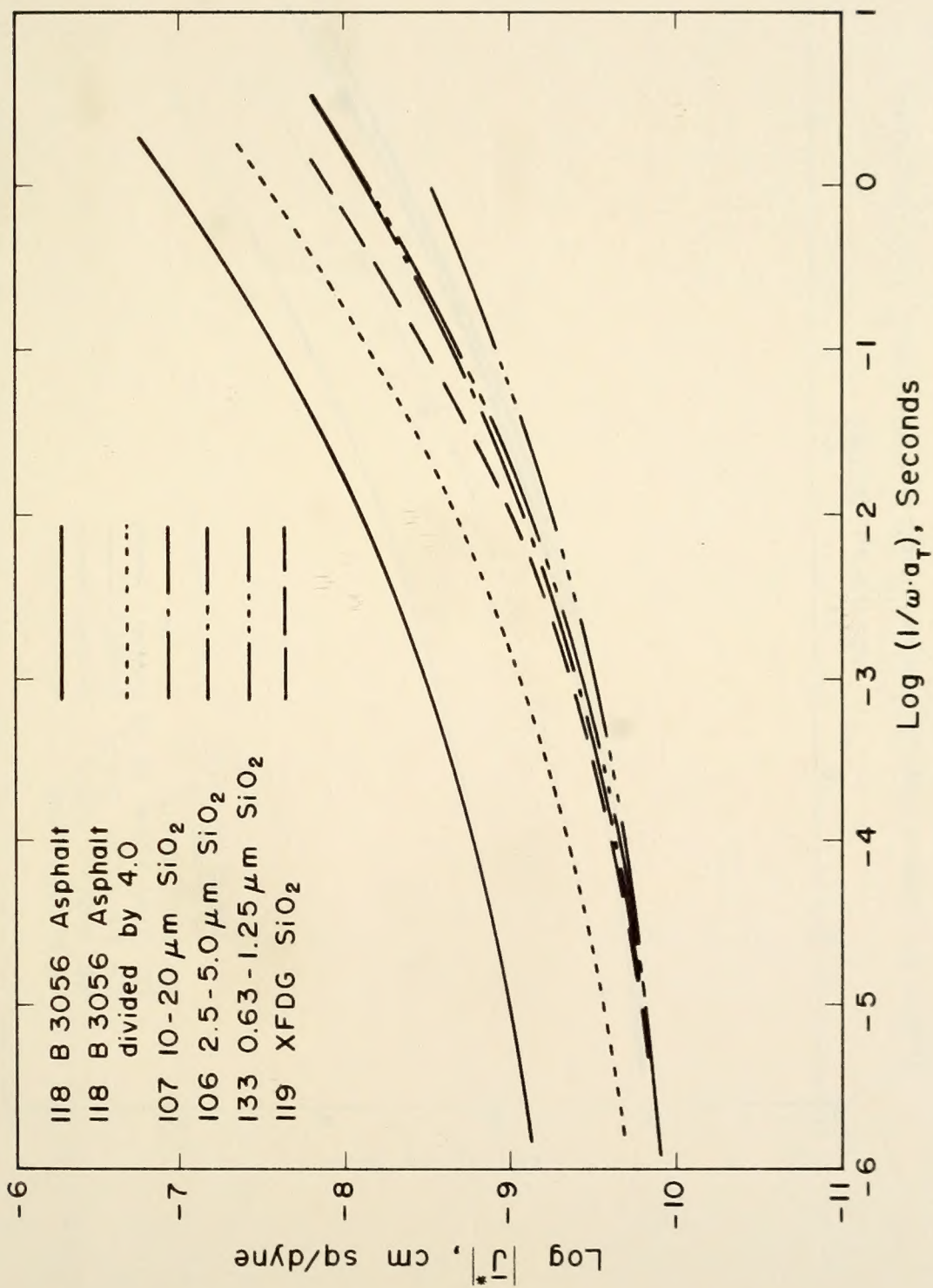


Figure 68. $|J^*|$, B3056 - SiO₂ Mixtures

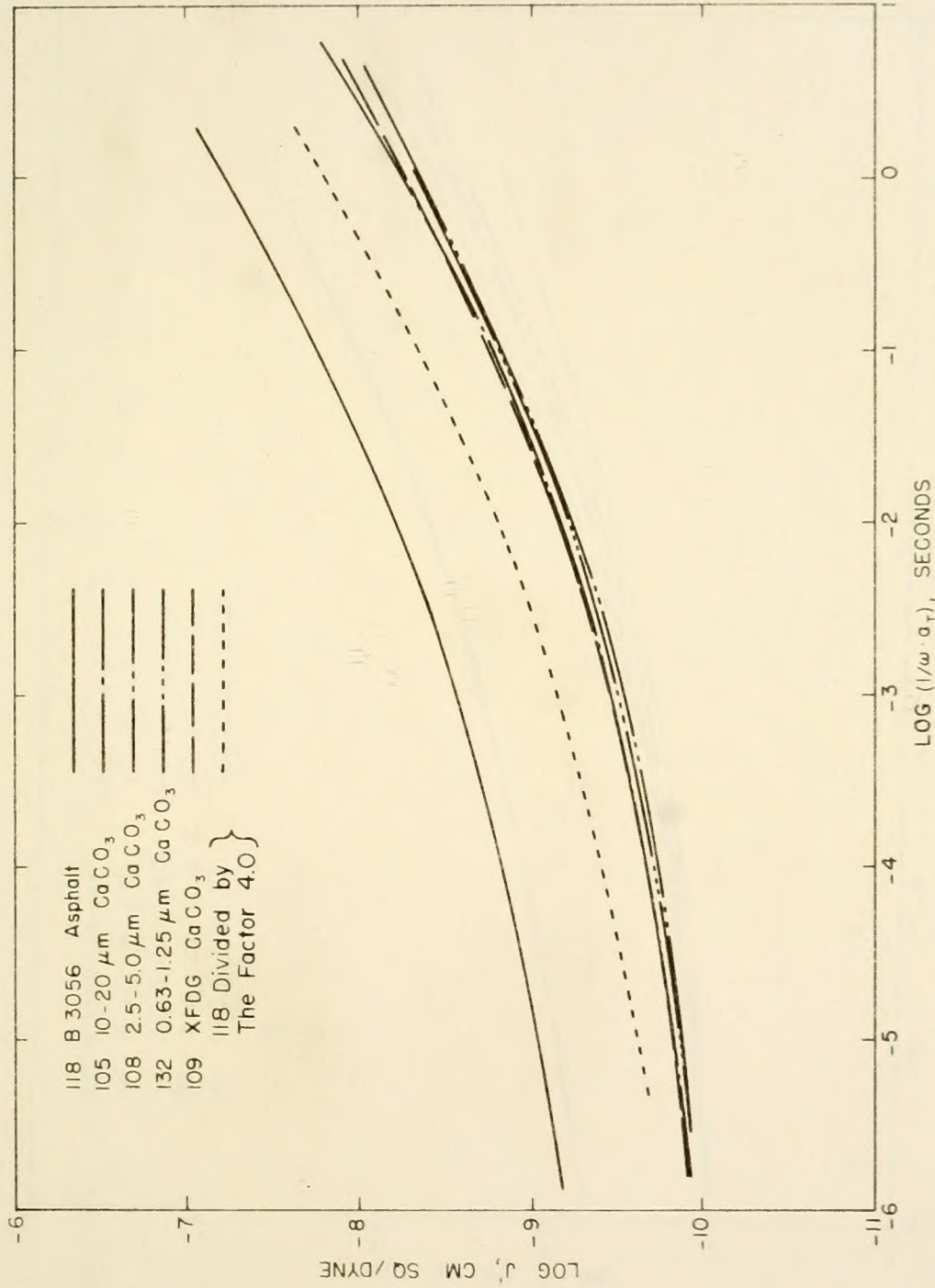


Figure 69. Comparison of Storage Compliance for B3056, CaCO_3 Mixtures.

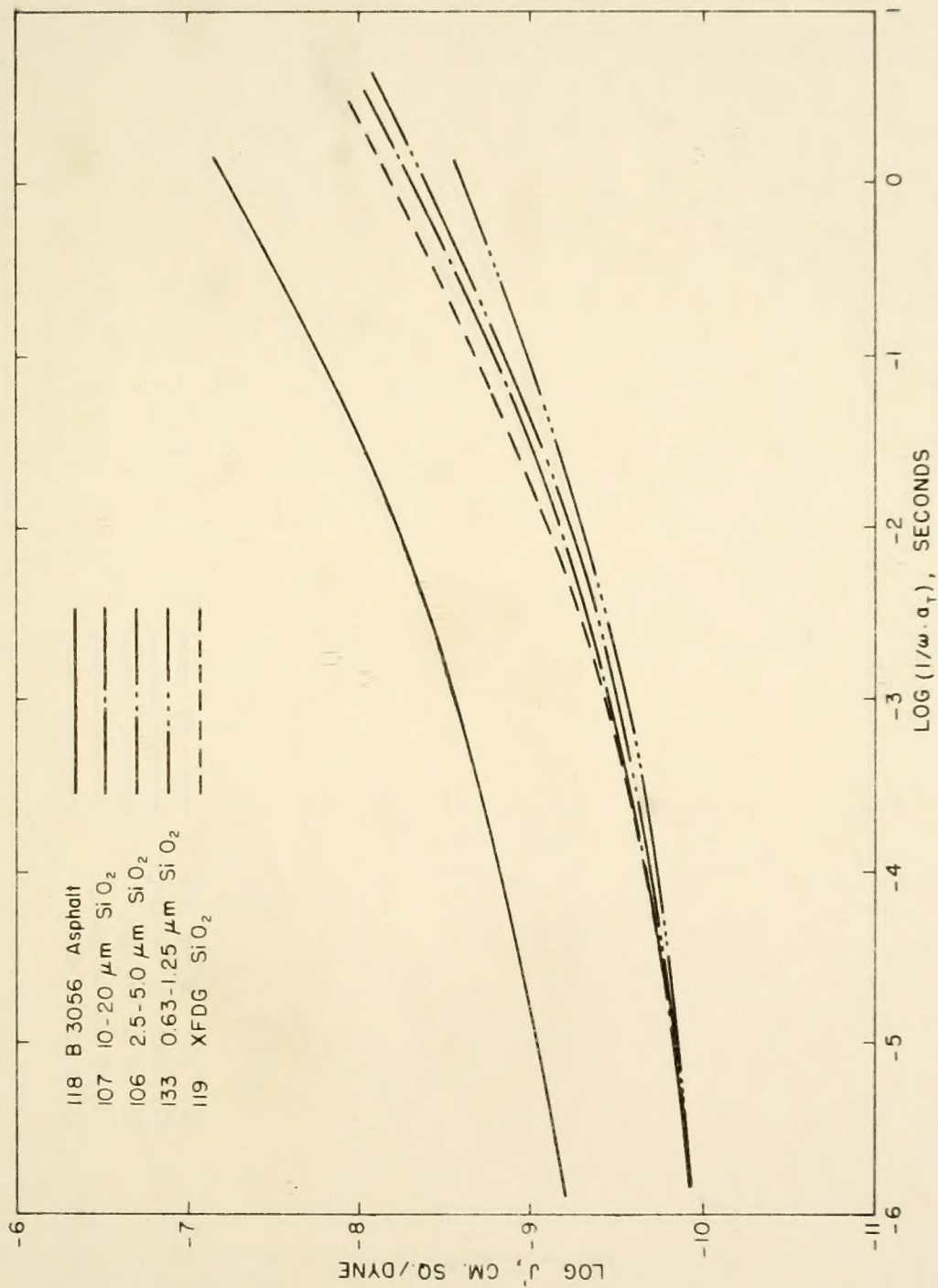


Figure 70. Comparison of Storage Compliance for B3056, SiO_2 Mixtures.

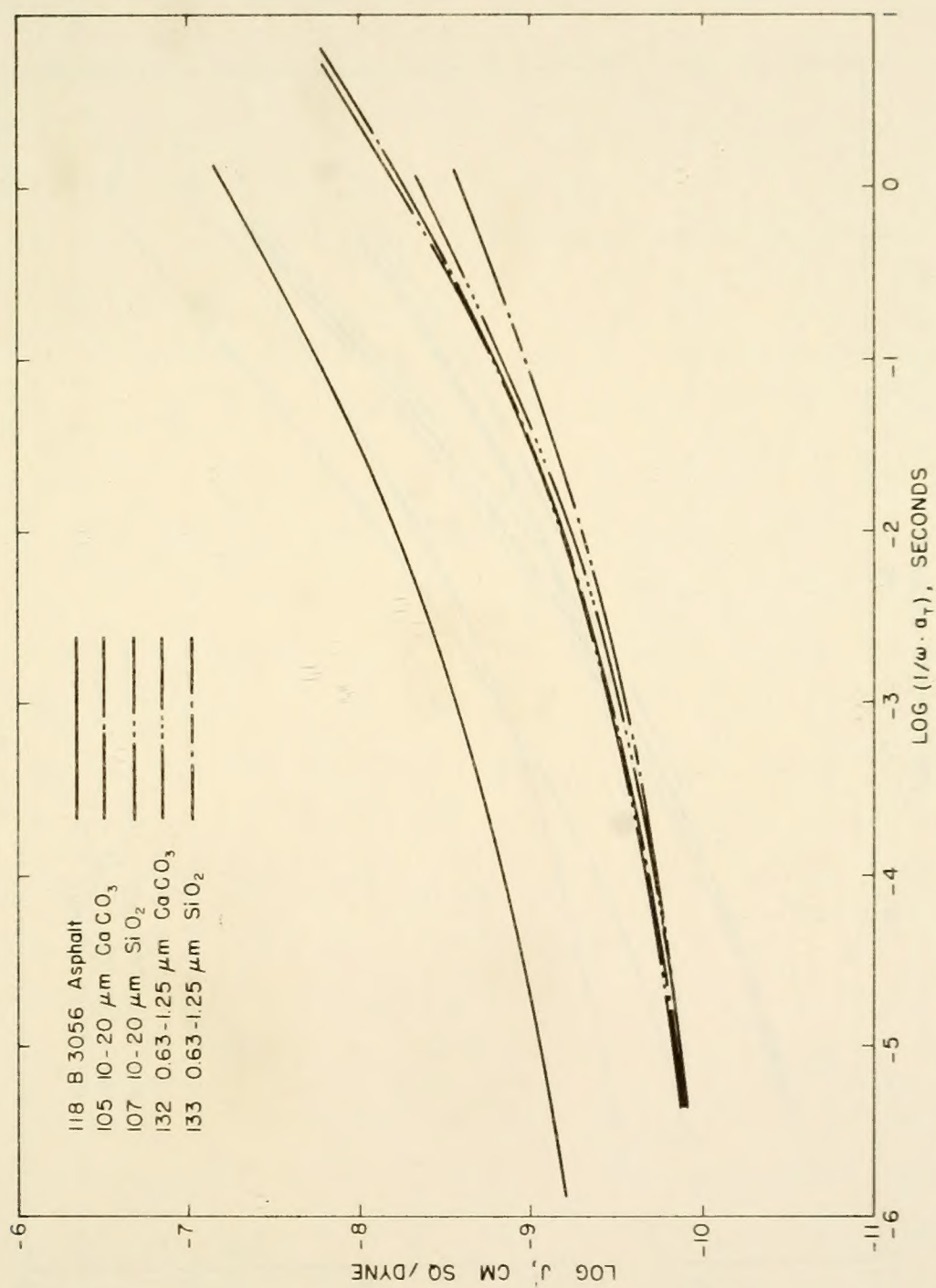


Figure 71. Effect of Filler Type on Storage Compliance, B3056 Mixtures.

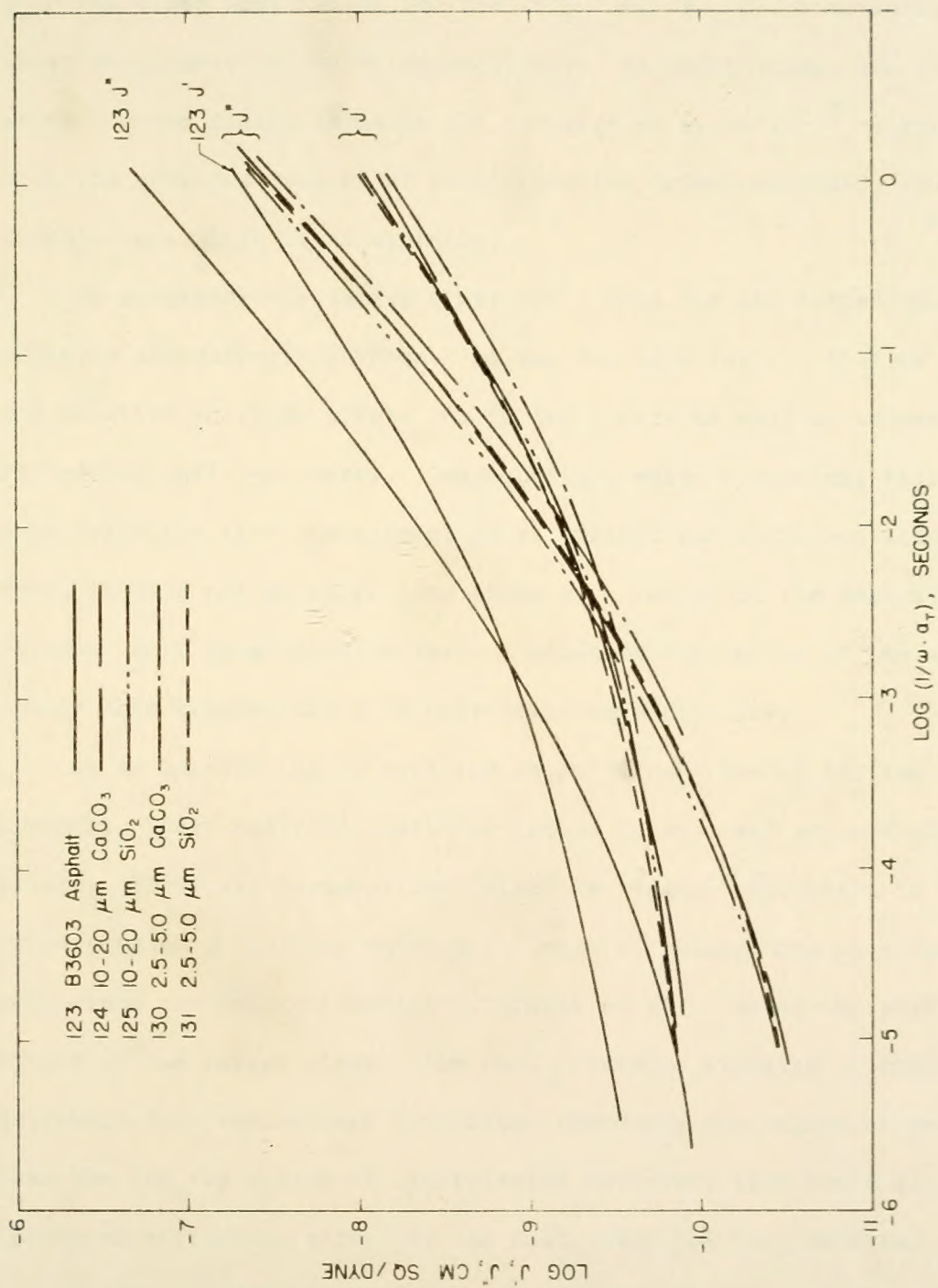


Figure 72. Storage and Loss Compliance for B3603 Mixtures.

The effect of the fillers at long times is best observed by examining creep compliance, $J(t)$; at long times $J(t)$ approaches $t/\eta + J_e$. The creep compliances for the CaCO_3 and SiO_2 B3056 mixtures are shown in Figures 73 and 74 respectively. At short times, the compliances for the filled asphalts all converge at about 10^{-10} cm sq/dyne. From the previous results of predicting the creep compliance from the dynamic data, this is as expected.

At progressively larger times the curves for the filled and unfilled asphalts increasingly diverge. As was the case for J' , this is true of the relative position within the filled curves as well as between the filled and unfilled curves. Consequently, while a vertical shift may well bring the short term compliances (filled and unfilled) into agreement, it will not do so at long times as a result of the separation effect. This separation reflects a relative stiffening of the material and is more predominant with decreasing particle size.

It is interesting to note the relative position of the two XFDG powders. These materials were dry ground to size and are definitely graded. Their air permeability "size" is roughly equivalent to the corresponding 2.5-5.0 μm material. (Table 2) Using this as a basis of comparison the apparent effect of gradation is to lower the stiffening effect at the longer times. The CaCO_3 would be expected to contain more extremely fine contaminant (recalling these are not washed or sedimented) than the SiO_2 by virtue of its relative softness; this could explain the increased stiffening effect of the CaCO_3 over the SiO_2 material.

Figure 75 presents the creep compliances for the coarse and fine extremes of the CaCO_3 and SiO_2 powders (B3056 asphalt). While the short

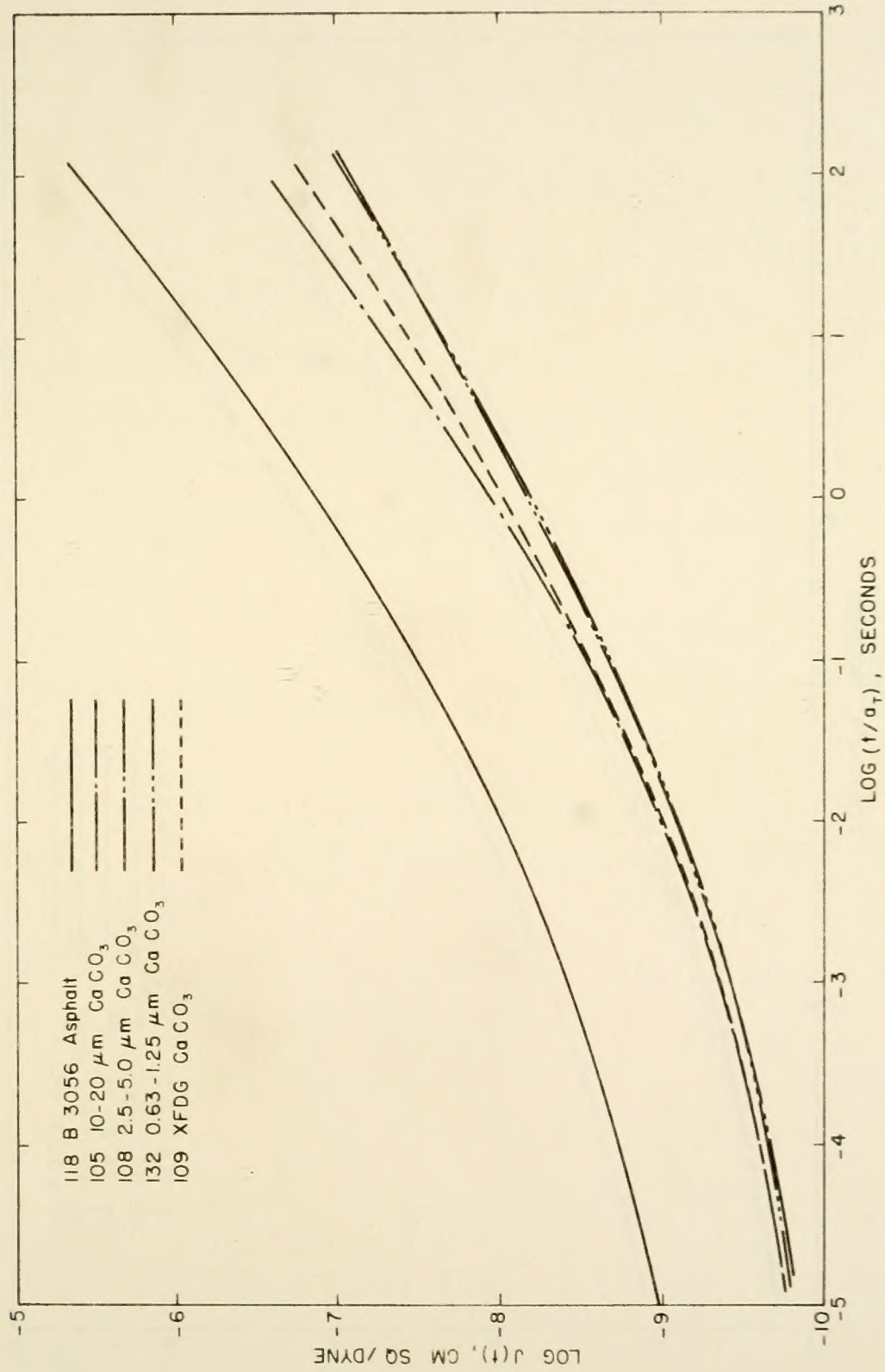


Figure 73. Creep Compliance for CaCO_3 Mixtures, B3056 Asphalt.

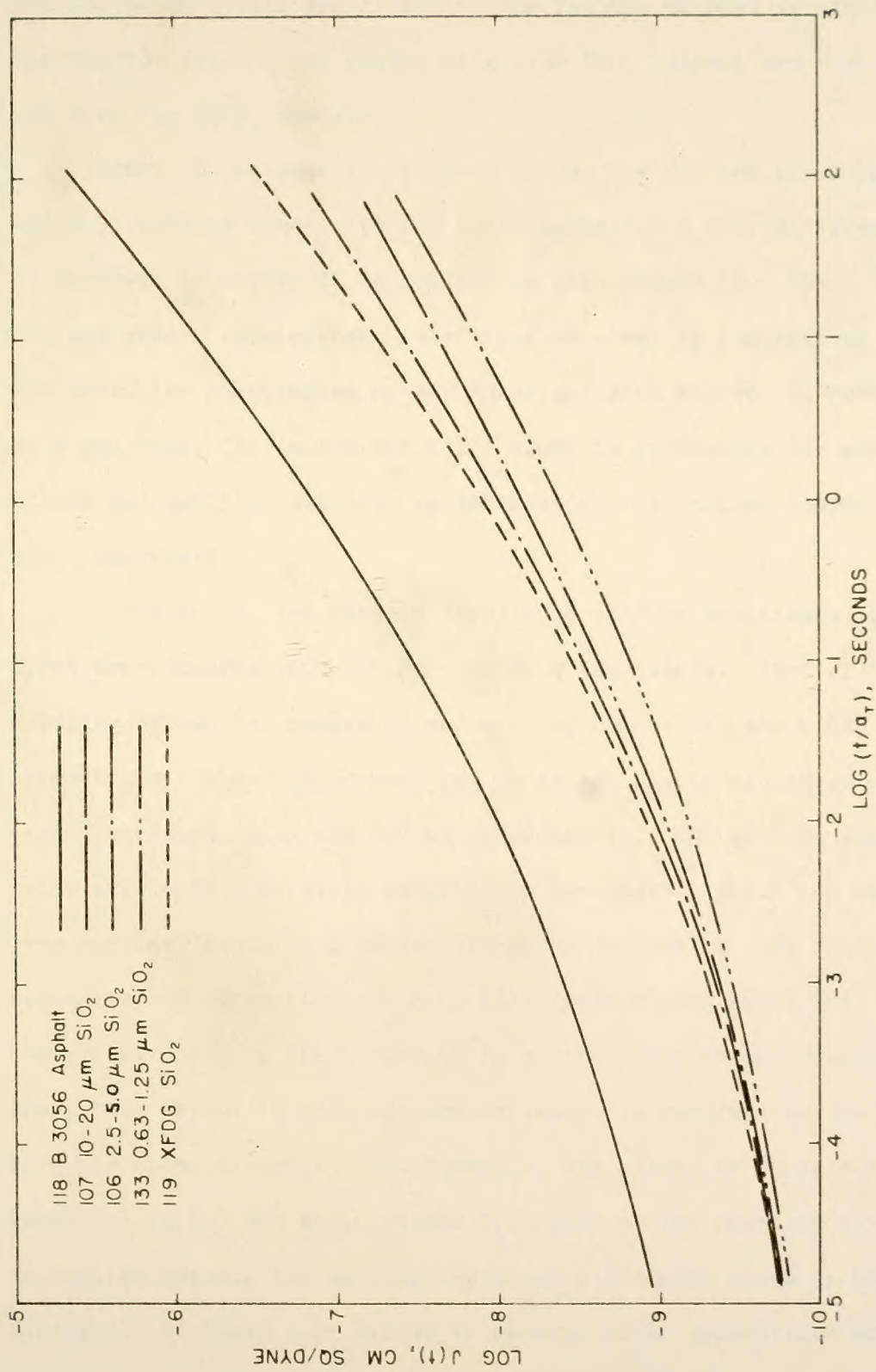


Figure 74. Creep Compliance for SiO_2 Mixtures, B3056 Asphalt.

time convergence is about 10^{-10} cm sq/dyne, it is at the long times that the differing stiffening effect of the fillers becomes apparent. From the curves, for a given powder size, the SiO_2 powders are more reinforcing than the CaCO_3 powders.

Figure 76 presents the results of the 2.5-5.0 and 10-20 μm CaCO_3 and SiO_2 powders mixed with the B3603 asphalt. A very different pattern is observed in Figure 76 in comparison with Figure 75. There is no decided effect from either filler type or size: in contrast to the B3056 mixtures, the compliances appear invariant with respect to both filler size and type. At long times a 1:1 slope is approached for both the filled and unfilled asphalts in contrast to the shallow slopes for the B3056 materials.

In Figure 77, the dynamic compliance of four additional mineral types are compared with the fine calcite and quartz. The $< 2.5 \mu\text{m}$ apatite, bytownite, magnesite and microcline are all about the same air permeability "size" ($0.53\text{-}0.61 \mu\text{m}$) while the quartz and calcite are one-sized materials, 0.59 and $1.4 \mu\text{m}$ respectively. The apatite and microcline are quite similar in behavior to the quartz, while the CaCO_3 , as seen earlier, exhibits a lesser degree of stiffening. In contrast, the magnesite and bytownite both exhibit a greater stiffening than the quartz. The effect shown by the bytownite is particularly strong because the short time asymptote also appears decreased in contrast to the effect from the other minerals. Additionally, the bytownite shows a marked reduction in Δa_T and an increased T_g . None of the measured powder properties explain the varying degree of stiffening shown by the four minerals. Although they differ in mineralogical composition an undetected

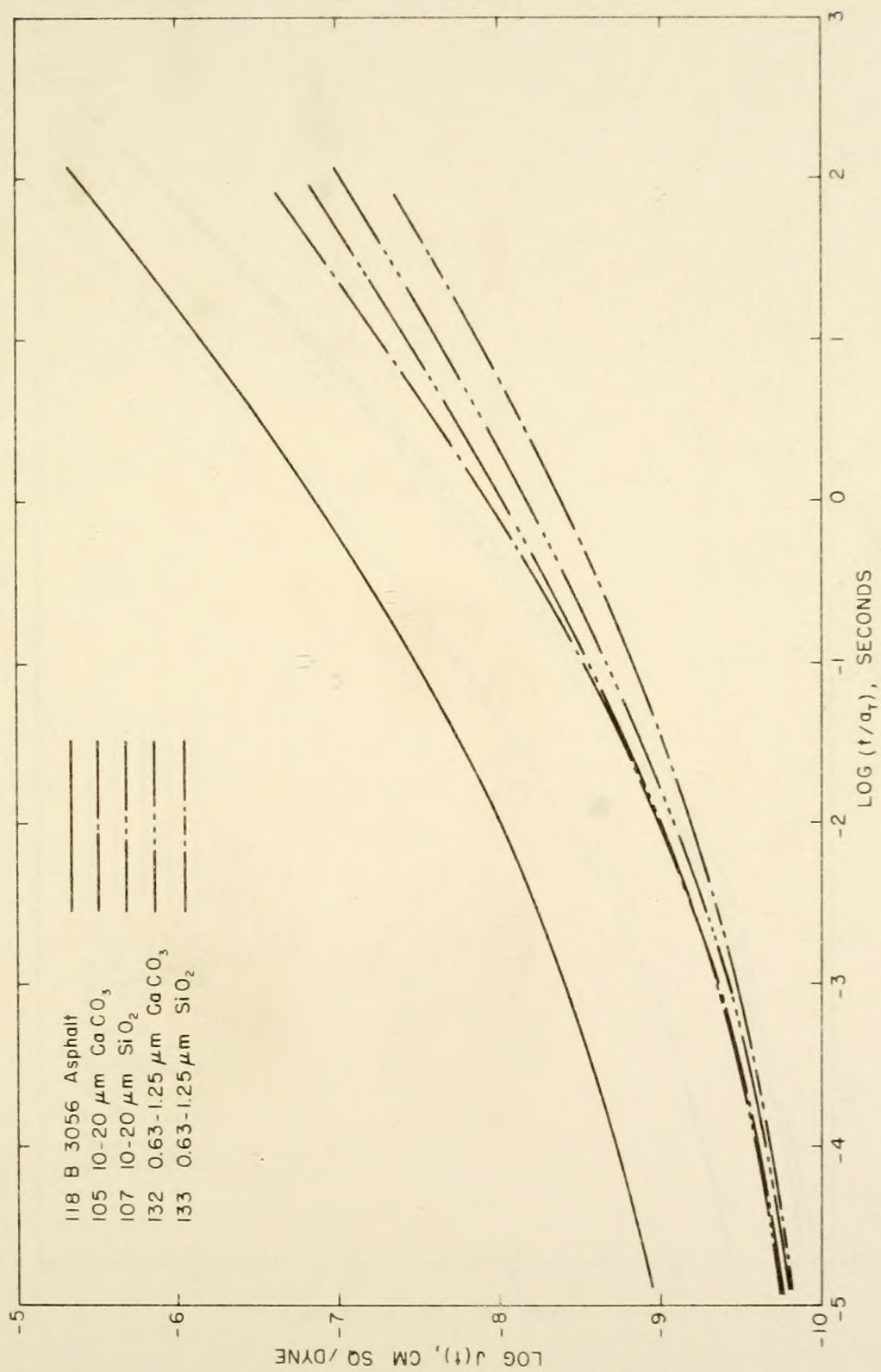


Figure 75. Creep Compliance, SiO_2 and CaCO_3 Mixtures Compared.

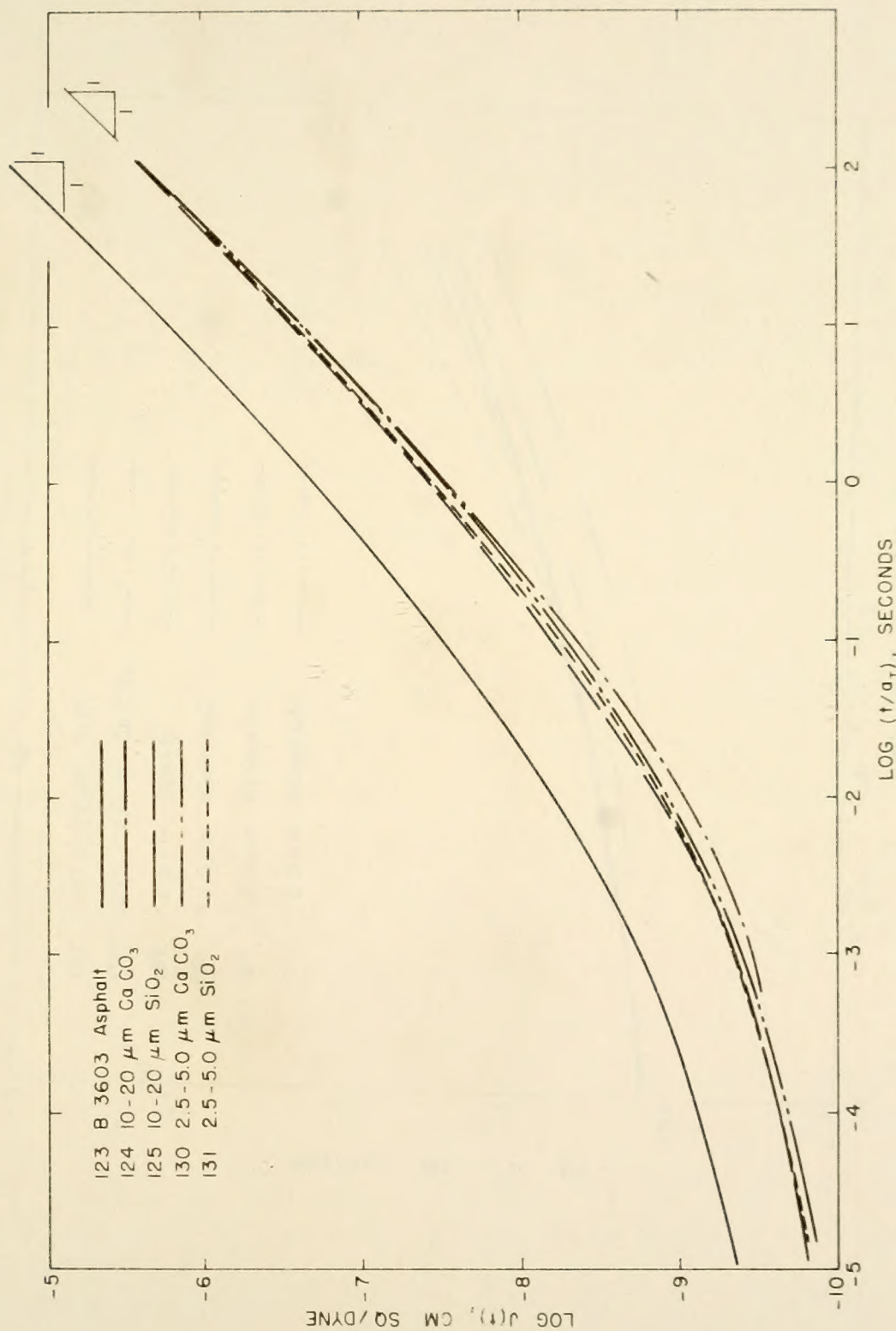


Figure 76. Creep Compliance for B3603 Mixtures, B3603 Asphalt.

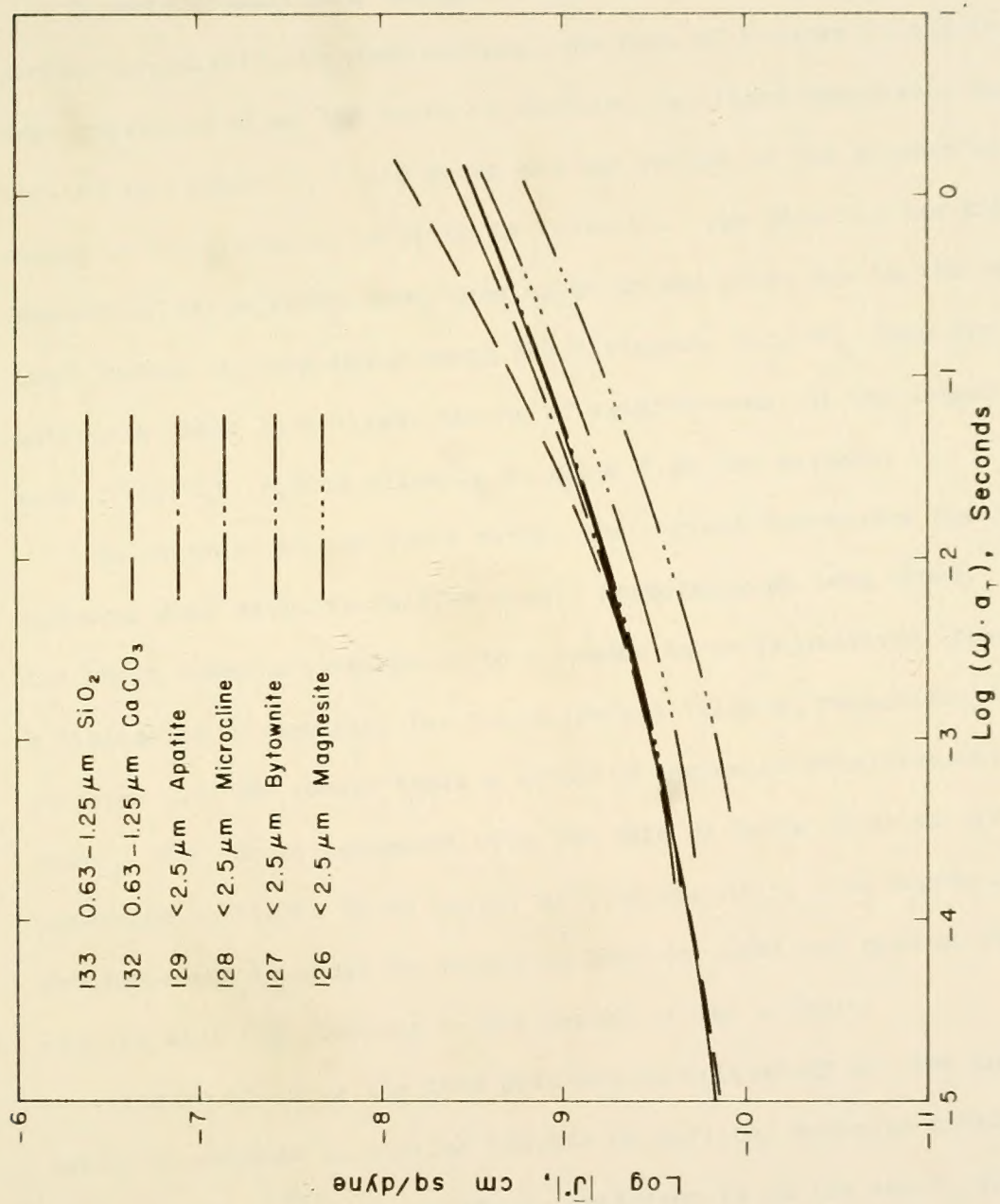


Figure 77. $|J^*|$, < 2.5 μm B3056 Mixtures.

difference in particle shape or gradation may well explain their differing behavior.

To more dramatically emphasize the reinforcement effect of the various asphalt-filler combinations, the data of Figures 75 and 76 have been recalculated as the ratio of unfilled to filled compliance and plotted in Figure 78. Also shown are the ratios of the extrapolated steady state viscosity as given in Table 15. The data for the B3603 asphalt-filler mixtures have been taken as one curve due to the relatively small change in compliance among the different fillers. Even for these materials there is a slight degree of reinforcement at the longer times, with $J^0(t)/J(t)$ rising slightly to about 7 at 200 seconds.

In contrast to the B3603 curve, the various curves for the B3056 mixtures show definite reinforcement, especially at long times. At the short times a convergence to a common curve is observed, revealing a similarity of behavior for the different fillers, regardless of size or type. At the longer times a dramatic degree of reinforcement is shown. This is in agreement with the data of Table 15 which are presented in Figure 78 as values of limiting η/η_0 . The degree of reinforcement is shown to depend on both the size and type of filler and, in addition, depends on the nature of the asphalt.

Figure 79 shows the data obtained in this study for the unfilled asphalts compared to similar results on unfilled asphalts obtained by other authors.⁽⁷⁴⁾ An important comparison is at the short times where a common asymptote is observed, in agreement with data from several other reports.^(51,74) At short times $J(t) \rightarrow |\bar{J}^*| = 1/|\bar{G}^*| \rightarrow 1/G(t)$ ⁽³⁵⁾ and a direct comparison between the reciprocal of the modulus, G , and

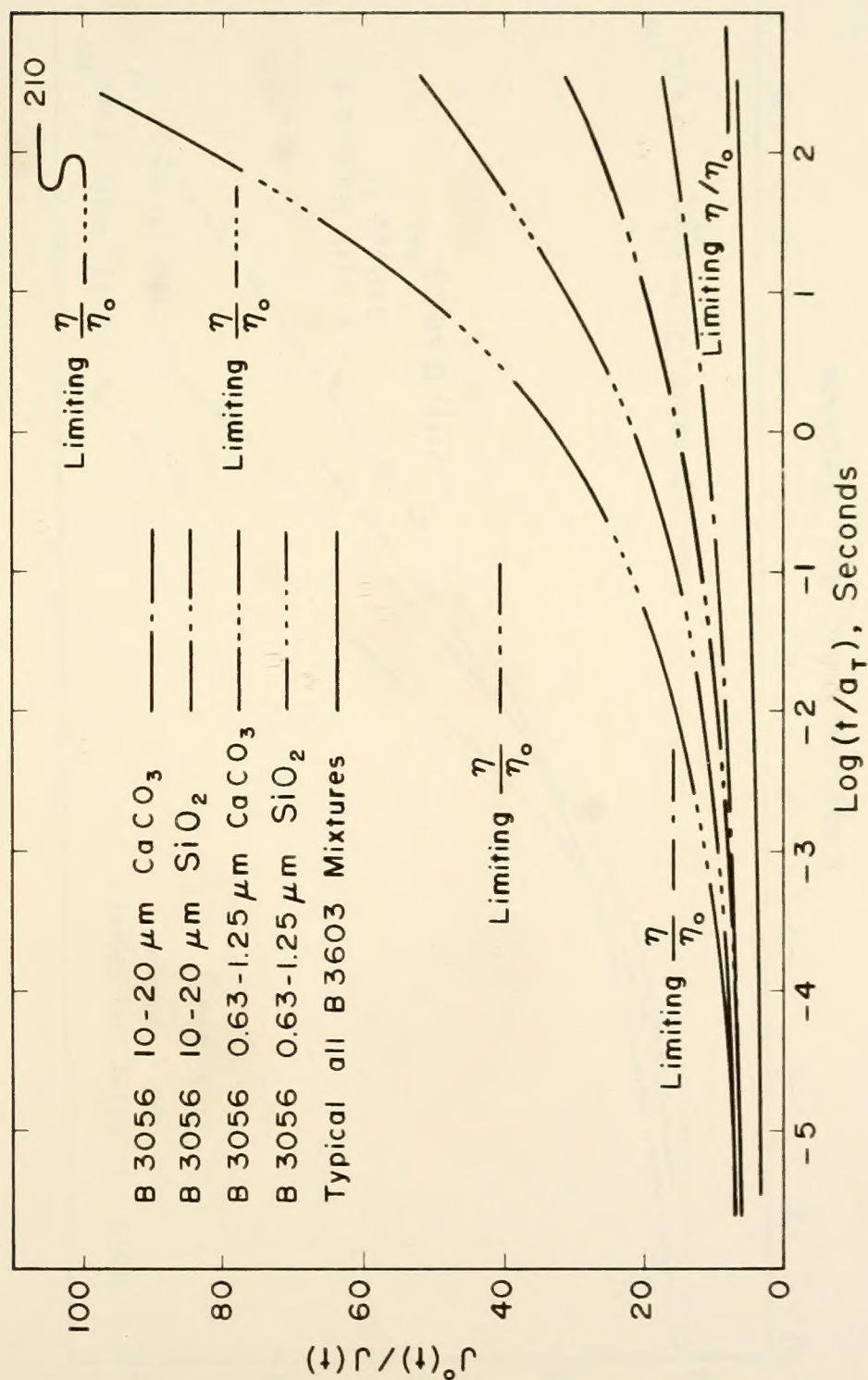


Figure 78. Ratio, $J^\circ(t)/J(t)$ for Selected B3056 and B3603 Mixtures

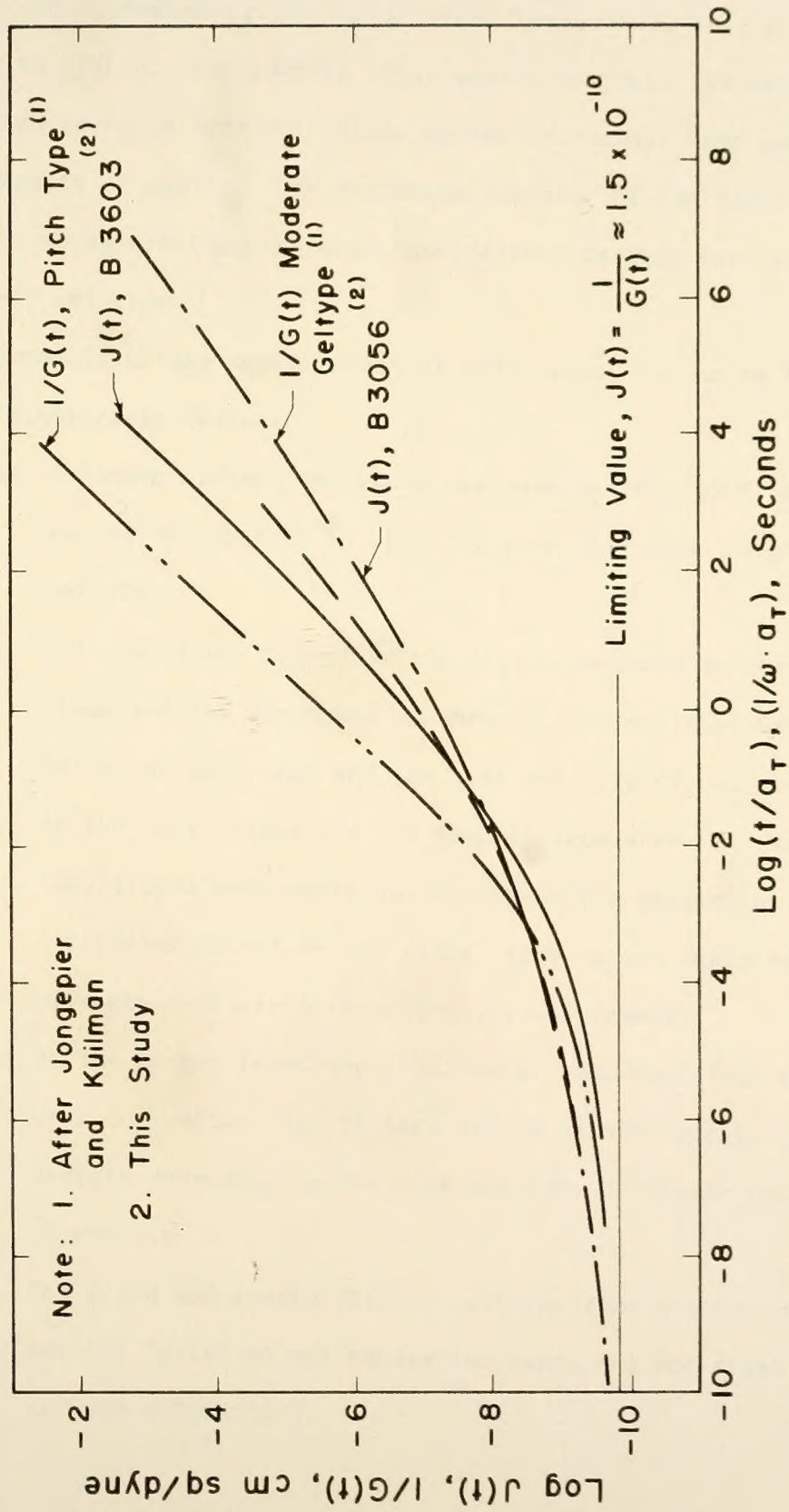


Figure 79. Comparison of the Results of the Unfilled Asphalts With Those of Other Authors.

compliance, J , is valid. At the intermediate times $|\bar{J}^*| = 1/|\bar{G}^*|$ and, using the approximation of van der Poel (page 120), $J(t)$ is approximately equal to $1/G(t)$. Considering these approximations, the data for the unfilled asphalts from this study appear reasonable when compared to the results of others. The differing behavior of the B3603 and B3056 asphalt is apparent and is shown intermediate between the pitch and moderate gel type.

Summarizing the measurements of compliance, it can be stated that, for the materials tested:

1. A common glassy compliance was observed for both the B3603 and B3056 asphalts in spite of very differing long-term behavior.
2. The compliance values of the filled asphalts at the short times and low temperatures where J_g predominates were independent of asphalt type and the size and type of filler.
3. At the short times and low temperatures where J_g predominates traditional semi-empirical equations for predicting the stiffening effect of the filler were valid, implying a lack of asphalt-filler interaction (reinforcement).
4. At the longer times the traditional semi-empirical methods were not valid. The fillers may be reinforcing to varying degrees depending on the size and type of filler and type of asphalt.
5. One sized and graded fillers with the same average air permeability "size" do not behave the same; the one sized material is more reinforcing.

Miscellaneous

Retardation Spectra

As described in a previous section, the retardation spectra were calculated from the combined shifted and calculated creep compliance data. As seen in Figures 80 through 82, the time scale of the experimental data was insufficient to completely describe $L(\tau)$. At the longer times $L(\tau)$ typically reaches a peak and then falls off.⁽³⁵⁾ True steady state flow is attained only after sufficient time such that $L(\tau)$ vanishes and there is no longer any contribution to compliance from the retardation process. The plotted retardation data (Figures 80 through 82) imply a continued contribution to compliance from $L(\tau)$. This is in agreement with the non-steady state behavior of the B3056 asphalt (pages 104 and 125) and may explain the minor differences in the various calculated and measured coefficients of viscosity for the B3603 asphalt.

The trends in $L(\tau)$ are very similar to those in $J(t)$, however this is to be expected because $L(\tau)$ is closely related to the slope of $J(t)$.⁽³⁵⁾ There is more of a tendency to retain the shape of the unfilled curve with the spectra data than with the compliance data although some divergence is still noted at the longer times.

Landel⁽⁵⁶⁾ points out that it is improper to reduce the spectra by the ratio given by the various equations predicting the volume filling effect of the filler and instead corrects on the basis that only that per cent of the volume represented by the binder volume can exhibit retardation phenomena. Following this procedure, at short times the spectra for filled polyisobutylene were brought into good

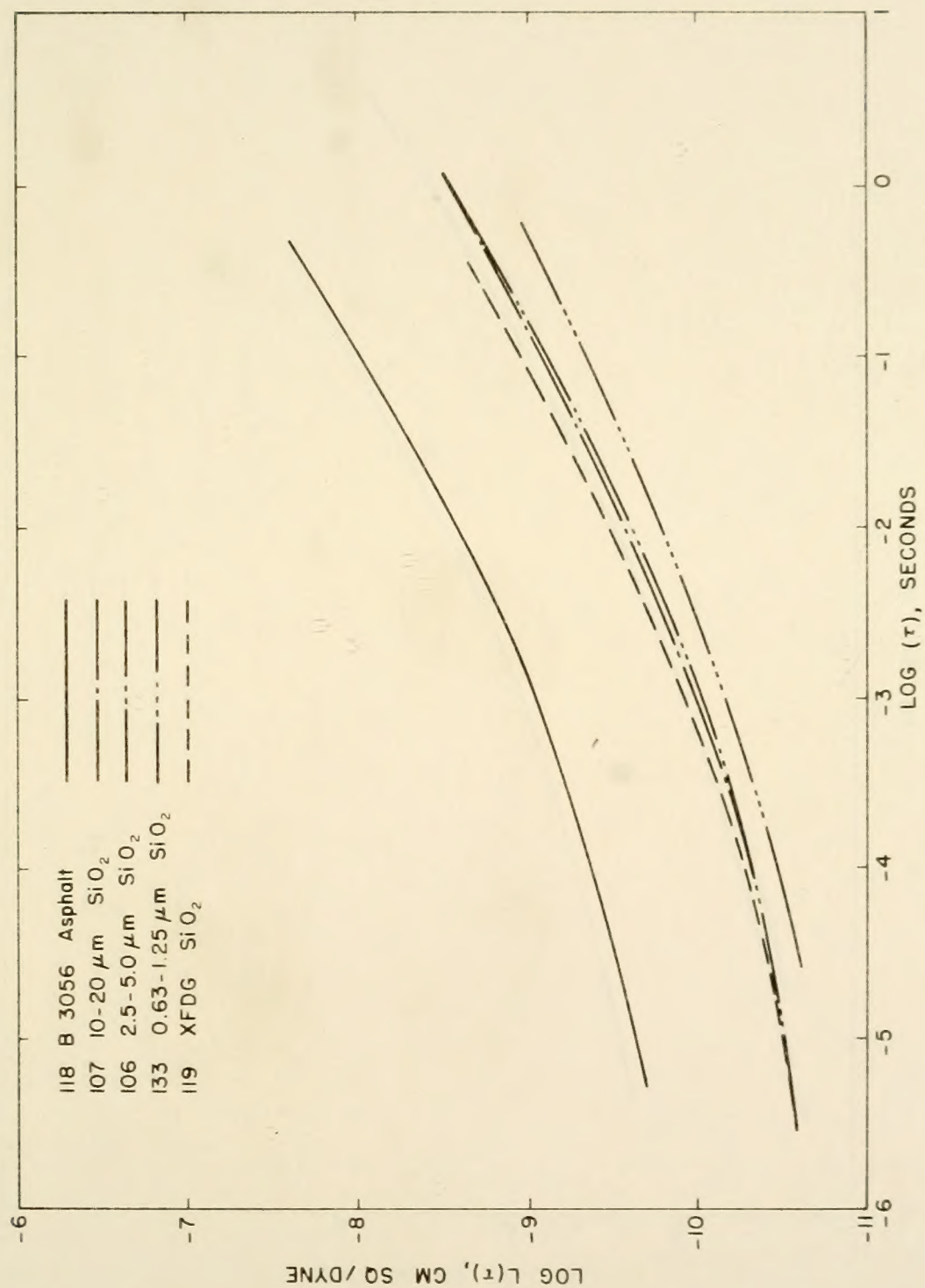


Figure 80. Retardation Spectra, SiO_2 - B3056 Mixtures.

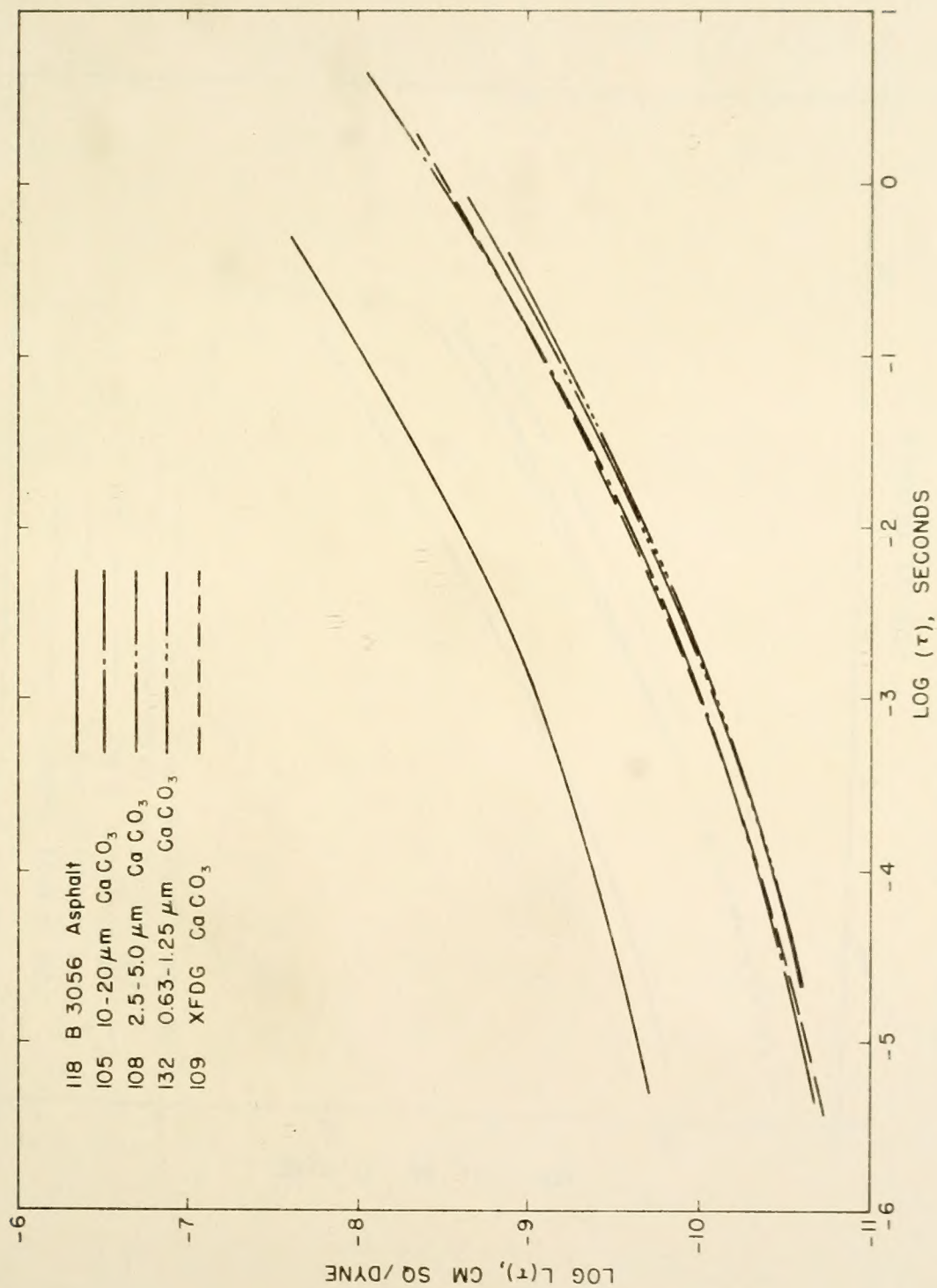


Figure 81. Retardation Spectra, CaCO_3 - B3056 Mixtures.

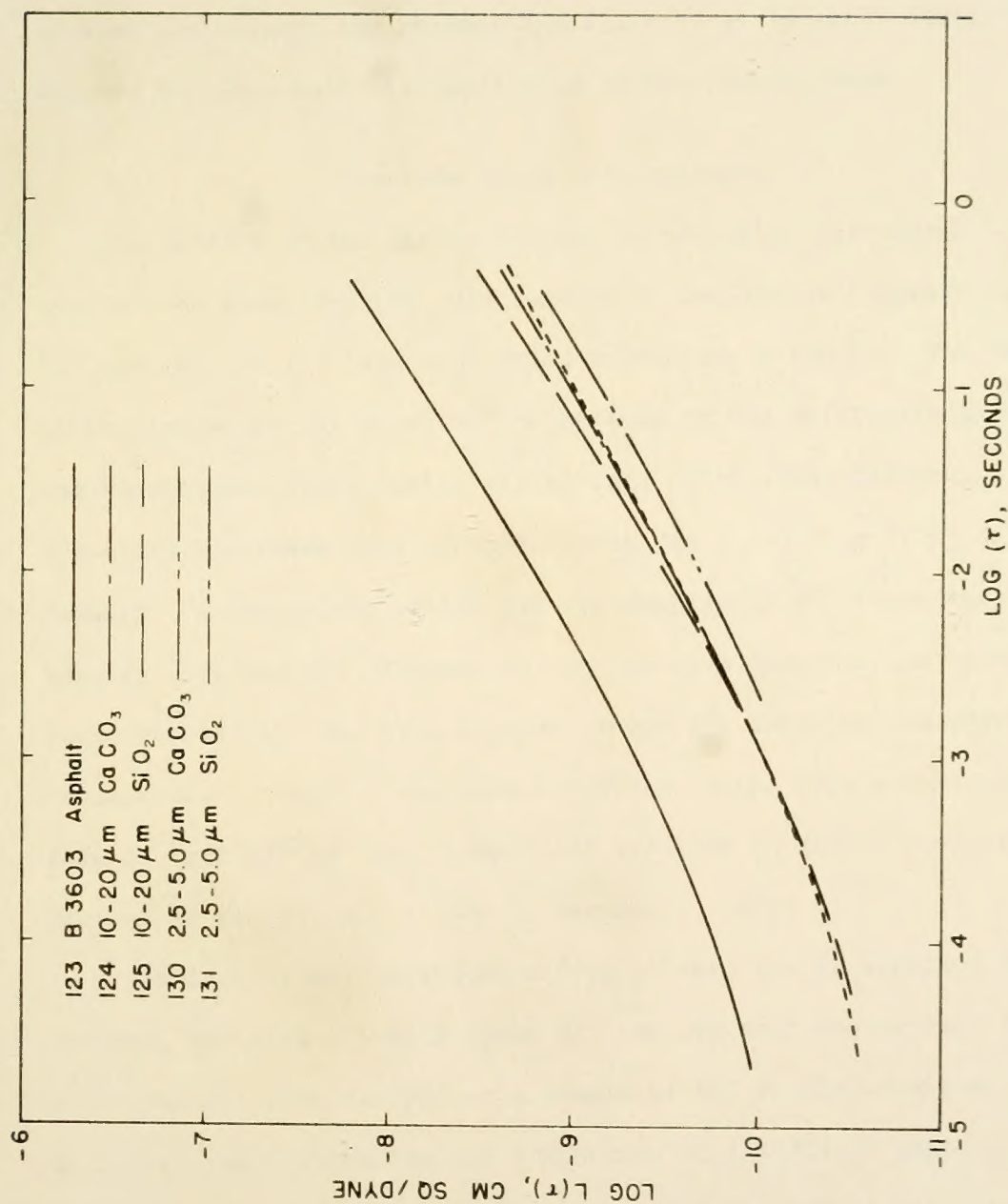


Figure 82. Retardation Spectra, B3603 Mixtures.

agreement with the spectra for the unfilled polyiso-butylene. At long times the remaining shift of the spectra to longer times is explained by the increased entanglement coupling in the polymer caused by adhesion between the polymer and filler. It is questionable as to whether the phenomenon is applicable in the present case.

Specimen Aging and Treatment

The effect of the mixing process on the creep and dynamic compliance of the plain asphalts was seen to be negligible (compare 117 and 118 and 122 and 123 tabulated data, Appendices G and I). The vacuum mixing procedure was resorted to because of the difficulty in obtaining homogeneous mixes during air mixing. With great difficulty two air-mixed specimens were produced using the 2.5-5.0 μm CaCO_3 and SiO_2 powders. A comparison of the dynamic compliance for these two samples (120 and 121, Figures 30 and 31) with their vacuum mixed counterparts (106 and 108, Figures 24 and 26) fails to indicate any considerable effect on the compliance due to the type of mixing. The same is true of the creep compliance (Figures 54 and 55 compared to Figures 48 and 50) and of the a_T parameter, Table 8.

The lack of any treatment effect between the as supplied and the desired, unfilled asphalts (page 32) implies that the asphalt in the mixes has not been altered as a result of the vacuum treatment alone. Therefore, when comparing the properties of the filled asphalt to the unfilled asphalt it is unlikely that any mixing effect other than that due to any asphalt-mineral interaction is present.

A second experiment was designed to evaluate the effect of an undisturbed hold period between mixing and testing. Samples 130-133 were prepared and tested in the usual manner and then allowed to remain undisturbed at room temperature for two months. After this hold period the samples were remounted and tested (labeled 230-233, corresponding to 130-133 except held for 2 months). After being tested and demounted the samples were first heated to about 160 F, the side bars of the sample mounts loosened and the plates worked (slid) with respect to each other to effect large strains (thousand per cent and more) in the material. These samples were labeled as 300's corresponding in description to 130 to 133.

The effect of the aging process on the values of a_T is shown in Table 8. The two B3603 mixtures retain the same T_g regardless of treatment. The two B3056 materials show a rise in T_g (as reflected in T_g) due to aging but the unaged values are regained during the heating process. The rise is small however, 3° for the CaCO_3 material and 6° for the SiO_2 . It is interesting to note that the rise corresponds to the increased interaction previously noted for the CaCO_3 and SiO_2 materials.

Figures 83 through 86 present the loss and storage compliance for each of the four mixtures. In general, the effect of aging is to stiffen the mixtures, but this effect is lost on reheating and reworking. Rather surprisingly all the reheated curves lie at or above the original (100's) curves. This is difficult to explain and may or may not be a result of experimental error. At any rate, the effect of aging is small, representing a change of fifty per cent or less in the compliance.

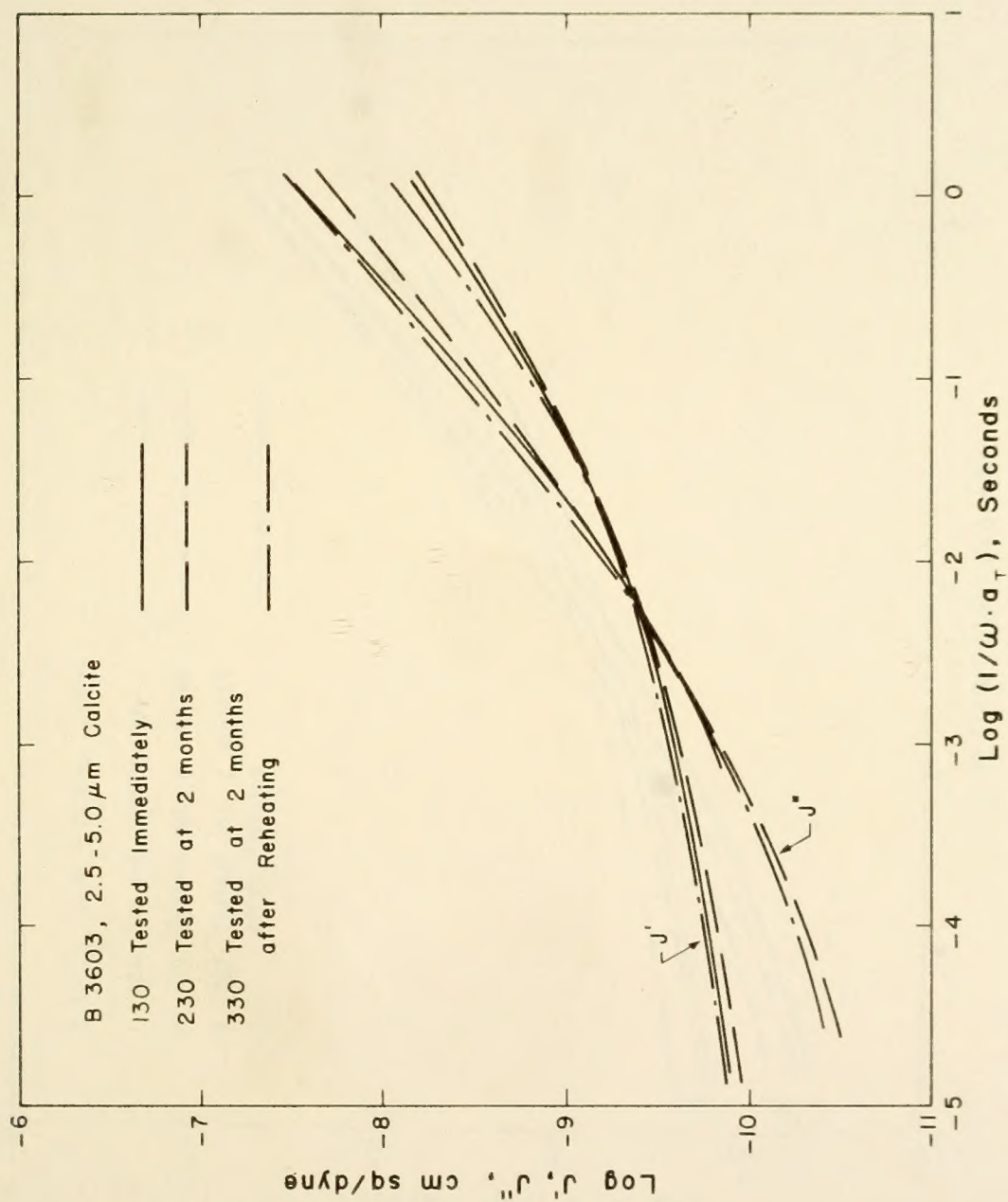


Figure 83. J' , J'' for Unaged and Aged B3603, 2.5-5.0 μm Calcite.

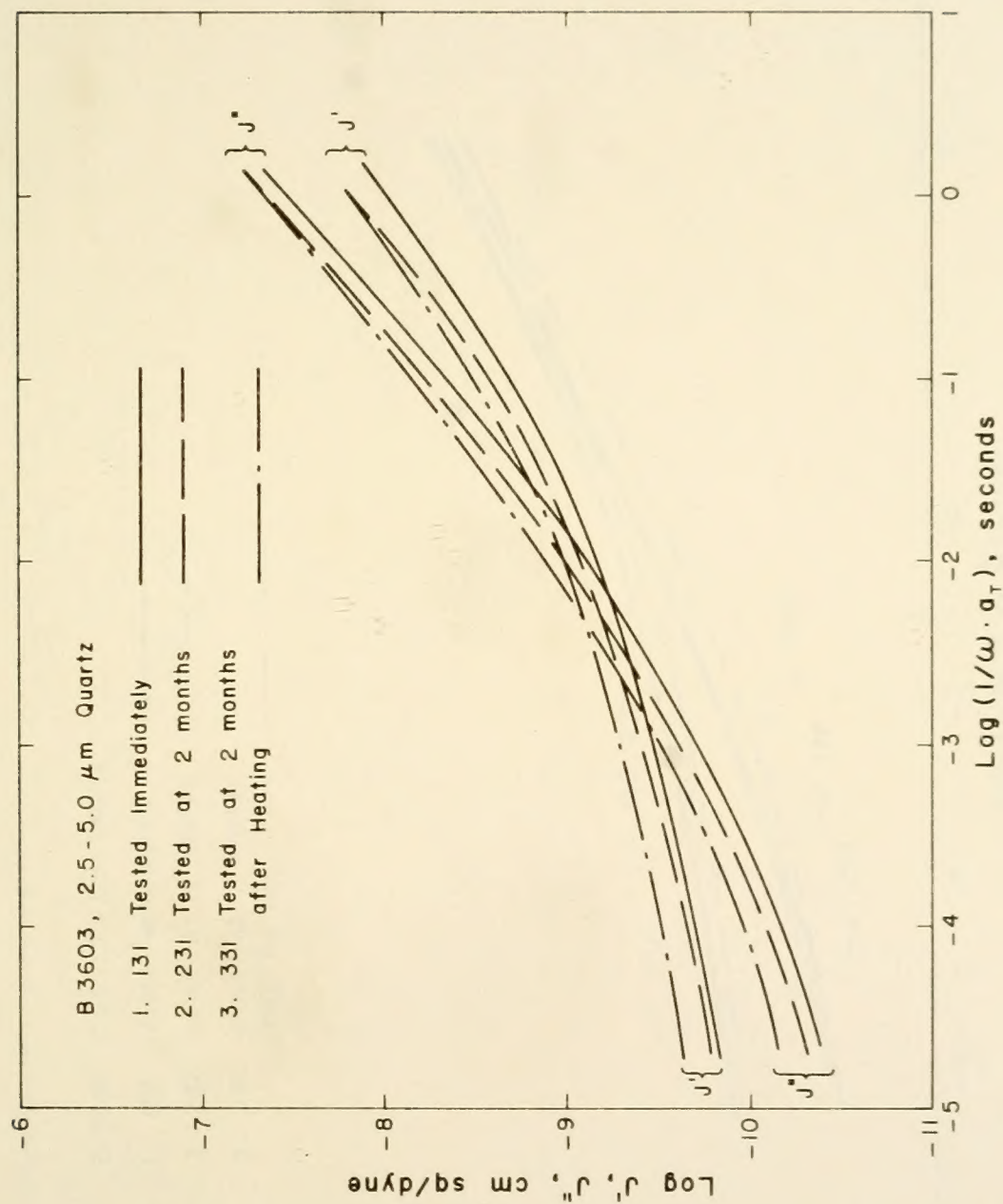


Figure 84. J' , J'' for Unaged and Aged B3603, 2.5-5.0 μm Quartz.

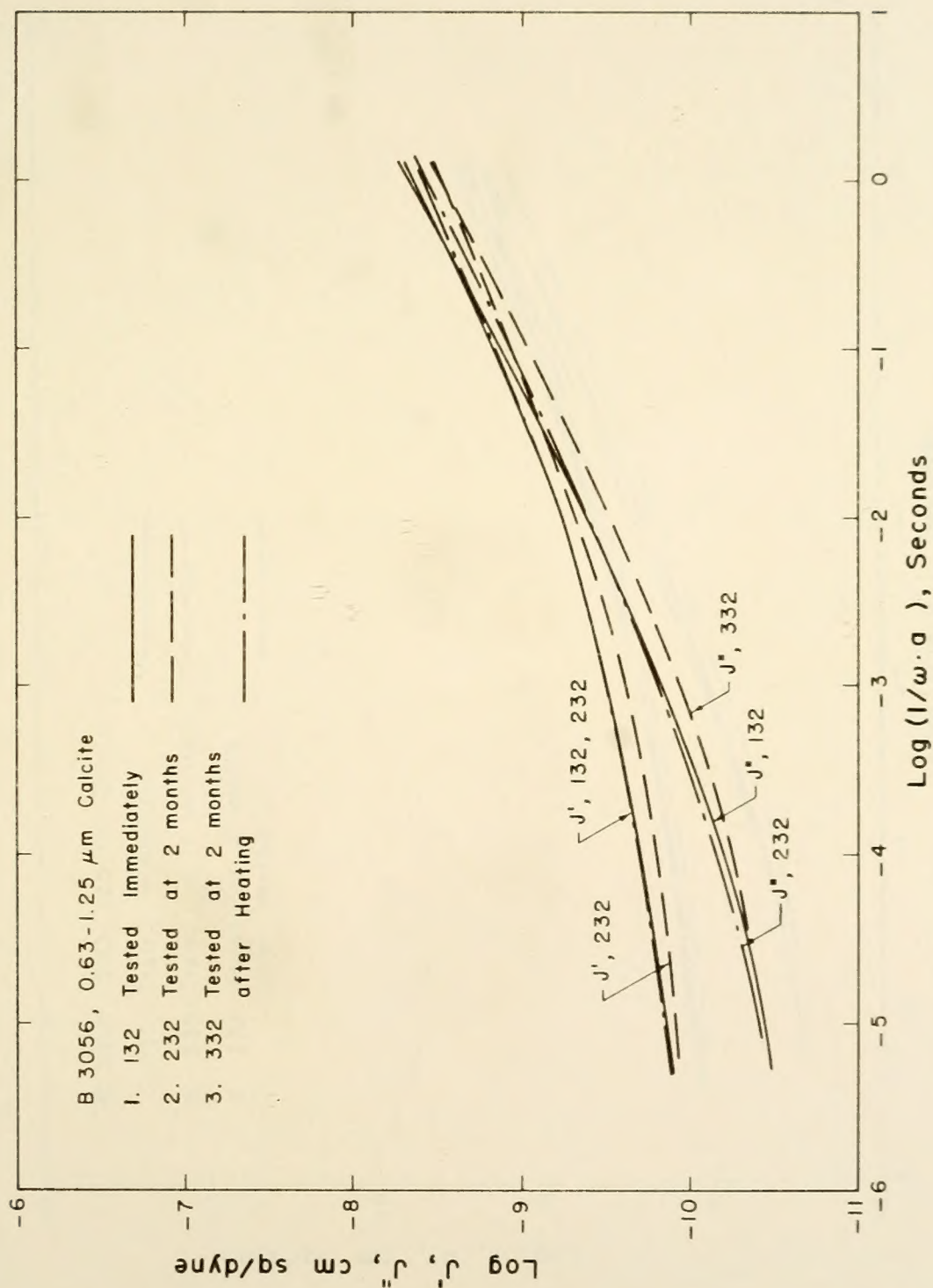


Figure 85. J' , J'' for Unaged and Aged B3056, 0.63-1.25 μm Calcite.

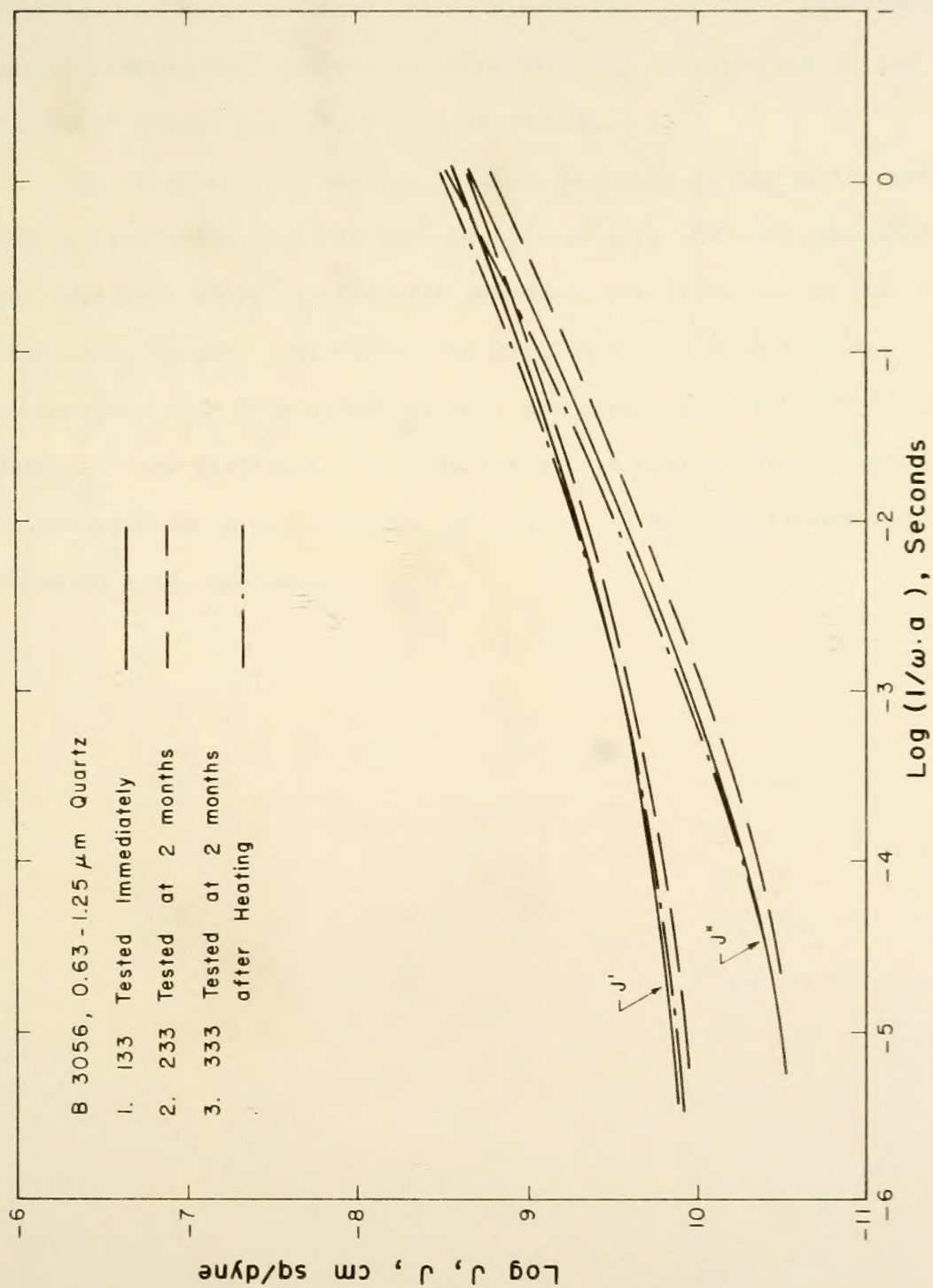


Figure 86: J' , J'' for Unaged and Aged B3056, 0.63-1.25 μ m Quartz.

If the stiffening apparent in the aged materials was due to a thixotropic effect in the asphalt it was not destroyed during the testing. As with the other tests, steady state dynamic behavior was reached immediately indicating no destruction of structure at the levels of stress and strain used in testing.

Any thixotropic effect or possible bridging of asphalt structure between particles that may have been present in the aged specimens was not destroyed except by the heat and excessive straining of the remolding process. Therefore, any structure developed with age is broken down only with excessive heat and straining. The reversible nature of the stiffening would indicate that preferential adsorption is probably not a satisfactory explanation of the reinforcement of the unheated aged specimens.

CONCLUSIONS

Mixing of Asphalt and Mineral Powder

In the course of the work, homogeneous mixtures of asphalt and mineral powder were required. From the work done in developing a suitable mixing technique, it can be concluded that:

1. Mixing under vacuum substantially increases the homogeneity of very fine powder-asphalt mixtures.
2. The vacuum mixing technique as developed in this study does not affect the measured compliance of either the filled or the unfilled asphalts. Except for mineral-asphalt interaction, the two asphalts tested are unchanged by the vacuum mixing process.

Surface Characterization

An extensive physico-chemical characterization of the mineral surface was anticipated prior to the start of the project. With the completion of the study it is concluded that, although this indeed looks like a very promising approach, a truly interdisciplinary effort between asphalt chemist and surface chemist will be needed to accomplish it.

Material Characterization

Prior to the examination of asphalt-mineral interaction a satisfactory method of material characterization was sought: one that would allow the evaluation of asphalt-mineral interaction. A linear viscoelastic representation was hypothesized. From the mechanical measurements it can be concluded that:

1. Over the range tested, both the filled and unfilled asphalts are linear viscoelastic by virtue of:
 - A. Compliance being independent of stress level.
 - B. Sinusoidal input yielding a sinusoidal output.
 - C. Superposition of creep data.
 - D. Interconvertibility of creep and dynamic data.
2. Neither filled nor unfilled material undergoes a measurable thixotropic or structural change when exposed to a stress field within the domain of linear behavior.
3. Both the filled and unfilled asphalts can be represented as thermorheologically simple; however, a single set of constants in the WLF equation are not satisfactory to describe both asphalts. If the standard form of the WLF equation is used this is equivalent to requiring a variable $T_s - T_g$ temperature.
4. Dilatometric and mechanically determined ($T_s - T_g$) values of T_g are compatible provided a variable value of $T_s - T_g$ is used.

5. Reasonable values of T_g can be generated dilatometrically using the micro samples (1/8 inch thick by 3/4 inch diameter) and technique described, as long as proper cell design and experimental care is exercised.
6. A rather simple bath may be used to determine the glass transition temperature, without recourse to complicated electronic controllers, etc. as long as proper attention to experimental detail is taken.

Interaction

Having concluded that both the filled and unfilled materials can be represented as linear viscoelastic, the various linear viscoelastic parameters were examined for evidence of mineral-asphalt interactions. From this examination it is concluded that:

1. Asphalt-mineral powder composites can definitely exhibit asphalt-mineral interaction and, because differing degrees of reinforcement are observed with:
 - A. The same mineral powder but different asphalt types,
 - B. Powders physically similar but of varying composition, and
 - C. Similar powders and asphalt but varying powder size,it can be concluded that the reinforcement is truly an interaction between surface and asphalt.

2. At short times all asphalts exhibit the same value of compliance. Each of the filled systems at the short test times are non-interacting and conform to the classical behavior for non-interacting filled systems. Therefore, while classical theories can predict short term behavior, long term behavior can not be predicted from volume concentration and physical filler characteristics alone.
3. The mechanism of reinforcement is uncertain but is most probably explained by a surface induced structure in the asphalt. This structure is not broken down during moderate straining. Preferential adsorption seems an improbable explanation.
4. The form of the temperature dependence is not altered by the reinforcing effect of the filler. The same values of a_T apply to both the filled and unfilled asphalts.
5. Dilatometric glass transition temperatures, for the interacting asphalt, vary with filler size (interaction) whereas the mechanically determined values do not.

From this result it is concluded that a different mechanism is operative in the volume expansion behavior than shear behavior.
6. Graded and one sized materials with the same average size do not generate the same degree of reinforcement. The parameters as given by Rigden⁽¹¹⁾ are not in themselves sufficient to predict the effect of size for an interacting filler-asphalt composite.

RECOMMENDATIONS FOR FURTHER RESEARCH

A rational characterization of the mineral surface chemistry pertinent to the adsorption mechanism is needed. Undoubtedly, collaboration between the surface and asphalt chemist will be required. The problem is complicated by the complex and as yet undefined nature of the asphalt. In addition, because the interaction mechanism is undefined, and perhaps variable with asphalt and mineral, the different surface chemistry parameters that should be evaluated are also uncertain.

An examination of the IR spectra of different asphalts adsorbed on various mineral surfaces or even variously treated glass surfaces should provide some insight into any adsorbed species that may promote reinforcement. A systematic variation in asphalt composition may also provide some clue as to the mechanism.

In regard to the evaluation of interaction, the short term behavior can logically be disregarded and instead a one temperature creep test conducted. The work of this study has served to isolate the time-temperature range over which reinforcement can be expected. Also, it appears that beads may be used in lieu of natural powders in the study of interaction. These may be processed in a range of essentially one sized fractions of varying composition. Different

surfactants may also be applied to the glass to generate different surface conditions.

No attempt was made to establish the stress-strain dependency of linear behavior or the effect of filler and asphalt-filler interaction on the range of linear behavior. A logical extension would, therefore, be the establishment of the range of stress and strain over which the concluded linear behavior is valid.

Time-temperature superposition was found valid over the range of time and temperature tested. It would be of interest to duplicate some of the testing on a wide range rheogoniometer such as reported in the literature⁽⁸⁰⁾ to see if the superposition holds at the time-temperature extremes, and, especially, to see if it is affected by the interaction between filler and asphalt.

It is reported for other materials that if the compliance is shown time-temperature shiftable, other parameters such as breaking strength are also shiftable in spite of their occurring in a non-linear region. It should be established whether or not the interactions are also carried over into the failure properties of the mixtures. It may well be that trends in the compliance are reflected in the failure parameters.

The reinforcement was attributed to a mineral surface-asphalt interaction. If correct, this interaction should be present regardless of the extent of the surface. When present on larger sized aggregate, the interaction may well play a role in the cracking behavior of bituminous concrete. The presence of the interaction isolated in

this study should be examined in the light of the behavior of bituminous concrete, both because an altered filler-bitumen system may affect overall behavior and because interaction may affect failure behavior.

LIST OF REFERENCES •

LIST OF REFERENCES

1. "The Asphalt Handbook", Manual Series No. 4 (MS-4) April, 1965 ed., Asphalt Institute, 1965.
2. Goetz, W. H. and Wood, L. E., "Bituminous Materials and Mixtures", Section 18, "Highway Engineering Handbook", Woods, K. B., ed., McGraw Hill, New York, 1960.
3. Allen, T., "Particle Size Measurements", Chapman and Hall, London, 1968.
4. Hough, B. K., "Basic Soils Engineering", Ronald Press, New York, 1957.
5. Benson, F. J., "Effects of Aggregate Size, Shape, and Surface Texture on the Properties of Bituminous Mixtures - A Literature Survey", Highway Research Board SR 109, 12 (1970).
6. Herrin, Moreland, and Goetz, W. H., "Effect of Aggregate Shape on Stability of Bituminous Mixes", Proc. Highway Research Board, 33, 293 (1954).
7. Richardson, Clifford, "The Modern Asphalt Pavement", J. Wiley and Sons, New York, 1914.
8. Traxler, R. N., "The Evaluation of Mineral Powders as Fillers for Asphalt", Proc. AAPT, 8, 60 (1937).
9. Traxler, R. N., "Asphalt: its Composition, Properties, and Uses", Reinhold, New York, 1961.
10. Mitchell, J. G., and Lee, A. R., "Evaluation of Fillers for Tar and Other Bituminous Surfacing", J. Soc. Chem. Ind., 58, 299 (1939).
11. Rigden, P. J., Road Research Technical Paper No. 28, Road Research Laboratory, Hammondsworth, Middlesex, H. M. S. O., London, 1954.
12. Winniford, R. S., "The Rheology of Asphalt-Filler Systems as Shown by the Microviscosimeter", ASTM STP 309, 109 (1961).

13. Warden, W. B., Hudson, S. B., and Howell, H. C., "Evaluation of Mineral Fillers in Terms of Practical Pavement Performance", Proc. AAPT, 28, 316 (1959).
14. Tunnicliff, D. G., "A Review of Mineral Filler", Proc. AAPT, 31, 118 (1962).
15. Tunnicliff, D. G., "Binding Effects of Mineral Filler", Proc. AAPT, 36, 114 (1967).
16. Van Wazer, J. R., et. al., "Viscosity and Flow Measurement - A Laboratory Handbook of Rheology", Interscience Publishers, New York, 1963.
17. Hurlbut, C. S., "Dana's Manual of Mineralogy", 17th ed., Wiley, New York, 1961.
18. Jackson, M. L., "Soils Chemical Analysis - Advanced Course", College of Agriculture, University of Wisconsin, Madison, Wis., 1956.
19. Herdan, G., "Small Particle Statistics", Elsevier Pub. Co., Amsterdam, 1953.
20. Cadle, R. D., "Particle Size Determination", Interscience, New York, 1955.
21. Carman, P. C., "Flow of Gasses Through Porous Media", New York Academic Press, 1956.
22. Ridgen, P. J., "The Specific Surface of Powders - A Modification of the Theory of the Air-Permeability Method", J. Soc. Chem. Ind., 66, 130 (1947).
23. Arnell, J. C., "Permeability Studies I. Surface Area Measurements Using a Modified Kozeny Equation", Can. J. Res. 24, 103 (1946).
24. Kamak, H. J., "Simple Air-Permeability Methods for Measuring Surface Areas of Fine Powders", Anal. Chem., 26, 1623 (1954).
25. Gregg, S. J. and Sing, K. S. W., "Adsorption, Surface Area and Porosity", Academic Press, London and New York, 1967.
26. Eilers, H., "The Colloidal Structure of Asphalt", J. of Physical and Colloid Chem., 53, 1195 (1949).
27. Kipling, J. J., "Adsorption from Solutions of Non-Electrolytes", Academic Press, New York, 1965.

28. Hammett, L. P., and Deyrup, A. J., "A Series of Simple Basic Indicators. I. The Acid Functions of Mixtures of Sulfuric and Perchloric Acids with Water", JACS, 54, 2720 (1932).
29. Benesi, H. A., "Acidity of Catalyst Surfaces. I. Acid Strength from Colors of Adsorbed Indicators", JACS, 78, 5490 (1956).
30. Schmidt, R. J. and Santucci, L. E., "A Practical Method for Determining the Glass Transition Temperature of Asphalts and Calculation of Their Low Temperature Viscosities", Proc. AAPT, 35, 61 (1966).
31. Welborn, J. Y., Oglio, E. R., and Zenewitz, J. A., "A Study of Viscosity-Graded Asphalt Cements", Proc. AAPT, 35, 19 (1966).
32. Halstead, W. J., Rostler, F. S. and White, R. M., "Properties of Highway Asphalts - Part III, Influence of Chemical Composition", Proc. AAPT, 35, 191 (1966).
33. Blokker, P. C. and van Hoorn, H., "Durability of Bitumen in Theory and Practice", Proc., Fifth World Petroleum Congress.
34. Daniel, I. M., "Theoretical Stress Analysis", in Brown, W. E., ed., Testing of Polymers, Vol. 4, Interscience Publishers, New York, 1968.
35. Ferry, J. D., "Viscoelastic Properties of Polymers", Wiley, New York, 1961.
36. Gross, B., "Theories of Viscoelasticity", Herman, Paris, 1953.
37. Bland, D. R., "The Theory of Linear Viscoelasticity," Pergamon Press, London, 1960.
38. Lee, E. H., "Stress Analysis in Viscoelastic Bodies", Quart. Appl. Math., 13, 183 (1955).
39. Schapery, R. A., "Stress Analysis of Viscoelastic Composite Materials", J. Composite Materials, 1, 228 (1967).
40. Moavenzadeh, F. and Soussou, J., "Viscoelastic Constitutive Equation for Sand Asphalt Mixtures", Highway Research Board, HRR 256, 36 (1968).
41. Williams, M. L., "Structural Analysis of Viscoelastic Materials", AIAA Journal, 2, 785 (1964).
42. Fung, Y. C., "Foundations of Solid Mechanics", Prentice-Hall, Englewood Cliffs, New Jersey, 1965.

43. Wylie, C. R. Jr., "Advanced Engineering Mathematics", 2nd ed., McGraw Hill, New York, 1960.
44. Malmstadt, H. V., Enke, C. G., and Toren, E. C. Jr., "Electronics for Scientists", Benjamin, New York, 1963.
45. Lee, T., "Methods of Determining Dynamic Properties of Viscoelastic Solids Employing Forced Vibrations", J. Appl. Physics, 34, 5 (1963).
46. Williams, M. L., Landel, R. F., and Ferry, J. D., "The Temperature Dependence of Relaxation Mechanisms in Amorphous Polymers and Other Glass Forming Liquids", JACS, 77, 3701 (1955).
47. Krokosky, Edward, "Behavior of Time-Dependent Composite Materials", in Broutman, L. J., Krock, R. H., Ed., Modern Composite Materials, Addison-Wesley, 1967.
48. Wada, Y., Hirose, H., "Glass Transition Phenomena and Rheological Properties of Petroleum Asphalt", J. Phys. Soc. Japan, 15, 1885, (1960).
49. Smith, T. L., "Dependence of the Ultimate Properties of a GR-S Rubber on Strain Rate and Temperature", J. Polymer Sci., 32, 99 (1958).
50. Shoor, S. K., Majidzadeh, K., and Schweyer, H. E., "Temperature-Flow Functions for Certain Asphalt Cements", Highway Research Board, HRR 134, 63 (1966).
51. Sisko, A. W. and Brunstrum, L. C., "Relation of Asphalt Rheological Properties to Pavement Durability", Highway Research Board, NCHRP Report 67, 1969.
52. Ferry, J. D., and Landel, R. F., "Molecular Friction Coefficients in Polymers and Their Temperature Dependence", Kolloid - Z., 148, 1 (1956).
53. Brodnyan, J. G., "Use of Rheological and Other Data in Asphalt Engineering Problems", Highway Research Board Bull. 192, 1 (1958).
54. Ninomiya, K. and Ferry, J. D., "Some Approximate Equations Useful in the Phenomenological Treatment of Linear Viscoelastic Data", J. Colloid. Sci., 14, 36 (1959).
55. Williams, M. L., and Ferry, J. D., "Several Approximation Calculations of Mechanical and Electrical Relaxation and Retardation Distributions", J. Polymer Sci., 11, 169, (1953).

56. Landel, R. J., "The Dynamic Mechanical Properties of a Model Filled System: Polyisobutylene Glass Beads", *Trans. Soc. Rheol.*, 2, 53 (1958).
57. Buche, F., "Physical Properties of Polymers", Interscience, New York, 1962.
58. Bartenev, G. M., et. al., "A Contribution to the Theory of the Structural Glass Transition", *J. Polymer Sci.*, 7, 2147 (1969).
59. Kauzmann, W., "The Nature of the Glassy State and the Behavior of Liquids at Low Temperatures", *Chem. Rev.*, 43, 219 (1948).
60. Barrall, E. M., et. al., "Asphalt Transition at Low Temperatures. Measurements Using Recording Thermal Expansion Apparatus", *Am. Chem. Soc., Div. Retrol. Chem., Preprints*, 9 (2), B27 (1964).
61. Lange, N. A., ed., "Handbook of Chemistry", 10th edition, McGraw Hill, New York, 1967.
62. van der Poel, C., "A General System Describing the Visco-elastic Properties of Bitumens and Its Relation to Routine Test Data", *J. Appl. Chem.*, 4, 221 (1954).
63. van der Poel, C., "Time and Temperature Effects on the Deformation of Asphaltic Bitumens and Bitumen-Mineral Mixtures", *SPE Journal*, 47 (1955).
64. Ninomiya, K., "An Extrapolation Method for Estimating Steady-Flow Viscosity and Steady State Compliance from Creep Data", *JACS*, 67, 1152 (1963).
65. Kraus, G., "Interactions between Elastomers and Reinforcing Fillers", in Kraus, G., *Reinforcement of Elastomers*, Interscience, New York, 1965.
66. Secor, K. E., and Monosmith, C. L., "Viscoelastic Response of Asphalt Paving Slabs under Creep Loading", *Highway Research Board, HRR* 67, 84 (1965).
67. Pagen, C. A., "A Study of the Temperature-Dependent Rheological Characteristics of Asphalt-Concrete", *Highway Research Board, HRR* 158, 116 (1967).
68. Haas, R. C. G., "Thermal Shrinkage Cracking of Some Ontario Pavements", D. H. O. Report No. RR 161, Dept. of Highways, Downsview, Ontario.

69. Davis, E. R., Krokosky, E. M., Tons, E., "Stress Relaxation of Bituminous Concrete in Tension", Highway Research Board, HRR 67, 38 (1965).
70. Metzner, A. B., and Whetlock, M., "Flow Behavior of Concentrated (Dilatent) Suspensions", Trans. Soc. Rheol., 2, 239 (1958).
71. Nielsen, L. E., "Creep and Dynamic Mechanical Properties of Filled Polyethylenes", Trans. Soc. Rheol., 13, 141 (1969).
72. Schwarzl, F. R., et. al., "Mechanical Properties of Highly Filled Elastomers. I. Relationship between Filler Characteristics, Shear Moduli, and Tensile Properties", 4th Int. Cong. on Rheology, Part 3, Interscience Pub., 241 (1965).
73. Landel, R. F., and Smith, T. L., "Viscoelastic Properties of Rubberlike Composite Propellants and Filled Elastomers", ARS Journal, 31, 599 (1961).
74. Jongepier, R., Kuilman, B., "Characteristics of the Rheology of Bitumens", Proc. AAPT, 30, 98 (1969).
75. Einstein, A., Ann. Physik, 19, 289 (1906), 34, 591 (1911).
76. Guth, E., "Theory of Filler Reinforcement", J. Appl. Physics, 16, 20 (1945).
77. Smallwood, H. M., "Limiting Law of the Reinforcement of Rubber", J. Appl. Phys., 15, 758 (1944).
78. Eilers, H., "Viscosity of Emulsions of a Highly Viscous Substance as a Function of Concentration", Kolloid-Z, 97, 313 (1941).
79. Hashin, Z., "On Viscoelastic Behavior of Two Phase Media", 4th Int. Cong. on Rheology, Part 3, Interscience Pub., 30 (1965).
80. Meryman, H. T., New York Academy of Sciences Annals, 85, 630 (1960).

APPENDICES

APPENDIX A

POWDER PREPARATION

The minerals were first crushed to a fine sand size with a steel mortar and pestle and then dry ground in a small porcelain ball mill with agate balls for 2 to 8 hours. Time of grinding was controlled by the amount and type of powder in the ball mill. X-ray diffraction patterns on the various powders did not show any impurities traceable to the grinding process.

The majority of the material produced by the ball mill was minus 200 sieve size. A passing 200 mesh-retained 400 mesh fraction ($37\text{ }\mu\text{m}$ to $74\text{ }\mu\text{m}$) was collected by wash sieving.

The minus $37\text{ }\mu\text{m}$ material was further fractionated through sedimentation in various aqueous solutions. Particles larger than $2.5\text{ }\mu\text{m}$ were sedimented under the force of gravity while particles less than $2.5\text{ }\mu\text{m}$ were sedimented in a centrifuge.

Stokes' Law was used to predict the time, t , that it took a particle of given diameter, d , to fall a given height, h ⁽¹⁸⁾. Therefore, after standing for the appropriate time, t , the suspensions contained only particles finer than a corresponding diameter, d . Unfortunately, the sediment also contained some particles finer than d as a consequence of having fallen less than the total suspension height, h . In order to obtain a sediment with its predominant material sized

greater than d , the sediment was repeatedly redispersed and decanted. The various sedimenting times used were calculated as suggested by Jackson⁽¹⁸⁾ and are presented in Table A1.

Considerable time was expended in finding, for each of the mineral types used, an appropriate sedimenting solution. It was required that the solution give good dispersion and yet not contain a dispersant that could not be easily removed by repeated washing.

The dispersion technique was considered effective when the sediment was a hard-packed deposit and the supernatant, for any given size, was clear after 4 or 5 repetitions. Generally, after 4 or 5 repetitions the sediment was so hard-packed that considerable energy was required with the plunger to redisperse it.

To limit interparticle interference and provide "clean" sediments with a minimum of resedimentation, the solids concentration was limited to 0.5 percent by volume. Stock sedimenting solutions containing dispersing agents, as described in Table A1, were mixed, deaired and stored for later use. Initial dispersion of the dry powder in the stock solution was achieved by mixing the two together in a mechanical mixer (ASTM D422) for at least 10 minutes. The dispersion was then wash sieved, deaired and allowed to age for an hour or more before beginning the sedimentation procedure.

Figure A1 shows the components used in the gravity sedimentation. The dispersion was poured from the mechanical mixer into the 1000 ml tall form beaker, brought to the 15 cm depth with stock solution, and then mixed with a special plunger.

Table A1. Specific Gravity and Time of Fall for Powders

Material	Specific Gravity*	Sediment Solution**	Size, μ m	Sedimentation Process	Time of fall, min.
Calcite	2.72	A	20.0	gravity	6
			10.0		25
			5.0		99
			2.5		396
			1.25	centrifuge,*** 750 rpm	12
Quartz	2.65	B	.63	1500 rpm	12
			20.0	gravity	13
			10.0		52
			5.0		206
			2.5		825
			1.25	centrifuge***, 1000 rpm	14
			.63	1500 rpm	24

* From reference (17).

** Solutions as follows:

A. 2.0 grams $\text{Na}_2\text{SiO}_3 \cdot 9\text{H}_2\text{O}$ /liter water

B. 20% ethanol -80% water (by weight).

*** 6.94 in. to top of sediment, 3.50 in. to top of fluid; from axis of rotation

Table A1, cont.

Material	Specific Gravity*	Sediment Solution**	Size, μ m	Sedimentation Process	Time of fall, min.
Apatite	3.18	C	10.0	gravity	20
			2.5		311
Bytownite	2.74	C	10.0	gravity	25
			2.5		391
Magnesite	3.04	A	10.0	gravity	21
			2.5		332
Microcline	2.55	C	10.0	gravity	28
			2.5		438

* From reference (17).

** Solutions as follow:

C. 0.111 grams NaCO_3 /liter water.

A. 2.0 grams $\text{Na}_2\text{SiO}_3 \cdot 9\text{H}_2\text{O}$ /liter water.

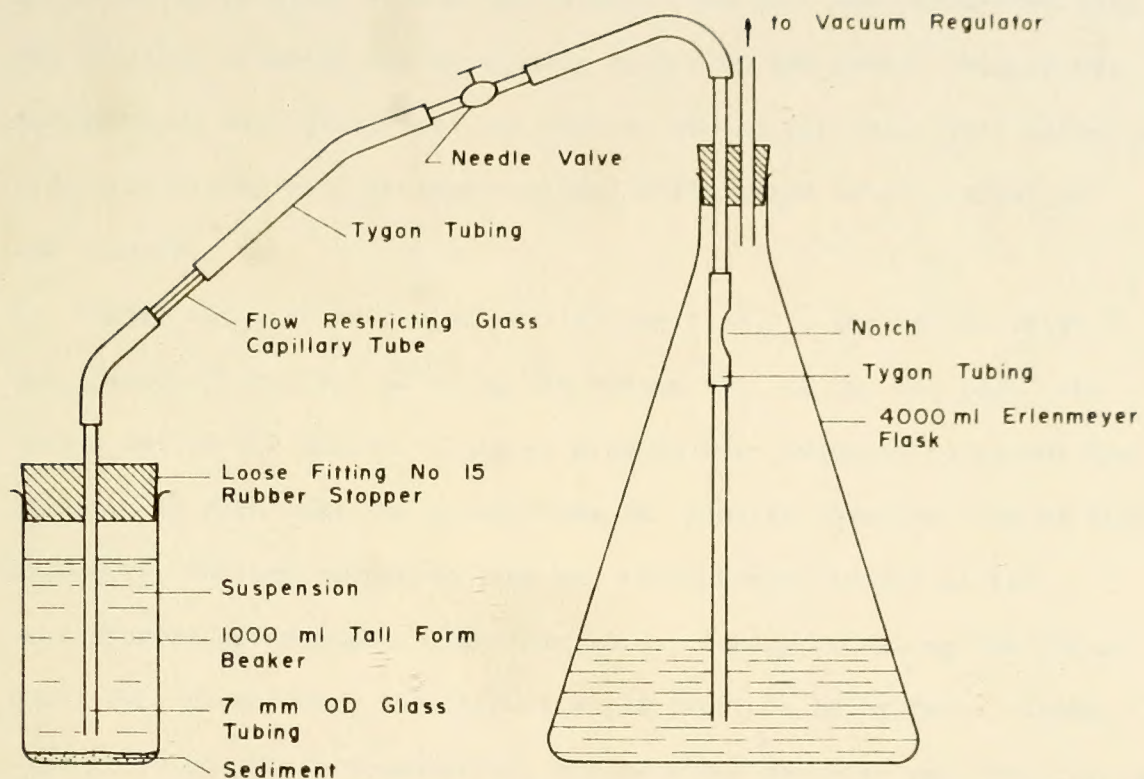


Figure A1. Schematic of Gravity Sedimentation Equipment.

The plunger was a stainless steel rod fitted with a $1/8$ inch thick stainless steel disc. The diameter of the disc was such that it would easily slide inside the beaker. The disc was perforated with 18, $1/4$ -inch diameter holes, equally spaced on two radii. Mixing was accomplished with short vertical strokes of the plunger. This technique gave good mixing with minimum residual disturbance after removal of the plunger.

After the dispersion had settled for time, t , the needle valve was opened, Figure A1, allowing the vacuum (15. cm Hg) to "pull" the decant out of the beaker. Several minutes were required to decant the liquid. In each case the decant time was shorter than the time of fall. Therefore, the sedimentation time was effectively stopped at the beginning of decantation. In other words, during decanting the liquid level fell faster than the largest sized particle being fractionated.

After the first decantation, the decanted material was transferred to a second beaker, dispersed, and allowed to sediment for time, t_2 , corresponding to the next finer size, d_2 . The process was then duplicated for t_3 , etc., until the finest size desired was sedimented.

Fresh sedimentation fluid was always added to the sediment of the coarsest fraction but the sediments of the succeeding fractions were always dispersed in the fluid decanted from the preceding (coarser) fraction. In this way the use of fluid and loss of material was minimized. Generally, four or five decantings were sufficient to produce a clear decant.

The same procedure was followed in the centrifuge sedimentation except that flat-bottomed stainless steel cups were used (6 cm diameter

by 11.5 cm deep) and the decant was poured off rather than "pulled" off. This was possible because the sediment was extremely hard-packed; as much as 30 minutes of vigorous stirring with the plunger was required to re-disperse the sediment. Scraping the bottom was to be avoided as it only produced lumps of powder that could not be broken down and dispersed.

At the end of the sedimentation procedure the material was washed repeatedly in distilled water until the sediment became loose or flocculated, assumingly free of dispersing agent. Attempts to dry the finer fractions in an oven were unsuccessful because after drying the powders were aggregated or even caked and bricklike. For this reason a freeze-drying process was used.

The freeze-drying apparatus is shown in Figure A2. The frozen sample was held under vacuum at approximately -10°C , upstream from a liquid nitrogen trap (approximately -190°C). The equilibrium water vapor pressure over the trap (-190°C) was much lower than that over the sample (-10°C). This pressure gradient resulted in a net flow of the water vapor from over the sample to the trap where it was frozen out. (80)

In this way water was removed from the frozen suspension, passing from the solid ice directly to the gaseous state, eliminating the compacting effect of the meniscus of liquid water. Powders dried in this manner were fluffy and free of aggregation. Following freeze drying, the powders were oven dried and stored in closed bottles for further use.

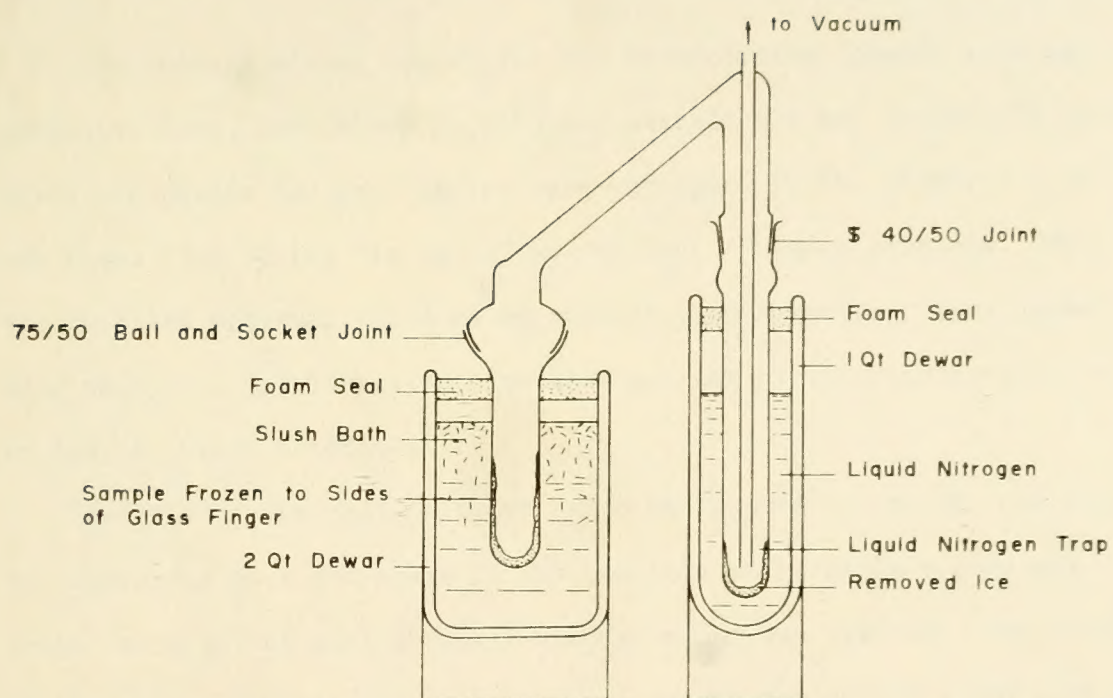


Figure A2. Freeze Dry Apparatus.

APPENDIX B

MIXING PROCEDURE

Preliminary mixing operations for incorporating powder with asphalt indicated that, when mixed in air, the asphalt did not completely penetrate the powder and gas bubbles were entrapped in the mixtures. It was found that mixing "in vacuo" solved both of these problems. The vacuum-mixed material was free of bubbles, has a smooth creamy appearance when hot, and lacked the isolated patches of uncoated powder found in the air-mixed material.

Details of the equipment are shown in Figures B1 and B2. By placing the equipment on a hot plate it was possible to maintain a constant temperature in the mixing beaker when a vacuum was applied. The pressure in the mixing chamber during mixing was maintained at 3-4 mm of mercury (absolute).

The mixing temperature was measured with a thermocouple immersed in the asphalt in the mixing beaker. The measurement was made while the chamber was evacuated and the asphalt was being stirred. The mixing temperature was 330 F.

Several features of the mixing equipment shown in Figure B2 are:

1. a well to accommodate a 10 ml "mixing beaker", a quartz powder seat in the bottom of the well to enhance the conduction of heat between the beaker and hot plate below;

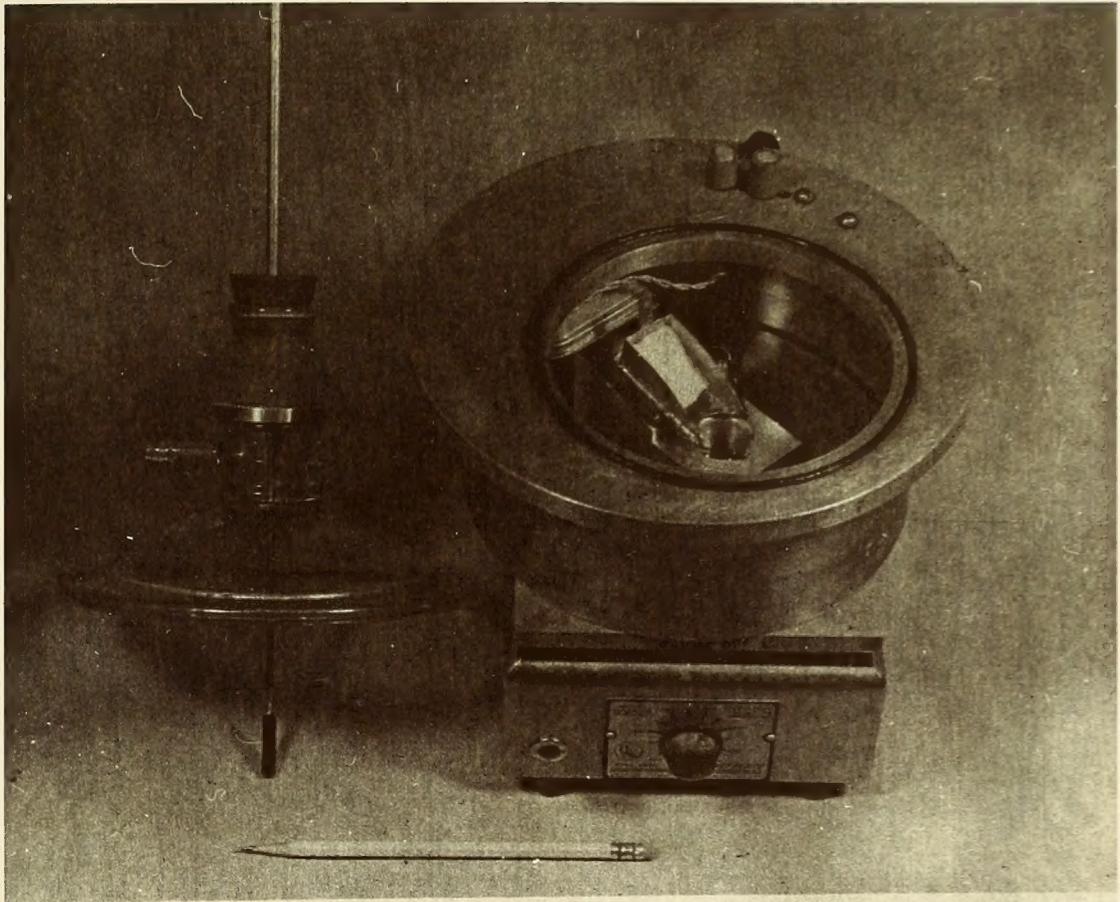


Figure B1. Photograph of Mixing Equipment.

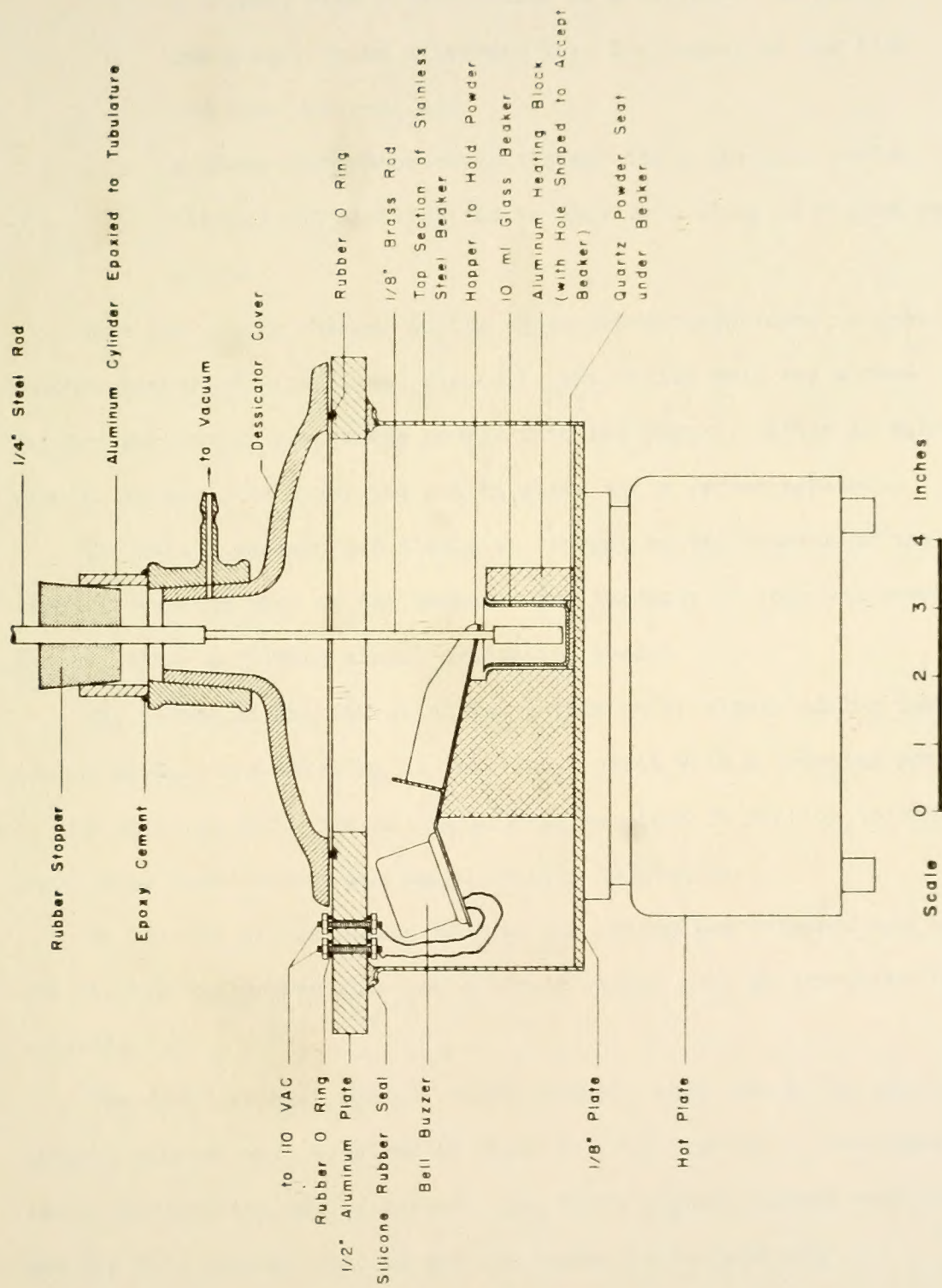


Figure B2. Schematic of Mixing Equipment.

2. a hopper, with a bell buzzer as a vibrator, to permit the powder to be dispersed into the beaker at the time and rate desired; and
3. a glass desiccator cover fitted with a one-hole rubber stopper and a mixing rod to provide a means of mixing the sample.

With the mixing chamber at its equilibrium temperature, a pre-weighed beaker of asphalt was placed in the mixing well and a pre-weighed portion of powder was poured into the hopper. After 10 minutes warming in air, the cover was put in place and a vacuum applied.

The vacuum was applied slowly to prevent sudden foaming of the asphalt over the side of the beaker. Any tendency to foam was essentially over after a fifteen minute evacuation period.

The actual mixing operation was initiated by slowly adding powder to the asphalt and stirring it into the asphalt with a rotating movement of the stirring rod. The mixing process required 30 minutes to complete. Total time under vacuum was approximately 45 minutes.

At the end of the mixing process the vacuum was released and the hot mixture was poured into the silicone rubber mold as described in Appendix C.

The B3603 asphalt foamed rather severely when vacuum was applied. Several minutes were required to apply the full vacuum or the asphalt would overflow the mixing beaker. The B3056 asphalt foamed very little and the full vacuum could be applied almost instantaneously.

APPENDIX C

PREPARATION OF TEST SPECIMENS FOR GLASS
TRANSITION TEMPERATURE AND SHEAR TESTING

Specimens were formed in a silicone rubber mold. This mold, shown in Step 1 of Figure C1, is a 3/16-inch thick silicone rubber casting. The specimens were formed in the four cavities, each 1/8-inch deep by 3/4-inch in diameter. The bottoms of the cavities were provided with a radius to prevent the entrapment of air during filling. Two or four specimens were formed according to whether or not duplicate shear test specimens were to be prepared.

At the completion of the mixing process the hot material was poured directly into the mold which had been preheated on a hot plate to about 250 F. After filling, the mold was held on the hot plate for 10 to 15 minutes so that the mixture could flow level with the top of the mold.

Upon cooling, the discs of sample material were easily popped from the flexible rubber mold. If glass transition measurements were to be made, the discs of sample material were placed in the T_g dilatometer. These same discs were later transferred to the shear plates to form shear-test specimens.

There were two reasons for casting the disc-shaped specimens. First, the round disc provided a sample convenient for the T_g dilatometer. Second, it provided a method for obtaining a reproduceable sample shape and volume between the shear plates. When squeezed, the

Each mixture that was produced was given a three digit "batch" number. A tabulation of these numbers and an appropriate description for each number is given in Table 5. Note that 117 and 122 were not mixtures to the extent that they were asphalts tested as supplied, without deairing. Samples 118 and 123 were plain asphalts, but were deaired and stirred; they were "mixed" in the same manner as the composites.

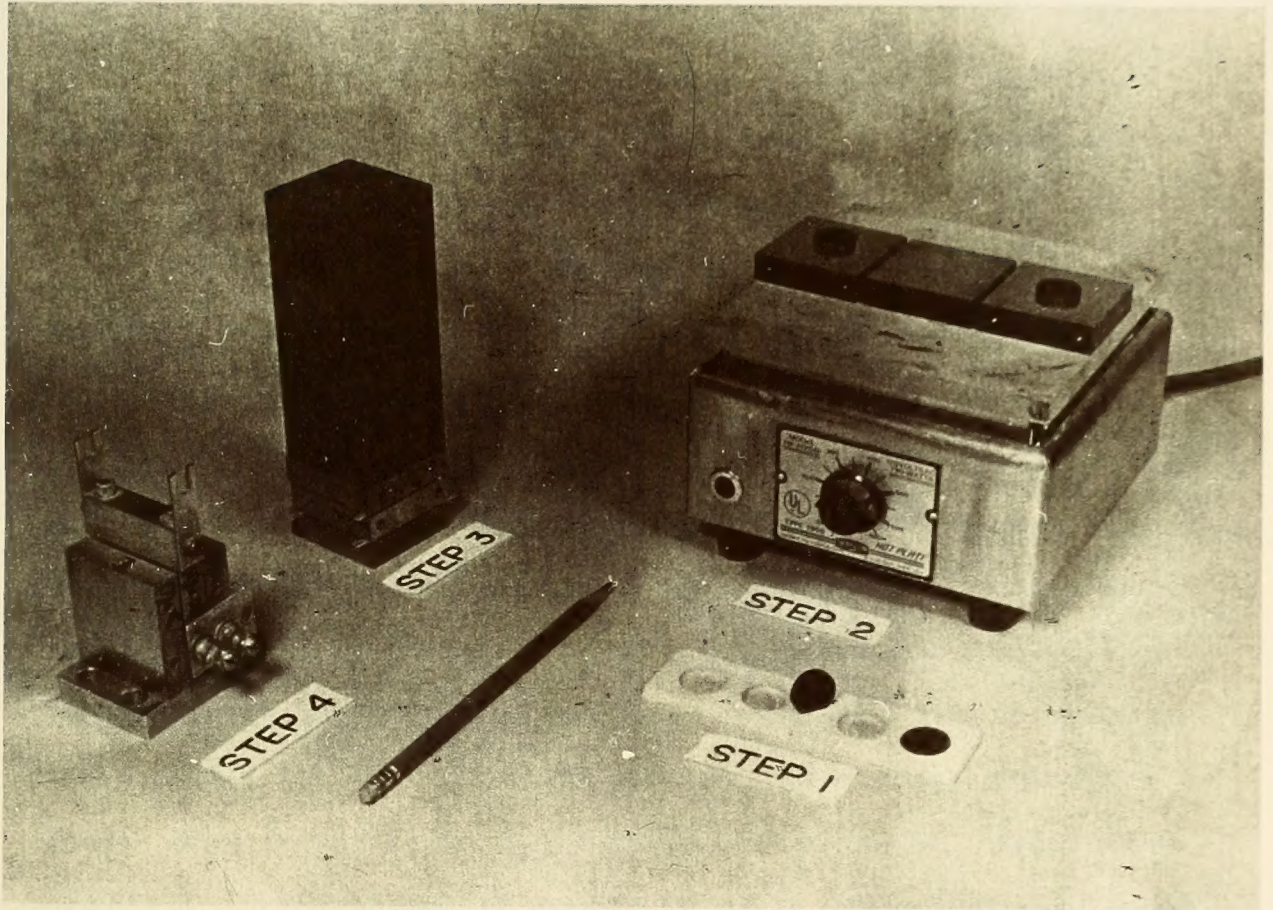


Figure C1. Test Specimen Preparation Sequence.

round discs retained their shape and a straight-forward calculation of shearing area could be made with the new sample diameter. In order to prevent unwanted eccentric forces in the shear plate assembly, equal shearing area and thickness must be present in each sample portion. This was insured by controlling the sample volume as described above and by controlling the thickness as described below.

The shear plates were assembled as shown in the sequence in Figure C1. Step 1 shows the silicone rubber mold, while Step 2 shows the discs of sample material on the preheated sample plates.

In Step 3 a weight is shown squeezing the plates together, forming a sample the thickness of the feeler gages. An assembled set of plates, with the side bars locked in place is shown in Step 4. The assembling was done while the material was relatively warm and free to flow, eliminating the possibility of building in stresses during assembly. Upon cooling, the thickness of the assembled three sample plates with sample material between was determined with a micrometer. By subtracting the plate thicknesses, an average thickness for the two portions of sample material between the plates was determined. The thickness was approximately 0.020 inches per side for the unfilled material and 0.040 inches for the filled material.

The shearing area was determined by separating the plates at the end of the testing. This was done by supporting the outer plates and striking the center plate sharply with a hammer, stripping one face of each of the two portions of sample material from the steel plates. The sample diameter was then easily measured with a pair of calipers.

An area for the material mounted on each side of the center plate was calculated and the two values added together to give the total sheared area. The sheared area was generally about 10 square centimeters per side.

During the testing and data reduction, the material was identified by a sample (mixture) number and by the number of the shear plate on which the sample was mounted. Unless given separately, the sample/plate numbers were given as the three digit sample number followed by a slash and the plate number. Later, when the data were plotted, the plate number was dropped and an average value for the one or more plates was presented. The mixture properties associated with each sample number are documented in Table 5.

APPENDIX D

SHEAR TEST PROCEDURES

The original objective was to perform the shear testing at low strains, hopefully in a region where the material exhibited linear behavior. Within this context, it was felt that once the specimens were formed they should remain essentially undisturbed until tested. The preparation, mounting, and testing procedure was designed to accomplish this end.

Description of Shear Test Apparatus

Figure D1 gives an overall view of the test set-up while Figure D2 details the components mounted in the sample bath. The shear testing, both dynamic and creep, was done in an MTS Testing Machine. Test temperatures of 5, 15, and 25 C, ± 0.05 C, were maintained by circulating water from a secondary bath to the sample bath mounted on the lower head (hydraulic actuator) of the machine. The bath was a six-inch lucite cylinder insulated with glass wool. A circular weir at the top of the bath controlled the water level. This is shown in Figure D2.

The bottom of the sample bath was fitted with a flat, steel plate, drilled and tapped to accommodate the preassembled sample plates shown in Figure B3. The load cell was fixed to the upper, rigid head of the machine and provided readout and feedback for control of the various

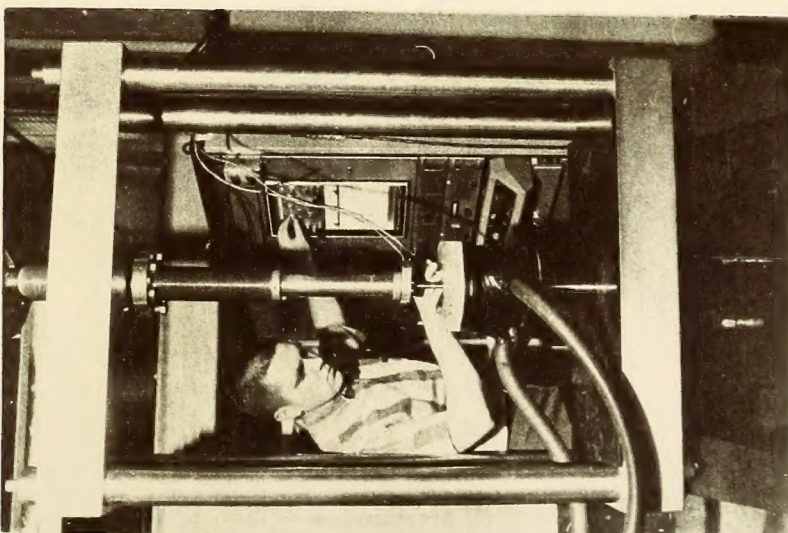


Figure D1. Overall Picture of Test Set, Up.

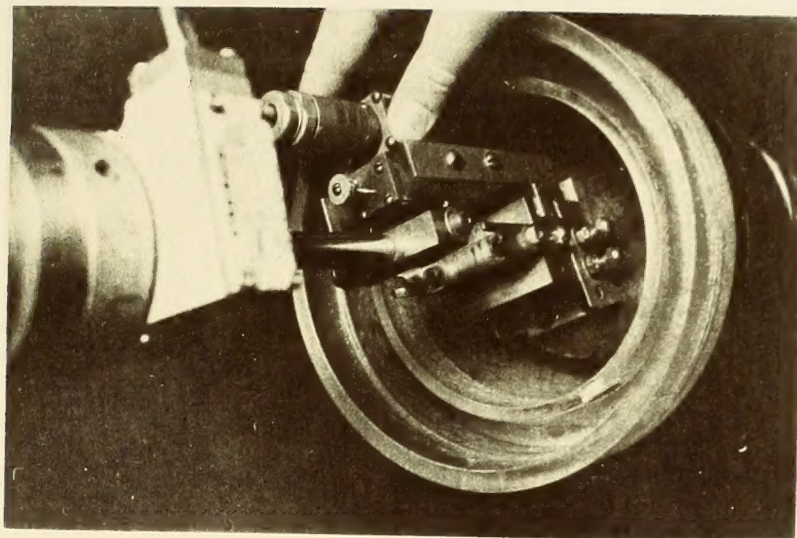


Figure D2. Details of Plate Assembly being Mounted in Water Bath.

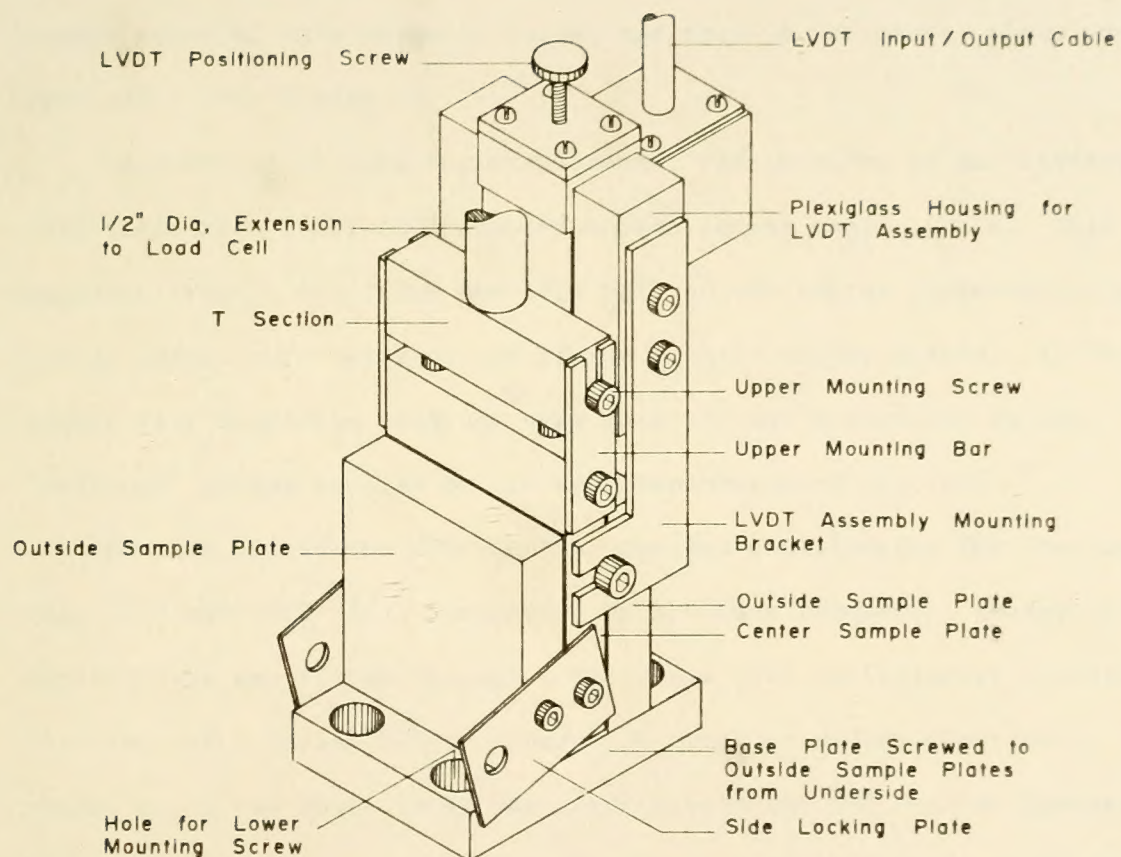


Figure D3. Assembled Sample Plates.

loading functions (input) imposed on the sample material. With the sample base plate screwed to the bottom of the bath and with the side locking plates loosened, force generated by displacing the hydraulic actuator was transmitted to the outside sample plates through the sample material as a shearing force, and then to the center plate and load cell. See Figure D3.

Measurement of shearing displacement was provided by an accessory LVDT (Linearsyn 595DT-100) mounted on the center sample plate. This assembly (Figure D4) fixes the LVDT coil to the center plate while the spring loaded core bears on one of the outside sample plates. In this manner very sensitive readings were possible and errors due to any "softness" in the machine or its appurtenances were omitted.

Modules within the MTS Machine provided conditioning for the load cell (DC) and LVDT (AC). Depending on the test frequency, readout of dynamic data was either through a Tektronix 502A oscilloscope (Polaroid pictures) or a Varian X-Y recorder. In order to reduce electronic noise, an RC low pass filter was used between the MTS Machine modules and the oscilloscope. While the filter did produce a phase shift in both signals, it was balanced such that the phase shift between the signals was zero. A filter attenuation factor was determined experimentally for each frequency used and was applied to the recorder sensitivity during the data reduction. See Table D1.

The readout of the creep data was through a two channel recorder (Brush 280). In a few instances the low pass filter was used in recording the creep data and the filter attenuation factor was applied accordingly.

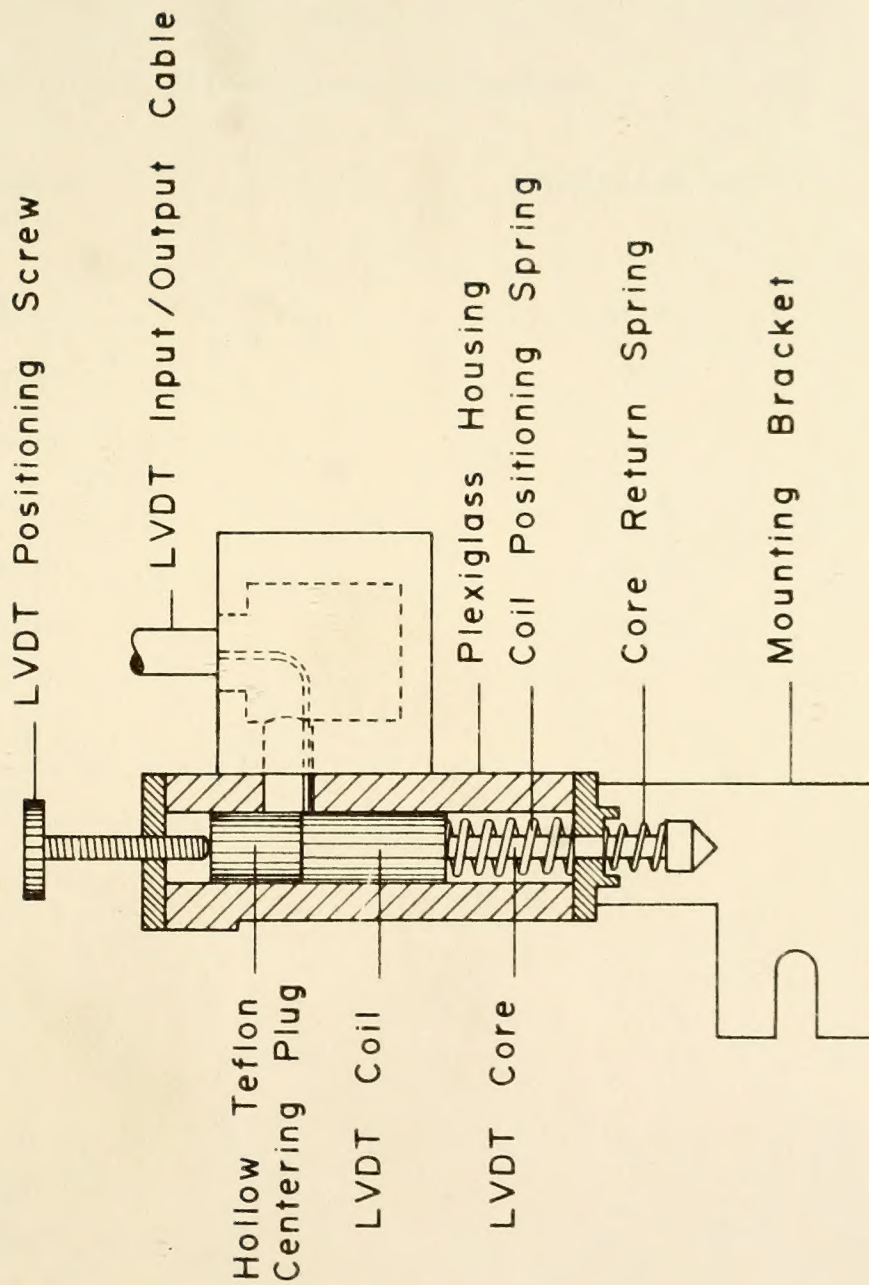


Figure D4. LVDT Assembly.

Table D1
Filter Attenuation Factors

Frequency Hertz	Attenuation Factor
50.3	12.0
15.9	3.96
5.03	1.59
1.59	1.12
<1.59	1.12
Creep	1.12

Most of the dynamic measurements were taken at frequencies of 15.9, 5.03, 1.59, 0.503, and 0.159 Hertz. This represents the satisfactory range of the machine for this particular test set-up. At 25 C with frequencies less than 0.159 Hertz, drift in the machine gave meandering Lissajous patterns (hysteresis loops) and data interpretation was difficult. At these lower frequencies the loads required for linear behavior often approached 500 grams or less. Frequencies above 15.9 Hertz exceeded the hydraulic pump capacity of the machine. Considering that the work was done with a 5,000 pound actuator, the control of the machine cannot be faulted.

The ramp or rise time used in applying the creep load was 0.063 seconds, selected for convenience of machine operation.

Mounting Sequence

Prior to mounting in the test bath, the assembled plates were held in the secondary bath for at least one hour (within 0.2 C of test temperature).

The mounting of the assembled sample plates was as follows (see Figure D3):

1. Position the assembled sample plates (without the LVDT assembly in place) in the test bath and start the lower mounting screws into their threads.
2. Program a small compressive load and slide the upper mounting bars under the upper mounting screws. Finger tighten.
3. Carefully tighten the lower mounting screws.
4. Tighten the upper mounting screws.

5. Install the LVDT assembly by sliding the mounting bracket under the two screws on either side of the center sample plate. Tighten screws to secure LVDT assembly to the center sample plate.
6. Zero the LVDT using the positioning screw.

At this point the shearing stress in the sample was essentially zero. After removal of the side locking bar the various loading patterns were programmed onto the sample. In this way the strain history of the sample was easily monitored and controlled such that its magnitude was less than that encountered during the actual testing.

De-mounting consisted of the above procedure in reverse with, of course, the side locking bar clamped to prevent excessive straining.

Testing Sequence

Tests in both dynamic and creep shear were performed at 25, 15, and 5 C in that sequence. The samples were remounted at each test temperature.

At each temperature the dynamic tests were made in the order of decreasing frequency followed by the creep tests. When more than one stress level was used, generally the larger stress was used first.

A flow chart depicting the timing used in sample making and testing is given in Figure D5.

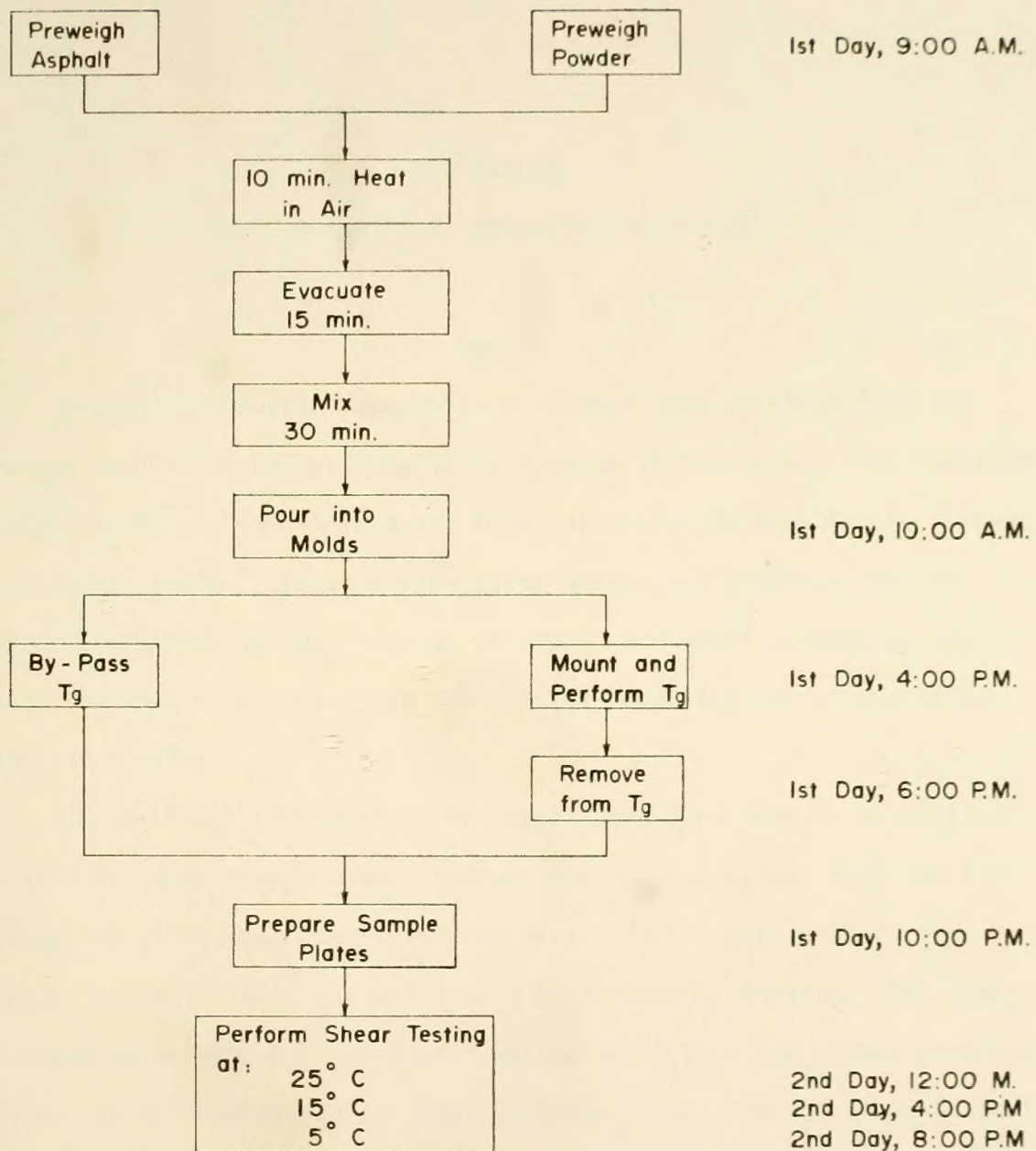


Figure D5. Flow Chart for Testing Sequence.

APPENDIX E

GLASS TRANSITION TEMPERATURE EQUIPMENT

Bath

Reasonably constant temperature changes were obtained from the rather simple but well-insulated bath shown in Figure E1. The insulation material was closed-cell plastic foam two inches or more thick, coated with epoxy resin. The stainless steel beaker was supported on the upper insulation by the flare at its top. The upper insulation was in turn fastened to a supporting stand. The lower section of insulation was removeable.

The methanol in the stainless steel beaker was cooled by pumping liquid nitrogen from a dewar, through the filling spout, into the tin liner until it just overflowed the weir. As the bath cooled, the liquid nitrogen level was maintained by occasional pumping. The pumping was accomplished by pressurizing the dewar with the rubber pressure bulb. About four liters of liquid nitrogen were required to cool the 3.5 liters of commercial grade methanol to about -60°C .

When the desired temperature had been reached, the lower section containing the liquid nitrogen was lowered and removed. It was replaced with a second section, similar in dimensions, but without the tin liner, weir, and filling spout. At -60°C with the second section in place, the bath was sufficiently insulated that, with the stirrer running, a gain in temperature of only 0.13°C per minute was noted.

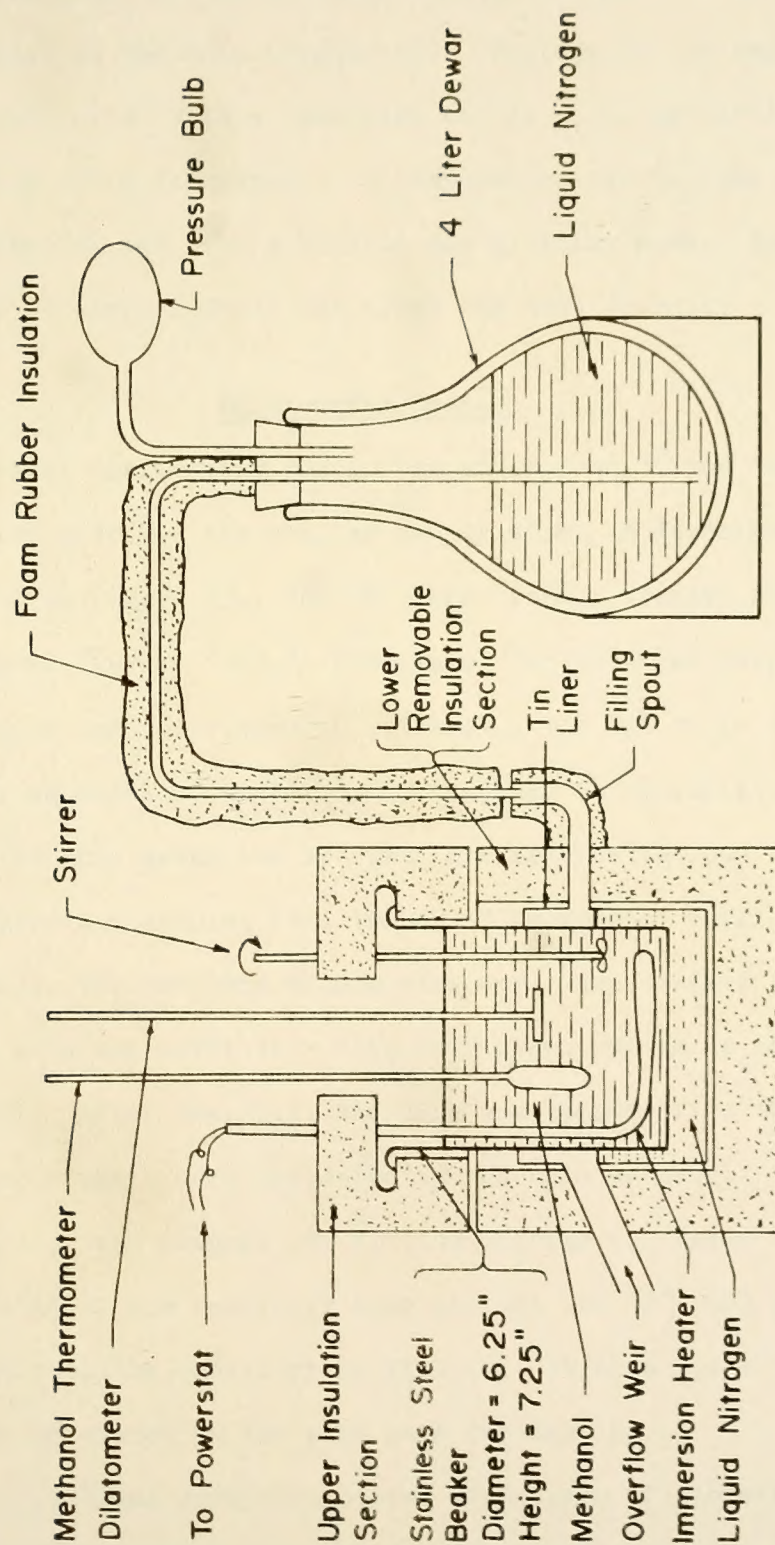


Figure E1. Controlled Temperature Bath.

The temperature in the bath was raised to ambient with a 500 watt heater immersed in the bath (Figure E1). Voltage to the immersion heater was controlled with a powerstat at 111 volts up to -20 C and at 118 volts from -20 C to ambient. A temperature versus time plot is given in Figure E2 for both a falling and a rising mode. Note that the cooling rate is approximately two times the heating rate.

Dilatometer Design

The initial dilatometer design was after Schmidt and Santucci (30) with provision made for the smaller sample size. A description of this cell is given in Figure E3. The "O" rings were a special silicone rubber compound (Parker 5383-7) formulated for both low temperature characteristics and resistance to methanol. The "O" rings were kept stored under methanol to minimize any tendency to entrap air.

The cells were assembled by first placing the various chamber parts, along with a sample, in a 100 by 50 centimeter Petri dish filled with methanol. The contents of the dish were then deaired by placing the dish in a vacuum dessicator with sufficient vacuum to make the methanol boil. After deairing, the dish was removed from the dessicator and the various parts were assembled immersed in methanol. With the smaller "O" ring and compression fitting lightly tightened in place, the process of sliding the capillary tube through the "O" ring displaced enough fluid into the capillary to fill it. At this point the assembly was ready to be placed in the test bath for testing.

Several problems were encountered with these dilatometers. The aluminum reacted with the methanol in some unknown way and became

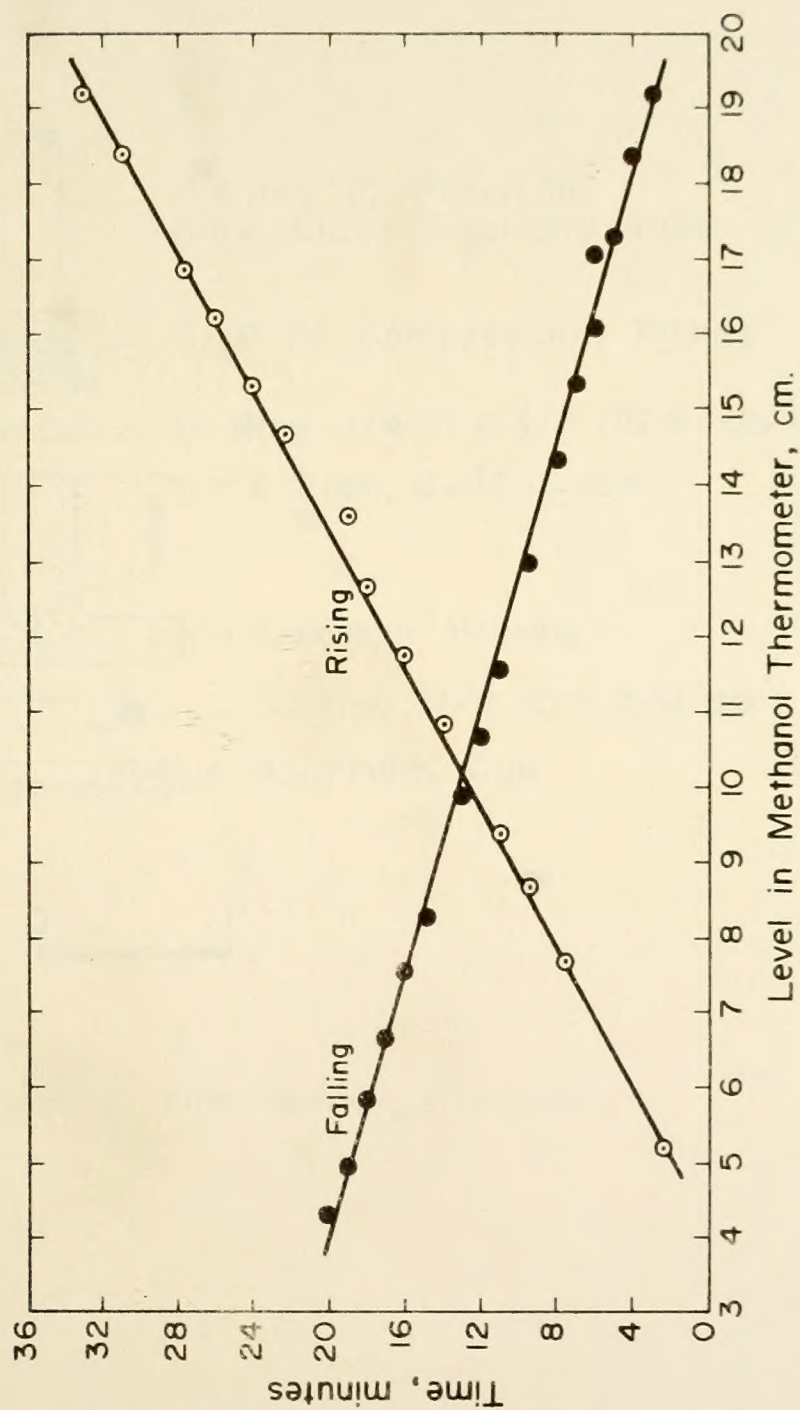
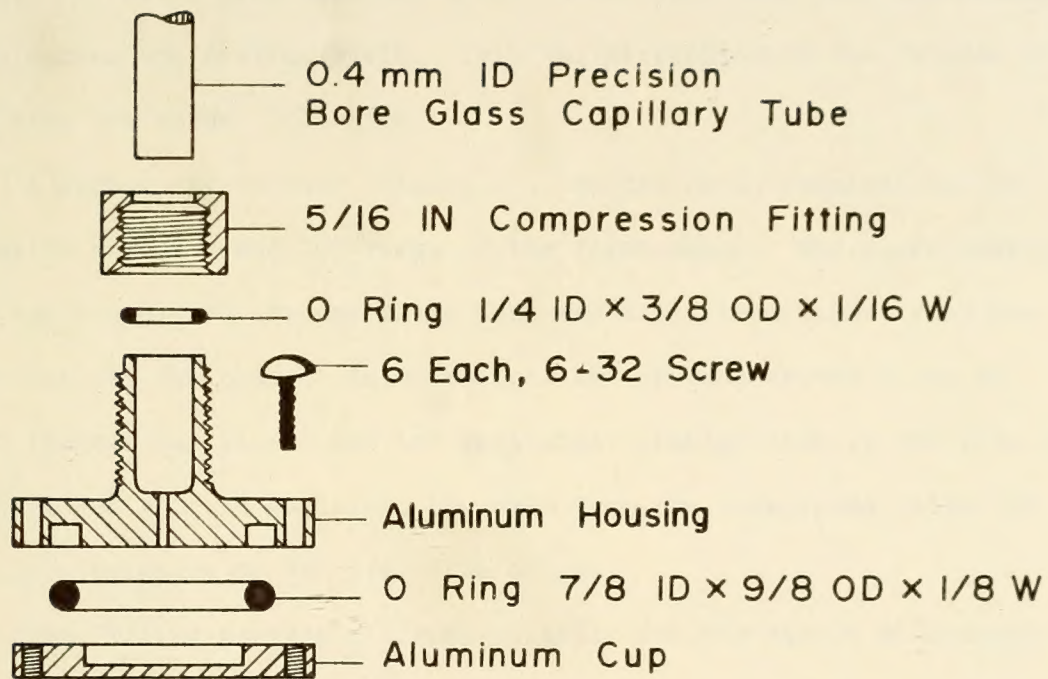


Figure E2. Typical Time-Temperature Plot from T_g Bath.



Scale 0 1"

Figure E3. First Design T_g Dilatometer.

pitted and porous with time. As the dilatometers were cooled they often developed slight leaks as evidenced by excessive lowering of the methanol in the capillary tubes. These leaks were probably at the "O" rings. On other occasions the level in the capillary rose unaccountably high during the heating cycle. This was attributed to the release of gas from the rubber "O" rings.

A second dilatometer, Figure E4, was designed, eliminating the metallic surfaces and "O" rings of the first model. The glass sample cup was blown onto the capillary tube and a silicone rubber seal was cast against the glass. An occasional set of data showed signs of cell leakage but it was not the persistent problem that it was with the initial design. In addition, the data from the redesigned cells did not give evidence of the evolution of gas.

The filling process differed slightly for the second dilatometer design. The sample and cover plate were placed in the Petri dish and deaired. A six-inch length of rubber tubing was slipped onto the open end of the capillary. Two pinch cocks were placed on the rubber tubing: one at the open end, the second an inch or so away. The tubing was then pinched with the thumb and forefinger and the cell end inserted into the methanol. Upon releasing the tubing, the methanol was sucked into the capillary. Next the cell was placed over the sample and cover plate and held in place with light pressure. Releasing the second pinch cock created enough suction so that the cell could be lifted intact from the Petri dish and the spring clip installed. The first pinch cock was then released and the tubing removed. Only light pressure was applied to the spring clip: the elimination of leaks depended more on the

I have been thinking of you very much lately, and wondering how you are getting on. I hope you are well and happy. I have been very busy lately, but I have managed to find some time to write to you. I have been thinking of you very much lately, and wondering how you are getting on. I hope you are well and happy. I have been very busy lately, but I have managed to find some time to write to you.

I have been thinking of you very much lately, and wondering how you are getting on. I hope you are well and happy. I have been very busy lately, but I have managed to find some time to write to you. I have been thinking of you very much lately, and wondering how you are getting on. I hope you are well and happy. I have been very busy lately, but I have managed to find some time to write to you.

I have been thinking of you very much lately, and wondering how you are getting on. I hope you are well and happy. I have been very busy lately, but I have managed to find some time to write to you. I have been thinking of you very much lately, and wondering how you are getting on. I hope you are well and happy. I have been very busy lately, but I have managed to find some time to write to you.

I have been thinking of you very much lately, and wondering how you are getting on. I hope you are well and happy. I have been very busy lately, but I have managed to find some time to write to you. I have been thinking of you very much lately, and wondering how you are getting on. I hope you are well and happy. I have been very busy lately, but I have managed to find some time to write to you.

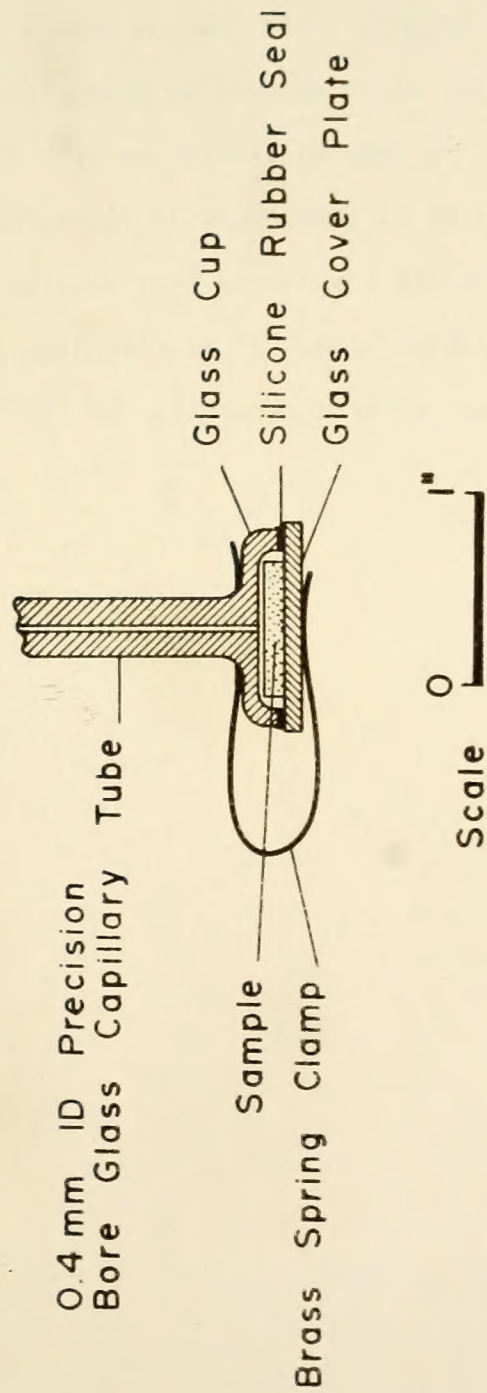


Figure E4. Second Design T_g Dilatometer.

quality of the mating surfaces than on compressing the rubber gasket.

No provision was made for coating or otherwise protecting the asphalt before it was placed in the cell. None of the filled materials stuck to the glass or aluminum as long as their first contact was under the methanol. A few, occasional patches of sticking did occur with the unfilled asphalt but it was judged to be insignificant.

Several samples were weighed before and after being used in the T_g determination. No gain or loss in sample weight was observed in the weightings taken with an analytical balance (nearest 0.1 mg).

APPENDIX F

REDUCTION OF DYNAMIC TEST DATA

The two sinusoidal functions, displacement and load, were recorded on the x and y axes of either an oscilloscope (high frequencies) or an x-y recorder (low frequencies). When two sinusoidal functions are combined in this manner, the result is an ellipse or hysteresis loop, generally called a Lissajous pattern.⁽⁴⁴⁾

An individual pattern was produced for each temperature, frequency, and load level. Sample patterns from the oscilloscope and x-y recorder are shown in Figures F1 and F2.

A transparent overlay was placed over each pattern and the distances a , X_0 , and Y_0 were scaled as labelled in Figure F3. Special care was taken to keep the grid parallel to the x and y axes during the scaling process, particularly when scaling a .

The values of $|\bar{J}^*|$ were calculated according to

$$|\bar{J}^*| = \frac{Y_0}{\sigma_0} \quad 8$$

where γ_0 and σ_0 , the peak to peak strain and stress were calculated by applying the appropriate scale factors (recorder sensitivity) to the values of X_0 and Y_0 .

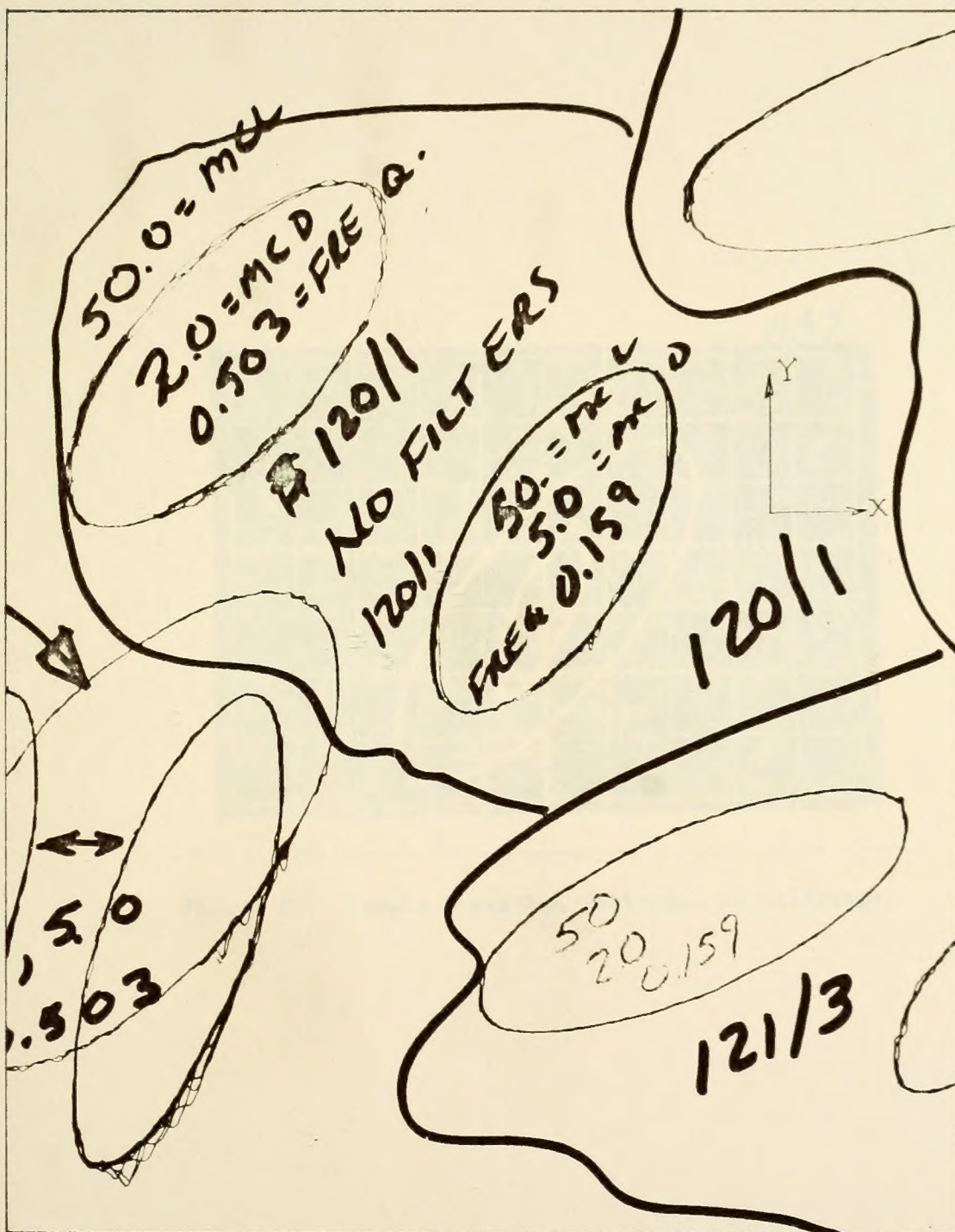


Figure F1. Sample Lissajous Patterns, x-y Recorder.

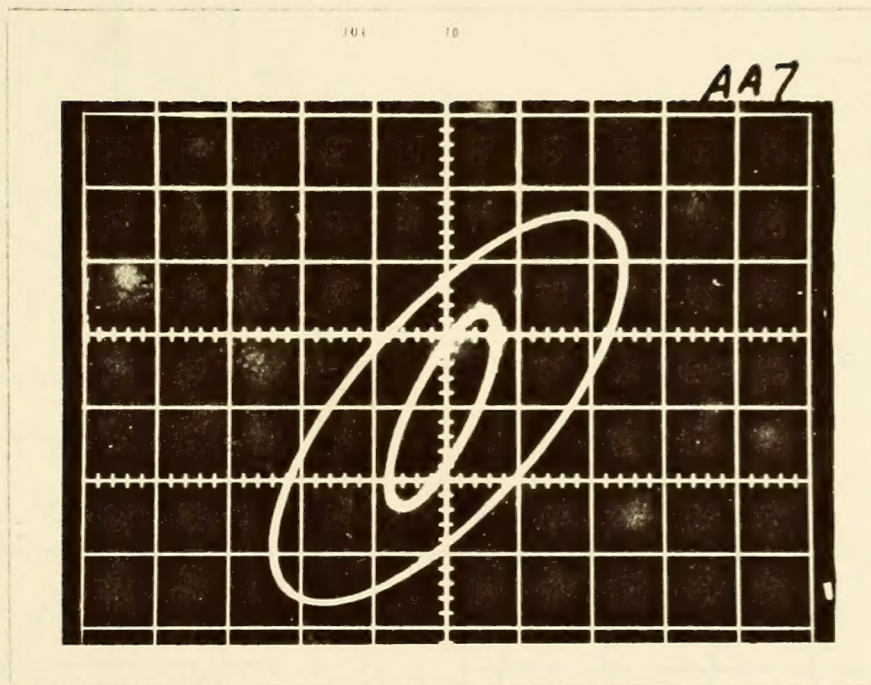


Figure F2. Sample Lissajous Patterns, Oscilloscope.

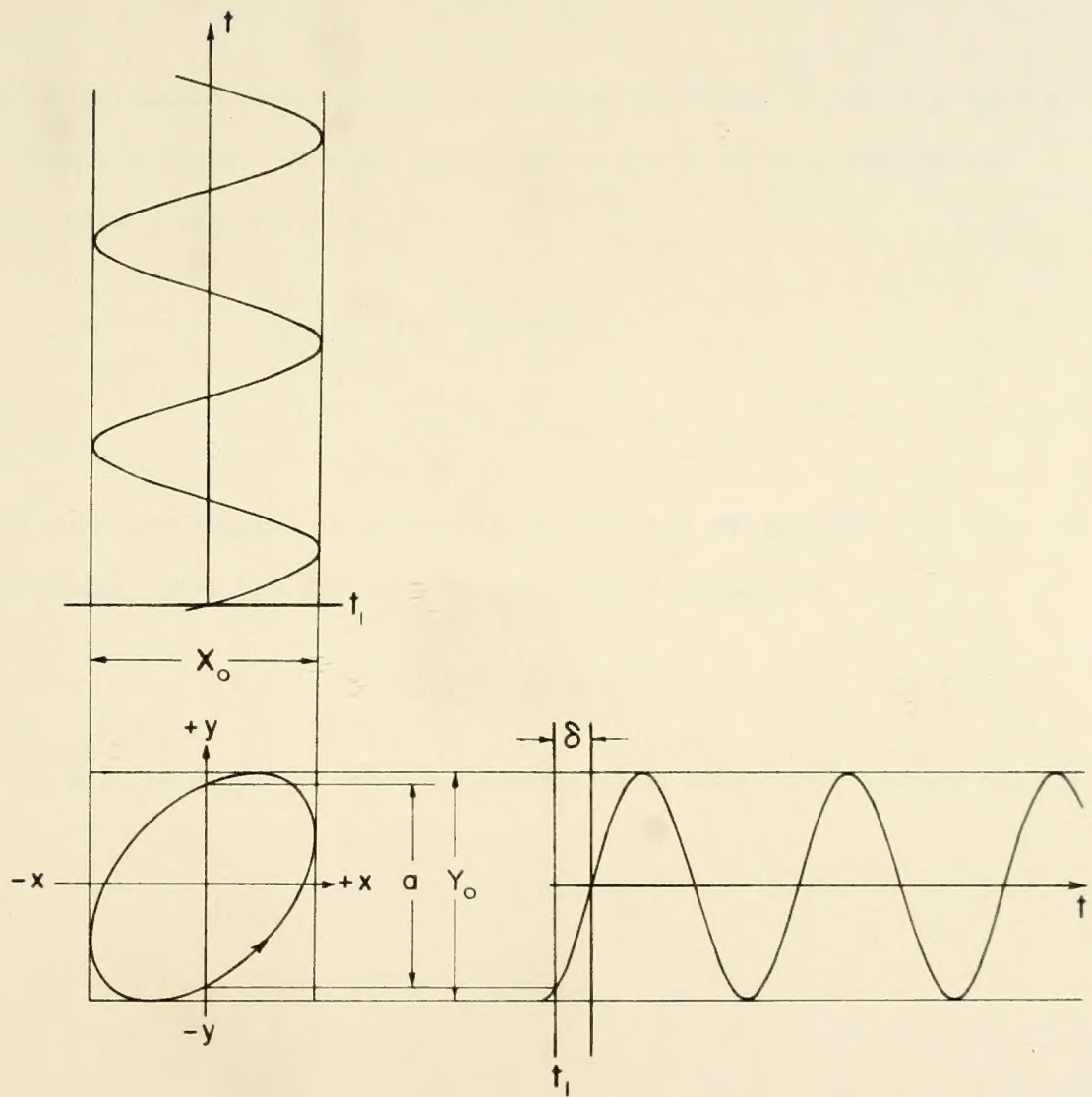


Figure F3. Schematic Lissajous Pattern.

The phase angle, δ , was calculated from

$$\delta = \sin^{-1} \frac{a}{Y_0}$$

This relationship is visualized by looking at Figure F3 where y equals $a/2$ when x is zero. Because both x and y are sine functions we can write, with x lagging y by δ ,

$$y = \frac{Y_0}{2} \sin(\omega t) \quad F1$$

$$x = \frac{X_0}{2} \sin(\omega t - \delta) \quad F2$$

where ω is the angular frequency in radians per second and t is time in seconds. When $y = a/2$, $x = 0$, and, from equation F2

$$\sin(\omega t - \delta) = 0$$

and ωt must be equal to $2n\pi + \delta$. Substituting this into equation F1,

$$y = \frac{a}{2} = \frac{Y_0}{2} \sin(2n\pi + \delta)$$

or

$$\sin \delta = \frac{a}{Y_0}$$

and

$$\delta = \sin^{-1} \left(\frac{a}{Y_0} \right) \quad F3$$

The components, J' and J'' were then calculated as

$$J' = |\bar{J}^*| \cos \delta$$

$$J'' = |\bar{J}^*| \sin \delta$$

Calculated values of $|\bar{J}^*|$, J' and J'' were multiplied by T/T_0 . The actual reduction of the data was done on an electronic computer, the data transferred to cards and plotted on a CALCOMP x-y plotter. The program used to reduce the data is given in Appendix G along with sample raw data and a complete listing of the reduced data. A sample hand calculation for one test point follows on the next three pages. The data for this calculation is drawn from the sample data sheet of Figure F4 as scaled from Figures F1 and F2.

1. Sample #120/1, 25°C, 50.3 cycles/second
see sample data and data sheet Figures F1, F2, and F4 for data used in calculation below.

2. Notation:

a: hgt. of Lissajous pattern at zero strain

A: area of one side of shear sample, cm^2

F: correction factor to correct for filter attenuation

J', J'': in phase and out of phase compliance components
 cm^2/dyne .

MC: recorder sensitivity, millivolts/division

X₀: number of chart divisions, displacement

R: sensitivity of MTS output signal, grams or inch/division

T: test temperature, °K

T₀: reference temperature, 298°K (25°C)

Th: thickness of both sides of sample, inch.

Y₀: number of chart divisions, peak to peak, load.

δ: phase angle, degrees

σ₀: maximum, peak to peak, shear stress, dynes/cm²

ε₀: maximum, peak to peak, strain, inches/inch.

3. Maximum shear stress, σ₀

σ₀ = Load, dynes / Area 2 sides, cm²

$$\sigma_0 = \frac{(MC)(Y_0)(R)(F)980}{2A}$$

$$\sigma_0 = \frac{(50 \cancel{\text{mV}}/\cancel{\text{div}})(26.6 \cancel{\text{div}})(\frac{50,000 \cancel{\text{gram}}}{10,000 \cancel{\text{mV}}})(12.0)(980 \frac{\text{dyne}}{\cancel{\text{gram}}})}{(2)(10.18 \text{ cm}^2)}$$

$$\sigma_0 = 3.84 \times 10^6 \text{ dynes/cm}^2$$

4. Maximum shear strain, γ_0

$\gamma_0 = \text{displacement} / \text{thickness, one side of sample}$

$$\gamma_0 = \frac{(MC) (\chi_0) (R) (F)}{Th/2}$$

$$\gamma_0 = \frac{(0.5 \text{ mv/div}) (14.5 \text{ div}) (0.01 \text{ in}/10,000 \text{ mv}) (12.0)}{0.0808 \text{ in}/2}$$

$$\boxed{\gamma_0 = 0.00215 \text{ in/in}}$$

5. Phase angle, δ

$$\delta = \sin^{-1} \frac{a}{Y_0}$$

$$\delta = \sin^{-1} \frac{16.8}{26.6}$$

$$\boxed{\delta = 39.2^\circ}$$

6. $\log |\bar{J}^*|$, absolute value of complex compliance

$$\log |\bar{J}^*| = \log \frac{\epsilon}{\sigma_0} \cdot \frac{T}{T_0} = \log \gamma_0 - \log \sigma_0 + \log \frac{T}{T_0}$$

$$\log |\bar{J}^*| = \log 0.00215 - \log 3.84 \times 10^6 + \log 1.0$$

$$\log |\bar{J}^*| = -2.667 - 6.584 - 0$$

$$\boxed{\log |\bar{J}^*| = -9.25}$$

7. $\log J'$, log of storage compliance

$$\log J' = \log |\bar{J}^*| + \log \cos \delta$$

$$\log J' = \log |\bar{J}^*| + \log \cos 39.2^\circ$$

$$\log J' = -9.25 + (-0.11)$$

$$\boxed{\log J' = -9.36}$$

8. $\log J''$, log of loss compliance

$$\log J'' = \log |\bar{J}^*| + \log \sin \delta$$

$$\log J'' = \log |\bar{J}^*| + \log 39.2^\circ$$

$$\log J'' = -9.25 + (-0.20)$$

$$\boxed{\log J'' = -9.45}$$

APPENDIX G

REDUCED DYNAMIC DATA

The next pages contain the reduced dynamic data preceded by the reduction program and a set of sample data. The program was processed by a CDC 6500 electronic computer.

PROGRAM

```

C *****
C PROGRAM TO REDUCE DYNAMIC DATA
C *****

REAL MCL, MCD, LAG, JSTAR, JREAL, JLOSS, LJSTAR
REAL LJREAL, LJLOSS, LHEC, LTDEL
INTEGER TYPE, SAMPLE, PLATE

C *****
C DIVD = CHART DIVISIONS ON X AXIS
C DIVL = CHART DIVISIONS ON Y AXIS
C MCD * RANGED * 0.01 IS READOUT CONSTANT FOR X AXIS
C MCL * RANGEL * 49. IS READOUT CONSTANT FOR Y AXIS
C REMAINING VARIABLES ARE SELF EVIDENT
C *****

C *****
C READ IN CONSTANTS USED IN DATA REDUCTION, PRINT COLUMN HEADINGS
C *****

1 READ(5,500) SAMPLE, PLATE, TEMP, N, THICK, AREA, RANGEL, RANGED
  IF(EOF,5)999,2
C *****
C DIVIDE THICKNESS OF TWO SIDES BY TWO = THICKNESS OF ONE SIDE
C *****
2 THICK = THICK / 2.
  WRITE( 6,600 ) SAMPLE, PLATE, TEMP, AREA, THICK

```



```

C *****
C READ IN DATA, DO REDUCTION AND PRINT AND PUNCH OUT DATA
C *****

3 Z = 0.0
DO 199 I=1,N
  READ(5,501) FREQ, MCL, DIVL, MCD, DIVD, LAG, TYPE
  IF( FREQ .NE. Z ) WRITE(6,601)
  Z = FREQ
  STRESS = ( DIVL / AREA ) * ( MCL * RANGEL * 49. )
  PCT = ( DIVD / THICK ) * ( MCD * 0.01 * RANGED )
  JSTAR = (PCT / (100.*STRESS)) * ((273.+TEMP) / 298.)
  ZILCH = 1. - (LAG*LAG) / (DIVL*DIVL)
  IF ( ZILCH ) 199,199,121
121 JREAL = JSTAR * SQRT ( ZILCH )
  JLOSS = JSTAR * LAG / DIVL
  LJSTAR = ALOG10(JSTAR)
  LJREAL = ALOG10(JREAL)
  LJLOSS = ALOG10(JLOSS)
  LTDEL = ALOG10 ( JLOSS / JREAL )
  LREC = ALOG10 ( ( 1.0 ) / ( FREQ * 6.283 ) )
C *****
C APPLY FILTER ATTENUATION FACTOR TO TYPE 2 DATA
C *****
  IF ( TYPE .EQ. 3 ) GO TO 122
  PCT = PCT * 1.05
  IF( FREQ .EQ. 1.59 ) PCT = 1.12 * PCT
  IF( FREQ .EQ. 5.03 ) PCT = 1.59 * PCT
  IF( FREQ .EQ. 15.9 ) PCT = 3.96 * PCT
  IF( FREQ .EQ. 50.3 ) PCT = 12.0 * PCT
122 WRITE( 6,603 ) LREC, PCT, LJSTAR, LJREAL, LJLOSS, LTDEL
199 CONTINUE
  WRITE( 6,604 )
  GO TO 1

500 FORMAT( I3, I1, F4.1, I2, F5.4, F4.2, F4.1, F5.4 )
501 FORMAT( F5.2, F4.1, F3.1, F5.2, F3.1, F4.1, I2 )
600 FORMAT( 1H , 15X, 6HSAMPLE, I4, 2X, 5HPLATE, I2, 6X,
  $F6.1, 11H DEG. CENT., //, 21X,
  $22HAREA SHEARED, ONE SIDE, F7.2, 8H CM. SQ., /, 21X,
  $22HSAMPLE THICK, ONE SIDE, F8.4, 4H IN., //,
  $16X, 3HLOG, 4X, 3HPCT, 5X, 2(3HLOG, 5X),
  $13HLOG LOG TAN, /, 16X,
  $43H1/W STRAIN IJ*I JREAL JLOSS DELTA, /, 15X, 45(1H-))
601 FORMAT( 1H )
603 FORMAT( 1H , 14X, F5.2, F7.3, 3F8.2, F7.2)
604 FORMAT( 1H1 )

999 STOP
END

```


Sample Data

1201	250	6	04081018	50	01			
50.3	50	266	5	145	168	3	120/1-25	
15.9	50	529	5	481	361	3	120/1-25	
5.03	50	338	5	434	235	3	120/1-25	
1.59	50	477	10	542	353	3	120/1-25	
.503	50	290	20	273	216	2	120/1-25	
.159	50	295	50	209	221	2	120/1-25	
1204	250	6	0796	995	50	01		
50.3	50	105	5	114	119	3	120/4-25	
15.9	50	352	5	325	229	3	120/4-25	
5.03	50	411	5	632	284	2	120/4-25	
1.59	50	492	10	655	352	4	120/4-25	
.503	50	225	20	272	162	2	120/4-25	
.159	50	225	20	515	170	2	120/4-25	
1201	150	5	04081018	50	01			
15.9	100	316	05	185	145	3	120/1-15	
5.03	100	522	05	413	268	3	120/1-15	
1.59	100	745	05	818	413	3	120/1-15	
.503	200	280	20	241	161	2	120/1-15	
.159	200	271	20	377	170	2	120/1-15	
1204	150	7	0796	995	50	01		
15.9	100	352	10	124	167	3	120/4-15	
5.03	100	647	10	319	341	3	120/4-15	
1.59	100	712	10	511	418	3	120/4-15	
.503	200	244	20	263	147	2	120/4-15	
.503	200	248	20	249	148	2	120/4-15	
.503	200	247	20	273	142	2	120/4-15	
.159	200	240	50	180	160	2	120/4-15	
1201	50	5	04081018	50	01			
50.3	100	139	02	74	41	3	120/1-5	
15.9	100	457	02	305	135	3	120/1-5	
5.03	200	451	02	699	140	3	120/1-5	
5.03	200	425	02	654	132	3	120/1-5	
1.59	200	647	05	505	223	3	120/1-5	
1204	50	6	0796	995	50	01		
50.3	50	312	02	110	75	3	120/4-5	
15.9	200	187	02	290	45	3	120/4-5	
5.03	200	461	02	784	120	3	120/4-5	
1.59	200	651	05	578	207	3	120/4-5	
.503	200	548	05	634	193	2	120/4-5	
.159	200	558	10	430	235	2	120/4-5	

Reduced Data

The pages that follow present copies of the computer printout of the reduced data. Each "block" of data represents one sample-plate combination for one temperature. In general, one page contains one sample number. The pages are arranged by increasing sample number.

Table 5 in the main text gives a description for each sample. When more than one plate number per sample is given, a duplicate test is indicated.

SAMPLE 105 PLATE 1									
AREA SHEARED, ONE SIDE									
SAMPLE THICK, ONE SIDE									
5.0 DEG. CENT.									
LOG	PCT	LOG	LOG	LOG	LOG	LOG	LOG	LOG	LOG
1/W	STRAIN	IJ*1	JREAL	JLOSS	DELTA	1/W	STRAIN	IJ*1	JREAL
-1.50	.121	-8.95	-9.00	-9.01	-.01	-2.50	.005	-9.21	-9.23
-1.50	.227	-8.82	-8.97	-8.96	.01	-2.00	.017	-9.84	-10.42
-1.00	.312	-8.59	-8.79	-8.71	.04	-1.50	.027	-9.74	-10.33
-1.00	.110	-8.62	-8.84	-8.72	.12	-1.00	.047	-9.71	-10.17
-1.50	.152	-8.33	-8.56	-8.41	.15	-1.50	.037	-9.51	-10.01
.00	.313	-8.02	-8.28	-8.11	.17	.00	.044	-9.53	-10.57
.00	.156	-7.72	-8.00	-7.79	.21				

SAMPLE 105 PLATE 1									
AREA SHEARED, ONE SIDE									
SAMPLE THICK, ONE SIDE									
15.0 DEG. CENT.									
LOG	PCT	LOG	LOG	LOG	LOG	LOG	LOG	LOG	LOG
1/W	STRAIN	IJ*1	JREAL	JLOSS	DELTA	1/W	STRAIN	IJ*1	JREAL
-2.00	.018	-9.54	-9.58	-9.53	-.35	-1.50	.055	-9.41	-9.75
-1.50	.065	-9.41	-9.46	-9.45	-.28	-1.50	.033	-9.43	-9.77
-1.50	.033	-9.43	-9.48	-9.47	-.29	-1.00	.141	-9.25	-9.53
-1.00	.141	-9.25	-9.33	-9.53	-.20	-1.50	.060	-9.09	-9.35
-1.50	.060	-9.09	-9.16	-9.35	-.14	.00	.045	-8.89	-9.10
.00	.045	-8.89	-8.99	-9.10	-.11				

SAMPLE 105 PLATE 4

15.0 DEG. CENT.

AREA SHEARED, ONE SIDE

SAMPLE THICK, ONE SIDE

9.90 CM. SQ.

.0406 IN.

LOG	PCT	LOG	LOG	LOG	LOG	LOG	LOG	LOG	LOG
1/W	STRAIN	IJ*1	JREAL	JLOSS	DELTA	1/W	STRAIN	IJ*1	JREAL
-2.00	.015	-9.57	-9.62	-9.91	-.29	-1.50	.055	-9.42	-9.72
-1.50	.055	-9.42	-9.48	-9.72	-.24	-1.00	.044	-9.27	-9.53
-1.00	.044	-9.27	-9.35	-9.53	-.18	-1.50	.054	-9.10	-9.33
-1.50	.054	-9.10	-9.20	-9.33	-.13	.00	.079	-8.87	-9.05
.00	.079	-8.87	-9.00	-9.05	-.04				

SAMPLE 104 PLATE 4

25.0 DEG. CENT.

AREA SHEARED, ONE SIDE

SAMPLE THICK, ONE SIDE

9.90 CM. SQ.

.0406 IN.

LOG	PCT	LOG	LOG	LOG	LOG	LOG	LOG	LOG	LOG
1/W	STRAIN	IJ*1	JREAL	JLOSS	DELTA	1/W	STRAIN	IJ*1	JREAL
-1.50	.091	-8.82	-8.98	-8.97	.00	-1.50	.172	-8.81	-8.96
-1.50	.172	-8.81	-8.97	-8.96	.01	-1.00	.236	-8.57	-8.78
-1.00	.236	-8.57	-8.78	-8.68	.10	-1.50	.244	-8.29	-8.51
-1.50	.244	-8.29	-8.51	-8.38	.13	.00	.529	-7.95	-8.27
.00	.529	-7.95	-8.27	-8.01	.24	.50	.302	-7.65	-7.71
.50	.302	-7.65	-7.95	-7.71	.24	.50	.302	-7.67	-7.73
1.00	.680	-7.34	-7.66	-7.39	.28				

SAMPLE 106 PLATE 2 25.0 DEG. CENT.

AREA SHEARED, ONE SIDE					9.97 CM. SQ.				
SAMPLE THICK, ONE SIDE					.0409 IN.				
LOG	PCT	LOG	LOG	LOG TAN	LOG	LOG	LOG	LOG TAN	LOG TAN
1/4	STRAIN	LOG	JREAL	JLOSS	DELTA	LOG	JREAL	JLOSS	DELTA
-1.50	.045	-4.92	-9.04	-9.11	-.07	-1.50	-9.04	-9.11	-.07
-1.50	.187	-4.88	-9.01	-9.05	-.04	-1.50	-9.01	-9.05	-.04
-1.00	.493	-4.63	-8.80	-8.76	.04	-1.50	-8.80	-8.76	.04
-1.50	.364	-5.40	-8.56	-8.54	.02	-1.50	-8.56	-8.54	.02
.00	.713	-8.11	-8.32	-8.21	.11	.00	-8.32	-8.21	.11
.00	.315	-8.16	-8.37	-8.26	.10	.00	-8.37	-8.26	.10
.50	.203	-7.99	-8.15	-8.13	.02	.50	-8.15	-8.13	.02

SAMPLE 106 PLATE 2 15.0 DEG. CENT.

AREA SHEARED, ONE SIDE					9.97 CM. SQ.				
SAMPLE THICK, ONE SIDE					.0409 IN.				
LOG	PCT	LOG	LOG	LOG TAN	LOG	LOG	LOG	LOG TAN	LOG TAN
1/4	STRAIN	LOG	JREAL	JLOSS	DELTA	LOG	JREAL	JLOSS	DELTA
-2.00	.017	-9.56	-9.61	-9.94	-.33	-2.00	-9.61	-9.94	-.33
-1.50	.031	-9.44	-9.52	-9.78	-.24	-1.50	-9.52	-9.78	-.24
-1.50	.063	-9.44	-9.49	-9.79	-.30	-1.50	-9.49	-9.79	-.30
-1.00	.064	-9.31	-9.38	-9.60	-.22	-1.00	-9.38	-9.60	-.22
-.50	.054	-9.15	-9.24	-9.40	-.16	-.50	-9.24	-9.40	-.16
.00	.084	-8.97	-9.06	-9.19	-.13	.00	-9.06	-9.19	-.13

SAMPLE 106 PLATE 2

AREA SHEARED, ONE SIDE					9.97 CM. SQ.				
SAMPLE THICK, ONE SIDE					.0409 IN.				
LOG	PCT	LOG	LOG	LOG TAN	LOG	LOG	LOG	LOG TAN	LOG TAN
1/4	STRAIN	LOG	JREAL	JLOSS	DELTA	LOG	JREAL	JLOSS	DELTA
-2.50	.004	-9.92	-9.94	-10.41	-.44	-2.50	-9.94	-10.41	-.44
-2.00	.004	-9.84	-9.87	-10.32	-.45	-2.00	-9.87	-10.32	-.45
-2.00	.010	-9.83	-9.85	-10.34	-.53	-2.00	-9.85	-10.34	-.53
-1.50	.014	-9.77	-9.79	-10.28	-.44	-1.50	-9.79	-10.28	-.44
-1.50	.027	-9.75	-9.74	-10.33	-.54	-1.50	-9.74	-10.33	-.54
-1.00	.020	-9.69	-9.72	-10.11	-.39	-1.00	-9.72	-10.11	-.39
-1.00	.044	-9.70	-9.74	-10.09	-.35	-1.00	-9.74	-10.09	-.35
-.50	.044	-9.60	-9.63	-10.03	-.41	-.50	-9.63	-10.03	-.41
.00	.024	-9.53	-9.58	-9.87	-.29	.00	-9.58	-9.87	-.29
.00	.050	-9.44	-9.54	-9.45	-.31	.00	-9.54	-9.45	-.31
.50	.040	-9.34	-9.43	-9.70	-.27	.50	-9.43	-9.70	-.27

SAMPLE 106 PLATE 3 25.0 DEG. CENT.

AREA SHEARED, ONE SIDE					9.63 CM. SQ.				
SAMPLE THICK, ONE SIDE					.0410 IN.				
LOG	PCT	LOG	LOG	LOG TAN	LOG	LOG	LOG	LOG TAN	LOG TAN
1/4	STRAIN	LOG	JREAL	JLOSS	DELTA	LOG	JREAL	JLOSS	DELTA
-1.50	.064	-4.96	-9.04	-9.14	-.04	-1.50	-9.04	-9.14	-.04
-1.50	.130	-4.94	-9.06	-9.12	-.05	-1.50	-9.06	-9.12	-.05
-1.00	.214	-8.75	-8.89	-8.91	-.02	-1.00	-8.89	-8.91	-.02
-1.00	.074	-8.77	-8.91	-8.92	-.01	-1.00	-8.91	-8.92	-.01
-1.50	.174	-4.52	-8.65	-8.68	-.03	-1.50	-8.65	-8.68	-.03
.00	.317	-8.25	-8.43	-8.34	.04	.00	-8.43	-8.34	.04
.50	.172	-8.04	-8.22	-8.25	-.03	.50	-8.22	-8.25	-.03
.50	.171	-8.08	-8.24	-8.21	.03	.50	-8.24	-8.21	.03

SAMPLE 106 PLATE 3 15.0 DEG. CENT.

AREA SHEARED, ONE SIDE					9.63 CM. SQ.				
SAMPLE THICK, ONE SIDE					.0410 IN.				
LOG	PCT	LOG	LOG	LOG TAN	LOG	LOG	LOG	LOG TAN	LOG TAN
1/4	STRAIN	LOG	JREAL	JLOSS	DELTA	LOG	JREAL	JLOSS	DELTA
-2.00	.014	-9.62	-9.67	-9.96	-.29	-2.00	-9.67	-9.96	-.29
-1.50	.064	-9.47	-9.53	-9.79	-.27	-1.50	-9.53	-9.79	-.27
-1.50	.073	-9.49	-9.55	-9.81	-.26	-1.50	-9.55	-9.81	-.26
-1.00	.060	-9.34	-9.43	-9.62	-.19	-1.00	-9.43	-9.62	-.19
-1.00	.123	-9.33	-9.40	-9.61	-.21	-1.00	-9.40	-9.61	-.21
-1.00	.024	-9.34	-9.47	-9.54	-.12	-1.00	-9.47	-9.54	-.12
-.50	.045	-9.21	-9.31	-9.44	-.13	-.50	-9.31	-9.44	-.13
.00	.067	-9.03	-9.13	-9.24	-.12	.00	-9.13	-9.24	-.12
.00	.070	-9.02	-9.13	-9.22	-.09	.00	-9.13	-9.22	-.09

SAMPLE 106 PLATE 3

AREA SHEARED, ONE SIDE					9.63 CM. SQ.				
SAMPLE THICK, ONE SIDE					.0410 IN.				
LOG	PCT	LOG	LOG	LOG TAN	LOG	LOG	LOG	LOG TAN	LOG TAN
1/4	STRAIN	LOG	JREAL	JLOSS	DELTA	LOG	JREAL	JLOSS	DELTA
-2.00	.013	-9.87	-9.90	-10.34	-.44	-2.00	-9.90	-10.34	-.44
-1.50	.023	-9.82	-9.84	-10.29	-.44	-1.50	-9.84	-10.29	-.44
-1.00	.041	-9.74	-9.73	-10.14	-.35	-1.00	-9.73	-10.14	-.35
-.50	.044	-9.64	-9.70	-10.11	-.41	-.50	-9.70	-10.11	-.41
.00	.060	-9.54	-9.62	-9.87	-.30	.00	-9.62	-9.87	-.30

SAMPLE 10M PLATE 1										15.0 DEG. CENT.										5.0 DEG. CENT.									
AREA SHEARED, ONE SIDE										9.50 CM. SQ.										9.50 CM. SQ.									
SAMPLE THICK, ONE SIDE										.0418 IN.										.0418 IN.									
LOG	PCT	LOG	LOG	LOG	LOG	LOG	LOG	LOG	LOG	LOG	PCT	LOG	LOG	LOG	LOG	LOG	LOG	LOG	LOG	LOG	PCT	LOG	LOG	LOG	LOG	LOG	LOG	LOG	LOG
1/4	STRAIN	1/4	STRAIN	1/4	STRAIN	1/4	STRAIN	1/4	STRAIN	1/4	STRAIN	1/4	STRAIN	1/4	STRAIN	1/4	STRAIN	1/4	STRAIN	1/4	STRAIN	1/4	STRAIN	1/4	STRAIN	1/4	STRAIN	1/4	STRAIN
-2.00	.034	-9.15	-9.24	-9.39	-9.14	-9.50	.014	-9.58	-9.62	-9.94	-9.36	-1.50	.034	-9.46	-9.51	-9.82	-9.31	-1.50	.034	-9.46	-9.51	-9.82	-9.31	-1.50	.034	-9.46	-9.51	-9.82	-9.31
-1.50	.101	-8.95	-9.07	-9.14	-9.07	-1.00	.064	-9.32	-9.38	-9.63	-9.25	-1.00	.064	-9.32	-9.38	-9.63	-9.25	-1.00	.064	-9.32	-9.38	-9.63	-9.25	-1.00	.064	-9.32	-9.38	-9.63	-9.25
-1.00	.213	-8.71	-8.86	-8.86	.00	-.50	.086	-9.16	-9.23	-9.45	-.22	-.50	.086	-9.16	-9.23	-9.45	-.22	-.50	.086	-9.16	-9.23	-9.45	-.22	-.50	.086	-9.16	-9.23	-9.45	-.22
-.50	.161	-8.47	-8.61	-8.63	-.01	.00	.207	-8.95	-9.05	-9.17	-.12	.00	.207	-8.95	-9.05	-9.17	-.12	.00	.207	-8.95	-9.05	-9.17	-.12	.00	.207	-8.95	-9.05	-9.17	-.12
.00	.241	-8.22	-8.39	-8.36	.03	.00	.100	-8.97	-9.06	-9.19	-.13	.00	.100	-8.97	-9.06	-9.19	-.13	.00	.100	-8.97	-9.06	-9.19	-.13	.00	.100	-8.97	-9.06	-9.19	-.13
.00	.073	-8.22	-8.38	-8.35	.03	.50	.044	-8.75	-8.84	-8.95	-.06	.50	.044	-8.75	-8.84	-8.95	-.06	.50	.044	-8.75	-8.84	-8.95	-.06	.50	.044	-8.75	-8.84	-8.95	-.06
.50	.116	-7.99	-8.14	-8.11	.07																								

SAMPLE 10M PLATE 4										15.0 DEG. CENT.										5.0 DEG. CENT.									
AREA SHEARED, ONE SIDE										9.20 CM. SQ.										9.20 CM. SQ.									
SAMPLE THICK, ONE SIDE										.0416 IN.										.0416 IN.									
LOG	PCT	LOG	LOG	LOG	LOG	LOG	LOG	LOG	LOG	LOG	PCT	LOG	LOG	LOG	LOG	LOG	LOG	LOG	LOG	LOG	PCT	LOG	LOG	LOG	LOG	LOG	LOG	LOG	LOG
1/4	STRAIN	1/4	STRAIN	1/4	STRAIN	1/4	STRAIN	1/4	STRAIN	1/4	STRAIN	1/4	STRAIN	1/4	STRAIN	1/4	STRAIN	1/4	STRAIN	1/4	STRAIN	1/4	STRAIN	1/4	STRAIN	1/4	STRAIN	1/4	STRAIN
-2.00	.040	-4.15	-4.26	-4.35	-.09	-2.00	.010	-9.64	-9.68	-10.01	-.33	-2.00	.010	-9.64	-9.68	-10.01	-.33	-2.00	.010	-9.64	-9.68	-10.01	-.33	-2.00	.010	-9.64	-9.68	-10.01	-.33
-1.50	.101	-4.95	-5.08	-5.12	-.04	-1.50	.024	-9.51	-9.57	-9.83	-.24	-1.50	.024	-9.51	-9.57	-9.83	-.24	-1.50	.024	-9.51	-9.57	-9.83	-.24	-1.50	.024	-9.51	-9.57	-9.83	-.24
-1.00	.244	-4.70	-4.86	-4.85	.01	-1.00	.051	-9.39	-9.46	-9.67	-.21	-1.00	.051	-9.39	-9.46	-9.67	-.21	-1.00	.051	-9.39	-9.46	-9.67	-.21	-1.00	.051	-9.39	-9.46	-9.67	-.21
-.50	.245	-4.45	-4.61	-4.60	.02	-.50	.036	-9.22	-9.33	-9.42	-.09	-.50	.036	-9.22	-9.33	-9.42	-.09	-.50	.036	-9.22	-9.33	-9.42	-.09	-.50	.036	-9.22	-9.33	-9.42	-.09
.00	.205	-4.20	-4.38	-4.33	.05	.00	.054	-9.03	-9.15	-9.21	-.07	.00	.054	-9.03	-9.15	-9.21	-.07	.00	.054	-9.03	-9.15	-9.21	-.07	.00	.054	-9.03	-9.15	-9.21	-.07
.50	.114	-3.94	-4.14	-4.09	.09	.00	.120	-8.94	-9.10	-9.20	-.09	.00	.120	-8.94	-9.10	-9.20	-.09	.00	.120	-8.94	-9.10	-9.20	-.09	.00	.120	-8.94	-9.10	-9.20	-.09

SAMPLE 104 PLATE 3 25.0 DEG. CENT.									
AREA SHEARED, ONE SIDE 9.20 CM. SQ.									
SAMPLE THICK, ONE SIDE .0406 IN.									
LOG	PCT	LOG	LOG	LOG	LOG	LOG	LOG	LOG	LOG
1/4 STRAIN	1/41	1/41	1/41	1/41	1/41	1/41	1/41	1/41	1/41
-1.50	.100	-4.83	-8.97	-4.99	-.03				
-1.00	.121	-4.61	-4.76	-4.76	-.01				
-1.00	.061	-4.63	-4.79	-4.77	.01				
.00	.143	-4.06	-4.24	-4.17	.11				
.00	.142	-4.04	-4.30	-4.14	.12				
.50	.276	-7.74	-8.01	-7.88	.12				
SAMPLE 104 PLATE 3 15.0 DEG. CENT.									
AREA SHEARED, ONE SIDE 9.20 CM. SQ.									
SAMPLE THICK, ONE SIDE .0406 IN.									
LOG	PCT	LOG	LOG	LOG	LOG	LOG	LOG	LOG	LOG
1/4 STRAIN	1/41	1/41	1/41	1/41	1/41	1/41	1/41	1/41	1/41
-2.00	.017	-9.53	-4.58	-9.49	-.31				
-1.50	.056	-9.34	-4.54	-9.70	-.24				
-1.00	.054	-9.26	-4.34	-9.52	-.14				
-1.00	.111	-9.25	-9.32	-9.53	-.21				
-.50	.045	-9.04	-9.16	-9.33	-.14				
-.50	.047	-9.07	-9.15	-9.32	-.17				
.00	.155	-8.87	-8.38	-9.07	-.09				
SAMPLE 104 PLATE 3 5.0 DEG. CENT.									
AREA SHEARED, ONE SIDE 9.20 CM. SQ.									
SAMPLE THICK, ONE SIDE .0406 IN.									
LOG	PCT	LOG	LOG	LOG	LOG	LOG	LOG	LOG	LOG
1/4 STRAIN	1/41	1/41	1/41	1/41	1/41	1/41	1/41	1/41	1/41
-2.00	.010	-9.62	-9.44	-10.19	-.55				
-2.00	.009	-9.85	-9.45	-10.41	-.55				
-1.50	.032	-9.76	-9.80	-10.35	-.55				
-1.00	.053	-9.71	-9.74	-10.22	-.43				
-.50	.047	-9.61	-9.65	-10.03	-.34				
-.50	.017	-9.65	-9.70	-10.03	-.33				
.00	.023	-9.51	-9.57	-9.84	-.24				
SAMPLE 104 PLATE 4 25.0 DEG. CENT.									
AREA SHEARED, ONE SIDE 9.72 CM. SQ.									
SAMPLE THICK, ONE SIDE .0401 IN.									
LOG	PCT	LOG	LOG	LOG	LOG	LOG	LOG	LOG	LOG
1/4 STRAIN	1/41	1/41	1/41	1/41	1/41	1/41	1/41	1/41	1/41
-1.50	.119	-4.84	-4.97	-4.01	-.04				
-1.50	.059	-4.45	-4.44	-4.02	-.04				
-1.00	.143	-4.62	-4.74	-4.77	.00				
-.50	.114	-4.34	-4.50	-4.44	.03				
-.50	.242	-4.33	-4.50	-4.47	.04				
.00	.227	-4.06	-4.27	-4.16	.11				
.50	.173	-7.74	-8.01	-7.88	.13				
SAMPLE 104 PLATE 4 15.0 DEG. CENT.									
AREA SHEARED, ONE SIDE 9.72 CM. SQ.									
SAMPLE THICK, ONE SIDE .0401 IN.									
LOG	PCT	LOG	LOG	LOG	LOG	LOG	LOG	LOG	LOG
1/4 STRAIN	1/41	1/41	1/41	1/41	1/41	1/41	1/41	1/41	1/41
-2.00	.015	-9.54	-9.41	-9.44	-.24				
-1.50	.044	-9.43	-9.50	-9.71	-.21				
-.50	.044	-9.10	-9.20	-9.32	-.12				
-.50	.176	-9.08	-9.14	-9.32	-.14				
.00	.145	-8.87	-8.99	-9.05	-.04				
SAMPLE 104 PLATE 4 5.0 DEG. CENT.									
AREA SHEARED, ONE SIDE 9.72 CM. SQ.									
SAMPLE THICK, ONE SIDE .0401 IN.									
LOG	PCT	LOG	LOG	LOG	LOG	LOG	LOG	LOG	LOG
1/4 STRAIN	1/41	1/41	1/41	1/41	1/41	1/41	1/41	1/41	1/41
-2.00	.000	-9.45	-9.26	-10.59	-.61				
-2.00	.001	-9.24	-9.21	-10.44	-.57				
-2.00	.001	-9.47	-9.44	-10.44	-.50				
-.50	.003	-9.44	-9.47	-10.10	-.44				
.00	.004	-9.34	-9.34	-9.92	-.33				
.00	.002	-9.54	-9.44	-9.91	-.33				

SAMPLE 116 PLATE 1 25.0 DEG. CENT.

AREA SHEARED, ONE SIDE 9.92 CM. SQ.
 SAMPLE THICK, ONE SIDE .0404 IN.

LOG 1/W	PCT STRAIN	LOG IJ*1	LOG JREAL	LOG JLOSS	LOG TAN DELTA
-2.50	.019	-8.52	-8.63	-8.71	-.08
-2.50	.046	-8.52	-8.62	-8.73	-.10
-2.00	.058	-8.33	-8.45	-8.51	-.06
-2.00	.491	-8.27	-8.41	-8.43	-.02
-1.50	.759	-8.04	-8.20	-8.17	.03
-1.50	.361	-8.07	-8.21	-8.22	-.00
-1.00	1.048	-7.76	-7.98	-7.86	.12
-1.00	2.006	-7.78	-8.00	-7.88	.12
-1.00	.491	-7.79	-8.00	-7.89	.11
-.50	4.857	-7.47	-7.71	-7.55	.15
-.50	.645	-7.49	-7.71	-7.58	.13
-.50	2.353	-7.48	-7.72	-7.57	.14

SAMPLE 116 PLATE 2 25.0 DEG. CENT.

AREA SHEARED, ONE SIDE 9.41 CM. SQ.
 SAMPLE THICK, ONE SIDE .0055 IN.

LOG 1/W	PCT STRAIN	LOG IJ*1	LOG JREAL	LOG JLOSS	LOG TAN DELTA
-2.50	.251	-8.48	-8.59	-8.67	-.08
-2.50	.120	-8.48	-8.60	-8.67	-.08
-2.50	.071	-8.49	-8.58	-8.71	-.13
-2.00	.505	-8.24	-8.39	-8.39	-.00
-2.00	.245	-8.26	-8.41	-8.42	-.01
-1.50	.704	-8.03	-8.19	-8.16	.03
-1.50	.360	-8.02	-8.18	-8.15	.03
-1.50	1.552	-7.98	-8.16	-8.11	.06
-1.00	4.288	-7.71	-7.95	-7.79	.16
-1.00	2.131	-7.71	-7.94	-7.80	.15
-1.00	1.047	-7.71	-7.95	-7.80	.15
-.50	4.212	-7.40	-7.67	-7.48	.19
-.50	2.127	-7.40	-7.68	-7.47	.21
-.50	5.082	-6.42	-6.72	-6.48	.24
-.50	9.198	-7.36	-7.64	-7.43	.21
.00	4.489	-7.08	-7.40	-7.13	.27
.00	1.105	-7.09	-7.45	-7.14	.31
.00	2.196	-7.09	-7.43	-7.14	.29
.00	9.391	-7.06	-7.41	-7.11	.30
.00	9.364	-7.06	-7.42	-7.11	.31

SAMPLE 117 PLATE 1 25.0 DEG. CENT.

AREA SHEARED, ONE SIDE 17.50 CM. SQ.
SAMPLE THICK, ONE SIDE .0204 IN.

LOG 1/4	PCT STRAIN	LOG IJ*1	LOG JREAL	LOG JLOSS	LOG TAN DELTA
-2.50	.041	-4.29	-4.39	-4.50	-.11
-2.00	.175	-4.05	-4.19	-4.22	-.03
-1.50	.757	-7.81	-7.99	-7.95	.04
-1.00	2.065	-7.54	-7.75	-7.64	.10
-.50	4.495	-7.22	-7.49	-7.30	.19
-.50	4.754	-7.22	-7.50	-7.29	.20
.00	2.347	-6.89	-7.19	-6.96	.24
.00	2.750	-6.89	-7.21	-6.95	.24

SAMPLE 117 PLATE 1 15.0 DEG. CENT.

AREA SHEARED, ONE SIDE 17.50 CM. SQ.
SAMPLE THICK, ONE SIDE .0204 IN.

LOG 1/4	PCT STRAIN	LOG IJ*1	LOG JREAL	LOG JLOSS	LOG TAN DELTA
-2.00	.051	-8.65	-8.71	-8.94	-.23
-1.50	.113	-8.50	-8.57	-8.76	-.19
-1.00	.240	-8.32	-8.42	-8.55	-.13
-.50	.323	-8.10	-8.21	-8.30	-.09
.00	.552	-7.89	-8.02	-8.06	-.04

SAMPLE 117 PLATE 1 5.0 DEG. CENT.

AREA SHEARED, ONE SIDE 17.50 CM. SQ.
SAMPLE THICK, ONE SIDE .0204 IN.

LOG 1/4	PCT STRAIN	LOG IJ*1	LOG JREAL	LOG JLOSS	LOG TAN DELTA
-2.50	.017	-9.16	-9.19	-9.60	-.41
-2.00	.049	-9.08	-9.13	-9.44	-.31
-1.50	.053	-9.09	-9.14	-9.45	-.31
-1.00	.072	-8.99	-9.05		-.24
-.50	.164	-8.74	-8.84	-9.04	-.22
-.50	.230	-8.74	-8.81	-9.03	-.22
.00	.272	-8.62	-8.69	-8.94	-.19
.00	.332	-8.59	-8.66	-8.95	-.19

SAMPLE 117 PLATE 2 25.0 DEG. CENT.

AREA SHEARED, ONE SIDE 18.10 CM. SQ.
SAMPLE THICK, ONE SIDE .0203 IN.

LOG 1/4	PCT STRAIN	LOG IJ*1	LOG JREAL	LOG JLOSS	LOG TAN DELTA
-2.50	.046	-4.30	-4.40	-4.52	-.12
-2.00	.214	-4.03	-4.17	-4.19	-.02
-1.50	.640	-7.81	-7.98	-7.94	.04
-1.00	1.726	-7.53	-7.74	-7.63	.11
-.50	2.174	-7.23	-7.50	-7.30	.20
-.50	2.651	-7.23	-7.44	-7.31	.17
.00	2.974	-6.89	-7.21	-6.95	.24
.00	3.564	-6.89	-7.21	-6.94	.27

SAMPLE 117 PLATE 2 15.0 DEG. CENT.

AREA SHEARED, ONE SIDE 18.10 CM. SQ.
SAMPLE THICK, ONE SIDE .0203 IN.

LOG 1/4	PCT STRAIN	LOG IJ*1	LOG JREAL	LOG JLOSS	LOG TAN DELTA
-2.00	.066	-8.67	-8.74	-8.95	-.21
-1.50	.132	-8.51	-8.59	-8.76	-.17
-1.00	.266	-8.34	-8.43	-8.57	-.14
-.50	.352	-8.10	-8.21	-8.30	-.09
-.50	.420	-8.15	-8.26	-8.34	-.04
.00	.525	-7.89	-7.94	-8.03	-.04
.00	.589	-7.98	-8.02	-8.04	-.02

SAMPLE 117 PLATE 2 5.0 DEG. CENT.

AREA SHEARED, ONE SIDE 18.10 CM. SQ.
SAMPLE THICK, ONE SIDE .0203 IN.

LOG 1/4	PCT STRAIN	LOG IJ*1	LOG JREAL	LOG JLOSS	LOG TAN DELTA
-2.50	.015	-9.14	-9.22	-9.60	-.38
-2.00	.044	-9.04	-9.13	-9.44	-.31
-1.50	.062	-9.04	-9.10	-9.35	-.25
-1.00	.100	-8.92	-8.99	-9.18	-.22
-.50	.207	-8.70	-8.74	-9.01	-.25
-.50	.214	-8.62	-8.69	-8.92	-.23
.00	.253	-8.55	-8.63	-8.82	-.19
.00	.298	-8.55	-8.62	-8.81	-.18

SAMPLE 11B PLATE 3 25.0 DEG. CENT.									
AREA SHEARED, ONE SIDE 14.90 CM. SQ.									
SAMPLE THICK, ONE SIDE .0204 IN.									
LOG	PCT	LOG	LOG	LOG	LOG	LOG	LOG	LOG	LOG
1/2	STRAIN	1/2	JREAL	JLOSS	DELTA	1/2	STRAIN	1/2	JREAL
-2.50	.049	-8.24	-9.39	-8.44	-.08	-2.50	.019	-9.17	-9.19
-2.00	.195	-8.04	-8.19	-8.20	-.01	-2.00	.060	-9.04	-9.04
-1.50	.190	-7.80	-7.97	-7.94	.03	-1.50	.100	-8.95	-8.99
-1.00	.521	-7.80	-7.97	-7.92	.05	-1.00	.194	-8.81	-8.86
-1.00	2.612	-7.42	-7.454	-7.52	.12	-1.00	.731	-8.57	-8.72
-1.00	1.360	-7.40	-7.454	-7.49	.15	-1.00	.274	-8.70	-8.76
-1.50	1.42	-7.20	-7.47	-7.28	.19	.00	.412	-8.52	-8.59
.00	6.590	-6.88	-7.21	-6.94	.27	.00	.693	-8.51	-8.58

SAMPLE 11B PLATE 3
AREA SHEARED, ONE SIDE 14.90 CM. SQ.
SAMPLE THICK, ONE SIDE .0204 IN.

LOG PCT LOG LOG LOG LOG LOG LOG LOG LOG
1/2 STRAIN 1/2 JREAL JLOSS DELTA

SAMPLE 11B PLATE 4 25.0 DEG. CENT.									
AREA SHEARED, ONE SIDE 14.75 CM. SQ.									
SAMPLE THICK, ONE SIDE .0202 IN.									
LOG	PCT	LOG	LOG	LOG	LOG	LOG	LOG	LOG	LOG
1/2	STRAIN	1/2	JREAL	JLOSS	DELTA	1/2	STRAIN	1/2	JREAL
-2.50	.052	-8.34	-8.47	-8.54	-.07	-2.50	.014	-9.14	-9.22
-2.00	.197	-8.12	-8.27	-8.26	.02	-2.00	.081	-9.04	-9.08
-1.50	.624	-7.88	-8.06	-8.00	.05	-1.50	.121	-8.94	-8.92
-1.00	1.741	-7.59	-7.80	-7.69	.11	-1.00	.247	-8.83	-8.88
-1.50	2.634	-7.24	-7.51	-7.37	.14	-1.00	.341	-8.71	-8.76
-1.50	2.154	-7.29	-7.55	-7.37	.14	-1.00	.335	-8.71	-8.78
.00	3.035	-6.97	-7.24	-7.03	.25	.00	.401	-8.87	-8.88
.00	3.815	-6.95	-7.25	-7.01	.24	.00	.466	-8.85	-8.83

SAMPLE 11B PLATE 4 25.0 DEG. CENT.
AREA SHEARED, ONE SIDE 14.75 CM. SQ.
SAMPLE THICK, ONE SIDE .0202 IN.

LOG PCT LOG LOG LOG LOG LOG LOG LOG LOG
1/2 STRAIN 1/2 JREAL JLOSS DELTA

SAMPLE 11B PLATE 4 25.0 DEG. CENT.
AREA SHEARED, ONE SIDE 14.75 CM. SQ.
SAMPLE THICK, ONE SIDE .0202 IN.

LOG PCT LOG LOG LOG LOG LOG LOG LOG LOG
1/2 STRAIN 1/2 JREAL JLOSS DELTA

SAMPLE 119 PLATE 1 25.0 DEG. CENT.

AREA SHEARED, ONE SIDE 9.75 CM. SQ.
SAMPLE THICK, ONE SIDE .0405 IN.

LOG 1/4	PCT STRAIN	LOG 1J*1	LOG JREAL	LOG JLOSS	LOG TAN DELTA
-2.00	.042	-9.00	-9.12	-9.18	-.06
-1.50	.126	-8.76	-8.90	-8.92	-.02
-1.00	.339	-8.64	-8.70	-8.57	.13
-.50	.192	-8.26	-8.53	-8.34	.19
.00	.407	-7.93	-8.25	-7.98	.27
-.50	.571	-8.15	-8.40	-8.23	.17
.00	1.194	-7.83	-8.12	-7.89	.23

SAMPLE 119 PLATE 1 15.0 DEG. CENT.

AREA SHEARED, ONE SIDE 9.75 CM. SQ.
SAMPLE THICK, ONE SIDE .0405 IN.

LOG 1/4	PCT STRAIN	LOG 1J*1	LOG JREAL	LOG JLOSS	LOG TAN DELTA
-2.00	.024	-9.51	-9.57	-9.41	-.25
-1.50	.053	-9.38	-9.45	-9.66	-.21
-1.00	.107	-9.23	-9.32	-9.44	-.16
.00	.216	-8.80	-8.94	-8.95	-.01
-.50	.150	-9.02	-9.12	-9.24	-.12

SAMPLE 119 PLATE 1 5.0 DEG. CENT.

AREA SHEARED, ONE SIDE 9.75 CM. SQ.
SAMPLE THICK, ONE SIDE .0405 IN.

LOG 1/4	PCT STRAIN	LOG 1J*1	LOG JREAL	LOG JLOSS	LOG TAN DELTA
-2.00	.014	-9.59	-9.94	-10.20	-.24
-1.50	.024	-9.84	-9.94	-10.11	-.19
-1.00	.024	-9.45	-9.94	-10.10	-.16
-1.00	.049	-9.75	-9.79	-10.10	-.31
-.50	.059	-9.42	-9.68	-9.94	-.25
.00	.083	-9.22	-9.55	-9.74	-.19
-.50	.071	-9.80	-9.85	-9.93	-.27
.00	.100	-9.45	-9.53	-9.75	-.22

SAMPLE 119 PLATE 2 25.0 DEG. CENT.

AREA SHEARED, ONE SIDE 9.75 CM. SQ.
SAMPLE THICK, ONE SIDE .0404 IN.

LOG 1/4	PCT STRAIN	LOG 1J*1	LOG JREAL	LOG JLOSS	LOG TAN DELTA
-2.00	.043	-8.99	-9.11	-9.19	-.09
-1.50	.151	-8.76	-8.89	-8.94	-.05
-1.00	.342	-8.52	-8.70	-8.64	.06
-.50	.658	-8.20	-8.40	-8.31	.09
.00	.941	-7.89	-8.16	-7.97	.19
.00	.952	-7.90	-8.19	-7.96	.23

SAMPLE 119 PLATE 2 15.0 DEG. CENT.

AREA SHEARED, ONE SIDE 9.75 CM. SQ.
SAMPLE THICK, ONE SIDE .0404 IN.

LOG 1/4	PCT STRAIN	LOG 1J*1	LOG JREAL	LOG JLOSS	LOG TAN DELTA
-2.00	.024	-9.52	-9.57	-9.47	-.30
-1.50	.050	-9.39	-9.45	-9.70	-.24
-1.00	.101	-9.24	-9.31	-9.50	-.19
-.50	.134	-9.04	-9.13	-9.27	-.15
.00	.229	-8.41	-8.44	-8.94	-.05
.00	.254	-8.76	-8.90	-8.42	-.02

SAMPLE 119 PLATE 2 5.0 DEG. CENT.

AREA SHEARED, ONE SIDE 9.75 CM. SQ.
SAMPLE THICK, ONE SIDE .0404 IN.

LOG 1/4	PCT STRAIN	LOG 1J*1	LOG JREAL	LOG JLOSS	LOG TAN DELTA
-2.00	.013	-9.80	-9.94	-10.37	-.24
-1.50	.014	-9.74	-9.74	-10.30	-.24
-1.00	.041	-9.47	-9.70	-10.15	-.24
-1.00	.074	-9.65	-9.69	-10.14	-.25
-.50	.071	-9.55	-9.59	-9.94	-.26
.00	.045	-9.83	-9.94	-9.74	-.24
-.50	.084	-9.83	-9.87	-9.94	-.24
.00	.114	-9.40	-9.45	-9.74	-.24

SAMPLE 119 PLATE 3 25.0 DEG. CENT.									
AREA SHEARED, ONE SIDE 9.45 CM. SQ. SAMPLE THICK, ONE SIDE .0204 IN.									
LOG	PCT	LOG	LOG	LOG	LOG	LOG	LOG	LOG	LOG
1/W	STRAIN	LOG	LOG	LOG	LOG	LOG	LOG	LOG	LOG
1/W	STRAIN	LOG	LOG	LOG	LOG	LOG	LOG	LOG	LOG
1/W	STRAIN	LOG	LOG	LOG	LOG	LOG	LOG	LOG	LOG
-2.00	.084	-8.98	-9.09	-9.17	-9.07				
-1.50	.335	-8.73	-8.84	-8.90	-9.02				
-1.00	.859	-8.49	-8.58	-8.60	.08				
-.50	.174	-8.28	-8.31	-8.38	.13				
-.50	.503	-8.25	-8.34	-8.34	.13				
.00	.991	-7.95	-8.22	-8.03	.19				

SAMPLE 119 PLATE 3 15.0 DEG. CENT.									
AREA SHEARED, ONE SIDE 9.45 CM. SQ. SAMPLE THICK, ONE SIDE .0204 IN.									
LOG	PCT	LOG	LOG	LOG	LOG	LOG	LOG	LOG	LOG
1/W	STRAIN	LOG	LOG	LOG	LOG	LOG	LOG	LOG	LOG
1/W	STRAIN	LOG	LOG	LOG	LOG	LOG	LOG	LOG	LOG
1/W	STRAIN	LOG	LOG	LOG	LOG	LOG	LOG	LOG	LOG
-2.00	.034	-9.45	-9.50	-9.50	-9.77	-9.26			
-1.50	.067	-9.32	-9.39	-9.39	-9.50	-9.20			
-1.00	.170	-9.20	-9.28	-9.28	-9.45	-9.17			
-.50	.190	-9.01	-9.11	-9.11	-9.24	-9.13			
-.50	.198	-8.94	-9.09	-9.09	-9.22	-9.13			
.00	.235	-8.82	-8.97	-8.97	-9.08	-9.01			

SAMPLE 119 PLATE 3 5.0 DEG. CENT.									
AREA SHEARED, ONE SIDE 9.45 CM. SQ. SAMPLE THICK, ONE SIDE .0204 IN.									
LOG	PCT	LOG	LOG	LOG	LOG	LOG	LOG	LOG	LOG
1/W	STRAIN	LOG	LOG	LOG	LOG	LOG	LOG	LOG	LOG
1/W	STRAIN	LOG	LOG	LOG	LOG	LOG	LOG	LOG	LOG
1/W	STRAIN	LOG	LOG	LOG	LOG	LOG	LOG	LOG	LOG
-2.00	.024	-9.75	-9.78	-9.78	-10.16	-9.38			
-1.50	.050	-9.70	-9.75	-9.75	-10.05	-9.31			
-1.00	.064	-9.63	-9.67	-9.67	-10.02	-9.35			
-1.00	.082	-9.63	-9.67	-9.67	-10.05	-9.39			
-.50	.064	-9.57	-9.51	-9.51	-9.93	-9.31			
-.50	.084	-9.53	-9.58	-9.58	-9.90	-9.33			
.00	.108	-9.44	-9.49	-9.49	-9.74	-9.27			

SAMPLE 119 PLATE 4 25.0 DEG. CENT.									
AREA SHEARED, ONE SIDE 9.45 CM. SQ. SAMPLE THICK, ONE SIDE .0200 IN.									
LOG	PCT	LOG	LOG	LOG	LOG	LOG	LOG	LOG	LOG
1/W	STRAIN	LOG	LOG	LOG	LOG	LOG	LOG	LOG	LOG
1/W	STRAIN	LOG	LOG	LOG	LOG	LOG	LOG	LOG	LOG
1/W	STRAIN	LOG	LOG	LOG	LOG	LOG	LOG	LOG	LOG
-2.00	.090	-8.97	-9.11	-9.13	-9.03				
-1.50	.368	-8.72	-8.89	-8.85	.04				
-1.00	.851	-8.47	-8.58	-8.57	.11				
-.50	.703	-8.19	-8.42	-8.28	.15				
.00	1.129	-7.88	-8.17	-7.95	.22				

SAMPLE 119 PLATE 4 15.0 DEG. CENT.									
AREA SHEARED, ONE SIDE 9.45 CM. SQ. SAMPLE THICK, ONE SIDE .0200 IN.									
LOG	PCT	LOG	LOG	LOG	LOG	LOG	LOG	LOG	LOG
1/W	STRAIN	LOG	LOG	LOG	LOG	LOG	LOG	LOG	LOG
1/W	STRAIN	LOG	LOG	LOG	LOG	LOG	LOG	LOG	LOG
1/W	STRAIN	LOG	LOG	LOG	LOG	LOG	LOG	LOG	LOG
-2.00	.039	-9.44	-9.49	-9.49	-9.80	-9.31			
-1.50	.073	-9.33	-9.39	-9.39	-9.62	-9.22			
-1.00	.147	-9.20	-9.26	-9.26	-9.48	-9.21			
-.50	.197	-9.03	-9.12	-9.12	-9.25	-9.13			
-.50	.243	-9.01	-9.09	-9.09	-9.25	-9.16			
.00	.197	-8.83	-8.95	-8.95	-9.02	-9.06			
.02	.238	-8.81	-8.92	-8.92	-9.00	-9.08			

SAMPLE 119 PLATE 4 5.0 DEG. CENT.									
AREA SHEARED, ONE SIDE 9.45 CM. SQ. SAMPLE THICK, ONE SIDE .0200 IN.									
LOG	PCT	LOG	LOG	LOG	LOG	LOG	LOG	LOG	LOG
1/W	STRAIN	LOG	LOG	LOG	LOG	LOG	LOG	LOG	LOG
1/W	STRAIN	LOG	LOG	LOG	LOG	LOG	LOG	LOG	LOG
1/W	STRAIN	LOG	LOG	LOG	LOG	LOG	LOG	LOG	LOG
-2.00	.022	-9.77	-9.79	-9.79	-10.29	-9.50			
-1.50	.057	-9.72	-9.74	-9.74	-10.23	-9.50			
-1.00	.072	-9.66	-9.70	-9.70	-10.07	-9.37			
-1.00	.075	-9.66	-9.68	-9.68	-10.05	-9.37			
-.50	.044	-9.64	-9.68	-9.68	-10.01	-9.32			
-.50	.051	-9.64	-9.68	-9.68	-10.04	-9.37			
.00	.075	-9.48	-9.53	-9.53	-9.74	-9.25			

SAMPLE 120 PLATE 1 25.0 DEG. CENT.									
AREA SHEARED, ONE SIDE 10.18 CM. SQ.									
SAMPLE THICK, ONE SIDE .0404 IN.									
LOG	PCT	LOG	LOG	LOG	LOG TAN	LOG	PCT	LOG	LOG TAN
1/4	STRAIN	LOG	LOG	LOG	DELTA	1/4	STRAIN	LOG	DELTA
-2.50	.014	-9.25	-9.36	-9.45	-.09	-2.50	.023	-9.54	-9.59
-2.00	.060	-9.03	-9.17	-9.20	-.03	-1.50	.051	-9.41	-9.47
-1.50	.054	-8.84	-8.92	-9.04	-.01	-1.00	.101	-9.26	-9.34
-1.00	.134	-8.63	-8.80	-8.76	.04	-.50	.125	-9.07	-9.15
-.50	.142	-8.41	-8.59	-8.54	.05	.00	.146	-8.85	-9.05
.00	.272	-8.14	-8.32	-8.26	.05				

SAMPLE 120 PLATE 1 15.0 DEG. CENT.									
AREA SHEARED, ONE SIDE 10.18 CM. SQ.									
SAMPLE THICK, ONE SIDE .0404 IN.									
LOG	PCT	LOG	LOG	LOG	LOG TAN	LOG	PCT	LOG	LOG TAN
1/4	STRAIN	LOG	LOG	LOG	DELTA	1/4	STRAIN	LOG	DELTA
-2.00	.023	-9.54	-9.59	-9.67	-.29	-1.50	.051	-9.41	-9.47
-1.00	.101	-9.26	-9.34	-9.52	-.14	-.50	.125	-9.07	-9.31
.00	.146	-8.85	-9.05	-9.05	-.09				

SAMPLE 120 PLATE 1 5.0 DEG. CENT.									
AREA SHEARED, ONE SIDE 10.18 CM. SQ.									
SAMPLE THICK, ONE SIDE .0404 IN.									
LOG	PCT	LOG	LOG	LOG	LOG TAN	LOG	PCT	LOG	LOG TAN
1/4	STRAIN	LOG	LOG	LOG	DELTA	1/4	STRAIN	LOG	DELTA
-2.50	.004	-9.94	-10.01	-10.52	-.51	-2.00	.015	-9.89	-10.42
-1.50	.035	-9.43	-9.45	-10.34	-.49	-1.00	.032	-9.43	-10.34
-1.00	.062	-9.73	-9.74	-10.19	-.44				

SAMPLE 120 PLATE 4 25.0 DEG. CENT.									
AREA SHEARED, ONE SIDE 9.95 CM. SQ.									
SAMPLE THICK, ONE SIDE .0394 IN.									
LOG	PCT	LOG	LOG	LOG	LOG TAN	LOG	PCT	LOG	LOG TAN
1/4	STRAIN	LOG	LOG	LOG	DELTA	1/4	STRAIN	LOG	DELTA
-2.50	.014	-9.22	-9.33	-9.44	-.11	-2.00	.041	-9.03	-9.21
-1.50	.133	-8.80	-8.95	-8.96	-.02	-1.00	.139	-8.97	-9.19
-1.00	.165	-8.57	-8.72	-8.71	.01	-.50	.131	-9.00	-9.23
-.50	.144	-8.31	-8.47	-8.45	.02	.00	.237	-8.73	-8.91
.00	.272	-8.03	-8.21	-8.15	.06				

SAMPLE 120 PLATE 4 15.0 DEG. CENT.									
AREA SHEARED, ONE SIDE 9.95 CM. SQ.									
SAMPLE THICK, ONE SIDE .0394 IN.									
LOG	PCT	LOG	LOG	LOG	LOG TAN	LOG	PCT	LOG	LOG TAN
1/4	STRAIN	LOG	LOG	LOG	DELTA	1/4	STRAIN	LOG	DELTA
-2.00	.031	-9.44	-9.51	-9.74	-.27	-1.50	.080	-9.31	-9.59
-1.00	.128	-9.15	-9.24	-9.34	-.14	-.50	.139	-8.97	-9.19
.00	.237	-8.73	-8.91	-8.91	-.05				

SAMPLE 120 PLATE 4 5.0 DEG. CENT.									
AREA SHEARED, ONE SIDE 9.95 CM. SQ.									
SAMPLE THICK, ONE SIDE .0394 IN.									
LOG	PCT	LOG	LOG	LOG	LOG TAN	LOG	PCT	LOG	LOG TAN
1/4	STRAIN	LOG	LOG	LOG	DELTA	1/4	STRAIN	LOG	DELTA
-2.50	.004	-9.97	-9.99	-10.44	-.41	-2.00	.015	-9.93	-10.45
-1.50	.035	-9.47	-9.47	-10.34	-.47	-1.00	.073	-9.44	-10.17
-1.00	.073	-9.44	-9.44	-10.17	-.47	-.50	.064	-9.56	-10.31
.00	.113	-9.44	-9.44	-9.41	-.33				

SAMPLE 121 PLATE 2 25.0 DEG. CENT.

AREA SHEARED, ONE SIDE 9.62 CM. SQ.
SAMPLE THICK, ONE SIDE .0403 IN.

LOG PCT LOG LOG LOG LOG TAN
1/4 STRAIN 1.01 JREAL JLOSS DELTA

-2.50 .014 -9.25 -9.35 -9.48 -.13
-2.00 .040 -9.07 -9.18 -9.28 -.10
-1.50 .069 -8.87 -8.99 -9.04 -.05
-1.00 .236 -8.60 -8.76 -8.74 .02
-.50 .253 -8.33 -8.49 -8.47 .02
-.50 .238 -8.36 -8.51 -8.50 .01
.00 .405 -8.07 -8.27 -8.19 .07

SAMPLE 121 PLATE 2 15.0 DEG. CENT.

AREA SHEARED, ONE SIDE 9.62 CM. SQ.
SAMPLE THICK, ONE SIDE .0403 IN.

LOG PCT LOG LOG LOG LOG TAN
1/4 STRAIN 1.01 JREAL JLOSS DELTA

-2.00 .014 -9.55 -9.59 -9.93 -.34
-1.50 .061 -9.42 -9.47 -9.74 -.27
-1.00 .143 -9.25 -9.33 -9.52 -.14
-.50 .093 -9.08 -9.17 -9.32 -.14
.00 .150 -8.87 -8.94 -9.07 -.09

SAMPLE 121 PLATE 2 5.0 DEG. CENT.

AREA SHEARED, ONE SIDE 9.62 CM. SQ.
SAMPLE THICK, ONE SIDE .0403 IN.

LOG PCT LOG LOG LOG LOG TAN
1/4 STRAIN 1.01 JREAL JLOSS DELTA

-2.50 .005 -9.95 -9.97 -10.50 -.53
-2.00 .012 -9.84 -9.90 -10.43 -.53
-1.50 .033 -9.83 -9.84 -10.34 -.54
-1.00 .057 -9.76 -9.77 -10.24 -.44
-.50 .034 -9.73 -9.77 -10.13 -.34
-.50 .044 -9.67 -9.71 -10.11 -.40
.00 .054 -9.55 -9.51 -9.89 -.24

SAMPLE 121 PLATE 3 25.0 DEG. CENT.

AREA SHEARED, ONE SIDE 10.12 CM. SQ.
SAMPLE THICK, ONE SIDE .0402 IN.

LOG PCT LOG LOG LOG LOG TAN
1/4 STRAIN 1.01 JREAL JLOSS DELTA

-2.50 .014 -9.25 -9.34 -9.48 -.14
-2.00 .050 -9.04 -9.16 -9.22 -.05
-1.50 .068 -8.85 -8.98 -9.02 -.04
-1.00 .136 -8.63 -8.78 -8.78 -.00
-.50 .107 -8.39 -8.55 -8.53 .02
.00 .143 -8.13 -8.30 -8.27 .03

SAMPLE 121 PLATE 3 15.0 DEG. CENT.

AREA SHEARED, ONE SIDE 10.12 CM. SQ.
SAMPLE THICK, ONE SIDE .0402 IN.

LOG PCT LOG LOG LOG LOG TAN
1/4 STRAIN 1.01 JREAL JLOSS DELTA

-2.00 .022 -9.56 -9.61 -9.93 -.32
-1.50 .051 -9.43 -9.48 -9.74 -.29
-1.00 .101 -9.30 -9.36 -9.59 -.22
-.50 .132 -9.10 -9.14 -9.36 -.14
.00 .214 -8.89 -9.00 -9.09 -.09

SAMPLE 121 PLATE 3 5.0 DEG. CENT.

AREA SHEARED, ONE SIDE 10.12 CM. SQ.
SAMPLE THICK, ONE SIDE .0402 IN.

LOG PCT LOG LOG LOG LOG TAN
1/4 STRAIN 1.01 JREAL JLOSS DELTA

-2.50 .005 -9.94 -9.95 -10.50 -.46
-2.00 .011 -9.83 -9.81 -10.44 -.41
-1.50 .031 -9.84 -9.84 -10.34 -.51
-1.00 .055 -9.75 -9.77 -10.24 -.46
-.50 .031 -9.66 -9.70 -10.06 -.36
.00 .054 -9.53 -9.57 -9.89 -.29

SAMPLE 122 PLATE 1 25.0 DEG. CENT.											
AREA SHEARED, ONE SIDE 17.40 CM. SQ.					15.0 DEG. CENT.						
SAMPLE THICK, ONE SIDE .0203 IN.					SAMPLE THICK, ONE SIDE .0203 IN.						
LOG	PCT	LOG	LOG	LOG TAN	LOG	PCT	LOG	LOG	LOG TAN		
1/W	STRAIN	1/W	JREAL	JLOSS	DELTA	1/W	STRAIN	1/W	JREAL	JLOSS	DELTA
-2.50	.012	-8.54	-8.76	-8.63	.14	-2.00	.020	-8.92	-9.05	-9.09	-.04
-2.00	.057	-8.23	-8.57	-8.28	.29	-1.50	.072	-8.68	-8.85	-8.81	.04
-1.50	.225	-8.21	-8.53	-8.27	.27	-1.00	.038	-8.71	-8.84	-8.83	.06
-1.00	.367	-7.85	-8.29	-7.88	.60	-1.00	.167	-8.40	-8.53	-8.59	.14
-1.00	1.276	-7.46	-8.03	-7.47	.56	-1.00	.110	-8.40	-8.53	-8.59	.14
-1.50	1.444	-7.04	-7.70	-7.05	.66	-.50	.234	-8.10	-8.40	-8.17	.23
.00	2.276	-6.62	-7.44	-6.63	.81	.00	.291	-7.75	-8.12	-7.80	.32
.00	1.309	-6.60	-7.38	-6.61	.77	.00	.564	-7.73	-8.15	-7.77	.38

SAMPLE 122 PLATE 2 25.0 DEG. CENT.											
AREA SHEARED, ONE SIDE 18.77 CM. SQ.											
SAMPLE THICK, ONE SIDE .0201 IN.											
LOG	PCT	LOG	LOG	LOG	LOG	LOG	LOG	LOG	LOG	LOG	LOG
1/W	STRAIN	1/W	JREAL	JLOSS	DELTA	1/W	STRAIN	1/W	JREAL	JLOSS	DELTA
-2.450	.015	-8.57	-8.81	-8.66	.15	-2.00	.021	-9.01	-9.21	-9.12	.08
-2.00	.070	-8.23	-8.59	-8.28	.31	-1.50	.099	-8.74	-8.97	-8.83	.15
-1.50	.237	-7.83	-8.27	-7.86	.42	-1.50	.062	-8.79	-9.04	-8.68	.16
-1.50	.305	-7.88	-8.24	-7.87	.41	-1.00	.206	-8.43	-8.72	-8.49	.23
-1.00	1.145	-7.44	-8.01	-7.46	.55	-1.00	.294	-8.42	-8.71	-8.49	.22
-1.00	.309	-7.46	-8.04	-7.48	.56	-1.00	.060	-8.44	-8.69	-8.64	.25
-1.50	.476	-7.05	-7.77	-7.06	.71	-1.50	.168	-8.15	-8.60	-8.18	.42
-1.50	1.062	-7.04	-7.81	-7.04	.77	-1.50	.211	-8.15	-8.55	-8.18	.37
.00	3.671	-6.58	-7.86	-6.59	.85	.00	.279	-7.74	-8.26	-7.80	.46
						.00	.074	-8.37	-7.91	-7.91	.46

SAMPLE 122 PLATE 2 15.0 DEG. CENT.									
AREA SHEARED, ONE SIDE 17.77 CM. SQ.									
SAMPLE THICK, ONE SIDE .0201 IN.									
LOG 1/W	PCT STRAIN	LOG 1/W	LOG JREAL	LOG JLOSS	LOG DELTA	LOG 1/W	PCT STRAIN	LOG JREAL	LOG JLOSS
-2.00	.021	-9.01	-9.21	-9.12	.04	-2.00	.021	-9.01	-9.12
-1.50	.094	-8.74	-8.97	-8.83	.15	-1.50	.094	-8.74	-8.83
-1.50	.062	-8.79	-9.04	-8.88	.16	-1.50	.062	-8.79	-8.88
-1.00	.206	-8.63	-8.72	-8.69	.23	-1.00	.206	-8.63	-8.69
-1.00	.294	-8.42	-8.71	-8.69	.22	-1.00	.294	-8.42	-8.69
-1.00	.060	-8.54	-8.84	-8.64	.25	-1.00	.060	-8.54	-8.64
-1.50	.168	-8.15	-8.60	-8.18	.42	-1.50	.168	-8.15	-8.18
-1.50	.211	-8.15	-8.55	-8.18	.37	-1.50	.211	-8.15	-8.55
.00	.274	-7.74	-8.26	-7.80	.44	.00	.274	-7.74	-7.80
.00	.109	-7.84	-8.37	-7.91	.46	.00	.109	-7.84	-7.91

SAMPLE 122 PLATE 2 25.0 DEG. CENT.											
AREA SHEARED, ONE SIDE 14.77 CM. SQ.											
SAMPLE THICK, ONE SIDE .0201 IN.											
LOG	PCT	LOG	LOG	LOG	LOG	LOG	LOG	LOG	LOG		
1/W	STRAIN	1/W	JREAL	JLOSS	DELTA	1/W	STRAIN	1/W	STRAIN		
-2.50	.015	-8.57	-9.81	-8.66	.15	-2.50	.015	-8.57	-9.81	-8.66	.15
-2.00	.070	-8.23	-8.59	-8.28	.31	-2.00	.070	-8.23	-8.59	-8.28	.31
-1.50	.237	-7.83	-8.27	-7.86	.42	-1.50	.237	-7.83	-8.27	-7.86	.42
-1.50	.305	-7.84	-8.24	-7.87	.41	-1.50	.305	-7.84	-8.24	-7.87	.41
-1.00	1.145	-7.44	-8.01	-7.46	.55	-1.00	1.145	-7.44	-8.01	-7.46	.55
-1.00	.304	-7.46	-8.04	-7.48	.56	-1.00	.304	-7.46	-8.04	-7.48	.56
-1.50	.476	-7.05	-7.77	-7.06	.71	-1.50	.476	-7.05	-7.77	-7.06	.71
-1.50	1.062	-6.04	-7.81	-6.04	.77	-1.50	1.062	-6.04	-7.81	-6.04	.77
.00	3.471	-6.54	-7.84	-6.59	.95	.00	3.471	-6.54	-7.84	-6.59	.95

SAMPLE 124 PLATE 1										25.0 DEG. CENT.										SAMPLE 124 PLATE 1										15.0 DEG. CENT.										SAMPLE 124 PLATE 1										5.0 DEG. CENT.									
AREA SHEARED, ONE SIDE					9.38 CM. SQ.					AREA SHEARED, ONE SIDE					9.38 CM. SQ.					AREA SHEARED, ONE SIDE					9.38 CM. SQ.					AREA SHEARED, ONE SIDE					9.38 CM. SQ.					AREA SHEARED, ONE SIDE					9.38 CM. SQ.														
SAMPLE THICK, ONE SIDE					.0402 IN.					SAMPLE THICK, ONE SIDE					.0402 IN.					SAMPLE THICK, ONE SIDE					.0402 IN.					SAMPLE THICK, ONE SIDE					.0402 IN.					SAMPLE THICK, ONE SIDE					.0402 IN.														
LOG	PCT	LOG	LOG	LOG TAN	LOG	PCT	LOG	LOG	LOG TAN	LOG	PCT	LOG	LOG	LOG TAN	LOG	PCT	LOG	LOG	LOG TAN	LOG	PCT	LOG	LOG	LOG TAN	LOG	PCT	LOG	LOG	LOG TAN	LOG	PCT	LOG	LOG	LOG TAN																									
1/2	STRAIN	IJ	1	DELTA	JG	1	STRAIN	IJ	1	DELTA	JG	1	STRAIN	IJ	1	DELTA	JG	1	STRAIN	IJ	1	DELTA	JG	1	STRAIN	IJ	1	DELTA	JG	1	STRAIN	IJ	1	DELTA	JG																								
2.00	.038	-9.00	-9.23	-9.09	.15	-2.00	.009	-9.57	-9.55	-9.85	-2.00	.008	-9.92	-10.04	-5.2	-2.00	.016	-9.69	-9.30	-10.49	-5.4	-1.50	.024	-9.45	-9.37	-10.30	-5.3	-1.50	.011	-9.84	-9.32	-10.30	-5.3																										
2.00	.019	-9.01	-9.26	-9.09	.17	-2.00	.017	-9.56	-9.53	-9.85	-2.00	.016	-9.69	-10.49	-5.4	-1.50	.024	-9.45	-9.37	-10.30	-5.3	-1.50	.011	-9.84	-9.32	-10.30	-5.3	-1.50	.011	-9.84	-9.32	-10.30	-5.3																										
1.50	.048	-8.71	-9.08	-8.75	.33	-1.50	.012	-9.43	-9.53	-9.64	-1.50	.024	-9.45	-9.37	-10.30	-5.3	-1.50	.024	-9.45	-9.37	-10.30	-5.3	-1.50	.011	-9.84	-9.32	-10.30	-5.3	-1.50	.011	-9.84	-9.32	-10.30	-5.3																									
1.50	.109	-8.71	-9.03	-8.77	.27	-1.50	.031	-9.40	-9.50	-9.64	-1.50	.031	-9.40	-9.50	-9.64	-1.50	.031	-9.40	-9.50	-9.64	-1.50	.031	-9.40	-9.50	-9.64	-1.50	.031	-9.40	-9.50	-9.64	-1.50	.031	-9.40	-9.50	-9.64																								
1.00	.378	-8.33	-8.79	-8.36	.43	-1.00	.056	-9.19	-9.33	-9.34	-1.00	.056	-9.19	-9.33	-9.34	-1.00	.056	-9.19	-9.33	-9.34	-1.00	.056	-9.19	-9.33	-9.34	-1.00	.056	-9.19	-9.33	-9.34	-1.00	.056	-9.19	-9.33	-9.34																								
1.00	.484	-7.92	-8.42	-7.94	.44	-1.00	.031	-9.20	-9.35	-9.36	-1.00	.031	-9.20	-9.35	-9.36	-1.00	.031	-9.20	-9.35	-9.36	-1.00	.031	-9.20	-9.35	-9.36	-1.00	.031	-9.20	-9.35	-9.36	-1.00	.031	-9.20	-9.35	-9.36																								
.50	.702	-7.49	-8.17	-7.50	.67	-.50	.175	-8.92	-9.12	-9.02	.10	.074	-9.57	-9.63	-9.90	-5.27	-.50	.175	-8.92	-9.12	-9.02	.10	.074	-9.57	-9.63	-9.90	-5.27	-.50	.175	-8.92	-9.12	-9.02	.10	.074	-9.57	-9.63	-9.90																						
.00	.00	.00	.00	.00	.25	.00	.213	-8.60	-8.91	-8.66	.25	.074	-9.57	-9.63	-9.90	-5.27	.00	.213	-8.60	-8.91	-8.66	.25	.074	-9.57	-9.63	-9.90	-5.27	.00	.213	-8.60	-8.91	-8.66	.25	.074	-9.57	-9.63	-9.90																						

[illegible]

SAMPLE 124 PLATE 3 15.0 DEG. CENT.									
AREA SHEARED, ONE SIDE 13.424 CM. SQ.									
SAMPLE THICK, ONE SIDE .0399 IN.									
LOG	PCT	LOG	LOG	LOG	LOG	LOG	LOG	LOG	LOG
1/W	STRAIN	1.01	JZEL	JZEL	JLOSS	DELTA	DELTA	DELTA	DELTA
2.00	.013	-9.52	-9.59	-9.61	-9.81	-22			
2.00	.013	-9.54	-9.61	-9.61	-9.82	-21			
1.50	.018	-9.39	-9.49	-9.49	-9.61	-11			
1.50	.037	-9.39	-9.48	-9.48	-9.61	-13			
1.00	.075	-9.16	-9.31	-9.31	-9.31	.00			
.750	.100	-8.88	-9.10	-9.10	-8.98	.12			
.750	.050	-8.89	-9.10	-9.10	-8.99	.10			
.500	.105	-8.57	-8.86	-8.86	-8.63	.23			

SAMPLE 124 PLATE 1 25.0 DEG. CENT.									
AREA SHEARED, ONE SIDE		9.38 CM. SQ.							
SAMPLE THICK, ONE SIDE		.0402 IN.							
LOG	PCT	LOG	LOG	LOG	LOG	LOG	LOG	LOG	LOG
1/W	STRAIN	1/W	JREAL	JLOSS	DELTA				
2.00	.034	-8.93	-9.13	-9.03	.10				
2.00	.065	-8.95	-9.15	-9.06	.09				
1.50	.143	-8.72	-9.02	-8.78	.25				
1.50	.090	-8.74	-9.04	-8.80	.24				
1.00	.166	-8.37	-8.78	-8.41	.37				
1.00	.306	-8.36	-8.80	-8.39	.41				
2.00	.013	-8.94	-9.27	-9.05	.22				
2.00	.028	-8.96	-9.25	-9.03	.22				
1.50	.065	-8.68	-9.07	-8.72	.35				
1.00	.221	-8.31	-8.77	-8.34	.43				
1.00	.089	-8.31	-8.79	-8.35	.44				
.50	.266	-7.88	-8.42	-7.90	.52				
.00	.745	-7.43	-8.02	-7.45	.57				

[illegible]

SAMPLE 126 PLATE 3 25.0 DEG. CENT.

AREA SHEARED, ONE SIDE SAMPLE THICK, ONE SIDE					
9.37 CM. SQ. .0399 IN.					
LOG 1/W	PCT STRAIN	LOG IJ*1	LOG JREAL	LOG JLOSS	LOG TAN DELTA
-2.00	.021	-9.38	-9.44	-9.68	-.24
-2.00	.043	-9.36	-9.42	-9.67	-.25
-1.50	.085	-9.22	-9.29	-9.50	-.22
-1.50	.043	-9.22	-9.29	-9.50	-.22
-1.00	.088	-9.07	-9.15	-9.32	-.17
-1.00	.044	-9.06	-9.14	-9.30	-.15
-.50	.148	-8.86	-8.94	-9.10	-.16
-.50	.318	-8.82	-8.93	-9.03	-.11
.00	.263	-8.60	-8.74	-8.76	-.03
.00	.412	-8.59	-8.73	-8.74	-.01
.00	.408	-8.58	-8.73	-8.73	.00

SAMPLE 126 PLATE 3 15.0 DEG. CENT.

AREA SHEARED, ONE SIDE SAMPLE THICK, ONE SIDE					
9.37 CM. SQ. .0399 IN.					
LOG 1/W	PCT STRAIN	LOG IJ*1	LOG JREAL	LOG JLOSS	LOG TAN DELTA
-2.00	.010	-9.72	-9.75	-10.16	-.40
-2.00	.020	-9.72	-9.74	-10.21	-.47
-1.50	.028	-9.63	-9.66	-10.07	-.41
-1.50	.058	-9.62	-9.64	-10.09	-.45
-1.00	.052	-9.52	-9.56	-9.91	-.35
-1.00	.107	-9.50	-9.54	-9.92	-.39
-.50	.029	-9.42	-9.47	-9.77	-.30
-.50	.063	-9.38	-9.43	-9.75	-.32
-.50	.114	-9.38	-9.42	-9.76	-.34
.00	.163	-9.22	-9.29	-9.53	-.24
.00	.077	-9.24	-9.31	-9.53	-.22

SAMPLE 127 PLATE 2 25.0 DEG. CENT.

AREA SHEARED, ONE SIDE SAMPLE THICK, ONE SIDE					
9.24 CM. SQ. .0403 IN.					
LOG 1/W	PCT STRAIN	LOG IJ*1	LOG JREAL	LOG JLOSS	LOG TAN DELTA
-2.00	.019	-9.61	-9.67	-9.90	-.23
-2.00	.026	-9.58	-9.64	-9.89	-.24
-1.50	.065	-9.42	-9.50	-9.68	-.18
-1.50	.032	-9.44	-9.51	-9.70	-.19
-1.00	.046	-9.26	-9.35	-9.49	-.14
-1.00	.096	-9.24	-9.33	-9.46	-.13
-.50	.208	-9.01	-9.12	-9.21	-.09
-.50	.102	-9.02	-9.13	-9.22	-.09
.00	.075	-8.85	-8.95	-9.08	-.13
.00	.164	-8.81	-8.91	-9.03	-.12

SAMPLE 127 PLATE 2 15.0 DEG. CENT.

AREA SHEARED, ONE SIDE SAMPLE THICK, ONE SIDE					
9.24 CM. SQ. .0403 IN.					
LOG 1/W	PCT STRAIN	LOG IJ*1	LOG JREAL	LOG JLOSS	LOG TAN DELTA
-1.50	.042	-9.77	-9.80	-10.17	-.37
-1.50	.021	-9.77	-9.80	-10.16	-.35
-2.00	.014	-9.89	-9.92	-10.33	-.41
-1.00	.028	-9.65	-9.70	-10.01	-.31
-1.00	.058	-9.65	-9.69	-10.02	-.33
-.50	.043	-9.51	-9.56	-9.83	-.28
-.50	.089	-9.49	-9.55	-9.83	-.28
.00	.131	-9.33	-9.40	-9.62	-.22
.00	.062	-9.35	-9.41	-9.65	-.24

SAMPLE 128 PLATE 1 25.0 DEG. CENT.

AREA SHEARED, ONE SIDE 9.08 CM. SQ. SAMPLE THICK, ONE SIDE .0405 IN.					
LOG 1/W	PCT STRAIN	LOG IJ*1	LOG JREAL	LOG JLOSS	LOG TAN DELTA
-2.00	.044	-9.25	-9.31	-9.56	-.25
-2.00	.023	-9.25	-9.31	-9.58	-.27
-1.50	.071	-9.09	-9.15	-9.38	-.23
-1.50	.137	-9.08	-9.15	-9.36	-.21
-1.00	.194	-8.91	-9.00	-9.17	-.17
-1.00	.103	-8.91	-9.00	-9.16	-.16
-.50	.152	-8.73	-8.81	-8.99	-.18
-.50	.321	-8.71	-8.79	-8.97	-.17
.00	.117	-8.56	-8.64	-8.82	-.14
.00	.240	-8.53	-8.63	-8.77	-.14

SAMPLE 128 PLATE 1 15.0 DEG. CENT.

AREA SHEARED, ONE SIDE 9.08 CM. SQ. SAMPLE THICK, ONE SIDE .0405 IN.					
LOG 1/W	PCT STRAIN	LOG IJ*1	LOG JREAL	LOG JLOSS	LOG TAN DELTA
-2.00	.026	-9.60	-9.63	-10.09	-.47
-2.00	.016	-9.62	-9.64	-10.08	-.44
-1.50	.039	-9.50	-9.53	-9.95	-.42
-1.50	.079	-9.50	-9.52	-9.96	-.44
-1.00	.055	-9.38	-9.42	-9.78	-.36
-1.00	.056	-9.37	-9.41	-9.76	-.36
-.50	.098	-9.24	-9.28	-9.63	-.35
-.50	.162	-9.24	-9.28	-9.62	-.34
.00	.140	-9.07	-9.12	-9.40	-.27
.00	.070	-9.08	-9.14	-9.40	-.26

SAMPLE 129 PLATE 4 25.0 DEG. CENT.

AREA SHEARED, ONE SIDE 8.92 CM. SQ. SAMPLE THICK, ONE SIDE .0358 IN.					
LOG 1/W	PCT STRAIN	LOG IJ*1	LOG JREAL	LOG JLOSS	LOG TAN DELTA
-2.00	.070	-9.17	-9.24	-9.46	-.22
-2.00	.033	-9.20	-9.27	-9.49	-.22
-1.50	.082	-9.04	-9.11	-9.31	-.20
-1.50	.041	-9.04	-9.11	-9.32	-.20
-1.00	.102	-8.87	-8.95	-9.12	-.17
-1.00	.190	-8.83	-8.92	-9.07	-.15
-.50	.337	-8.62	-8.71	-8.88	-.17
-.50	.159	-8.64	-8.72	-8.87	-.15
.00	.308	-8.44	-8.54	-8.66	-.12
.00	.145	-8.45	-8.55	-8.68	-.13

SAMPLE 129 PLATE 4 15.0 DEG. CENT.

AREA SHEARED, ONE SIDE 8.92 CM. SQ. SAMPLE THICK, ONE SIDE .0358 IN.					
LOG 1/W	PCT STRAIN	LOG IJ*1	LOG JREAL	LOG JLOSS	LOG TAN DELTA
-2.00	.014	-9.58	-9.61	-10.04	-.43
-2.00	.028	-9.58	-9.60	-10.06	-.46
-1.50	.031	-9.47	-9.51	-9.91	-.41
-1.50	.063	-9.47	-9.50	-9.91	-.41
-1.00	.059	-9.36	-9.40	-9.73	-.33
-1.00	.062	-9.37	-9.41	-9.79	-.38
-.50	.082	-9.19	-9.24	-9.56	-.32
-.50	.163	-9.19	-9.24	-9.56	-.32
.00	.241	-9.02	-9.08	-9.33	-.25
.00	.117	-9.04	-9.09	-9.36	-.27

SAMPLE 130 PLATE 3 25.0 DEG. CENT.									
AREA SHEARED, ONE SIDE 8.96 CM. SQ.									
SAMPLE THICK, ONE SIDE .0402 IN.									
LOG	PCT	LOG	LOG	LOG	LOG	LOG	LOG	LOG	LOG
1/4	STRAIN	IJ-I	JREAL	JLOSS	DELTA	LOG	LOG	LOG	LOG

-2.00	.013	-9.11	-9.32	-9.21	.11	-2.00	.013	-9.58	-9.63
-2.00	.027	-9.09	-9.31	-9.19	.13	-2.00	.025	-9.57	-9.63
-1.50	.070	-9.77	-9.08	-9.83	.25	-1.50	.032	-9.43	-9.52
-1.50	.141	-9.76	-9.08	-9.82	.27	-1.50	.064	-9.42	-9.51
-1.00	.077	-9.41	-9.85	-9.44	.41	-1.00	.048	-9.22	-9.37
-1.00	.152	-9.41	-9.84	-9.44	.40	-1.00	.093	-9.22	-9.38
-1.50	.534	-7.98	-9.69	-9.00	.68				
-1.50	.263	-9.00	-9.51	-9.03	.49				
-1.50	.134	-7.99	-9.50	-9.01	.49				
.00	.357	-7.57	-9.20	-7.58	.62				
.00	.174	-7.57	-9.25	-7.58	.67				
.00	.175	-7.55	-9.22	-7.56	.66				

SAMPLE 131 PLATE 2 25.0 DEG. CENT.									
AREA SHEARED, ONE SIDE 10.58 CM. SQ.									
SAMPLE THICK, ONE SIDE .0402 IN.									
LOG	PCT	LOG	LOG	LOG	LOG	LOG	LOG	LOG	LOG
1/4	STRAIN	IJ-I	JREAL	JLOSS	DELTA	LOG	LOG	LOG	LOG

-2.00	.020	-9.39	-9.19	-9.10	.10	-2.00	.004	-9.45	-9.52
-2.00	.040	-9.39	-9.22	-9.08	.14	-2.00	.016	-9.48	-9.54
-1.50	.046	-9.67	-9.38	-9.74	.24	-1.50	.029	-9.31	-9.40
-1.50	.179	-9.65	-9.37	-9.71	.26	-1.50	.059	-9.31	-9.40
-1.00	.100	-9.32	-9.73	-9.35	.34	-1.00	.068	-9.10	-9.25
-1.00	.199	-9.31	-9.75	-9.34	.41	-1.00	.139	-9.09	-9.24
-1.50	.574	-7.89	-9.44	-7.90	.54	-1.00	.127	-9.82	-9.01
-1.50	.274	-7.90	-9.39	-7.93	.46	-1.50	.047	-9.81	-9.39
.00	.757	-7.46	-9.05	-7.47	.57	.00	.143	-9.47	-9.40
.00	.374	-7.46	-9.01	-7.47	.54	.00	.069	-9.51	-9.40
						.00	.142	-9.49	-9.40

SAMPLE 131 PLATE 2 5.0 DEG. CENT.									
AREA SHEARED, ONE SIDE 10.58 CM. SQ.									
SAMPLE THICK, ONE SIDE .0402 IN.									
LOG	PCT	LOG	LOG	LOG	LOG	LOG	LOG	LOG	LOG
1/4	STRAIN	IJ-I	JREAL	JLOSS	DELTA	LOG	LOG	LOG	LOG

-2.00	.004	-9.42	-9.43	-9.43	.40	-2.00	.004	-9.42	-9.43
-2.00	.014	-9.42	-9.43	-9.43	.35	-2.00	.014	-9.42	-9.43
-1.50	.018	-9.74	-9.74	-9.74	.50	-1.50	.018	-9.74	-9.74
-1.50	.036	-9.75	-9.75	-9.75	.52	-1.50	.036	-9.75	-9.75
-1.00	.034	-9.63	-9.63	-9.63	.43	-1.00	.034	-9.63	-9.63
-1.00	.097	-9.63	-9.63	-9.63	.41	-1.00	.097	-9.63	-9.63
-1.50	.075	-9.47	-9.47	-9.47	.31	-1.50	.075	-9.47	-9.47

SAMPLE 132 PLATE 4 25.0 DEG. CENT.													SAMPLE 132 PLATE 4 15.0 DEG. CENT.													SAMPLE 132 PLATE 4 5.0 DEG. CENT.																																																																																																																																																																																																																																																																																																																																																																																																																																																																																																																																																																																																																																																																																																																																																																																																																																																																																																																																																																																																																																																																										
AREA SHEARED, ONE SIDE SAMPLE THICK, ONE SIDE													AREA SHEARED, ONE SIDE SAMPLE THICK, ONE SIDE													AREA SHEARED, ONE SIDE SAMPLE THICK, ONE SIDE																																																																																																																																																																																																																																																																																																																																																																																																																																																																																																																																																																																																																																																																																																																																																																																																																																																																																																																																																																																																																																																																										
LOG	PCT	LOG	LOG	LOG	LOG	LOG	LOG	LOG	LOG	LOG	LOG	LOG	LOG	PCT	LOG	LOG	LOG	LOG	LOG	LOG	LOG	PCT	LOG	LOG	LOG	LOG	LOG	LOG	LOG	LOG	PCT	LOG	LOG	LOG	LOG	LOG	LOG	LOG	LOG	LOG	LOG	LOG	LOG	LOG	LOG	LOG	LOG	LOG	LOG	LOG	LOG	LOG	LOG	LOG	LOG	LOG	LOG	LOG	LOG	LOG	LOG	LOG	LOG	LOG	LOG	LOG	LOG	LOG	LOG	LOG	LOG	LOG	LOG	LOG	LOG	LOG	LOG	LOG	LOG	LOG	LOG	LOG	LOG	LOG	LOG	LOG	LOG	LOG	LOG	LOG	LOG	LOG	LOG	LOG	LOG	LOG	LOG	LOG	LOG	LOG	LOG	LOG	LOG	LOG	LOG	LOG	LOG	LOG	LOG	LOG	LOG	LOG	LOG	LOG	LOG	LOG	LOG	LOG	LOG	LOG	LOG	LOG	LOG	LOG	LOG	LOG	LOG	LOG	LOG	LOG	LOG	LOG	LOG	LOG	LOG	LOG	LOG	LOG	LOG	LOG	LOG	LOG	LOG	LOG	LOG	LOG	LOG	LOG	LOG	LOG	LOG	LOG	LOG	LOG	LOG	LOG	LOG	LOG	LOG	LOG	LOG	LOG	LOG	LOG	LOG	LOG	LOG	LOG	LOG	LOG	LOG	LOG	LOG	LOG	LOG	LOG	LOG	LOG	LOG	LOG	LOG	LOG	LOG	LOG	LOG	LOG	LOG	LOG	LOG	LOG	LOG	LOG	LOG	LOG	LOG	LOG	LOG	LOG	LOG	LOG	LOG	LOG	LOG	LOG	LOG	LOG	LOG	LOG	LOG	LOG	LOG	LOG	LOG	LOG	LOG	LOG	LOG	LOG	LOG	LOG	LOG	LOG	LOG	LOG	LOG	LOG	LOG	LOG	LOG	LOG	LOG	LOG	LOG	LOG	LOG	LOG	LOG	LOG	LOG	LOG	LOG	LOG	LOG	LOG	LOG	LOG	LOG	LOG	LOG	LOG	LOG	LOG	LOG	LOG	LOG	LOG	LOG	LOG	LOG	LOG	LOG	LOG	LOG	LOG	LOG	LOG	LOG	LOG	LOG	LOG	LOG	LOG	LOG	LOG	LOG	LOG	LOG	LOG	LOG	LOG	LOG	LOG	LOG	LOG	LOG	LOG	LOG	LOG	LOG	LOG	LOG	LOG	LOG	LOG	LOG	LOG	LOG	LOG	LOG	LOG	LOG	LOG	LOG	LOG	LOG	LOG	LOG	LOG	LOG	LOG	LOG	LOG	LOG	LOG	LOG	LOG	LOG	LOG	LOG	LOG	LOG	LOG	LOG	LOG	LOG	LOG	LOG	LOG	LOG	LOG	LOG	LOG	LOG	LOG	LOG	LOG	LOG	LOG	LOG	LOG	LOG	LOG	LOG	LOG	LOG	LOG	LOG	LOG	LOG	LOG	LOG	LOG	LOG	LOG	LOG	LOG	LOG	LOG	LOG	LOG	LOG	LOG	LOG	LOG	LOG	LOG	LOG	LOG	LOG	LOG	LOG	LOG	LOG	LOG	LOG	LOG	LOG	LOG	LOG	LOG	LOG	LOG	LOG	LOG	LOG	LOG	LOG	LOG	LOG	LOG	LOG	LOG	LOG	LOG	LOG	LOG	LOG	LOG	LOG	LOG	LOG	LOG	LOG	LOG	LOG	LOG	LOG	LOG	LOG	LOG	LOG	LOG	LOG	LOG	LOG	LOG	LOG	LOG	LOG	LOG	LOG	LOG	LOG	LOG	LOG	LOG	LOG	LOG	LOG	LOG	LOG	LOG	LOG	LOG	LOG	LOG	LOG	LOG	LOG	LOG	LOG	LOG	LOG	LOG	LOG	LOG	LOG	LOG	LOG	LOG	LOG	LOG	LOG	LOG	LOG	LOG	LOG	LOG	LOG	LOG	LOG	LOG	LOG	LOG	LOG	LOG	LOG	LOG	LOG	LOG	LOG	LOG	LOG	LOG	LOG	LOG	LOG	LOG	LOG	LOG	LOG	LOG	LOG	LOG	LOG	LOG	LOG	LOG	LOG	LOG	LOG	LOG	LOG	LOG	LOG	LOG	LOG	LOG	LOG	LOG	LOG	LOG	LOG	LOG	LOG	LOG	LOG	LOG	LOG	LOG	LOG	LOG	LOG	LOG	LOG	LOG	LOG	LOG	LOG	LOG	LOG	LOG	LOG	LOG	LOG	LOG	LOG	LOG	LOG	LOG	LOG	LOG	LOG	LOG	LOG	LOG	LOG	LOG	LOG	LOG	LOG	LOG	LOG	LOG	LOG	LOG	LOG	LOG	LOG	LOG	LOG	LOG	LOG	LOG	LOG	LOG	LOG	LOG	LOG	LOG	LOG	LOG	LOG	LOG	LOG	LOG	LOG	LOG	LOG	LOG	LOG	LOG	LOG	LOG	LOG	LOG	LOG	LOG	LOG	LOG	LOG	LOG	LOG	LOG	LOG	LOG	LOG	LOG	LOG	LOG	LOG	LOG	LOG	LOG	LOG	LOG	LOG	LOG	LOG	LOG	LOG	LOG	LOG	LOG	LOG	LOG	LOG	LOG	LOG	LOG	LOG	LOG	LOG	LOG	LOG	LOG	LOG	LOG	LOG	LOG	LOG	LOG	LOG	LOG	LOG	LOG	LOG	LOG	LOG	LOG	LOG	LOG	LOG	LOG	LOG	LOG	LOG	LOG	LOG	LOG	LOG	LOG	LOG	LOG	LOG	LOG	LOG	LOG	LOG	LOG	LOG	LOG	LOG	LOG	LOG	LOG	LOG	LOG	LOG	LOG	LOG	LOG	LOG	LOG	LOG	LOG	LOG	LOG	LOG	LOG	LOG	LOG	LOG	LOG	LOG	LOG	LOG	LOG	LOG	LOG	LOG	LOG	LOG	LOG	LOG	LOG	LOG	LOG	LOG	LOG	LOG	LOG	LOG	LOG	LOG	LOG	LOG	LOG	LOG	LOG	LOG	LOG	LOG	LOG	LOG	LOG	LOG	LOG	LOG	LOG	LOG	LOG	LOG	LOG	LOG	LOG	LOG	LOG	LOG	LOG	LOG	LOG	LOG	LOG	LOG	LOG	LOG	LOG	LOG	LOG	LOG	LOG	LOG	LOG	LOG	LOG	LOG	LOG	LOG	LOG	LOG	LOG	LOG	LOG	LOG	LOG	LOG	LOG	LOG	LOG	LOG	LOG	LOG	LOG	LOG	LOG	LOG	LOG	LOG	LOG	LOG	LOG	LOG	LOG	LOG	LOG	LOG	LOG	LOG	LOG	LOG	LOG	LOG	LOG	LOG	LOG	LOG	LOG	LOG	LOG	LOG	LOG	LOG	LOG	LOG	LOG	LOG	LOG	LOG	LOG	LOG	LOG	LOG	LOG	LOG	LOG	LOG	LOG	LOG	LOG	LOG	LOG	LOG	LOG	LOG	LOG	LOG	LOG	LOG	LOG	LOG	LOG	LOG	LOG	LOG	LOG	LOG	LOG	LOG	LOG	LOG	LOG	LOG	LOG	LOG	LOG	LOG	LOG	LOG	LOG	LOG	LOG	LOG	LOG	LOG	LOG	LOG	LOG	LOG	LOG	LOG	LOG	LOG	LOG	LOG	LOG	LOG	LOG	LOG	LOG	LOG	LOG	LOG	LOG	LOG	LOG	LOG	LOG	LOG	LOG	LOG	LOG	LOG	LOG	LOG	LOG	LOG	LOG	LOG	LOG	LOG	LOG	LOG	LOG	LOG	LOG	LOG	LOG	LOG	LOG	LOG	LOG	LOG	LOG	LOG	LOG	LOG	LOG	LOG	LOG	LOG	LOG	LOG	LOG	LOG	LOG	LOG	LOG	LOG	LOG	LOG	LOG	LOG	LOG	LOG	LOG	LOG	LOG	LOG	LOG	LOG	LOG	LOG	LOG	LOG	LOG	LOG	LOG	LOG	LOG	LOG	LOG	LOG	LOG	LOG	LOG	LOG	LOG	LOG	LOG	LOG	LOG	LOG	LOG	LOG	LOG	LOG	LOG	LOG	LOG	LOG	LOG	LOG	LOG	LOG	LOG	LOG	LOG	LOG	LOG	LOG	LOG	LOG	LOG	LOG	LOG	LOG	LOG	LOG	LOG	LOG	LOG	LOG	LOG	LOG	LOG	LOG	LOG	LOG	LOG	LOG	LOG	LOG	LOG	LOG	LOG	LOG	LOG	LOG	LOG	LOG	LOG	LOG	LOG	LOG	LOG	LOG	LOG	LOG	LOG	LOG	LOG	LOG	LOG	LOG	LOG	LOG	LOG	LOG	LOG	LOG	LOG	LOG	LOG	LOG	LOG	LOG	LOG	LOG	LOG	LOG	LOG	LOG	LOG	LOG	LOG	LOG	LOG	LOG	LOG	LOG	LOG	LOG	LOG	LOG	LOG	LOG	LOG	LOG	LOG	LOG	LOG	LOG	LOG	LOG	LOG	LOG	LOG	LOG	LOG	LOG	LOG	LOG	LOG	LOG	LOG	LOG	LOG	LOG	LOG	LOG	LOG	LOG	LOG	LOG	LOG	LOG	LOG	LOG	LOG

SAMPLE 230 PLATE 3 25.0 DEG. CENT.									
AREA SHEARED, ONE SIDE 8.96 CM. SQ. .0404 IN.									
SAMPLE THICK, ONE SIDE									
LOG	PCT	LOG	LOG	LOG	LOG	LOG	LOG	LOG	LOG
1/W	STRAIN	IJOI	JREAL	JLOSS	DELTA	DELTA	DELTA	DELTA	DELTA
-2.00	.019	-9.07	-9.32	-9.15	.17				
-2.00	.037	-9.08	-9.31	-9.18	.12				
-2.00	.016	-9.15	-9.41	-9.22	.19				
-2.00	.035	-9.11	-9.36	-9.20	.16				
-1.50	.049	-8.85	-9.17	-8.90	.27				
-1.50	.101	-8.83	-9.14	-8.89	.25				
-1.00	.095	-8.49	-8.90	-8.53	.37				
-1.00	.196	-8.67	-8.94	-8.50	.44				
-1.50	.445	-8.06	-8.59	-8.08	.51				
-1.50	.441	-8.06	-8.50	-8.08	.52				
-1.50	.207	-8.09	-8.54	-8.11	.52				
.00	.436	-7.68	-8.15	-7.70	.44				
.00	.195	-7.72	-8.17	-7.75	.43				

SAMPLE 230 PLATE 3 15.0 DEG. CENT.									
AREA SHEARED, ONE SIDE 8.96 CM. SQ. .0404 IN.									
SAMPLE THICK, ONE SIDE									
LOG	PCT	LOG	LOG	LOG	LOG	LOG	LOG	LOG	LOG
1/W	STRAIN	IJOI	JREAL	JLOSS	DELTA	DELTA	DELTA	DELTA	DELTA
-2.00	.015	-9.60	-9.66	-9.92	-.27				
-2.00	.007	-9.61	-9.68	-9.89	-.21				
-1.50	.035	-9.46	-9.55	-9.69	-.15				
-1.50	.020	-9.46	-9.54	-9.69	-.15				
-1.00	.081	-9.24	-9.34	-9.40	-.02				
-1.00	.043	-9.27	-9.42	-9.42	-.00				
-1.50	.175	-8.95	-9.15	-9.06	.09				
-1.50	.116	-8.95	-9.16	-9.06	.11				
-1.50	.057	-8.97	-9.17	-9.08	.09				
.00	.244	-8.64	-8.94	-8.70	.24				
.00	.120	-8.64	-8.93	-8.71	.22				

SAMPLE 230 PLATE 3 5.0 DEG. CENT.									
AREA SHEARED, ONE SIDE 8.96 CM. SQ. .0404 IN.									
SAMPLE THICK, ONE SIDE									
LOG	PCT	LOG	LOG	LOG	LOG	LOG	LOG	LOG	LOG
1/W	STRAIN	IJOI	JREAL	JLOSS	DELTA	DELTA	DELTA	DELTA	DELTA
-2.00	.014	-9.89	-9.91	-10.49	-.59				
-2.00	.007	-9.94	-9.96	-10.53	-.57				
-1.50	.041	-9.86	-9.88	-10.41	-.53				
-1.50	.021	-9.86	-9.86	-10.34	-.53				
-1.00	.042	-9.73	-9.75	-10.18	-.42				
-1.00	.031	-9.73	-9.75	-10.16	-.40				
-1.50	.064	-9.60	-9.64	-9.97	-.33				
-1.50	.067	-9.61	-9.65	-9.97	-.32				
-1.50	.041	-9.60	-9.65	-9.95	-.29				
-1.50	.039	-9.61	-9.66	-9.96	-.29				
.00	.077	-9.45	-9.53	-9.71	-.19				
.00	.037	-9.46	-9.53	-9.73	-.20				

SAMPLE 231 PLATE 2 25.0 DEG. CENT.									
AREA SHEARED, ONE SIDE 10.58 CM. SQ. .0402 IN.									
SAMPLE THICK, ONE SIDE									
LOG	PCT	LOG	LOG	LOG	LOG	LOG	LOG	LOG	LOG
1/W	STRAIN	IJOI	JREAL	JLOSS	DELTA	DELTA	DELTA	DELTA	DELTA
-2.00	.050	-8.88	-9.13	-8.96	.17				
-2.00	.025	-8.88	-9.14	-8.96	.18				
-1.50	.214	-8.56	-8.90	-8.61	.29				
-1.50	.108	-8.56	-8.90	-8.62	.28				
-1.00	.207	-8.21	-8.54	-8.24	.40				
-1.00	.101	-8.21	-8.63	-8.25	.38				
-1.50	.571	-7.79	-8.24	-7.81	.43				
-1.50	.282	-7.79	-8.30	-7.81	.44				
.00	.373	-7.38	-7.90	-7.40	.49				

SAMPLE 231 PLATE 2 15.0 DEG. CENT.									
AREA SHEARED, ONE SIDE 10.58 CM. SQ. .0402 IN.									
SAMPLE THICK, ONE SIDE									
LOG	PCT	LOG	LOG	LOG	LOG	LOG	LOG	LOG	LOG
1/W	STRAIN	IJOI	JREAL	JLOSS	DELTA	DELTA	DELTA	DELTA	DELTA
-2.00	.019	-9.43	-9.50	-9.71	-.21				
-2.00	.009	-9.44	-9.51	-9.73	-.22				
-1.50	.027	-9.25	-9.35	-9.47	-.12				
-1.50	.055	-9.25	-9.35	-9.47	-.12				
-1.00	.050	-9.01	-9.17	-9.16	.01				
-1.00	.036	-9.04	-9.19	-9.18	.00				
-1.50	.125	-8.73	-8.94	-8.83	.11				
-1.50	.063	-8.73	-8.94	-8.83	.11				
.00	.266	-8.40	-8.74	-8.45	.29				
.00	.132	-8.40	-8.72	-8.46	.27				

SAMPLE 231 PLATE 2 5.0 DEG. CENT.									
AREA SHEARED, ONE SIDE 10.58 CM. SQ. .0402 IN.									
SAMPLE THICK, ONE SIDE									
LOG	PCT	LOG	LOG	LOG	LOG	LOG	LOG	LOG	LOG
1/W	STRAIN	IJOI	JREAL	JLOSS	DELTA	DELTA	DELTA	DELTA	DELTA
-2.00	.019	-9.74	-9.75	-10.34	-.59				
-2.00	.009	-9.76	-9.78	-10.30	-.51				
-1.50	.042	-9.69	-9.71	-10.18	-.47				
-1.50	.021	-9.69	-9.68	-10.11	-.44				
-1.00	.040	-9.55	-9.58	-9.95	-.36				
-1.00	.041	-9.54	-9.58	-9.94	-.36				
-1.50	.082	-9.39	-9.45	-9.71	-.24				
-1.50	.035	-9.41	-9.48	-9.68	-.21				
.00	.110	-9.22	-9.32	-9.44	-.12				
.00	.053	-9.23	-9.34	-9.43	-.09				

SAMPLE 233 PLATE 1 25.0 DEG. CENT.									
AREA SHEARED, ONE SIDE 9.25 CM. SQ.									
SAMPLE THICK, ONE SIDE .0402 IN.									
LOG	PCT	LOG	LOG	LOG	LOG	LOG	LOG	LOG	LOG
1/W	STRAIN	IJ	JREAL	JLOSS	DELTA	1/W	STRAIN	IJ	JREAL
-2.00	.021	-9.29	-9.35	-9.59	-1.24	-2.00	.015	-9.88	-9.89
-2.00	.010	-9.32	-9.38	-9.63	-1.25	-1.50	.042	-9.84	-9.85
-1.50	.073	-9.16	-9.23	-9.46	-1.24	-1.50	.021	-9.82	-9.83
-1.50	.037	-9.16	-9.21	-9.47	-1.26	-1.00	.051	-9.73	-9.74
-1.00	.094	-9.00	-9.08	-9.27	-1.20	-1.00	.031	-9.72	-9.73
-1.00	.058	-8.99	-9.06	-9.26	-1.20	-.50	.100	-9.62	-9.64
-.50	.248	-8.77	-8.86	-9.02	-1.16	-.50	.050	-9.62	-9.64
-.50	.117	-8.80	-8.87	-9.07	-1.20	.00	.047	-9.52	-9.55
.00	.244	-8.59	-8.68	-8.82	-1.14	.00	.054	-9.51	-9.54

SAMPLE 233 PLATE 1 5.0 DEG. CENT.									
AREA SHEARED, ONE SIDE 9.25 CM. SQ.									
SAMPLE THICK, ONE SIDE .0402 IN.									
LOG	PCT	LOG	LOG	LOG	LOG	LOG	LOG	LOG	LOG
1/W	STRAIN	IJ	JREAL	JLOSS	DELTA	1/W	STRAIN	IJ	JREAL
-2.00	.015	-9.88	-9.89	-10.52	-.63	-2.00	.016	-9.91	-9.93
-1.50	.042	-9.84	-9.85	-10.46	-.51	-1.50	.013	-9.95	-9.97
-1.50	.021	-9.82	-9.83	-10.42	-.54	-1.50	.014	-9.91	-9.95
-1.00	.051	-9.73	-9.74	-10.30	-.52	-1.00	.040	-9.81	-9.84
-1.00	.031	-9.72	-9.73	-10.27	-.53	-1.00	.014	-9.84	-9.88
-.50	.100	-9.62	-9.64	-10.12	-.47	-.50	.018	-9.77	-9.81
-.50	.050	-9.62	-9.64	-10.10	-.48	-.50	.030	-9.72	-9.76
.00	.047	-9.52	-9.55	-9.96	-.41	-.50	.046	-9.68	-9.72
.00	.054	-9.51	-9.54	-9.94	-.39	-.50	.057	-9.67	-9.71

SAMPLE 232 PLATE 4 25.0 DEG. CENT.									
AREA SHEARED, ONE SIDE 8.96 CM. SQ.									
SAMPLE THICK, ONE SIDE .0398 IN.									
LOG	PCT	LOG	LOG	LOG	LOG	LOG	LOG	LOG	LOG
1/W	STRAIN	IJ	JREAL	JLOSS	DELTA	1/W	STRAIN	IJ	JREAL
-2.00	.013	-9.23	-9.30	-9.50	-1.20	-2.00	.024	-9.63	-9.66
-2.00	.027	-9.23	-9.31	-9.48	-1.17	-2.00	.012	-9.63	-9.66
-1.50	.043	-9.05	-9.14	-9.29	-1.15	-1.50	.027	-9.48	-9.52
-1.50	.045	-9.04	-9.14	-9.27	-1.13	-1.50	.055	-9.48	-9.53
-1.00	.050	-8.84	-8.95	-9.04	-.09	-1.00	.089	-9.34	-9.40
-1.00	.046	-8.85	-8.97	-9.05	-.09	-1.00	.045	-9.34	-9.40
-.50	.189	-8.60	-8.72	-8.78	-.06	-.50	.182	-9.15	-9.22
-.50	.093	-8.61	-8.73	-8.79	-.06	-.50	.091	-9.15	-9.21
.00	.164	-8.37	-8.51	-8.54	-.04	.00	.231	-8.95	-9.05
.00	.087	-8.38	-8.52	-8.54	-.03	.00	.142	-8.95	-9.05

SAMPLE 232 PLATE 4 15.0 DEG. CENT.									
AREA SHEARED, ONE SIDE 8.96 CM. SQ.									
SAMPLE THICK, ONE SIDE .0398 IN.									
LOG	PCT	LOG	LOG	LOG	LOG	LOG	LOG	LOG	LOG
1/W	STRAIN	IJ	JREAL	JLOSS	DELTA	1/W	STRAIN	IJ	JREAL
-2.00	.024	-9.63	-9.66	-10.03	-.37	-2.00	.016	-9.91	-9.93
-2.00	.012	-9.63	-9.66	-10.05	-.39	-1.50	.013	-9.95	-9.97
-1.50	.027	-9.48	-9.52	-9.87	-.35	-1.50	.014	-9.91	-9.95
-1.50	.055	-9.48	-9.53	-9.84	-.32	-1.00	.040	-9.81	-9.84
-1.00	.089	-9.34	-9.40	-9.65	-.25	-1.00	.014	-9.84	-9.88
-1.00	.045	-9.34	-9.40	-9.66	-.26	-.50	.018	-9.77	-9.81
-.50	.182	-9.15	-9.22	-9.42	-.20	-.50	.030	-9.72	-9.76
-.50	.091	-9.15	-9.21	-9.43	-.21	-.50	.046	-9.68	-9.72
.00	.231	-8.95	-9.05	-9.17	-.12	-.50	.057	-9.67	-9.71
.00	.142	-8.95	-9.05	-9.17	-.12	.00	.060	-9.54	-9.57

SAMPLE 232 PLATE 4 5.0 DEG. CENT.									
AREA SHEARED, ONE SIDE 8.96 CM. SQ.									
SAMPLE THICK, ONE SIDE .0398 IN.									
LOG	PCT	LOG	LOG	LOG	LOG	LOG	LOG	LOG	LOG
1/W	STRAIN	IJ	JREAL	JLOSS	DELTA	1/W	STRAIN	IJ	JREAL
-2.00	.016	-9.91	-9.93	-10.39	-.46	-2.00	.016	-9.91	-9.93
-1.50	.013	-9.95	-9.97	-10.31	-.43	-1.50	.013	-9.95	-9.97
-1.50	.014	-9.91	-9.95	-10.32	-.37	-1.50	.014	-9.91	-9.95
-1.00	.040	-9.81	-9.84	-10.24	-.40	-1.00	.040	-9.81	-9.84
-1.00	.014	-9.84	-9.88	-10.22	-.33	-1.00	.014	-9.84	-9.88
-.50	.018	-9.77	-9.81	-10.15	-.33	-.50	.018	-9.77	-9.81
-.50	.030	-9.72	-9.76	-10.12	-.37	-.50	.030	-9.72	-9.76
-.50	.046	-9.68	-9.72	-10.04	-.33	-.50	.046	-9.68	-9.72
-.50	.057	-9.67	-9.71	-10.05	-.33	-.50	.057	-9.67	-9.71
.00	.060	-9.54	-9.57	-9.96	-.24	.00	.060	-9.54	-9.57
.00	.028	-9.61	-9.67	-9.92	-.24	.00	.028	-9.61	-9.67

SAMPLE 232 PLATE 4 15.0 DEG. CENT.									
AREA SHEARED, ONE SIDE 8.96 CM. SQ.									
SAMPLE THICK, ONE SIDE .0398 IN.									
LOG	PCT	LOG	LOG	LOG	LOG	LOG	LOG	LOG	LOG
1/W	STRAIN	IJ	JREAL	JLOSS	DELTA	1/W	STRAIN	IJ	JREAL
-2.00	.014	-9.88	-9.89	-10.37	-.46	-2.00	.014	-9.88	-9.89
-1.50	.043	-9.85	-9.87	-10.34	-.41	-1.50	.043	-9.85	-9.87
-1.50	.021	-9.84	-9.87	-10.24	-.41	-1.50	.021	-9.84	-9.87
-1.00	.044	-9.79	-9.84	-10.17	-.33	-1.00	.044	-9.79	-9.84
-1.00	.041	-9.79	-9.82	-10.24	-.43	-1.00	.041	-9.79	-9.82
-.50	.074	-9.64	-9.67	-10.09	-.41	-.50	.074	-9.64	-9.67
-.50	.047	-9.66	-9.69	-10.05	-.38	-.50	.047	-9.66	-9.69

[illegible]

APPENDIX H

REDUCTION OF CREEP DATA

The creep data were generated by applying a step load (generally for 60 seconds) to the shear specimens and recording both the load and the resulting displacement on a two channel recorder. A sample of the recorder output is given in Figure H1. As noted in Figure H1, the recovery of the specimen after the removal of the step load was also recorded, generally for a period of time equal to that of the step function. (Because of reproduction limitations, the full recovery portion is not shown.)

Beginning at the loading time, values were scaled from the displacement curve at times of 1, 2, 4, etc. seconds. A similar scaling was done for the recovery portion at equivalent times beginning with the recovery or unload time. These two sets of displacement data were then added at equivalent times, giving a superposed curve with the time scale taken as the sum of the total time of the step load plus the recovery time. A sample data sheet is given in Figure H2.

As shown below in the sample calculations, values of stress and strain were reduced to the creep compliance $J(t)$

$$J(t) = \frac{\gamma(t)}{\sigma_0}$$

where $\gamma(t)$ is the strain as a function of time and σ_0 is the applied stress.

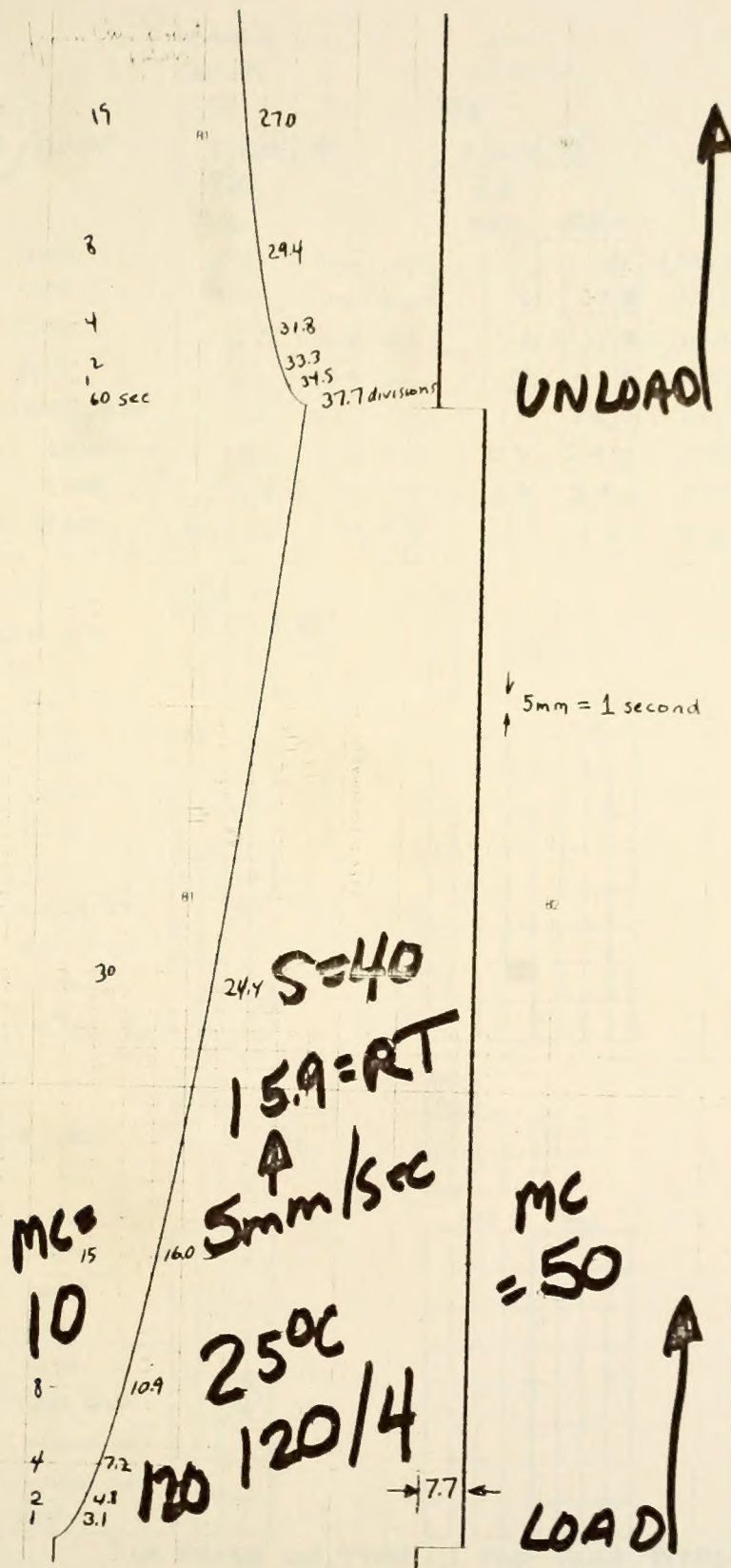


Figure H1. Sample Creep Curve.

✓
P

		HEADING CARD #1	LOAD CARD #2	RECOVERY CARD #3
ID				
SAMPLE / PLATE		1 2 0 X 4	1 2 0 X 4	1 2 0 X 4
TEMP, °C		25	25	25
		F4.1	F4.0 F4.1	F4.1
RANGE	LOAD	50	TIME - DIVD 1 31	TIME - DIVD 9 4 5
MC	LOAD	50	TIME - DIVD 2 4 8	TIME - DIVD 3 3 3
DIV	LOAD	7.7	TIME - DIVD 4 7 2	TIME - DIVD 3 1 8
MC	DISP	10	TIME - DIVD 8 1 0 9	TIME - DIVD 2 9 4
* FILTER--LOAD, DISP			TIME - DIVD 1 5 1 6 0	TIME - DIVD 2 7 0
THICK	2 SIDES, IN	0.796	TIME - DIVD 3 0 2 4 4	TIME - DIVD 2 3 6
AREA	1 SIDE, CM ²	9.95	TIME - DIVD 6 0 3 7 7	TIME - DIVD 2 0 0
RANGE	DISP	0.1	TIME - DIVD	TIME - DIVD

ID				
SAMPLE / PLATE				
TEMP, °C				
		F4.0	F4.1	F4.1
RANGE	LOAD			
MC	LOAD			
DIV	LOAD			
MC	DISP			
* FILTER--LOAD, DISP				
THICK	2 SIDES, IN			
AREA	1 SIDE, CM			
RANGE	DISP			

ID				
SAMPLE / PLATE				
TEMP, °C				
		F4.0	F4.1	F4.1
RANGE	LOAD			
MC	LOAD			
DIV	LOAD			
MC	DISP			
* FILTER--LOAD, DISP				
THICK	2 SIDES, IN			
AREA	1 SIDE, CM			
RANGE	DISP			

* IF FILTER ON, TYPE 1, 1 FOR LOAD, DISPLACEMENT

Figure H2. Sample Data Sheet, Creep.

Values of $\gamma(t)$ and σ were calculated by scaling the divisions from the strip chart recorder and multiplying by the appropriate scale factor. $J(t)$ was corrected to 298 K by multiplying by the ratio: (test temperature, K) / (298 K).

The data were actually reduced on an electronic computer, transferred to cards and plotted on an x-y CALCOMP plotter. The reduction program, along with a sample set of raw data is given in Appendix I. This is followed by a complete tabulation of the reduced creep data. A sample hand calculation for $120/4$ at 25 C is given on the following pages. The data for this calculation were taken from the sample data sheet in Figure H2.

1. Sample #120/4, 25°C

see sample data and data, Figures H1 and H2,
for the data used in following calculations.

2. Notation:

A: area of one side of shear sample, cm^2

F: correction factor to correct for filter attenuation

$F = 1.0$ when filters were not used. See Table D1.

$J(t)$: creep compliance, cm^2/dyne

MC: recorder sensitivity, millivolts/division

X_0 : number of chart divisions, displacement

R: sensitivity of MTS output signal, grams or inch/division

T: test temperature, °K

T_h : Thickness of both sides of sample, inch

T_0 : Reference temperature, 298°K (25°C)

Y_0 : number of chart divisions, height of step load

δ : phase angle, degrees

σ_0 : step shear stress, dynes/ cm^2

γ_0 : strain as function of time resulting from σ_0 , in/in.

3. STRESS, σ_0 , dynes/cm²

$$\sigma_0 = \text{Load, dynes} / \text{Area, cm}^2$$

$$\sigma_0 = \frac{(MC) (Y_0) (R) (F)^* (980)}{2. A}$$

$$\sigma_0 = \frac{(50. \frac{mv}{dw}) (7.7dw) (\frac{50,000g}{10,000mv}) (1.) (980 \frac{dyne}{gram})}{(2.) (9.95 \text{ cm}^2)}$$

$$\boxed{\sigma = 9.48 \times 10^4 \text{ dynes/cm}^2}$$

* No filter used, $\therefore F = 1.0$

4. STRAIN, γ , inches/inch, at 1. second.

$$\gamma = \text{displacement} / \text{thickness, one side}$$

$$\gamma = \frac{(MC) (X) (R) (F)^*}{Th / 2.}$$

$$\gamma = \frac{(10 \frac{mv}{dw}) (3.1dw) (\frac{0.01 \text{ inch}}{10,000mv}) (1.)}{0.0796 \text{ inch} / 2.}$$

$$\boxed{\gamma = 0.00078 \text{ in/in}}$$

5. $\log J(t)$, Creep compliance, cm^2/dyne

$$J(t) = \left[\gamma(t) / \sigma_0 \right] \frac{T}{T_0}$$

$$\log J(t) = \log \gamma - \log \sigma_0 + \log T/T_0$$

$$\log J(t) = \log 0.00078 - \log 9.48 \times 10^4 + \log \frac{298}{278}$$

$$\boxed{\log J(t) = -8.09}$$

6. Recovery portion:

$J(t)$, or more correctly the normalized recovery curve, is calculated as per above except N , step 4, is the number of chart divisions displacement after time, t , in recovery. The load is taken as the load applied during creep, ie the step load

7. Superposed portion:

$J(t)$ is calculated as per steps 3 through 5 except N in step 4 is taken as the sum of the divisions displacement after t' seconds recovery and the divisions displacement after t' seconds creep. The superposed time is the time at unload plus the time of recovery. Looking at 120/4, 25°C data sheet; the unload time is 60 seconds. After 30 seconds recovery, the displacement is 23.6. Adding 60 seconds and 30 seconds, superposed time is 90 seconds. Superposed calculated displacement is $23.6 + 24.4 = 48.0$ divisions.

APPENDIX I

REDUCED CREEP DATA

The next pages present the reduced creep data preceded by the reduction program and a set of sample data. The data are presented in the same format as used to input the program. The program was run on a CDC 6500 electronic computer.

Each creep curve was represented by three data cards. The first card contained identification and constants. The second card contained displacement and time data for creep and the third card contained the recovery displacement data at recovery times equivalent to the creep times.

Program

```

C      *****
C      *
C      *
C      *      REDUCTION OF CREEP DATA
C      *
C      *
C      *****

INTEGER SAMP, FILTER, PLATE
DIMENSION X(17), SEC(17), DIVD(9), LTIME(9)
REAL MCL, MCD, J, LTIME, LJ

C      *****
C      READ DATA.....ONE SET = 3 CARDS
C      FIRST CARD, CONSTANTS FOR THE DATA SET
C      SECOND CARD, CREEP TIME (I), DISPLACEMENT (I)
C      THIRD CARD, RECOVERY DISPLACEMENT (I) CORRESPONDING TO CREEP TIME (I)
C      IDO TRANSFERS TO CALCULATION OF ( CONSTANTS, LOAD, RECOVERY )
C      *****

1 READ (5,500) IDO, SAMP, PLATE, TEMP, (X(J), J=2,17)
   IF( EOF,5 ) 999, 2
2 IF( IDO )300, 100, 200

C      *****
C      COMPUTE CONSTANTS USED IN REDUCTION AND WRITE COLUMN HEADINGS
C      *****

100 RANGEL = X(2)
   MCL = X(3)
   DIVL = X(4)
   MCD = X(5)
   FILTER = X(6)
   IF ( FILTER .EQ. 110 .OR. FILTER .EQ. 100 ) DIVL = 1.05 * DIVL
   THICK = 0.001 * X(7) / 2.
   AREA = 0.1 * X(8)
   RANGED = 0.001 * X(9)
   STRESS = MCL * DIVL * RANGEL * 49. / AREA
   WRITE ( 6,600 ) SAMP, PLATE, TEMP, AREA, THICK
   GO TO 1

C      *****
C      COMPUTE LOAD PORTION
C      *****

200 WRITE (6,601)

```



```

DO 299 K=1,8
  IF ( X(2*K) * X(2*K+1) * THICK * STRESS ) 299, 299, 201
201 SEC(K) = X(2*K) * 10.
  UNLOAD = SEC(K)
  DIVD(K) = X(2*K+1)
  IF ( FILTER .EQ. 10 .OR. FILTER .EQ. 110 )
    $ DIVD(K) = 1.05 * DIVD(K)
  PCT = MCD * DIVD(K) * RANGED / (100. * THICK)
  LJ = ALOG10 ( ((TEMP+273.)/298.)*(PCT/(100.*STRESS)) )
  LTIME(K) = ALOG10( SEC(K) )
  WRITE ( 6,604 ) PCT, LTIME(K), LJ
299 CONTINUE
GO TO 1

```

```

C *****
C COMPUTE RECOVERY PORTION
C *****

```

```

300 WRITE (6,602)
DO 349 K=1,8
  M = K+1
  IF ( X(M) ) 349, 349, 301
301 IF ( FILTER .EQ. 10 .OR. FILTER .EQ. 110 ) X( M ) = 1.05 * X( M )
  IF( STRESS * THICK * SEC(K) ) 349, 349, 302
302 PCT = MCD * X(M) * RANGED / (100. * THICK)
  J = ( PCT / ( 100. * STRESS ) ) * ( TEMP+273. ) / 298.
  IF(J) 349,349,303
303 LJ = ALOG10(J)
  WRITE ( 6,604 ) PCT, LTIME(K), LJ
349 CONTINUE

```

```

C *****
C COMPUTE SUPERPOSED PORTION
C *****

```

```

WRITE(6,603)
DO 399 K=1,8
  IF( X(K+1) ) 399, 399, 305
305 SUMD = DIVD(K) * X(K+1)
  SEC(K) = UNLOAD + SEC(K)
  IF( STRESS * THICK * SEC(K) ) 399, 399, 306
306 PCT = MCD * SUMD * RANGED / (100. * THICK)
  J = ( PCT / ( 100. * STRESS ) ) * ( TEMP+273. ) / 298.
  IF ( J ) 399, 399, 307
307 LJ = ALOG10(J)
  LTIME(K) = ALOG10( SEC(K) )
  WRITE ( 6,604 ) PCT, LTIME(K), LJ
399 CONTINUE
WRITE( 6,605 )
GO TO 1

```

```

500 FORMAT (I2, I4, I2, 17F4.1)
600 FORMAT( 1H , //, 15X, 6HSAMPLE, 14, 1H/, 11, /,
  $21X, F4.1, 5H DEF., //, 15X, 6HAREA =, F6.2, 7H CM.SQ., /,
  $15X, 7HTHICK =, F6.4, 4H IN., ///, 15X, 17H PCT LOG LOG, /,
  $15X, 18HSTRAIN TIME J(T), // )
601 FORMAT ( 1H , 14X, 18HLOAD..... )
602 FORMAT ( 1H , /, 15X, 18HRECOVERY..... )
603 FORMAT ( 1H , /, 15X, 18HSUPERPOSED..... )
604 FORMAT( 1H , 14X, F5.3, F6.2, F7.2 )
605 FORMAT( 1H )
999 STOP
END

```


Reduced Data

The pages that follow contain a listing of the reduced creep data. In general, each page contains the data for one sample; each "block" of data represents one creep-recovery test.

The data may be identified as follows: the first three digits following "SAMPLE" correspond to a mixture number as described in Table 5. The number following the slash represents the particular set of sample plates used. When more than one set of sample plates is given per mixture number (eg. 105/1, 105/4) a duplicate set of plates is indicated.

Sample Data

120	4	25	50	50	77	10	0796	995	1					
3	120	4	25	1	31	2	48	4	72	8	109	15	160	30 244 60 277
-3	120	4	25	345	333	318	294	270	236	200				
	120	1	15	50	100	188	10	08081017	1					
3	120	1	15	1	33	2	43	4	60	8	82	15	112	30 160 60 232
-3	120	1	15	207	194	188	173	160	142					
	120	4	15	50	100	19	10	0796	995	1				
3	120	4	15	1	40	2	55	4	77	8	109	15	151	30 220 60 325
-3	120	4	15	291	280	267	250	230	207	182				
	120	1	5	50	500	13	5	08071017	1					
3	120	1	5	1	39	2	52	4	62	8	88	15	113	30 152 60 212
-3	120	1	5	173	164	152	139	121	105	88				
	120	4	5	50	500	95	5	0796	995	1				
3	120	4	5	1	40	2	49	4	61	8	70	15	100	30 134 60 181
-3	120	4	5	141	133	122	110	97	81	64				
	121	2	25	50	20	173	10	11	0806	961	1			
3	121	2	25	1	29	2	41	4	61	8	91	15	133	30 204 60 312
-3	121	2	25	289	280	267	250	231	210	185				
	121	3	25	50	20	173	10	11	08041011	1				
3	121	3	25	1	20	2	30	4	45	8	69	15	99	30 148 60 218
-3	121	3	25	199	190	180	167	151	132	113				
	121	2	15	50	100	188	5	0806	961	1				
3	121	2	15	1	58	2	79	4	110	8	152	15	210	30 303 60 400
-3	121	2	15	350	333	312	288	260	228	198				
	121	3	15	50	100	142	5	08041011	1					
3	121	3	15	1	31	2	45	4	63	8	90	15	123	30 178 60 252
-3	121	3	15	220	209	195	176	157	131	104				
	121	2	5	50	500	133	5	0806	961	1				
3	121	2	5	1	48	2	60	4	75	8	95	15	121	30 162 60 223
-3	121	2	5	180	170	159	143	128	111	95				
	121	3	5	50	200	33	5	08041011	1					
3	121	3	5	1	45	2	57	4	70	8	90	15	115	30 155 60 210
-3	121	3	5	165	155	144	130	115	98	80				

SAMPLE 105/1
25.0 DEG.

AREA = 9.63 CM.².
THICK = .0404 IN.

PCT LOG LOG
STRAIN TIME J(T)

LOAD.....
.094 0.00 -8.02
.148 .30 -7.83
.235 .60 -7.63
.368 .90 -7.43
.691 1.30 -7.16

RECOVERY.....
.632 0.00 -7.20
.606 .30 -7.21
.570 .60 -7.24
.523 .90 -7.28
.462 1.30 -7.33

SUPERPOSED.....
.725 1.32 -7.14
.754 1.34 -7.12
.805 1.38 -7.09
.892 1.45 -7.05
1.155 1.60 -6.93

SAMPLE 105/1
15.0 DEG.

AREA = 9.63 CM.².
THICK = .0404 IN.

PCT LOG LOG
STRAIN TIME J(T)

LOAD.....
.076 0.00 -8.82
.108 .30 -8.67
.144 .60 -8.54
.215 .90 -8.37
.316 1.20 -8.20
.437 1.43 -8.07

RECOVERY.....
.370 0.00 -8.14
.352 .30 -8.16
.324 .60 -8.19
.298 .90 -8.23
.267 1.20 -8.28

SUPERPOSED.....
.446 1.45 -8.05
.460 1.46 -8.04
.472 1.49 -8.03
.513 1.54 -7.99
.583 1.63 -7.94

SAMPLE 105/1
5.0 DEG.

AREA = 9.63 CM.².
THICK = .0404 IN.

PCT LOG LOG
STRAIN TIME J(T)

LOAD.....
.067 0.00 -9.38
.076 .30 -9.30
.094 .60 -9.21
.119 .90 -9.11
.159 1.20 -8.98
.217 1.51 -8.85
.253 1.64 -8.78

RECOVERY.....
.199 0.00 -8.89
.188 .30 -8.91
.171 .60 -8.95
.153 .90 -9.00
.135 1.20 -9.05

SUPERPOSED.....
.262 1.65 -8.77
.263 1.66 -8.76
.265 1.68 -8.76
.273 1.72 -8.75
.294 1.78 -8.72

SAMPLE 105/4
25.0 DEG.

AREA = 9.90 CM.².
THICK = .0406 IN.

PCT LOG LOG
STRAIN TIME J(T)

LOAD.....
.047 0.00 -8.02
.072 .30 -7.83
.122 .60 -7.60
.194 .90 -7.40
.316 1.20 -7.19
.626 1.61 -6.89

RECOVERY.....
.597 0.00 -6.91
.583 .30 -6.92
.561 .60 -6.94
.536 .90 -6.96
.500 1.20 -6.99
.446 1.61 -7.04

SUPERPOSED.....
.644 1.62 -6.88
.654 1.63 -6.87
.683 1.65 -6.85
.730 1.69 -6.82
.816 1.76 -6.77
1.072 1.91 -6.66

SAMPLE 105/4
15.0 DEG.

AREA = 9.90 CM.².
THICK = .0406 IN.

PCT LOG LOG
STRAIN TIME J(T)

LOAD.....
.081 0.00 -8.79
.108 .30 -8.67
.153 .60 -8.51
.225 .90 -8.35
.338 1.20 -8.17
.446 1.41 -8.05

RECOVERY.....
.378 0.00 -8.12
.360 .30 -8.14
.338 .60 -8.17
.306 .90 -8.21
.273 1.20 -8.26

SUPERPOSED.....
.458 1.43 -8.04
.467 1.45 -8.03
.491 1.48 -8.01
.530 1.53 -7.97
.611 1.62 -7.91

SAMPLE 105/4
5.0 DEG.

AREA = 9.90 CM.².
THICK = .0406 IN.

PCT LOG LOG
STRAIN TIME J(T)

LOAD.....
.045 0.00 -9.50
.054 .30 -9.42
.072 .60 -9.29
.095 .90 -9.17
.129 1.20 -9.04
.180 1.52 -8.89

RECOVERY.....
.140 0.00 -9.00
.129 .30 -9.04
.117 .60 -9.08
.108 .90 -9.12
.090 1.20 -9.19

SUPERPOSED.....
.185 1.53 -8.88
.183 1.54 -8.88
.189 1.57 -8.87
.203 1.61 -8.84
.219 1.69 -8.81

SAMPLE 106/2
25.0 DEG.

AREA = 9.97 CM.².
THICK = .0408 IN.

PCT LOG LOG
STRAIN TIME J(T)

LOAD.....
.064 0.00 -8.21
.089 .30 -8.07
.136 .60 -7.88
.193 .90 -7.73
.315 1.28 -7.52

RECOVERY.....
.257 0.00 -7.61
.239 .30 -7.64
.214 .60 -7.69
.193 .90 -7.73
.161 1.28 -7.81

SUPERPOSED.....
.322 1.30 -7.51
.329 1.32 -7.50
.350 1.36 -7.47
.384 1.43 -7.43
.475 1.58 -7.34

SAMPLE 106/2
15.0 DEG.

AREA = 9.97 CM.².
THICK = .0408 IN.

PCT LOG LOG
STRAIN TIME J(T)

LOAD.....
.054 0.00 -8.97
.075 .30 -8.82
.102 .60 -8.69
.143 .90 -8.54
.197 1.20 -8.40
.289 1.54 -8.23

RECOVERY.....
.236 0.00 -8.32
.223 .30 -8.35
.200 .60 -8.39
.179 .90 -8.44
.148 1.20 -8.52
.129 1.54 -8.59

SUPERPOSED.....
.289 1.56 -8.23
.298 1.57 -8.22
.302 1.59 -8.22
.322 1.63 -8.19
.345 1.71 -8.16
.418 1.85 -8.07

SAMPLE 106/2
5.0 DEG.

AREA = 9.97 CM.².
THICK = .0408 IN.

PCT LOG LOG
STRAIN TIME J(T)

LOAD.....
.043 0.00 -9.37
.050 .30 -9.30
.061 .60 -9.22
.075 .90 -9.13
.098 1.20 -9.01
.143 1.59 -8.85

RECOVERY.....
.111 0.00 -8.96
.107 .30 -8.97
.098 .60 -9.01
.089 .90 -9.05
.084 1.20 -9.07
.071 1.59 -9.15

SUPERPOSED.....
.154 1.60 -8.81
.157 1.61 -8.80
.159 1.63 -8.80
.164 1.67 -8.78
.184 1.74 -8.74
.214 1.89 -8.67

SAMPLE 106/3
25.0 DEG.

AREA = 9.63 CM.².
THICK = .0410 IN.

PCT LOG LOG
STRAIN TIME J(T)

LOAD.....
.071 0.00 -8.17
.100 .30 -8.02
.143 .60 -7.86
.196 .90 -7.73
.285 1.20 -7.56
.325 1.32 -7.51

RECOVERY.....
.267 0.00 -7.59
.242 .30 -7.63
.214 .60 -7.69
.185 .90 -7.75
.160 1.20 -7.81

SUPERPOSED.....
.339 1.34 -7.49
.342 1.36 -7.48
.357 1.40 -7.47
.381 1.46 -7.44
.446 1.57 -7.37

SAMPLE 106/3
15.0 DEG.

AREA = 9.63 CM.².
THICK = .0410 IN.

PCT LOG LOG
STRAIN TIME J(T)

LOAD.....
.053 0.00 -8.98
.071 .30 -8.86
.094 .60 -8.72
.128 .90 -8.60
.178 1.20 -8.46
.241 1.51 -8.33
.332 1.77 -8.19

RECOVERY.....
.289 0.00 -8.25
.276 .30 -8.27
.257 .60 -8.30
.232 .90 -8.35
.201 1.20 -8.41
.171 1.51 -8.48
.153 1.77 -8.53

SUPERPOSED.....
.342 1.78 -8.18
.348 1.79 -8.17
.355 1.80 -8.16
.360 1.83 -8.16
.380 1.88 -8.13
.412 1.96 -8.10
.485 2.07 -8.03

SAMPLE 106/3
5.0 DEG.

AREA = 9.63 CM.².
THICK = .0410 IN.

PCT LOG LOG
STRAIN TIME J(T)

LOAD.....
.050 0.00 -9.48
.062 .30 -9.38
.078 .60 -9.28
.098 .90 -9.18
.128 1.20 -9.07
.178 1.56 -8.93

RECOVERY.....
.134 0.00 -9.05
.125 .30 -9.08
.114 .60 -9.12
.103 .90 -9.16
.089 1.20 -9.23
.080 1.56 -9.27

SUPERPOSED.....
.184 1.57 -8.91
.187 1.58 -8.90
.193 1.60 -8.89
.201 1.64 -8.87
.217 1.72 -8.84
.258 1.86 -8.76

SAMPLE 107/2
25.0 DEG.
AREA = 8.49 CM.SQ.
THICK = .0437 IN.

PCT LOG LOG
STRAIN TIME J(T)

LOAD.....
.055 0.00 -8.02
.087 .30 -7.83
.127 .60 -7.69
.204 .90 -7.46
.327 1.20 -7.25
.528 1.49 -7.04

RECOVERY.....
.487 0.00 -7.08
.471 .30 -7.09
.451 .60 -7.11
.422 .90 -7.14
.387 1.20 -7.18
.350 1.49 -7.22

SUPERPOSED.....
.542 1.51 -7.03
.557 1.52 -7.02
.571 1.54 -7.01
.626 1.59 -6.97
.714 1.67 -6.91
.876 1.79 -6.82

SAMPLE 107/2
15.0 DEG.
AREA = 8.49 CM.SQ.
THICK = .0437 IN.

PCT LOG LOG
STRAIN TIME J(T)

LOAD.....
.075 0.00 -8.82
.100 .30 -8.69
.142 .60 -8.54
.204 .90 -8.38
.300 1.20 -8.21
.467 1.53 -8.02

RECOVERY.....
.404 0.00 -8.09
.387 .30 -8.10
.367 .60 -8.13
.337 .90 -8.16
.304 1.20 -8.21
.284 1.53 -8.24

SUPERPOSED.....
.474 1.54 -8.01
.487 1.56 -8.00
.509 1.58 -7.99
.541 1.62 -7.96
.604 1.70 -7.91
.751 1.83 -7.82

SAMPLE 107/2
5.0 DEG.
AREA = 8.49 CM.SQ.
THICK = .0437 IN.

PCT LOG LOG
STRAIN TIME J(T)

LOAD.....
.035 0.00 -9.53
.042 .30 -9.43
.052 .60 -9.15
.064 .90 -9.24
.085 1.18 -9.14
.113 1.48 -9.02
.155 1.78 -8.88
.194 1.96 -8.78

RECOVERY.....
.162 0.00 -8.86
.155 .30 -8.88
.147 .60 -8.90
.135 .90 -8.94
.127 1.18 -8.97
.113 1.48 -9.02

SUPERPOSED.....
.197 1.97 -8.78
.194 1.97 -8.77
.194 1.98 -8.77
.204 2.00 -8.76
.212 2.03 -8.74
.227 2.09 -8.71

SAMPLE 107/3
5.0 DEG.
AREA = 9.84 CM.SQ.
THICK = .0406 IN.

PCT LOG LOG
STRAIN TIME J(T)

LOAD.....
.058 0.00 -9.42
.070 .30 -9.33
.084 .60 -9.24
.104 .90 -9.15
.131 1.18 -9.06
.174 1.48 -8.93
.219 1.71 -8.84

RECOVERY.....
.164 0.00 -8.86
.155 .30 -8.99
.142 .60 -9.03
.124 .90 -9.08
.108 1.18 -9.15
.090 1.48 -9.22

SUPERPOSED.....
.223 1.72 -8.83
.225 1.72 -8.83
.228 1.74 -8.82
.234 1.77 -8.81
.239 1.82 -8.80
.264 1.91 -8.75

SAMPLE 107/3
25.0 DEG.
AREA = 9.84 CM.SQ.
THICK = .0406 IN.

PCT LOG LOG
STRAIN TIME J(T)

LOAD.....
.036 0.00 -8.13
.054 .30 -7.95
.074 .60 -7.79
.115 .90 -7.62
.176 1.20 -7.44
.270 1.51 -7.25
.333 1.65 -7.16

RECOVERY.....
.306 0.00 -7.20
.291 .30 -7.22
.279 .60 -7.24
.261 .90 -7.27
.239 1.20 -7.31
.216 1.51 -7.35

SUPERPOSED.....
.342 1.66 -7.15
.345 1.67 -7.15
.358 1.69 -7.13
.376 1.72 -7.11
.415 1.79 -7.07
.485 1.89 -7.00

SAMPLE 107/3
15.0 DEG.
AREA = 9.84 CM.SQ.
THICK = .0406 IN.

PCT LOG LOG
STRAIN TIME J(T)

LOAD.....
.054 0.00 -8.85
.074 .30 -8.71
.102 .60 -8.57
.142 .90 -8.43
.198 1.18 -8.28
.291 1.48 -8.11
.441 1.78 -7.93
.462 1.85 -7.91

RECOVERY.....
.414 0.00 -7.96
.399 .30 -7.98
.379 .60 -8.00
.358 .90 -8.02
.329 1.18 -8.06
.297 1.48 -8.11
.205 1.78 -8.27

SUPERPOSED.....
.467 1.85 -7.91
.473 1.86 -7.90
.482 1.87 -7.90
.500 1.89 -7.88
.527 1.93 -7.86
.588 2.00 -7.81
.645 2.11 -7.77

SAMPLE 107/3
5.0 DEG.
AREA = 9.84 CM.SQ.
THICK = .0406 IN.

PCT LOG LOG
STRAIN TIME J(T)

LOAD.....
.031 0.00 -9.39
.038 .30 -9.30
.045 .60 -9.22
.054 .90 -9.14
.072 1.18 -9.02
.090 1.48 -8.92
.120 1.78 -8.79
.129 1.88 -8.76

RECOVERY.....
.106 0.00 -8.85
.099 .30 -8.88
.092 .60 -8.91
.088 .90 -8.93
.077 1.18 -8.99
.070 1.48 -9.03
.054 1.78 -9.14

SUPERPOSED.....
.137 1.89 -8.74
.137 1.89 -8.74
.137 1.90 -8.74
.142 1.92 -8.72
.149 1.96 -8.70
.160 2.03 -8.67
.174 2.13 -8.63

SAMPLE 10R/1
25.0 DEG.
AREA = 9.50 CM.².
THICK = .0418 IN.

PCT LOG LOG
STRAIN TIME J(T)

LOAD.....
.028 0.00 -8.27
.042 .30 -8.09
.061 .60 -7.93
.087 .90 -7.78
.126 1.18 -7.62
.192 1.48 -7.43
.332 1.90 -7.20

RECOVERY.....
.311 0.00 -7.22
.299 .30 -7.24
.285 .60 -7.26
.265 .90 -7.29
.244 1.18 -7.33
.214 1.48 -7.38
.187 1.90 -7.45

SUPERPOSED.....
.339 1.91 -7.19
.341 1.91 -7.18
.346 1.92 -7.18
.353 1.94 -7.17
.370 1.98 -7.15
.410 2.04 -7.10
.519 2.20 -7.00

SAMPLE 10R/1
15.0 DEG.
AREA = 9.50 CM.².
THICK = .0418 IN.

PCT LOG LOG
STRAIN TIME J(T)

LOAD.....
.037 0.00 -8.89
.049 .30 -8.76
.065 .60 -8.64
.080 .90 -8.50
.119 1.18 -8.38
.168 1.48 -8.23
.281 1.91 -8.00

RECOVERY.....
.248 0.00 -8.06
.247 .30 -8.07
.227 .60 -8.10
.211 .90 -8.13
.196 1.18 -8.16
.175 1.48 -8.21

SUPERPOSED.....
.285 1.92 -8.00
.292 1.92 -7.99
.292 1.93 -7.99
.300 1.95 -7.98
.314 1.99 -7.96
.342 2.05 -7.92

SAMPLE 10R/1
5.0 DEG.
AREA = 9.50 CM.².
THICK = .0418 IN.

PCT LOG LOG
STRAIN TIME J(T)

LOAD.....
.035 0.00 -9.48
.038 .30 -9.44
.051 .60 -9.32
.063 .90 -9.23
.074 1.18 -9.15
.101 1.48 -9.02
.140 1.78 -8.88
.166 1.95 -8.80

RECOVERY.....
.154 0.00 -8.84
.127 .30 -8.92
.122 .60 -8.94
.114 .90 -8.97
.105 1.18 -9.00
.087 1.48 -9.08

SUPERPOSED.....
.189 1.96 -8.75
.164 1.96 -8.80
.173 1.97 -8.79
.176 1.99 -8.78
.180 2.02 -8.77
.189 2.08 -8.75

SAMPLE 10R/4
25.0 DEG.
AREA = 9.20 CM.².
THICK = .0416 IN.

PCT LOG LOG
STRAIN TIME J(T)

LOAD.....
.033 0.00 -8.20
.047 .30 -8.05
.070 .60 -7.88
.098 .90 -7.73
.137 1.18 -7.59
.198 1.48 -7.43
.349 1.90 -7.18

RECOVERY.....
.325 0.00 -7.22
.314 .30 -7.23
.298 .60 -7.25
.281 .90 -7.28
.260 1.18 -7.31
.233 1.48 -7.36
.211 1.90 -7.40

SUPERPOSED.....
.358 1.91 -7.17
.351 1.91 -7.17
.369 1.92 -7.16
.379 1.94 -7.15
.397 1.98 -7.13
.432 2.04 -7.09
.560 2.20 -6.98

SAMPLE 10R/4
15.0 DEG.
AREA = 9.20 CM.².
THICK = .0416 IN.

PCT LOG LOG
STRAIN TIME J(T)

LOAD.....
.026 0.00 -8.91
.035 .30 -8.79
.044 .60 -8.69
.056 .90 -8.58
.079 1.18 -8.43
.109 1.48 -8.30
.158 1.78 -8.13
.175 1.88 -8.09

RECOVERY.....
.160 0.00 -8.14
.154 .30 -8.16
.146 .60 -8.18
.140 .90 -8.20
.126 1.18 -8.25
.123 1.48 -8.26

SUPERPOSED.....
.186 1.88 -8.08
.190 1.89 -8.07
.190 1.90 -8.07
.197 1.92 -8.05
.205 1.95 -8.04
.232 2.02 -7.98

SAMPLE 10R/4
5.0 DEG.
AREA = 9.20 CM.².
THICK = .0416 IN.

PCT LOG LOG
STRAIN TIME J(T)

LOAD.....
.032 0.00 -9.54
.037 .30 -9.47
.049 .60 -9.35
.056 .90 -9.29
.072 1.18 -9.18
.093 1.48 -9.07
.133 1.81 -8.91

RECOVERY.....
.104 0.00 -9.01
.097 .30 -9.04
.091 .60 -9.06
.082 .90 -9.11
.070 1.18 -9.18
.065 1.48 -9.21
.053 1.81 -9.30

SUPERPOSED.....
.135 1.82 -8.89
.133 1.83 -8.90
.140 1.84 -8.88
.139 1.86 -8.88
.142 1.90 -8.87
.158 1.98 -8.83
.186 2.11 -8.75

SAMPLE 109/3
25.0 DEG.

AREA = 9.20 CM.SQ.
THICK = .0406 IN.

PCT LOG LOG
STRAIN TIME J(T)

LOAD.....
.034 -.30 -8.18
.050 0.00 -8.01
.076 .30 -7.84
.111 .60 -7.67
.167 .90 -7.49
.257 1.20 -7.30
.403 1.51 -7.11
.638 1.81 -6.91

RECOVERY.....
.620 -.30 -6.92
.608 0.00 -6.93
.596 .30 -6.94
.566 .60 -6.96
.536 .90 -6.98
.496 1.20 -7.02
.456 1.51 -7.06
.403 1.81 -7.11

SUPERPOSED.....
.654 1.81 -6.90
.654 1.81 -6.89
.665 1.82 -6.89
.678 1.83 -6.88
.703 1.86 -6.87
.753 1.90 -6.84
.852 1.98 -6.78
1.041 2.11 -6.70

SAMPLE 109/3
15.0 DEG.

AREA = 9.20 CM.SQ.
THICK = .0406 IN.

PCT LOG LOG
STRAIN TIME J(T)

LOAD.....
.076 0.00 -8.85
.101 .30 -8.73
.144 .60 -8.57
.205 .90 -8.42
.288 1.18 -8.27
.430 1.48 -8.09
.476 1.56 -8.05

RECOVERY.....
.405 0.00 -8.12
.383 .30 -8.14
.358 .60 -8.17
.322 .90 -8.22
.288 1.18 -8.27
.245 1.48 -8.34

SUPERPOSED.....
.480 1.57 -8.05
.484 1.58 -8.04
.502 1.60 -8.03
.527 1.64 -8.01
.575 1.71 -7.97
.674 1.82 -7.90

SAMPLE 109/3
5.0 DEG.

AREA = 9.20 CM.SQ.
THICK = .0406 IN.

PCT LOG LOG
STRAIN TIME J(T)

LOAD.....
.041 0.00 -9.30
.050 .30 -9.21
.063 .60 -9.12
.079 .90 -9.02
.101 1.20 -8.91
.129 1.51 -8.80
.176 1.81 -8.67
.192 1.90 -8.63

RECOVERY.....
.153 0.00 -8.73
.146 .30 -8.75
.137 .60 -8.78
.124 .90 -8.82
.111 1.20 -8.87
.099 1.51 -8.92

SUPERPOSED.....
.194 1.90 -8.63
.196 1.91 -8.62
.200 1.92 -8.61
.203 1.94 -8.61
.212 1.98 -8.59
.228 2.05 -8.56

SAMPLE 109/4
25.0 DEG.

AREA = 9.72 CM.SQ.
THICK = .0401 IN.

PCT LOG LOG
STRAIN TIME J(T)

LOAD.....
.047 0.00 -8.02
.073 .30 -7.84
.109 .60 -7.66
.165 .90 -7.48
.240 1.18 -7.32
.371 1.48 -7.13
.600 1.78 -6.92
.635 1.81 -6.90

RECOVERY.....
.596 0.00 -6.92
.580 .30 -6.93
.558 .60 -6.95
.529 .90 -6.97
.496 1.18 -7.00
.455 1.48 -7.04
.405 1.78 -7.09

SUPERPOSED.....
.644 1.82 -6.89
.653 1.83 -6.88
.667 1.84 -6.87
.695 1.86 -6.86
.736 1.90 -6.83
.825 1.98 -6.78
1.005 2.10 -6.70

SAMPLE 109/4
15.0 DEG.

AREA = 9.72 CM.SQ.
THICK = .0401 IN.

PCT LOG LOG
STRAIN TIME J(T)

LOAD.....
.033 0.00 -8.89
.045 .30 -8.75
.067 .60 -8.58
.098 .90 -8.41
.133 1.18 -8.28
.202 1.48 -8.10
.309 1.78 -7.92
.327 1.83 -7.89

RECOVERY.....
.307 0.00 -7.92
.293 .30 -7.94
.278 .60 -7.96
.256 .90 -8.00
.234 1.18 -8.03
.209 1.48 -8.08
.173 1.78 -8.17

SUPERPOSED.....
.340 1.84 -7.87
.338 1.85 -7.88
.345 1.86 -7.87
.355 1.88 -7.86
.369 1.92 -7.84
.411 1.99 -7.79
.482 2.11 -7.72

SAMPLE 109/4
5.0 DEG.

AREA = 9.72 CM.SQ.
THICK = .0401 IN.

PCT LOG LOG
STRAIN TIME J(T)

LOAD.....
.053 0.00 -9.45
.069 .30 -9.33
.084 .60 -9.25
.104 .90 -9.16
.127 1.18 -9.07
.173 1.48 -8.93
.231 1.78 -8.81
.269 1.91 -8.74

RECOVERY.....
.211 0.00 -8.85
.200 .30 -8.87
.189 .60 -8.90
.173 .90 -8.93
.155 1.18 -8.98
.135 1.48 -9.04
.109 1.78 -9.13

SUPERPOSED.....
.264 1.91 -8.75
.269 1.92 -8.74
.273 1.93 -8.74
.276 1.95 -8.73
.282 1.98 -8.72
.307 2.05 -8.68
.340 2.15 -8.64

SAMPLE 117/1
25.0 DEG.
AREA = 17.50 CM.².
THICK = .0204 IN.

PCT LOG LOG
STRAIN TIME J(T)

LOAD.....
.120 0.00 -6.78
.150 .30 -6.68
.271 .60 -6.43
.436 .90 -6.22
.676 1.18 -6.03
1.157 1.48 -5.79
1.954 1.78 -5.57

RECOVERY.....
1.879 0.00 -5.58
1.849 .30 -5.59
1.819 .60 -5.60
1.773 .90 -5.61
1.683 1.18 -5.63
1.638 1.48 -5.64
1.593 1.78 -5.66

SUPERPOSED.....
1.999 1.79 -5.56
1.999 1.79 -5.56
2.089 1.81 -5.54
2.209 1.83 -5.51
2.360 1.88 -5.48
2.795 1.95 -5.41
3.547 2.08 -5.31

SAMPLE 117/1
15.0 DEG.
AREA = 17.50 CM.².
THICK = .0204 IN.

PCT LOG LOG
STRAIN TIME J(T)

LOAD.....
.122 0.00 -7.77
.157 .30 -7.65
.222 .60 -7.51
.315 .90 -7.35
.437 1.18 -7.21
.673 1.48 -7.02
1.009 1.78 -6.85

RECOVERY.....
.930 0.00 -6.88
.902 .30 -6.90
.850 .60 -6.92
.809 .90 -6.94
.737 1.18 -6.98
.658 1.48 -7.03
.580 1.78 -7.09

SUPERPOSED.....
1.052 1.79 -6.83
1.059 1.79 -6.83
1.081 1.81 -6.82
1.124 1.83 -6.80
1.174 1.88 -6.78
1.331 1.95 -6.73
1.584 2.08 -6.65

SAMPLE 117/1
5.0 DEG.
AREA = 17.50 CM.².
THICK = .0204 IN.

PCT LOG LOG
STRAIN TIME J(T)

LOAD.....
.152 0.00 -8.56
.208 .30 -8.43
.268 .60 -8.32
.358 .90 -8.20
.465 1.18 -8.08
.666 1.48 -7.93
.923 1.77 -7.79

RECOVERY.....
.777 0.00 -7.86
.738 .30 -7.89
.680 .60 -7.92
.612 .90 -7.96
.547 1.18 -8.01
.465 1.48 -8.08
.376 1.77 -8.18

SUPERPOSED.....
.930 1.78 -7.78
.938 1.79 -7.78
.948 1.80 -7.77
.970 1.83 -7.76
1.013 1.87 -7.74
1.131 1.95 -7.70
1.299 2.07 -7.64

SAMPLE 117/2
25.0 DEG.
AREA = 18.10 CM.².
THICK = .0203 IN.

PCT LOG LOG
STRAIN TIME J(T)

LOAD.....
.302 0.00 -6.81
.453 .30 -6.63
.740 .60 -6.42
1.193 .90 -6.21
2.054 1.18 -5.98
3.142 1.48 -5.79
3.912 1.60 -5.70

RECOVERY.....
3.700 0.00 -5.72
3.625 .30 -5.73
3.504 .60 -5.74
3.338 .90 -5.77
3.172 1.18 -5.79
2.960 1.48 -5.82
2.870 1.60 -5.83

SUPERPOSED.....
4.002 1.61 -5.69
4.078 1.62 -5.68
4.244 1.64 -5.66
4.531 1.68 -5.63
5.226 1.74 -5.57
6.102 1.85 -5.50
6.781 1.90 -5.46

SAMPLE 117/2
25.0 DEG.
AREA = 18.10 CM.².
THICK = .0203 IN.

PCT LOG LOG
STRAIN TIME J(T)

LOAD.....
.121 0.00 -6.74
.181 .30 -6.57
.287 .60 -6.37
.453 .90 -6.17
.680 1.18 -5.99
1.133 1.48 -5.77
1.873 1.78 -5.55

RECOVERY.....
1.812 0.00 -5.57
1.797 .30 -5.57
1.752 .60 -5.58
1.692 .90 -5.60
1.661 1.18 -5.60
1.601 1.48 -5.62
1.586 1.78 -5.62

SUPERPOSED.....
1.933 1.79 -5.54
1.979 1.79 -5.53
2.039 1.81 -5.52
2.145 1.83 -5.49
2.341 1.88 -5.46
2.734 1.95 -5.39
3.459 2.08 -5.29

SAMPLE 117/2
15.0 DEG.
AREA = 18.10 CM.².
THICK = .0203 IN.

PCT LOG LOG
STRAIN TIME J(T)

LOAD.....
.085 0.00 -7.49
.136 .30 -7.68
.204 .60 -7.50
.287 .90 -7.35
.415 1.18 -7.19
.627 1.48 -7.01
.967 1.78 -6.82

RECOVERY.....
.876 0.00 -6.87
.853 .30 -6.88
.808 .60 -6.90
.763 .90 -6.93
.710 1.18 -6.96
.642 1.48 -7.00
.566 1.78 -7.06

SUPERPOSED.....
.950 1.79 -6.83
.989 1.79 -6.81
1.012 1.81 -6.80
1.050 1.83 -6.79
1.125 1.88 -6.76
1.269 1.95 -6.71
1.533 2.08 -6.62

SAMPLE 117/2
5.0 DEG.
AREA = 18.10 CM.².
THICK = .0203 IN.

PCT LOG LOG
STRAIN TIME J(T)

LOAD.....
.219 0.00 -8.49
.291 .30 -8.36
.381 .60 -8.24
.521 .90 -8.11
.686 1.18 -7.99
.936 1.48 -7.85
1.303 1.78 -7.71

RECOVERY.....
1.114 0.00 -7.78
1.057 .30 -7.80
.982 .60 -7.83
.902 .90 -7.87
.812 1.18 -7.92
.706 1.48 -7.98
.604 1.78 -8.05

SUPERPOSED.....
1.333 1.79 -7.70
1.348 1.79 -7.70
1.363 1.81 -7.69
1.423 1.83 -7.67
1.491 1.88 -7.65
1.647 1.95 -7.61
1.907 2.08 -7.55

SAMPLE 118/3
25.0 DEG.

AREA = 14.90 CM.².
THICK = .0204 IN.

PCT STRAIN	LOG TIME	LOG J(T)
LOAD.....		
.215	0.00	-6.87
.372	.30	-6.63
.630	.60	-6.40
1.066	.90	-6.17
1.694	1.18	-5.97
2.877	1.48	-5.74
RECOVERY.....		
2.820	0.00	-5.75
2.777	.30	-5.76
2.720	.60	-5.77
2.627	.90	-5.78
2.534	1.18	-5.80
2.398	1.48	-5.82
SUPERPOSED.....		
3.035	1.49	-5.72
3.149	1.51	-5.70
3.349	1.53	-5.68
3.693	1.58	-5.64
4.230	1.65	-5.58
5.275	1.78	-5.48

SAMPLE 118/3
15.0 DEG.

AREA = 14.90 CM.².
THICK = .0204 IN.

PCT STRAIN	LOG TIME	LOG J(T)
LOAD.....		
.129	0.00	-7.80
.186	.30	-7.64
.265	.60	-7.48
.386	.90	-7.32
.637	1.18	-7.10
.866	1.48	-6.97
1.360	1.78	-6.77
RECOVERY.....		
1.267	0.00	-6.80
1.231	.30	-6.82
1.174	.60	-6.84
1.109	.90	-6.86
1.038	1.18	-6.89
.945	1.48	-6.93
.859	1.78	-6.97
SUPERPOSED.....		
1.396	1.79	-6.76
1.417	1.79	-6.76
1.439	1.81	-6.75
1.496	1.83	-6.73
1.675	1.88	-6.68
1.811	1.95	-6.65
2.219	2.08	-6.56

SAMPLE 118/3
5.0 DEG.

AREA = 14.90 CM.².
THICK = .0204 IN.

PCT STRAIN	LOG TIME	LOG J(T)
LOAD.....		
.229	0.00	-8.47
.293	.30	-8.36
.386	.60	-8.24
.515	.90	-8.12
.680	1.18	-8.00
.930	1.48	-7.86
1.317	1.78	-7.71
RECOVERY.....		
1.084	0.00	-7.80
1.038	.30	-7.82
.970	.60	-7.84
.895	.90	-7.88
.802	1.18	-7.93
.691	1.48	-7.99
.583	1.78	-8.07
SUPERPOSED.....		
1.313	1.79	-7.71
1.331	1.79	-7.71
1.356	1.81	-7.70
1.410	1.83	-7.68
1.481	1.88	-7.66
1.621	1.95	-7.62
1.900	2.08	-7.55

SAMPLE 118/4
25.0 DEG.

AREA = 14.75 CM.².
THICK = .0202 IN.

PCT STRAIN	LOG TIME	LOG J(T)
LOAD.....		
.136	0.00	-6.95
.220	.30	-6.74
.379	.60	-6.50
.621	.90	-6.29
.977	1.18	-6.09
1.643	1.48	-5.86
2.801	1.78	-5.63
RECOVERY.....		
2.725	0.00	-5.64
2.687	.30	-5.65
2.627	.60	-5.66
2.559	.90	-5.67
2.504	1.18	-5.68
2.453	1.48	-5.69
2.423	1.78	-5.70
SUPERPOSED.....		
2.862	1.79	-5.62
2.907	1.79	-5.62
3.005	1.81	-5.60
3.180	1.83	-5.58
3.482	1.88	-5.54
4.096	1.95	-5.47
5.224	2.08	-5.36

SAMPLE 118/4
15.0 DEG.

AREA = 14.75 CM.².
THICK = .0202 IN.

PCT STRAIN	LOG TIME	LOG J(T)
LOAD.....		
.144	0.00	-7.75
.216	.30	-7.58
.324	.60	-7.40
.497	.90	-7.22
.743	1.18	-7.04
1.168	1.48	-6.84
1.867	1.78	-6.64
RECOVERY.....		
1.752	0.00	-6.67
1.702	.30	-6.68
1.637	.60	-6.70
1.550	.90	-6.72
1.456	1.18	-6.75
1.327	1.48	-6.79
1.175	1.78	-6.84
SUPERPOSED.....		
1.896	1.79	-6.63
1.918	1.79	-6.63
1.961	1.81	-6.62
2.048	1.83	-6.60
2.199	1.88	-6.57
2.495	1.95	-6.51
3.043	2.08	-6.43

SAMPLE 118/4
5.0 DEG.

AREA = 14.75 CM.².
THICK = .0202 IN.

PCT STRAIN	LOG TIME	LOG J(T)
LOAD.....		
.213	0.00	-8.50
.270	.30	-8.40
.360	.60	-8.27
.476	.90	-8.15
.634	1.18	-8.03
.880	1.48	-7.89
1.247	1.78	-7.73
RECOVERY.....		
1.060	0.00	-7.81
1.004	.30	-7.83
.937	.60	-7.86
.858	.90	-7.90
.771	1.18	-7.94
.667	1.48	-8.01
.562	1.78	-8.08
SUPERPOSED.....		
1.273	1.79	-7.73
1.276	1.79	-7.72
1.298	1.81	-7.72
1.334	1.83	-7.71
1.406	1.88	-7.68
1.547	1.95	-7.64
1.810	2.08	-7.57

SAMPLE 119/1
25.0 DEG.

AREA = 9.37 CM.SQ.
THICK = .0404 IN.

PCT LOG LOG
STRAIN TIME J(T)

LOAD.....
.134 0.00 -7.85
.234 .30 -7.61
.371 .60 -7.42
.606 .90 -7.20
.939 1.18 -7.01
1.582 1.48 -6.79
2.652 1.78 -6.56

RECOVERY.....
2.559 0.00 -6.58
2.497 .30 -6.59
2.435 .60 -6.60
2.336 .90 -6.62
2.213 1.18 -6.64
2.015 1.48 -6.68
1.755 1.78 -6.74

SUPERPOSED.....
2.695 1.79 -6.56
2.732 1.79 -6.55
2.804 1.81 -6.54
2.942 1.83 -6.52
3.152 1.88 -6.49
3.597 1.95 -6.43
4.413 2.08 -6.34

SAMPLE 119/1
15.0 DEG.

AREA = 9.37 CM.SQ.
THICK = .0404 IN.

PCT LOG LOG
STRAIN TIME J(T)

LOAD.....
.07 0.00 -8.72
.101 .30 -8.58
.144 .60 -8.42
.213 .90 -8.26
.302 1.18 -8.11
.462 1.48 -7.92
.710 1.78 -7.74

RECOVERY.....
.672 0.00 -7.76
.650 .30 -7.77
.621 .60 -7.79
.586 .90 -7.82
.541 1.18 -7.85
.489 1.48 -7.90
.420 1.78 -7.96

SUPERPOSED.....
.747 1.79 -7.71
.752 1.79 -7.71
.766 1.81 -7.70
.799 1.83 -7.69
.843 1.88 -7.66
.952 1.95 -7.61
1.130 2.08 -7.53

SAMPLE 119/1
5.0 DEG.

AREA = 9.37 CM.SQ.
THICK = .0404 IN.

PCT LOG LOG
STRAIN TIME J(T)

LOAD.....
.047 0.00 -9.45
.061 .30 -9.74
.080 .60 -9.22
.110 .90 -9.08
.144 1.18 -8.95
.210 1.48 -8.80
.292 1.78 -8.65

RECOVERY.....
.250 0.00 -8.73
.236 .30 -8.75
.224 .60 -8.77
.204 .90 -8.81
.183 1.18 -8.86
.154 1.48 -8.93
.127 1.78 -9.02

SUPERPOSED.....
.297 1.79 -8.05
.297 1.79 -8.45
.304 1.81 -8.64
.314 1.83 -8.63
.331 1.88 -8.60
.366 1.95 -8.56
.425 2.08 -8.49

SAMPLE 119/2
25.0 DEG.

AREA = 9.75 CM.SQ.
THICK = .0403 IN.

PCT LOG LOG
STRAIN TIME J(T)

LOAD.....
.055 0.00 -7.94
.089 .30 -7.73
.129 .60 -7.57
.198 .90 -7.38
.287 1.18 -7.22
.434 1.48 -7.04
.679 1.78 -6.85

RECOVERY.....
.649 0.00 -6.87
.639 .30 -6.87
.610 .60 -6.89
.585 .90 -6.91
.550 1.18 -6.94
.511 1.48 -6.97
.476 1.78 -7.00

SUPERPOSED.....
.704 1.79 -6.83
.729 1.79 -6.82
.739 1.81 -6.81
.783 1.83 -6.79
.838 1.88 -6.76
.947 1.95 -6.70
1.155 2.08 -6.62

SAMPLE 119/2
15.0 DEG.

AREA = 9.75 CM.SQ.
THICK = .0403 IN.

PCT LOG LOG
STRAIN TIME J(T)

LOAD.....
.062 0.00 -8.78
.082 .30 -8.66
.114 .60 -8.51
.166 .90 -8.35
.224 1.18 -8.22
.332 1.48 -8.05
.494 1.78 -7.88

RECOVERY.....
.444 0.00 -7.92
.421 .30 -7.95
.397 .60 -7.97
.367 .90 -8.01
.330 1.18 -8.05
.290 1.48 -8.11
.245 1.78 -8.18

SUPERPOSED.....
.506 1.79 -7.87
.503 1.79 -7.87
.517 1.81 -7.86
.533 1.83 -7.85
.555 1.88 -7.83
.622 1.95 -7.78
.741 2.08 -7.70

SAMPLE 119/2
5.0 DEG.

AREA = 9.75 CM.SQ.
THICK = .0403 IN.

PCT LOG LOG
STRAIN TIME J(T)

LOAD.....
.058 0.00 -9.33
.071 .30 -9.25
.080 .60 -9.15
.116 .90 -9.03
.150 1.18 -8.92
.204 1.48 -8.79
.275 1.78 -8.66

RECOVERY.....
.223 0.00 -8.75
.211 .30 -8.77
.197 .60 -8.80
.176 .90 -8.85
.150 1.18 -8.90
.136 1.48 -8.96
.118 1.78 -9.03

SUPERPOSED.....
.281 1.79 -8.65
.281 1.79 -8.45
.286 1.81 -8.64
.292 1.83 -8.63
.300 1.88 -8.61
.341 1.95 -8.57
.393 2.08 -8.50

SAMPLE 119/3
25.0 DEG.
AREA = 0.50 CM.².
THICK = .0204 IN.

PCT LOG LOG
STRAIN TIME J(T)

LOAD.....
.068 0.00 -7.99
.094 .30 -7.84
.166 .60 -7.61
.254 .90 -7.42
.391 1.18 -7.23
.577 1.48 -7.07
.861 1.78 -6.89

RECOVERY.....
.802 0.00 -6.92
.782 .30 -6.93
.767 .60 -6.94
.704 .90 -6.98
.685 1.18 -6.99
.597 1.48 -7.05
.538 1.78 -7.10

SUPERPOSED.....
.870 1.79 -6.89
.880 1.79 -6.88
.924 1.81 -6.86
.958 1.83 -6.84
1.074 1.88 -6.79
1.174 1.95 -6.76
1.399 2.08 -6.68

SAMPLE 119/3
15.0 DEG.
AREA = 0.50 CM.².
THICK = .0204 IN.

PCT LOG LOG
STRAIN TIME J(T)

LOAD.....
.122 0.00 -8.79
.161 .30 -8.67
.244 .60 -8.49
.347 .90 -8.34
.499 1.18 -8.18
.763 1.48 -8.00
1.169 1.78 -7.81

RECOVERY.....
1.066 0.00 -7.85
1.027 .30 -7.87
.978 .60 -7.89
.924 .90 -7.92
.846 1.18 -7.95
.760 1.48 -8.00
.685 1.78 -8.05

SUPERPOSED.....
1.188 1.79 -7.81
1.188 1.79 -7.81
1.222 1.81 -7.79
1.271 1.83 -7.78
1.345 1.88 -7.75
1.531 1.95 -7.70
1.853 2.08 -7.61

SAMPLE 119/3
5.0 DEG.
AREA = 0.50 CM.².
THICK = .0204 IN.

PCT LOG LOG
STRAIN TIME J(T)

LOAD.....
.120 0.00 -9.74
.147 .30 -9.25
.181 .60 -9.16
.232 .90 -9.05
.294 1.18 -8.95
.390 1.48 -8.82
.555 1.78 -8.67

RECOVERY.....
.443 0.00 -8.77
.414 .30 -8.80
.391 .60 -8.82
.352 .90 -8.87
.310 1.18 -8.91
.260 1.48 -8.99
.244 1.78 -9.03

SUPERPOSED.....
.562 1.79 -8.87
.565 1.79 -8.87
.572 1.81 -8.86
.584 1.83 -8.85
.614 1.88 -8.83
.667 1.95 -8.59
.800 2.08 -8.51

SAMPLE 119/4
25.0 DEG.
AREA = 0.45 CM.².
THICK = .0200 IN.

PCT LOG LOG
STRAIN TIME J(T)

LOAD.....
.100 0.00 -7.99
.165 .30 -7.78
.275 .60 -7.55
.450 .90 -7.34
.700 1.18 -7.15
1.105 1.48 -6.95
1.790 1.78 -6.74

RECOVERY.....
1.745 0.00 -6.75
1.700 .30 -6.76
1.645 .60 -6.78
1.565 .90 -6.80
1.485 1.18 -6.82
1.365 1.48 -6.86
1.250 1.78 -6.90

SUPERPOSED.....
1.845 1.79 -6.73
1.865 1.79 -6.72
1.920 1.81 -6.71
2.015 1.83 -6.69
2.185 1.88 -6.65
2.470 1.95 -6.60
3.040 2.08 -6.51

SAMPLE 119/4
15.0 DEG.
AREA = 0.45 CM.².
THICK = .0200 IN.

PCT LOG LOG
STRAIN TIME J(T)

LOAD.....
.115 0.00 -8.83
.160 .30 -8.68
.240 .60 -8.51
.345 .90 -8.35
.490 1.18 -8.20
.725 1.48 -8.03
1.105 1.78 -7.84

RECOVERY.....
1.000 0.00 -7.89
.960 .30 -7.91
.915 .60 -7.93
.850 .90 -7.96
.785 1.18 -7.99
.675 1.48 -8.06
.590 1.78 -8.12

SUPERPOSED.....
1.115 1.79 -7.84
1.120 1.79 -7.84
1.155 1.81 -7.83
1.195 1.83 -7.81
1.275 1.88 -7.78
1.400 1.95 -7.74
1.695 2.08 -7.66

SAMPLE 119/4
5.0 DEG.
AREA = 0.45 CM.².
THICK = .0200 IN.

PCT LOG LOG
STRAIN TIME J(T)

LOAD.....
.107 0.00 -9.39
.137 .30 -9.28
.175 .60 -9.18
.220 .90 -9.06
.300 1.18 -8.94
.400 1.48 -8.82
.565 1.78 -8.67

RECOVERY.....
.452 0.00 -8.77
.430 .30 -8.79
.400 .60 -8.82
.362 .90 -8.86
.322 1.18 -8.91
.272 1.48 -8.99
.222 1.78 -9.07

SUPERPOSED.....
.560 1.79 -8.87
.567 1.79 -8.87
.575 1.81 -8.86
.590 1.83 -8.85
.622 1.88 -8.83
.672 1.95 -8.59
.787 2.08 -8.53

SAMPLE 120/4
25.0 DEG.

AREA = 9.95 CM.².
THICK = .0398 IN.

PCT LOG LOG
STRAIN TIME J(T)

LOAD.....
.078 0.00 -8.09
.121 .30 -7.90
.181 .60 -7.72
.274 .90 -7.54
.402 1.18 -7.37
.613 1.48 -7.19
.947 1.78 -7.00

RECOVERY.....
.867 0.00 -7.04
.837 .30 -7.05
.799 .60 -7.07
.739 .90 -7.11
.678 1.18 -7.15
.593 1.48 -7.20
.503 1.78 -7.28

SUPERPOSED.....
.945 1.79 -7.00
.957 1.79 -7.00
.980 1.81 -6.99
1.013 1.83 -6.97
1.080 1.88 -6.94
1.206 1.95 -6.90
1.450 2.08 -6.82

SAMPLE 120/4
15.0 DEG.

AREA = 9.95 CM.².
THICK = .0398 IN.

PCT LOG LOG
STRAIN TIME J(T)

LOAD.....
.101 0.00 -8.68
.138 .30 -8.54
.193 .60 -8.40
.274 .90 -8.25
.379 1.18 -8.11
.553 1.48 -7.94
.817 1.78 -7.77

RECOVERY.....
.731 0.00 -7.82
.704 .30 -7.84
.671 .60 -7.86
.628 .90 -7.89
.578 1.18 -7.92
.520 1.48 -7.97
.457 1.78 -8.02

SUPERPOSED.....
.832 1.79 -7.76
.842 1.79 -7.76
.864 1.81 -7.75
.902 1.83 -7.73
.957 1.88 -7.70
1.073 1.95 -7.65
1.274 2.08 -7.58

SAMPLE 120/4
5.0 DEG.

AREA = 9.95 CM.².
THICK = .0398 IN.

PCT LOG LOG
STRAIN TIME J(T)

LOAD.....
.050 0.00 -9.40
.062 .30 -9.31
.077 .60 -9.21
.099 .90 -9.10
.126 1.18 -9.00
.168 1.48 -8.87
.227 1.78 -8.74

RECOVERY.....
.177 0.00 -8.85
.167 .30 -8.88
.153 .60 -8.91
.138 .90 -8.96
.122 1.18 -9.01
.102 1.48 -9.09
.080 1.78 -9.19

SUPERPOSED.....
.227 1.79 -8.74
.229 1.79 -8.74
.230 1.81 -8.74
.237 1.83 -8.72
.247 1.88 -8.70
.270 1.95 -8.67
.308 2.08 -8.61

SAMPLE 120/1
15.0 DEG.

AREA = 10.17 CM.².
THICK = .0404 IN.

PCT LOG LOG
STRAIN TIME J(T)

LOAD.....
.082 0.00 -8.76
.106 .30 -8.64
.149 .60 -8.50
.203 .90 -8.36
.277 1.18 -8.23
.396 1.48 -8.07
.574 1.78 -7.91

RECOVERY.....
.512 0.00 -7.96
.493 .30 -7.98
.455 .60 -8.00
.428 .90 -8.04
.396 1.18 -8.07
.351 1.48 -8.12

SUPERPOSED.....
.594 1.79 -7.90
.599 1.79 -7.89
.614 1.81 -7.88
.631 1.83 -7.87
.673 1.88 -7.84
.748 1.95 -7.80

SAMPLE 120/1
5.0 DEG.

AREA = 10.17 CM.².
THICK = .0403 IN.

PCT LOG LOG
STRAIN TIME J(T)

LOAD.....
.048 0.00 -9.54
.064 .30 -9.42
.077 .60 -9.34
.109 .90 -9.19
.140 1.18 -9.08
.188 1.48 -8.95
.263 1.78 -8.81

RECOVERY.....
.214 0.00 -8.89
.203 .30 -8.92
.188 .60 -8.95
.172 .90 -8.99
.150 1.18 -9.05
.130 1.48 -9.11
.109 1.78 -9.19

SUPERPOSED.....
.263 1.79 -8.81
.268 1.79 -8.80
.265 1.81 -8.80
.281 1.83 -8.78
.290 1.88 -8.76
.318 1.95 -8.72
.372 2.08 -8.65

SAMPLE 121/2
25.0 DEG.
AREA = 9.61 CM.SQ.
THICK = .0403 IN.

PCT STRAIN	LOG TIME	LOG J(T)
LOAD.....		
.076	0.00	-8.09
.107	.30	-7.94
.150	.60	-7.77
.237	.90	-7.59
.347	1.18	-7.43
.532	1.48	-7.24
.813	1.78	-7.06

PCT STRAIN	LOG TIME	LOG J(T)
RECOVERY.....		
.753	0.00	-7.09
.730	.30	-7.10
.696	.60	-7.12
.651	.90	-7.15
.602	1.18	-7.19
.547	1.48	-7.23
.482	1.78	-7.28

PCT STRAIN	LOG TIME	LOG J(T)
SUPERPOSED.....		
.820	1.79	-7.05
.836	1.79	-7.04
.855	1.81	-7.03
.888	1.83	-7.02
.948	1.88	-6.99
1.079	1.95	-6.93
1.295	2.08	-6.85

SAMPLE 121/2
15.0 DEG.
AREA = 9.61 CM.SQ.
THICK = .0403 IN.

PCT STRAIN	LOG TIME	LOG J(T)
LOAD.....		
.072	0.00	-8.84
.098	.30	-8.70
.136	.60	-8.56
.189	.90	-8.42
.261	1.18	-8.28
.376	1.48	-8.12
.496	1.78	-8.00

PCT STRAIN	LOG TIME	LOG J(T)
RECOVERY.....		
.434	0.00	-8.06
.413	.30	-8.08
.387	.60	-8.11
.357	.90	-8.14
.323	1.18	-8.19
.283	1.48	-8.24
.246	1.78	-8.31

PCT STRAIN	LOG TIME	LOG J(T)
SUPERPOSED.....		
.506	1.79	-7.99
.511	1.79	-7.99
.524	1.81	-7.98
.546	1.83	-7.96
.583	1.88	-7.93
.659	1.95	-7.88
.742	2.08	-7.83

SAMPLE 121/2
5.0 DEG.
AREA = 9.61 CM.SQ.
THICK = .0403 IN.

PCT STRAIN	LOG TIME	LOG J(T)
LOAD.....		
.060	0.00	-9.48
.076	.30	-9.39
.097	.60	-9.29
.118	.90	-9.19
.150	1.18	-9.08
.201	1.48	-8.96
.277	1.78	-8.82

PCT STRAIN	LOG TIME	LOG J(T)
RECOVERY.....		
.223	0.00	-8.91
.211	.30	-8.94
.197	.60	-8.96
.177	.90	-9.01
.150	1.18	-9.06
.138	1.48	-9.12
.118	1.78	-9.19

PCT STRAIN	LOG TIME	LOG J(T)
SUPERPOSED.....		
.283	1.79	-8.81
.285	1.79	-8.80
.290	1.81	-8.80
.295	1.83	-8.79
.309	1.88	-8.77
.339	1.95	-8.73
.395	2.08	-8.66

SAMPLE 121/3
25.0 DEG.
AREA = 10.11 CM.SQ.
THICK = .0402 IN.

PCT STRAIN	LOG TIME	LOG J(T)
LOAD.....		
.052	0.00	-8.23
.078	.30	-8.05
.118	.60	-7.87
.180	.90	-7.69
.259	1.18	-7.53
.387	1.48	-7.36
.569	1.78	-7.19

PCT STRAIN	LOG TIME	LOG J(T)
RECOVERY.....		
.520	0.00	-7.23
.496	.30	-7.25
.470	.60	-7.27
.436	.90	-7.31
.394	1.18	-7.35
.345	1.48	-7.41
.295	1.78	-7.47

PCT STRAIN	LOG TIME	LOG J(T)
SUPERPOSED.....		
.572	1.79	-7.19
.575	1.79	-7.19
.588	1.81	-7.18
.616	1.83	-7.15
.653	1.88	-7.13
.731	1.95	-7.08
.865	2.08	-7.01

SAMPLE 121/3
15.0 DEG.
AREA = 10.11 CM.SQ.
THICK = .0402 IN.

PCT STRAIN	LOG TIME	LOG J(T)
LOAD.....		
.039	0.00	-8.97
.056	.30	-8.80
.078	.60	-8.66
.112	.90	-8.50
.153	1.18	-8.37
.221	1.48	-8.21
.313	1.78	-8.06

PCT STRAIN	LOG TIME	LOG J(T)
RECOVERY.....		
.274	0.00	-8.11
.260	.30	-8.14
.243	.60	-8.17
.219	.90	-8.21
.195	1.18	-8.26
.163	1.48	-8.34
.129	1.78	-8.44

PCT STRAIN	LOG TIME	LOG J(T)
SUPERPOSED.....		
.312	1.79	-8.06
.316	1.79	-8.05
.321	1.81	-8.05
.331	1.83	-8.03
.348	1.88	-8.01
.384	1.95	-7.97
.443	2.08	-7.91

SAMPLE 121/3
5.0 DEG.
AREA = 10.11 CM.SQ.
THICK = .0402 IN.

PCT STRAIN	LOG TIME	LOG J(T)
LOAD.....		
.056	0.00	-9.49
.071	.30	-9.38
.087	.60	-9.29
.112	.90	-9.19
.144	1.18	-9.07
.193	1.48	-8.95
.261	1.78	-8.82

PCT STRAIN	LOG TIME	LOG J(T)
RECOVERY.....		
.205	0.00	-8.92
.193	.30	-8.95
.170	.60	-8.98
.162	.90	-9.03
.143	1.18	-9.08
.122	1.48	-9.15
.100	1.78	-9.24

PCT STRAIN	LOG TIME	LOG J(T)
SUPERPOSED.....		
.261	1.79	-8.82
.264	1.79	-8.81
.266	1.81	-8.81
.274	1.83	-8.80
.287	1.88	-8.78
.315	1.95	-8.74
.361	2.08	-8.68

SAMPLE 122/1
25.0 DEG.
AREA = 17.40 CM.SQ.
THICK = .0203 IN.

PCT LOG LOG
STRAIN TIME J(T)

LOAD.....
.118 0.00 -6.54
.207 .30 -6.29
.394 .60 -6.01
.720 .90 -5.75
1.291 1.18 -5.50
2.414 1.48 -5.23
4.631 1.78 -4.94

SAMPLE 122/1
15.0 DEG.
AREA = 17.40 CM.SQ.
THICK = .0203 IN.

PCT LOG LOG
STRAIN TIME J(T)

LOAD.....
.064 0.00 -7.12
.112 .30 -7.48
.202 .60 -7.22
.369 .90 -6.96
.640 1.18 -6.72
1.197 1.48 -6.45
1.970 1.72 -6.24

SAMPLE 122/1
5.0 DEG.
AREA = 17.40 CM.SQ.
THICK = .0203 IN.

PCT LOG LOG
STRAIN TIME J(T)

LOAD.....
.133 0.00 -8.63
.192 .30 -8.48
.276 .60 -8.32
.419 .90 -8.14
.634 1.18 -7.96
1.025 1.48 -7.75
1.684 1.78 -7.53

RECOVERY.....
1.956 0.00 -6.24
1.941 .30 -6.24
1.921 .60 -6.25
1.897 .90 -6.25
1.872 1.18 -6.24
1.833 1.48 -6.27

SUPERPOSED.....
2.020 1.73 -6.22
2.054 1.74 -6.22
2.123 1.76 -6.20
2.266 1.79 -6.17
2.512 1.83 -6.13
3.030 1.92 -6.05

RECOVERY.....
1.576 0.00 -7.56
1.537 .30 -7.57
1.484 .60 -7.59
1.433 .90 -7.60
1.370 1.18 -7.62
1.291 1.48 -7.65
1.217 1.78 -7.67

SUPERPOSED.....
1.704 1.79 -7.53
1.729 1.79 -7.52
1.764 1.81 -7.51
1.852 1.83 -7.49
2.015 1.88 -7.45
2.315 1.95 -7.39
2.901 2.08 -7.30

SAMPLE 122/2
25.0 DEG.

AREA = 18.77 CM.SQ.
THICK = .0200 IN.

PCT LOG LOG
STRAIN TIME J(T)

LOAD.....
.084 0.00 -6.58
.157 .30 -6.30
.314 .60 -6.00
.587 .90 -5.73
1.047 1.18 -5.48
1.959 1.48 -5.21
3.666 1.78 -4.93

RECOVERY.....
3.655 0.00 -4.94
3.655 .30 -4.94
3.645 .60 -4.94
3.645 .90 -4.94
3.645 1.18 -4.94
3.645 1.48 -4.94
3.645 1.78 -4.94

SUPERPOSED.....
3.730 1.79 -4.93
3.812 1.79 -4.92
3.950 1.81 -4.90
4.231 1.83 -4.87
4.692 1.88 -4.83
5.603 1.95 -4.75
7.311 2.08 -4.63

SAMPLE 122/2
25.0 DEG.

AREA = 18.77 CM.SQ.
THICK = .0200 IN.

PCT LOG LOG
STRAIN TIME J(T)

LOAD.....
.259 .40 -6.85
.429 .10 -6.64
.738 .18 -6.40
1.377 .48 -6.13
2.584 .78 -5.86

RECOVERY.....
2.554 .40 -5.86
2.524 .10 -5.87
2.484 .18 -5.87
2.454 .48 -5.88
2.424 .78 -5.88

SUPERPOSED.....
2.813 .81 -5.82
2.953 .83 -5.80
3.222 .88 -5.76
3.830 .95 -5.68
5.007 1.08 -5.57

SAMPLE 122/2
15.0 DEG.

AREA = 18.77 CM.SQ.
THICK = .0200 IN.

PCT LOG LOG
STRAIN TIME J(T)

LOAD.....
.045 0.00 -7.76
.075 .30 -7.54
.145 .60 -7.25
.264 .90 -6.99
.469 1.18 -6.74
.888 1.48 -6.47
1.696 1.78 -6.19

RECOVERY.....
1.681 0.00 -6.19
1.676 .30 -6.19
1.661 .60 -6.19
1.641 .90 -6.20
1.614 1.18 -6.21
1.581 1.48 -6.22
1.541 1.78 -6.23

SUPERPOSED.....
1.726 1.79 -6.18
1.751 1.79 -6.17
1.805 1.81 -6.16
1.905 1.83 -6.14
2.085 1.88 -6.10
2.469 1.95 -6.02
3.237 2.08 -5.90

SAMPLE 122/2
5.0 DEG.

AREA = 18.77 CM.SQ.
THICK = .0200 IN.

PCT LOG LOG
STRAIN TIME J(T)

LOAD.....
.150 0.00 -8.63
.214 .30 -8.48
.324 .60 -8.30
.499 .90 -8.11
.763 1.18 -7.93
1.247 1.48 -7.71
2.045 1.78 -7.50

RECOVERY.....
1.905 0.00 -7.53
1.865 .30 -7.54
1.815 .60 -7.55
1.746 .90 -7.57
1.661 1.18 -7.59
1.556 1.48 -7.62
1.446 1.78 -7.65

SUPERPOSED.....
2.055 1.77 -7.50
2.080 1.78 -7.49
2.140 1.79 -7.48
2.244 1.82 -7.46
2.424 1.86 -7.42
2.803 1.94 -7.35
3.491 2.06 -7.27

SAMPLE 123/3
25.0 DEG.

AREA = 17.55 CM.².
THICK = .0203 IN.

PCT LOG LOG
STRAIN TIME J(T)

LOAD.....
.079 0.00 -5.59
.129 .30 -6.37
.236 .60 -6.11
.433 .90 -5.85
.768 1.18 -5.40
1.458 1.48 -5.32
2.660 1.78 -5.06

RECOVERY.....
2.650 0.00 -5.06
2.640 .30 -5.06
2.631 .60 -5.06
2.611 .90 -5.07
2.611 1.18 -5.07
2.611 1.48 -5.07
2.611 1.78 -5.07

SUPERPOSED.....
2.720 1.79 -5.05
2.768 1.79 -5.04
2.867 1.81 -5.02
3.044 1.83 -5.00
3.379 1.88 -4.95
4.069 1.95 -4.87
5.271 2.08 -4.76

SAMPLE 123/3
25.0 DEG.

AREA = 17.55 CM.².
THICK = .0203 IN.

PCT LOG LOG
STRAIN TIME J(T)

LOAD.....
.138 0.00 -6.68
.274 .30 -6.38
.483 .60 -6.14
.906 .90 -5.86
1.655 1.18 -5.40
3.143 1.48 -5.32
3.704 1.56 -5.25

RECOVERY.....
3.675 0.00 -5.25
3.645 .30 -5.26
3.626 .60 -5.26
3.594 .90 -5.26
3.576 1.18 -5.27
3.567 1.48 -5.27

SUPERPOSED.....
3.813 1.57 -5.24
3.921 1.58 -5.23
4.108 1.60 -5.21
4.504 1.64 -5.17
5.232 1.71 -5.10
6.709 1.82 -4.99

SAMPLE 123/3
15.0 DEG.

AREA = 17.55 CM.².
THICK = .0203 IN.

PCT LOG LOG
STRAIN TIME J(T)

LOAD.....
.074 0.00 -7.75
.113 .30 -7.56
.197 .60 -7.32
.345 .90 -7.08
.596 1.18 -6.84
1.099 1.48 -6.57
1.974 1.76 -6.32

RECOVERY.....
1.936 0.00 -6.33
1.921 .30 -6.33
1.904 .60 -6.33
1.872 .90 -6.34
1.837 1.18 -6.35
1.793 1.48 -6.36

SUPERPOSED.....
2.010 1.77 -6.31
2.034 1.78 -6.31
2.103 1.79 -6.29
2.217 1.82 -6.27
2.433 1.86 -6.23
2.892 1.94 -6.15

SAMPLE 123/3
5.0 DEG.

AREA = 17.55 CM.².
THICK = .0203 IN.

PCT LOG LOG
STRAIN TIME J(T)

LOAD.....
.153 0.00 -8.46
.217 .30 -8.51
.310 .60 -8.36
.458 .90 -8.19
.675 1.18 -8.02
1.074 1.48 -7.82
1.724 1.78 -7.61

RECOVERY.....
1.611 0.00 -7.84
1.567 .30 -7.68
1.522 .60 -7.46
1.463 .90 -7.46
1.394 1.18 -7.70
1.054 1.48 -7.82
.975 1.78 -7.86

SUPERPOSED.....
1.764 1.79 -7.60
1.782 1.79 -7.60
1.833 1.81 -7.58
1.921 1.83 -7.56
2.069 1.88 -7.53
2.128 1.95 -7.52
2.700 2.08 -7.42

SAMPLE 123/4
25.0 DEG.

AREA = 19.39 CM.².
THICK = .0199 IN.

PCT LOG LOG
STRAIN TIME J(T)

LOAD.....
.060 0.00 -6.79
.111 .30 -6.53
.242 .60 -6.19
.474 .90 -5.89
.854 1.18 -5.64
1.703 1.48 -5.34
3.305 1.78 -5.05
4.534 1.92 -4.91

RECOVERY.....
4.494 0.00 -4.82
4.474 .30 -4.92
4.453 .60 -4.92
4.423 .90 -4.92
4.383 1.18 -4.93
4.302 1.48 -4.94
4.171 1.78 -4.95
4.060 1.92 -4.96

SUPERPOSED.....
4.554 1.93 -4.91
4.584 1.93 -4.91
4.695 1.94 -4.90
4.897 1.96 -4.88
5.239 2.00 -4.85
6.005 2.06 -4.79
7.476 2.16 -4.70
8.594 2.23 -4.64

SAMPLE 123/4
15.0 DEG.

AREA = 19.39 CM.².
THICK = .0199 IN.

PCT LOG LOG
STRAIN TIME J(T)

LOAD.....
.040 0.00 -7.77
.065 .30 -7.56
.106 .60 -7.35
.202 .90 -7.07
.338 1.18 -6.85
.594 1.48 -6.60
1.134 1.78 -6.32

RECOVERY.....
1.100 0.00 -6.33
1.103 .30 -6.33
1.093 .60 -6.34
1.064 .90 -6.35
1.048 1.18 -6.36
1.008 1.48 -6.37
.977 1.78 -6.39

SUPERPOSED.....
1.149 1.79 -6.32
1.169 1.79 -6.31
1.199 1.81 -6.30
1.270 1.83 -6.27
1.385 1.88 -6.24
1.602 1.95 -6.17
2.111 2.08 -6.05

SAMPLE 123/4
5.0 DEG.

AREA = 19.39 CM.².
THICK = .0199 IN.

PCT LOG LOG
STRAIN TIME J(T)

LOAD.....
.166 0.00 -8.66
.227 .30 -8.52
.322 .60 -8.37
.479 .90 -8.20
.710 1.18 -8.03
1.108 1.48 -7.84
1.809 1.78 -7.62

RECOVERY.....
1.683 0.00 -7.65
1.647 .30 -7.66
1.587 .60 -7.68
1.521 .90 -7.70
1.446 1.18 -7.72
1.350 1.48 -7.75
1.254 1.78 -7.78

SUPERPOSED.....
1.840 1.79 -7.61
1.874 1.79 -7.61
1.909 1.81 -7.60
2.000 1.83 -7.58
2.154 1.88 -7.55
2.458 1.95 -7.49
3.063 2.08 -7.39

SAMPLE 124/1
25.0 DEG.

AREA = 0.3R CM.SQ.
THICK = .0402 IN.

PCT LOG LOG
STRAIN TIME J(T)

LOAD.....
.129 0.00 -7.60
.243 .30 -7.32
.452 .60 -7.05
.845 .90 -6.78
1.84R 1.30 -6.44

RECOVERY.....
1.80R 0.00 -6.45
1.77R .30 -6.46
1.74R .60 -6.46
1.70R .90 -6.48
1.60R 1.30 -6.50

SUPERPOSED.....
1.93R 1.32 -6.42
2.02R 1.34 -6.40
2.201 1.38 -6.36
2.54R 1.45 -6.30
3.44R 1.60 -6.17

SAMPLE 124/1
25.0 DEG.

AREA = 0.3R CM.SQ.
THICK = .0402 IN.

PCT LOG LOG
STRAIN TIME J(T)

LOAD.....
.08R 0.00 -7.45
.157 .30 -7.18
.271 .60 -6.94
.511 .90 -6.66
1.90R 1.1R -6.41
2.17R 1.60 -6.04

RECOVERY.....
2.15R 0.00 -6.04
2.13R .30 -6.04
2.12R .60 -6.04
2.10R .90 -6.05
2.08R 1.1R -6.05
2.07R 1.60 -6.06

SUPERPOSED.....
2.23R 1.61 -6.02
2.29R 1.62 -6.01
2.40R 1.64 -5.99
2.61R 1.68 -5.96
2.99R 1.74 -5.90
4.24R 1.90 -5.74

SAMPLE 124/1
25.0 DEG.

AREA = 0.3R CM.SQ.
THICK = .0402 IN.

PCT LOG LOG
STRAIN TIME J(T)

LOAD.....
.052 0.00 -7.40
.094 .30 -7.14
.157 .60 -6.92
.282 .90 -6.66
.501 1.1R -6.42
.944 1.4R -6.14
1.92R 1.81 -5.83

RECOVERY.....
1.89R 0.00 -5.84
1.89R .30 -5.84
1.88R .60 -5.84
1.87R .90 -5.84
1.87R 1.1R -5.84

SUPERPOSED.....
1.951 1.82 -5.82
1.98R 1.83 -5.82
2.04R 1.84 -5.80
2.16R 1.86 -5.78
2.37R 1.90 -5.74

SAMPLE 124/1
15.0 DEG.

AREA = 0.3R CM.SQ.
THICK = .0402 IN.

PCT LOG LOG
STRAIN TIME J(T)

LOAD.....
.029 0.00 -8.63
.052 .30 -8.17
.08R .60 -8.15
.151 .90 -7.91
.25R 1.1R -7.48
.454 1.4R -7.43
.874 1.81 -7.14

RECOVERY.....
.85R 0.00 -7.15
.84R .30 -7.16
.837 .60 -7.16
.83R .90 -7.17
.80R 1.1R -7.18
.782 1.4R -7.19
.764 1.81 -7.20

SUPERPOSED.....
.88R 1.82 -7.14
.892 1.83 -7.14
.923 1.84 -7.12
.981 1.86 -7.09
1.062 1.90 -7.06
1.237 1.98 -6.99
1.63R 2.11 -6.87

SAMPLE 124/1
5.0 DEG.

AREA = 0.3R CM.SQ.
THICK = .0402 IN.

PCT LOG LOG
STRAIN TIME J(T)

LOAD.....
.08R 0.00 -9.34
.117 .30 -9.23
.157 .60 -9.10
.224 .90 -8.94
.32R 1.1R -8.78
.502 1.4R -8.59
.79R 1.7R -8.39

RECOVERY.....
.72R 0.00 -8.44
.701 .30 -8.45
.67R .60 -8.46
.64R .90 -8.48
.621 1.1R -8.50
.574 1.4R -8.53
.542 1.7R -8.56

SUPERPOSED.....
.81R 1.79 -8.39
.817 1.79 -8.38
.83R 1.81 -8.37
.87R 1.83 -8.35
.947 1.88 -8.32
1.07R 1.95 -8.26
1.337 2.08 -8.17

SAMPLE 124/1
25.0 DEG.

AREA = 0.3R CM.SQ.
THICK = .0402 IN.

PCT LOG LOG
STRAIN TIME J(T)

LOAD.....
.08R 0.00 -7.48
.14R .30 -7.25
.281 .60 -6.98
.542 .90 -6.69
.944 1.1R -6.45
1.923 1.52 -6.14

RECOVERY.....
1.89R 0.00 -6.15
1.88R .30 -6.15
1.87R .60 -6.15
1.863 .90 -6.16
1.84R 1.1R -6.16
1.84R 1.52 -6.16

SUPERPOSED.....
1.98R 1.53 -6.13
2.037 1.54 -6.12
2.161 1.57 -6.09
2.405 1.61 -6.05
2.797 1.68 -5.98
3.771 1.82 -5.85

SAMPLE 124/3
25.0 DEG.

AREA = 10.42 CM.SQ.
THICK = .0399 IN.

PCT LOG LOG
STRAIN TIME J(T)

LOAD.....
.024 0.00 -7.63
.053 .30 -7.32
.10R .60 -7.02
.211 .90 -6.72
.36R 1.1R -6.48
.732 1.4R -6.18
1.52R 1.82 -5.86

RECOVERY.....
1.52R 0.00 -5.86
1.52R .30 -5.86
1.52R .60 -5.86
1.52R .90 -5.86
1.52R 1.1R -5.86
1.52R 1.4R -5.86
1.52R 1.82 -5.86

SUPERPOSED.....
1.553 1.83 -5.85
1.57R 1.83 -5.85
1.632 1.85 -5.83
1.737 1.87 -5.81
1.89 1.91 -5.77
2.25R 1.98 -5.69
3.051 2.12 -5.54

SAMPLE 124/3
15.0 DEG.

AREA = 10.42 CM.SQ.
THICK = .0399 IN.

PCT LOG LOG
STRAIN TIME J(T)

LOAD.....
.029 0.00 -8.69
.05R .30 -8.35
.07R .60 -8.15
.132 .90 -7.93
.21R 1.1R -7.72
.38R 1.4R -7.46
.712 1.7R -7.20

RECOVERY.....
.703 0.00 -7.20
.692 .30 -7.21
.68R .60 -7.22
.674 .90 -7.22
.65R 1.1R -7.23
.637 1.4R -7.25
.611 1.7R -7.27

SUPERPOSED.....
.732 1.79 -7.19
.742 1.80 -7.18
.763 1.81 -7.17
.80R 1.84 -7.14
.874 1.88 -7.11
1.02R 1.96 -7.04
1.32R 2.09 -6.93

SAMPLE 124/3
5.0 DEG.

AREA = 10.42 CM.SQ.
THICK = .0399 IN.

PCT LOG LOG
STRAIN TIME J(T)

LOAD.....
.06R 0.00 -9.45
.087 .30 -9.33
.12R .60 -9.16
.18R .90 -9.00
.263 1.1R -8.84
.41R 1.4R -8.64
.78R 1.8R -8.37

RECOVERY.....
.732 0.00 -8.40
.711 .30 -8.41
.68R .60 -8.43
.66R .90 -8.44
.637 1.1R -8.46
.60R 1.4R -8.49
.54R 1.8R -8.53

SUPERPOSED.....
.797 1.89 -8.36
.797 1.89 -8.36
.81R 1.90 -8.35
.85R 1.92 -8.34
.90R 1.96 -8.31
1.01R 2.03 -8.28
1.33R 2.18 -8.14

SAMPLE 125/4
25.0 DEG.

AREA = 10.51 CM.SQ.
THICK = .0395 IN.

PCT	LOG	LOG
STRAIN	TIME	J(T)

LOAD.....

.042	0.00	-7.41
.069	.30	-7.20
.133	.60	-6.92
.244	.90	-6.65
.430	1.18	-6.41
.802	1.48	-6.14
1.492	1.77	-5.87

RECOVERY.....

1.487	0.00	-5.87
1.476	.30	-5.87
1.471	.60	-5.87
1.460	.90	-5.88
1.450	1.18	-5.88
1.439	1.48	-5.88
1.439	1.77	-5.88

SUPERPOSED.....

1.520	1.78	-5.86
1.545	1.79	-5.85
1.604	1.80	-5.84
1.704	1.83	-5.81
1.880	1.87	-5.77
2.241	1.95	-5.69
2.931	2.07	-5.57

SAMPLE 125/4
5.0 DEG.

AREA = 10.51 CM.SQ.
THICK = .0395 IN.

PCT	LOG	LOG
STRAIN	TIME	J(T)

LOAD.....

.093	0.00	-9.30
.127	.30	-9.16
.175	.60	-9.02
.250	.90	-8.87
.364	1.18	-8.70
.560	1.48	-8.52
.897	1.77	-8.31

RECOVERY.....

.804	0.00	-8.36
.788	.30	-8.37
.762	.60	-8.38
.727	.90	-8.40
.693	1.18	-8.42
.650	1.48	-8.45
.608	1.77	-8.48

SUPERPOSED.....

.897	1.78	-8.31
.916	1.79	-8.30
.937	1.80	-8.29
.977	1.83	-8.27
1.057	1.87	-8.24
1.211	1.95	-8.18
1.505	2.07	-8.09

SAMPLE 125/4
15.0 DEG.

AREA = 10.51 CM.SQ.
THICK = .0395 IN.

PCT	LOG	LOG
STRAIN	TIME	J(T)

LOAD.....

.029	0.00	-8.58
.053	.30	-8.32
.088	.60	-8.10
.159	.90	-7.84
.265	1.18	-7.62
.494	1.48	-7.35
.950	1.78	-7.07

RECOVERY.....

.924	0.00	-7.08
.916	.30	-7.09
.903	.60	-7.09
.889	.90	-7.10
.868	1.18	-7.11
.844	1.48	-7.12
.823	1.78	-7.13

SUPERPOSED.....

.953	1.79	-7.07
.969	1.79	-7.06
.990	1.81	-7.05
1.049	1.83	-7.03
1.134	1.88	-6.99
1.338	1.95	-6.92
1.772	2.08	-6.80

SAMPLE 127/2
25.0 DEG.
AREA = 0.24 CM.SQ.
THICK = .0403 IN.

PCT LOG LOG
STRAIN TIME J(T)

LOAD.....
.044 .30 -8.46
.074 .60 -8.25
.102 .90 -8.11
.145 1.18 -7.06
.161 1.48 -7.91
.213 1.78 -7.79

RECOVERY.....
.170 .30 -7.89
.165 .60 -7.90
.136 .90 -7.99
.131 1.18 -8.01
.092 1.48 -8.16
.068 1.78 -8.29

SUPERPOSED.....
.216 1.79 -7.79
.239 1.81 -7.74
.238 1.83 -7.75
.275 1.88 -7.68
.253 1.95 -7.72
.282 2.08 -7.67

SAMPLE 127/2
25.0 DEG.
AREA = 0.24 CM.SQ.
THICK = .0403 IN.

PCT LOG LOG
STRAIN TIME J(T)

LOAD.....
.054 .30 -8.18
.074 .60 -8.25
.090 .90 -8.13
.133 1.18 -8.00
.176 1.48 -7.88

RECOVERY.....
.130 .30 -8.01
.118 .60 -8.05
.099 .90 -8.13
.087 1.18 -8.18
.065 1.48 -8.31

SUPERPOSED.....
.186 1.51 -7.85
.192 1.53 -7.84
.199 1.58 -7.82
.220 1.65 -7.78
.241 1.78 -7.74

SAMPLE 127/2
15.0 DEG.
AREA = 0.24 CM.SQ.
THICK = .0403 IN.

PCT LOG LOG
STRAIN TIME J(T)

LOAD.....
.078 .30 -9.24
.104 .60 -9.11
.144 .90 -8.98
.192 1.18 -8.85
.261 1.48 -8.72
.387 1.83 -8.55

RECOVERY.....
.310 .30 -8.65
.288 .60 -8.68
.267 .90 -8.71
.239 1.18 -8.76
.211 1.48 -8.81
.180 1.83 -8.88

SUPERPOSED.....
.388 1.84 -8.55
.393 1.85 -8.54
.411 1.88 -8.52
.432 1.91 -8.50
.471 1.99 -8.46
.567 2.13 -8.38

SAMPLE 127/2
15.0 DEG.
AREA = 0.24 CM.SQ.
THICK = .0403 IN.

PCT LOG LOG
STRAIN TIME J(T)

LOAD.....
.062 0.00 -9.34
.084 .30 -9.21
.104 .60 -9.10
.144 .90 -8.98
.181 1.18 -8.88
.247 1.48 -8.74

RECOVERY.....
.195 0.00 -8.45
.177 .30 -8.49
.159 .60 -8.44
.135 .90 -8.01
.112 1.18 -9.09
.094 1.48 -9.16

SUPERPOSED.....
.257 1.49 -8.73
.262 1.51 -8.72
.268 1.53 -8.71
.274 1.58 -8.69
.293 1.65 -8.67
.341 1.78 -8.60

SAMPLE 126/3
15.0 DEG.
AREA = 0.37 CM.SQ.
THICK = .0399 IN.

PCT LOG LOG
STRAIN TIME J(T)

LOAD.....
.075 0.00 -9.26
.096 .30 -9.15
.127 .60 -9.03
.168 .90 -8.91
.219 1.18 -8.79
.288 1.48 -8.67
.391 1.78 -8.54
.435 1.88 -8.49

RECOVERY.....
.363 0.00 -8.87
.345 .30 -8.69
.317 .60 -8.63
.288 .90 -8.67
.259 1.18 -8.72
.214 1.48 -8.80
.169 1.78 -8.90

SUPERPOSED.....
.439 1.88 -8.49
.441 1.89 -8.49
.444 1.90 -8.48
.456 1.92 -8.47
.479 1.95 -8.45
.503 2.02 -8.43
.560 2.13 -8.38

SAMPLE 128/1
25.0 DEG.

AREA = 9.08 CM.SQ.
THICK = .0404 IN.

PCT STRAIN	LOG TIME	LOG J(T)
---------------	-------------	-------------

LOAD.....

.074	0.00	-8.56
.103	.30	-8.42
.132	.60	-8.31
.183	.90	-8.17
.235	1.18	-8.06
.309	1.48	-7.94
.426	1.78	-7.80

RECOVERY.....

.356	0.00	-7.88
.334	.30	-7.91
.307	.60	-7.94
.272	.90	-8.00
.244	1.18	-8.04
.200	1.48	-8.13
.161	1.78	-8.23

SUPERPOSED.....

.430	1.79	-7.80
.436	1.79	-7.79
.439	1.81	-7.79
.455	1.83	-7.77
.478	1.88	-7.75
.509	1.95	-7.72
.587	2.08	-7.66

SAMPLE 128/1
25.0 DEG.

AREA = 9.08 CM.SQ.
THICK = .0404 IN.

PCT STRAIN	LOG TIME	LOG J(T)
---------------	-------------	-------------

LOAD.....

.083	0.00	-8.51
.103	.30	-8.42
.131	.60	-8.31
.177	.90	-8.18
.222	1.18	-8.08
.297	1.48	-7.96

RECOVERY.....

.234	0.00	-8.06
.214	.30	-8.10
.190	.60	-8.15
.161	.90	-8.23
.135	1.18	-8.30
.100	1.48	-8.43

SUPERPOSED.....

.316	1.49	-7.93
.316	1.51	-7.93
.321	1.53	-7.92
.337	1.58	-7.90
.357	1.65	-7.88
.397	1.78	-7.83

SAMPLE 128/1
15.0 DEG.

AREA = 9.08 CM.SQ.
THICK = .0404 IN.

PCT STRAIN	LOG TIME	LOG J(T)
---------------	-------------	-------------

LOAD.....

.117	0.00	-9.08
.144	.30	-8.97
.188	.60	-8.87
.241	.90	-8.76
.308	1.18	-8.66
.404	1.48	-8.54
.534	1.78	-8.42
.560	1.83	-8.40

RECOVERY.....

.454	0.00	-8.49
.426	.30	-8.52
.387	.60	-8.56
.347	.90	-8.60
.303	1.18	-8.66
.253	1.48	-8.74
.204	1.78	-8.84

SUPERPOSED.....

.571	1.83	-8.39
.575	1.84	-8.39
.575	1.85	-8.39
.588	1.88	-8.38
.611	1.91	-8.36
.658	1.99	-8.33
.738	2.10	-8.28

SAMPLE 130/3
25.0 DEG.
AREA = 8.96 CM.SQ.
THICK = .0403 IN.

PCT LOG LOG
STRAIN TIME J(T)

LOAD.....
.094 0.00 -7.56
.187 .30 -7.26
.338 .60 -7.00
.628 .90 -6.73
.947 1.11 -6.55

RECOVERY.....
.932 0.00 -6.56
.916 .30 -6.57
.896 .60 -6.58
.886 .90 -6.58
.886 1.11 -6.58

SUPERPOSED.....
1.028 1.15 -6.52
1.107 1.18 -6.49
1.233 1.23 -6.44
1.509 1.32 -6.35
1.827 1.41 -6.27

SAMPLE 130/3
25.0 DEG.
AREA = 8.96 CM.SQ.
THICK = .0403 IN.

PCT LOG LOG
STRAIN TIME J(T)

LOAD.....
.057 0.00 -7.48
.104 .30 -7.22
.187 .60 -6.96
.350 .90 -6.68
.968 1.38 -6.25

RECOVERY.....
.958 0.00 -6.26
.947 .30 -6.26
.937 .60 -6.26
.926 .90 -6.27
.896 1.38 -6.28

SUPERPOSED.....
1.016 1.40 -6.23
1.051 1.41 -6.21
1.124 1.45 -6.19
1.286 1.51 -6.13
1.863 1.68 -5.97

SAMPLE 130/3
15.0 DEG.
AREA = 8.96 CM.SQ.
THICK = .0403 IN.

PCT LOG LOG
STRAIN TIME J(T)

LOAD.....
.030 0.00 -8.63
.050 .30 -8.41
.070 .60 -8.21
.144 .90 -7.95
.248 1.20 -7.71
.434 1.51 -7.47
.600 1.68 -7.33

RECOVERY.....
.587 0.00 -7.34
.575 .30 -7.35
.570 .60 -7.35
.550 .90 -7.36
.545 1.20 -7.37
.520 1.51 -7.39
.515 1.68 -7.39

SUPERPOSED.....
.617 1.69 -7.41
.625 1.70 -7.31
.649 1.72 -7.29
.701 1.75 -7.26
.793 1.81 -7.21
.954 1.90 -7.13
1.115 1.98 -7.06

SAMPLE 130/3
15.0 DEG.
AREA = 8.96 CM.SQ.
THICK = .0403 IN.

PCT LOG LOG
STRAIN TIME J(T)

LOAD.....
.030 0.00 -8.61
.052 .30 -8.36
.087 .60 -8.14
.149 .90 -7.91
.260 1.20 -7.66
.449 1.51 -7.43
.669 1.70 -7.25

RECOVERY.....
.644 0.00 -7.27
.642 .30 -7.27
.632 .60 -7.28
.620 .90 -7.29
.595 1.20 -7.31
.570 1.51 -7.32
.545 1.70 -7.34

SUPERPOSED.....
.674 1.71 -7.25
.694 1.72 -7.24
.719 1.73 -7.22
.768 1.76 -7.19
.855 1.82 -7.15
1.019 1.91 -7.07
1.214 2.00 -7.00

SAMPLE 131/2
25.0 DEG.
AREA = 10.58 CM.².
THICK = .0402 IN.

PCT STRAIN	LOG TIME	LOG J(T)
LOAD.....		
.104	0.00	-7.44
.183	.30	-7.20
.334	.60	-6.94
.600	.90	-6.68
RECOVERY.....		
.577	0.00	-6.70
.561	.30	-6.71
.550	.60	-6.72
.535	.90	-6.73
SUPERPOSED.....		
.681	.95	-6.43
.743	1.00	-6.59
.884	1.08	-6.51
1.135	1.20	-6.41

SAMPLE 131/2
25.0 DEG.
AREA = 10.58 CM.².
THICK = .0402 IN.

PCT STRAIN	LOG TIME	LOG J(T)
LOAD.....		
.052	0.00	-7.45
.091	.30	-7.20
.170	.60	-6.93
.316	.90	-6.66
.570	1.20	-6.40
.762	1.34	-6.28
RECOVERY.....		
.751	0.00	-6.29
.743	.30	-6.29
.730	.60	-6.30
.717	.90	-6.31
.694	1.20	-6.32
.678	1.34	-6.33
SUPERPOSED.....		
.803	1.36	-6.26
.835	1.38	-6.24
.900	1.41	-6.21
1.033	1.48	-6.15
1.273	1.58	-6.06
1.440	1.64	-6.01

SAMPLE 131/2
25.0 DEG.
AREA = 10.58 CM.².
THICK = .0402 IN.

PCT STRAIN	LOG TIME	LOG J(T)
LOAD.....		
.031	0.00	-7.49
.06	.30	-7.21
.115	.60	-6.93
.211	.90	-6.66
.370	1.18	-6.42
.678	1.48	-6.16
.960	1.65	-6.01
RECOVERY.....		
.947	0.00	-6.01
.930	.30	-6.02
.934	.60	-6.02
.918	.90	-6.02
.910	1.18	-6.03
.892	1.48	-6.04
.890	1.65	-6.04
SUPERPOSED.....		
.978	1.66	-6.00
.999	1.67	-5.99
1.049	1.69	-5.97
1.130	1.72	-5.94
1.281	1.78	-5.88
1.570	1.88	-5.79
1.850	1.95	-5.72

SAMPLE 131/2
15.0 DEG.
AREA = 10.58 CM.².
THICK = .0402 IN.

PCT STRAIN	LOG TIME	LOG J(T)
LOAD.....		
.022	0.00	-8.33
.030	.30	-8.21
.050	.60	-7.98
.080	.90	-7.78
.140	1.20	-7.51
.253	1.51	-7.28
.460	1.79	-7.02
RECOVERY.....		
.450	0.00	-7.03
.447	.30	-7.03
.442	.60	-7.03
.435	.90	-7.04
.422	1.20	-7.05
.417	1.51	-7.06
.410	1.79	-7.07
SUPERPOSED.....		
.472	1.80	-7.01
.477	1.81	-7.00
.492	1.82	-6.99
.514	1.85	-6.97
.571	1.89	-6.92
.671	1.97	-6.85
.870	2.09	-6.74

SAMPLE 131/2
15.0 DEG.
AREA = 10.58 CM.².
THICK = .0402 IN.

PCT STRAIN	LOG TIME	LOG J(T)
LOAD.....		
.020	0.00	-8.40
.030	.30	-8.23
.050	.60	-8.01
.080	.90	-7.80
.140	1.20	-7.53
.256	1.48	-7.29
RECOVERY.....		
.248	0.00	-7.31
.244	.30	-7.31
.241	.60	-7.32
.236	.90	-7.33
.229	1.20	-7.34
.224	1.48	-7.35
SUPERPOSED.....		
.268	1.49	-7.27
.276	1.51	-7.26
.291	1.53	-7.24
.316	1.58	-7.20
.378	1.66	-7.12
.480	1.78	-7.02

SAMPLE 131/2
15.0 DEG.
AREA = 10.58 CM.².
THICK = .0402 IN.

PCT STRAIN	LOG TIME	LOG J(T)
LOAD.....		
.020	0.00	-8.40
.030	.30	-8.23
.050	.60	-8.01
.082	.90	-7.79
.140	1.20	-7.53
.261	1.51	-7.29
.447	1.79	-7.05
RECOVERY.....		
.435	0.00	-7.06
.427	.30	-7.07
.422	.60	-7.08
.415	.90	-7.08
.400	1.20	-7.10
.385	1.51	-7.12
.360	1.79	-7.15
SUPERPOSED.....		
.455	1.79	-7.04
.457	1.80	-7.04
.472	1.81	-7.03
.497	1.84	-7.01
.549	1.89	-6.96
.646	1.97	-6.89
.807	2.09	-6.79

SAMPLE 132/4
25.0 DEG.

AREA = 8.96 CM.SQ.
THICK = .0398 IN.

PCT LOG LOG
STRAIN TIME J(T)

LOAD.....
.075 0.00 -8.19
.106 .30 -8.05
.156 .60 -7.88
.239 .90 -7.69
.354 1.20 -7.52
.523 1.48 -7.35

RECOVERY.....
.457 0.00 -7.41
.432 .30 -7.43
.402 .60 -7.47
.357 .90 -7.52
.307 1.20 -7.58
.259 1.48 -7.66

SUPERPOSED.....
.533 1.49 -7.34
.538 1.51 -7.34
.558 1.53 -7.32
.595 1.58 -7.30
.661 1.66 -7.25
.781 1.78 -7.18

SAMPLE 132/4
25.0 DEG.

AREA = 8.96 CM.SQ.
THICK = .0398 IN.

PCT LOG LOG
STRAIN TIME J(T)

LOAD.....
.166 0.00 -8.15
.246 .30 -7.97
.354 .60 -7.82
.496 .85 -7.68

RECOVERY.....
.364 0.00 -7.80
.332 .30 -7.85
.296 .60 -7.89
.256 .85 -7.96

SUPERPOSED.....
.536 .90 -7.64
.574 .95 -7.60
.651 1.04 -7.55
.744 1.15 -7.49

SAMPLE 132/4
25.0 DEG.

AREA = 8.96 CM.SQ.
THICK = .0398 IN.

PCT LOG LOG
STRAIN TIME J(T)

LOAD.....
.038 0.00 -8.19
.050 .30 -8.07
.075 .60 -7.89
.113 .90 -7.72
.166 1.20 -7.55
.244 1.51 -7.38
.347 1.77 -7.23

RECOVERY.....
.314 0.00 -7.27
.302 .30 -7.29
.281 .60 -7.32
.256 .90 -7.36
.231 1.20 -7.41
.201 1.51 -7.47
.163 1.77 -7.56

SUPERPOSED.....
.352 1.78 -7.22
.352 1.79 -7.22
.357 1.80 -7.22
.369 1.83 -7.20
.397 1.88 -7.17
.445 1.96 -7.12
.510 2.07 -7.06

SAMPLE 132/4
15.0 DEG.

AREA = 8.96 CM.SQ.
THICK = .0398 IN.

PCT LOG LOG
STRAIN TIME J(T)

LOAD.....
.055 0.00 -8.93
.075 .30 -8.80
.103 .60 -8.66
.146 .90 -8.51
.201 1.20 -8.37
.276 1.51 -8.24
.339 1.69 -8.15

RECOVERY.....
.289 0.00 -8.22
.271 .30 -8.24
.251 .60 -8.28
.226 .90 -8.32
.196 1.20 -8.38
.156 1.51 -8.48
.131 1.69 -8.56

SUPERPOSED.....
.344 1.70 -8.14
.347 1.71 -8.14
.354 1.72 -8.13
.372 1.76 -8.11
.397 1.81 -8.08
.432 1.91 -8.04
.470 1.99 -8.01

SAMPLE 132/4
5.0 DEG.

AREA = 8.96 CM.SQ.
THICK = .0398 IN.

PCT LOG LOG
STRAIN TIME J(T)

LOAD.....
.050 0.00 -9.46
.060 .30 -9.39
.075 .60 -9.29
.094 .90 -9.19
.123 1.20 -9.08
.162 1.51 -8.96
.204 1.78 -8.86

RECOVERY.....
.157 0.00 -8.97
.148 .30 -8.90
.136 .60 -8.83
.119 .90 -8.69
.103 1.20 -8.55
.085 1.51 -8.43
.063 1.78 -8.37

SUPERPOSED.....
.207 1.79 -8.85
.209 1.79 -8.85
.211 1.81 -8.84
.214 1.83 -8.84
.226 1.88 -8.81
.247 1.96 -8.77
.266 2.08 -8.74

SAMPLE 133/1
25.0 DEG.

AREA = 0.25 CM.².
THICK = .0402 IN.

PCT LOG LOG
STRAIN TIME J(T)

LOAD.....
.062 0.00 -8.54
.082 .30 -8.42
.112 .60 -8.29
.149 .90 -8.16
.190 1.20 -8.04
.274 1.51 -7.90
.368 1.78 -7.77

RECOVERY.....
.299 0.00 -7.86
.270 .30 -7.89
.261 .60 -7.92
.231 .90 -7.96
.204 1.20 -8.03
.174 1.51 -8.10
.149 1.78 -8.16

SUPERPOSED.....
.361 1.79 -7.78
.361 1.79 -7.78
.373 1.81 -7.76
.386 1.83 -7.75
.403 1.88 -7.73
.440 1.96 -7.69
.517 2.08 -7.62

SAMPLE 133/1
25.0 DEG.

AREA = 0.25 CM.².
THICK = .0402 IN.

PCT LOG LOG
STRAIN TIME J(T)

LOAD.....
.025 0.00 -8.56
.030 .30 -8.48
.040 .60 -8.36
.050 .90 -8.26
.070 1.20 -8.11
.087 1.51 -8.02
.110 1.78 -7.88

RECOVERY.....
.095 0.00 -7.98
.087 .30 -8.02
.077 .60 -8.07
.074 .90 -8.08
.062 1.20 -8.16
.050 1.51 -8.26
.045 1.78 -8.31

SUPERPOSED.....
.110 1.79 -7.88
.117 1.79 -7.89
.117 1.81 -7.89
.124 1.83 -7.86
.132 1.88 -7.84
.137 1.96 -7.82
.164 2.08 -7.74

SAMPLE 133/1
25.0 DEG.

AREA = 0.25 CM.².
THICK = .0402 IN.

PCT LOG LOG
STRAIN TIME J(T)

LOAD.....
.062 0.00 -8.54
.080 .30 -8.44
.104 .60 -8.32
.144 .90 -8.18
.194 1.20 -8.05
.240 1.48 -7.94

RECOVERY.....
.187 0.00 -8.07
.164 .30 -8.11
.149 .60 -8.16
.124 .90 -8.24
.100 1.20 -8.34
.075 1.48 -8.46

SUPERPOSED.....
.240 1.49 -7.94
.240 1.51 -7.94
.254 1.53 -7.93
.260 1.58 -7.91
.294 1.66 -7.87
.323 1.78 -7.83

SAMPLE 133/1
15.0 DEG.

AREA = 0.25 CM.².
THICK = .0402 IN.

PCT LOG LOG
STRAIN TIME J(T)

LOAD.....
.045 0.00 -9.32
.057 .30 -9.21
.075 .60 -9.10
.100 .90 -8.97
.130 1.20 -8.83
.194 1.51 -8.68
.254 1.74 -8.56

RECOVERY.....
.211 0.00 -8.64
.190 .30 -8.67
.187 .60 -8.70
.160 .90 -8.74
.152 1.20 -8.79
.137 1.51 -8.83
.124 1.74 -8.87

SUPERPOSED.....
.254 1.75 -8.56
.254 1.76 -8.56
.261 1.77 -8.55
.269 1.80 -8.54
.291 1.85 -8.51
.331 1.94 -8.45
.378 2.04 -8.39

SAMPLE 133/1
5.0 DEG.

AREA = 0.25 CM.².
THICK = .0402 IN.

PCT LOG LOG
STRAIN TIME J(T)

LOAD.....
.037 0.00 -9.50
.047 .30 -9.40
.055 .60 -9.34
.065 .90 -9.27
.077 1.20 -9.19
.100 1.51 -9.08
.124 1.78 -8.98

RECOVERY.....
.087 0.00 -9.14
.077 .30 -9.19
.075 .60 -9.20
.062 .90 -9.28
.050 1.20 -9.38
.042 1.51 -9.45

SUPERPOSED.....
.124 1.79 -8.98
.124 1.79 -8.98
.129 1.81 -8.96
.127 1.83 -8.97
.127 1.88 -8.97
.142 1.96 -8.92

SAMPLE 133/1
5.0 DEG.

AREA = 0.25 CM.².
THICK = .0402 IN.

PCT LOG LOG
STRAIN TIME J(T)

LOAD.....
.060 0.00 -9.50
.068 .30 -9.44
.085 .60 -9.35
.102 .90 -9.27
.127 1.20 -9.18
.150 1.51 -9.08
.194 1.78 -8.99

RECOVERY.....
.137 0.00 -9.14
.124 .30 -9.18
.112 .60 -9.23
.100 .90 -9.28
.081 1.20 -9.37
.063 1.51 -9.48
.050 1.78 -9.58

SUPERPOSED.....
.197 1.79 -8.99
.193 1.79 -8.99
.197 1.81 -8.99
.201 1.83 -8.98
.208 1.88 -8.96
.223 1.96 -8.93
.244 2.08 -8.89

